Technical University of Denmark

DTU

Annual progress report of the Condensed Matter Physics and Chemistry Department 1 January - 31 December 1999

Lebech, Bente

Publication date:
2000

Document Version
Publisher's PDF, also known as Version of record

Link back to DTU Orbit

Citation (APA):
Lebech, B. (Ed.) (2000). Annual progress report of the Condensed Matter Physics and Chemistry Department 1 January - 31 December 1999. (Denmark. Forskningscenter Risoe. Risoe-R; No. 1156(EN)).

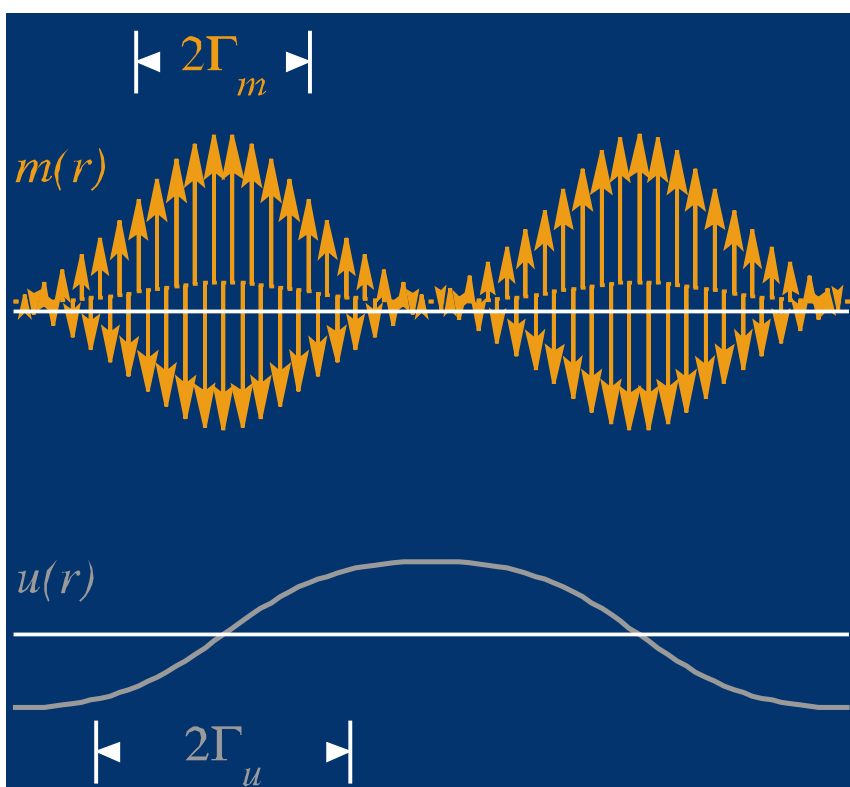**DTU Library**
Technical Information Center of Denmark

Annual Progress Report of the Condensed Matter Physics and Chemistry Department
1 January – 31 December 1999

Edited by B. Lebech

Abstract

The Condensed Matter Physics and Chemistry Department is concerned with both fundamental and applied research into the physical and chemical properties of materials. The principal activities in the year 1999 are presented in this progress report.

The research in physics is concentrated on neutron and X-ray scattering techniques and the problems studied include two- and three-dimensional structures, magnetic ordering and spin dynamics, superconductivity, phase transitions and nano-scale structures. The research in chemistry includes chemical synthesis and physico-chemical investigation of small molecules and polymers, with emphasis on polymers with new optical properties, block copolymers, surface-modified polymers and supramolecular structures. Theoretical work related to these problems is undertaken, including Monte Carlo simulation, computer simulation of molecules and polymers and methods of data analysis.

The readers are invited to contact the department or the authors of the individual contributions for more detailed information than can be given in this report. The postal address is: Condensed Matter Physics and Chemistry Department, Risø National Laboratory. P.O. Box 49, DK-4000 Roskilde, Denmark. E-mail addresses may be found one the last pages of this report or under the titles of the contributions.

Front cover illustration:
The field induced magnetic soliton in $GuGeO_3$ and the associated structural distortion (see section 2.2.1. of this report).

Back cover illustration:
AFM image of the worn surface of carbon fibre reinforced PEEK (see section 2.8.24. of this report).

Table of contents

1.   Introduction

Department of Condensed Matter Physics and Chemistry
Klaus Bechgaard

klaus.bechgaard@risoe.dk   http://www.risoe.dk/fys/department/introduction.htm

The research activities of the department aim at creating an understanding of the relation between the atomic and molecular configuration of materials and their structural, magnetical, electrical, optical, chemical or biological properties. In 1999 the activities were organised in three programmes: Macromolecular Materials Chemistry, Magnetism and Superconductivity and Surfaces and Interfaces.

In addition the department is in charge of a special user programme at DR3 steady state reactor supported by the Commission of the European Community (CEC) Training and Mobility of Researchers (TMR).

Relevance
The strategic goals of the department are identified along three main lines:
The department shall act as a link for academic and industrial researchers to international research at large facilities by providing internationally competitive neutron scattering facilities at DR3 and X-ray facilities at the synchroton at HASYLAB at Desy in Hamburg ,respectively. The specific research projects chosen fall within superconductivity, magnetism, polymer science and surface and interface science.

The department shall engage strongly in The Danish Polymer Center with the Technical University of Denmark to provide danish industry and academia with a strong potential for internationally competitive research and with well educated M.Sc. and Ph.D.

The department shall identify and engage in the research areas of the future (ex. nanophysics and –chemistry and biophysics) by thriving on the competencies obtained in in the fields mentioned above.

Dissemination of results
The results of the department are typically published in international journals or in the form of reports to the relevant funding agency.

During 1999 the departments researchers have participated in the filing of several patents, either as a result of ongoing collaborative programs or aimed at creating new business areas.

In collaborative programs with industry and public research institutions the competence and instrumental facilities are typically shared between the partners. As an example the newly installed surface science facilities can be mentioned. Also the Polymer Center aims at creating national competencies and facilities. Both have resulted in new "customers" for the department.

Several of the department's projects are performed in collaboration with industrial partners exercising their influence on the project goals.

The "industrial post-doc's" with Danfoss A/S and Haldor Topsøe A/S within tribology and catalysis have had a very strong influence on new ways of utilising the department's expertise and facilities.

Board members from Danish industry play an important role in the Danish Polymer Center and in DANSYNC when identifying research areas of relevance for Danish industry.

Danish universities

The department has a formalised collaboration with the Technical University of Denmark (The Polymer Center) and with The University of Copenhagen (Biophysics) and holds an external lectureship at the Ørsted Laboratory at University of Copenhagen. These collaborations have strong research and educational activities at the M.Sc. and at the Ph.D. level.

Most of the department's projects are in collaboration with partners at universities.

The department hosts a large number of other M.Sc., Ph.D. students and post-docs in specific projects with universities and is an active partner at summer schools etc.

Other Danish research institutions

The department collaborates in smaller projects with other public Danish research institutions (ex. Mikroelektronik Centret and Danish Technological Institute) but has no formal collaboration with the government research institutes.

Foreign universities and research institutes

The department's achievements in research depend strongly on international collaboration with researchers at universities and public and private research institutes. The department hosts many foreign researchers and the staff often visits foreign laboratories and institutions.

The visitors programme at DR3 is accommodating a very large number of foreign students during their project periods.

2.   Research Projects in the department

The work is divided in the following subject categories:

2.1. Theory

2.2. Magnetism

2.3. Superconducting materials and phenomena

2.4. Structures and defects

2.5. Structures and interfaces

2.6. Langmuir films

2.7. Microemulsions, surfactants and biological systems

2.8. Polymers

2.9. Organic chemistry

2.10. Instrumentation

2.11. Training and Mobility of Researchers - Access to Large Installations

2.1.   Theory

2.1.1.   Computer simulation of the phase diagram for the extended ASYNNNI model

P.-A. Lindgård, N. H. Andersen, *Condensed Matter Physics and Chemistry Department, Risø National Laboratory, Denmark* and D. Mønster, *UNI-C, Århus, Denmark*
e-mail: p.a.lindgard@risoe.dk   http://www.risoe.dk/fys/Employee/peli.htm

With the aim of getting a realistic calculation of the phase diagram for the oxygen ordering in $YBa_2Cu_3O_{6+x}$ we have studied the extended ASYNNNI model[1]. In addition to the usual interactions this model includes a next nearest neighbour interaction parameter, V_5, which effectively represents the relevant 2D Coulomb interactions with also more distant ions, while we have neglected the small 3D interaction (*i.e.* V_4=0). The detailed phase diagrams, shown for two values of V_5 in the figures, reveal several features, which have been observed experimentally[2], but previously not understood. We have found that the ordering vector q^* for alignment of copper-oxide chains along the *a*-axis varies semi-continuously in regions denoted $Q_{\neq}$ between the simpler commensurate ortho-II and –III structures. This is shown in the upper part of the figures for the lowest reduced temperature, $T^* \equiv k_B T/|V_1|$, studied, T^*=0.05, and at the onset of ordering, $T^* = T_Q$. A reasonable agreement between this and the prediction of a simple model[3] (dashed line) is obtained, however, we can support the underlying picture and several additional features are found. That is broad plateau-like peaks (the widths of which are indicated by vertical bars) and mixed phases (indicated by two q^* points at one *x* and the dashed regions). The detailed features for *x*<0.4 have not been observed experimentally. The reason for this is not yet understood.
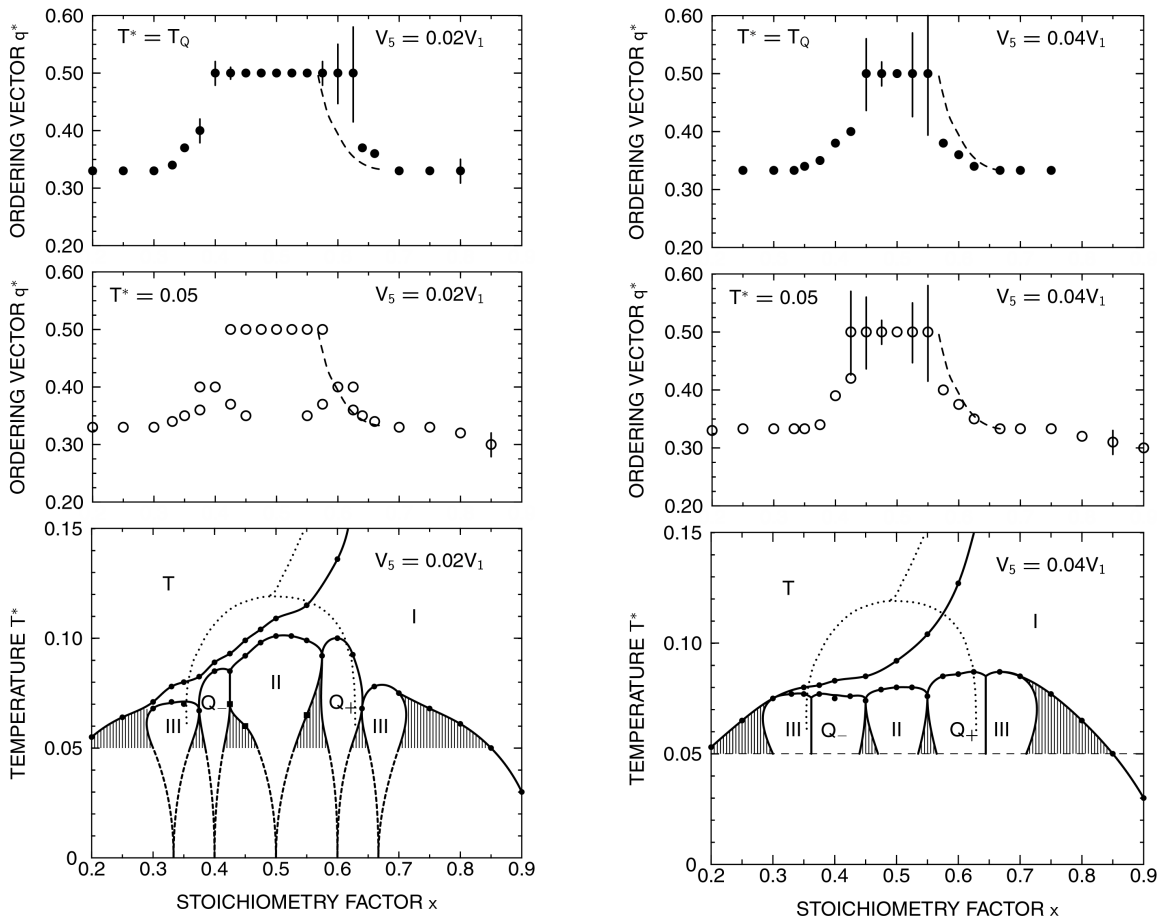
[1] D. Mønster, P.-A. Lindgård and N. H. Andersen, Phys. Rev. **B60**, 110 (1999).
[2] N. H. Andersen *et al.*, Physica C **317-318**, 259 (1999), P. Schleger, P. A. Hadfield, H. Casalta, N. H. Andersen, H. F. Poulsen, M. von Zimmermann, J. R. Schneider, R. Liang, P. Vosanjh and W. N. Hardy, Phys. Rev. Lett. **74**, 1446 (1995).
[3] A. G. Khatchaturian and J. W. Morris Jr., Phys. Rev. Lett. **64**, 76 (1989).

2.1.2. Field dependence of the π resonance in high-T_c superconductors: An SO(5)-based prediction

H. M. Rønnow, *Condensed Matter Physics and Chemistry Department, Risø National Laboratory, Denmark,* N. A. Mortensen, *Mikroelektronik Centret, Technical University of Denmark, Denmark,* H. Bruus and P. Hedegård, *Ørsted Laboratory, University of Copenhagen, Denmark*
e-mail: henrik.roennow@risoe.dk   http://www.risoe.dk/fys/Employee/hero.htm

The π resonance observed at $\omega_\pi \approx 41\,\text{meV}$ and $q = (\pi/a, \pi/a) \equiv Q$ in neutron scattering studies of YBa$_2$Cu$_3$O$_7$ and Bi$_2$Sr$_2$CaCu$_2$O$_{8+\delta}$ hold a key position in the understanding of high-T_c superconductivity[1]. A number of different models have been proposed to explain the π resonance[2]. In particular, Zhang[2] was inspired by the existence of antiferromagnetic (AFM) fluctuations within the superconducting (SC) state to suggest a unified theory of antiferromagnetism and d-wave superconductivity. The SC order parameter $\Psi = f\,e^{i\phi} \equiv n_1 + in_5$ and the AFM order parameter $m \equiv (n_2, n_3, n_4)$ are embedded within the SO(5) order parameter $n \equiv (n_1, n_2, n_3, n_4, n_5)$. Within the SO(5) space an effective Lagangian $\mathcal{L}(n)$ can be constructed such that it describes the low energy physics of the t-J model. The π resonance is directly present as fluctuations into the AFM subspace around a direction in the SC plane.

With the aim of making quantitative predictions that can provide experimental distinction between the different models, we have calculated the structure factor of the π resonance in the presence of an applied magnetic field. In the SO(5) theory[3], the magnetic field induced vortices are described by an order parameter, which for reasonably low fields within one unit cell of the vortex lattice is approximately given by $n(r) = (f(r)\cos\phi_r, 0, m(r), 0, f(r)\sin\phi_r)$, where $\phi_r = \arg(r)$ and $f(r) = 1$ except for close to the vortex core, where it vanishes on a length scale of ξ. The AFM order parameter $m = (1 - f^2)^{1/2}$ becomes non zero inside the vortex, but is irrelevant to the π-mode which is proportional to the SC order parameter: $\delta n(r, t) = (0, 0, 0, \delta\theta f(r)\cos\phi, \exp(i\omega_\pi t), 0)$. The dynamic structure factor is given by

$$S_{in}(q, \omega) = (\delta\theta)^2 \left| \sum_R e^{-i(q+Q)R} f(R)\cos\phi_R \right|^2 2\pi\delta(\omega - \omega_\pi) \qquad (1)$$

where the summation should run over one unit cell of the vortex lattice. As depicted in Fig. 1, the structure factor is distributed from the delta-function in zero field to a ring around Q of radius $\delta q = \pi/d$, where d is the vortex distance. This gives a $B^{1/2}$ field dependence as shown in Fig. 2, which could be detected as a broadening in q of a suitably optimised neutron scattering experiment. We conclude by pointing out that: *In the presence of an applied magnetic field, the amplitude of the π resonance is zero for* $q = (\pi, \pi)$!
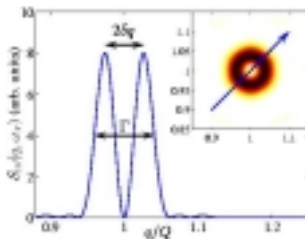
Fig. 1. The dynamic structure factor at $\omega = \omega_\pi$ as a function of q along the (π,π) - direction (for B = 10 T in YBa$_2$Cu$_3$O$_7$). The insert shows the almost isotropic response in the q-plane with the arrow indicating the (π,π) - direction.
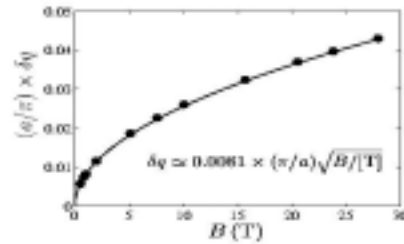
Fig. 2. The ring radius as a function of the magnetic field B. The calculated splitting ($\bullet$) has the expected $B^{1/2}$ behaviour. The numerical prefactor corresponds to a splitting of $\delta q = \pi/d$ where d is the vortex distance. (Numerical values for YBa$_2$Cu$_3$O$_7$ are used).

[1] J. Rossat-Mignod, L. P. Regnault, C. Vettier, P. Bourges, P. Burlet, J. Rossy, J. Y. Henry and G. Lapertot, Physica C **185-189**, 86 (1991), H. F. Fong, P. Bourges, Y. Sidis, L. P. Regnault, A. Ivanov, G. D. Gu, N. Koshizuka and B. Keimer, Nature **398,** 588 (1999).

[2] S.-C. Zhang, Science **275**, 1089 (1997), D. Z. Liu, Y. Zha and K. Levin, Phys. Rev. Lett. **75,** 4130 (1995), I. I. Mazin, V. M. Yakovenko, Phys. Rev. Lett. **75,** 4134 (1995).

[3] D. P. Arovas, A. J. Berlinsky, C. Kallin and S.-C. Zhang, Phys. Rev. Lett. **79**, 2871 (1997), H. Bruus, K. Astrup Eriksen, M. Hallundbæk and P. Hedegaard, Phys. Rev. **B59**, 4349 (1999).

2.1.3. Simulation of magnetic properties of small antiferromagnetic particles

P.-A. Lindgård, *Condensed Matter Physics and Chemistry Department, Risø National Laboratory, Denmark*

e-mail: p.a.lindgard@risoe.dk   http://www.risoe.dk/fys/Employee/peli.htm

In the quest for optimal and smaller scale information storage materials, the magnetic media still play a dominant role. Only recently has antiferromagnetic small particles been investigated for this purpose. It turns out that for nano-size particles the resulting magnetic moment can be surprisingly large, probably due to uncompensated spins. It is this total moment, which is of interest in the information storage, and brings the particles into the realm of superparamagnetism. There exists a much larger number of antiferromagnetic materials, than of ferro- or ferrimagnetic materials. It is therefore of interest to simulate the magnetic structure and the nature of the spin reversal in a magnetic field for small antiferromagnets. As a simple example a spherical cut NiO particle with 381 spins has been studied, as well as smaller ones. The structures is supposed to remain *fcc*, and the interaction constants $J_1 = 16K$ and $J_2 = -221K$ are known from spin wave measurements. The bulk structure is a simple type-II structure with ordering vector $q = (1,1,1)$. Surprisingly, for small particles it is found that a 2-*q* structure with simultaneous ordering in $q = (1,1,1)$ and $q = (-1,1,1)$ is more stable, with moments (•—) pointing perpendicular to each other in two out of four sublattices. See the figure to the left (top, viewed along $(1,1,1)$, below, only the middle plane), in agreement with a recent, different calculation[1]. However, even more surprisingly is that it is almost degenerate with a 4-*q* structure in which four out of eight sublattices can rotate essentially independent of each other, see figure centre and to the right. This makes it possible that the superparamagnetic relaxation, which in ferromagnets involves a rigid rotation of the particle spin, in antiferromagnets can involve partial rotations of the sublattices.

Of course the *fcc* structure is known to be highly frustrated, and the nearest neighbour interaction is cancelling for collinear spin arrangements. At higher temperatures a 'mean-field-like' compromise structure is found with about 60° relative angle between neighbouring spins. The problem with single and multiple *q* structure is familiar from the study of the nuclear magnetism in Cu[2]. Other materials, as hematite (α-Fe_2O_3) and maghemite (γ-Fe_2O_3), which have been investigated experimentally at Risø[3], have more complicated structures, but may therefore be simpler with respect to the frustration aspect.

<table>
<tr><td>2-*q*</td><td>4-*q*</td><td>4-*q*</td></tr>
</table>
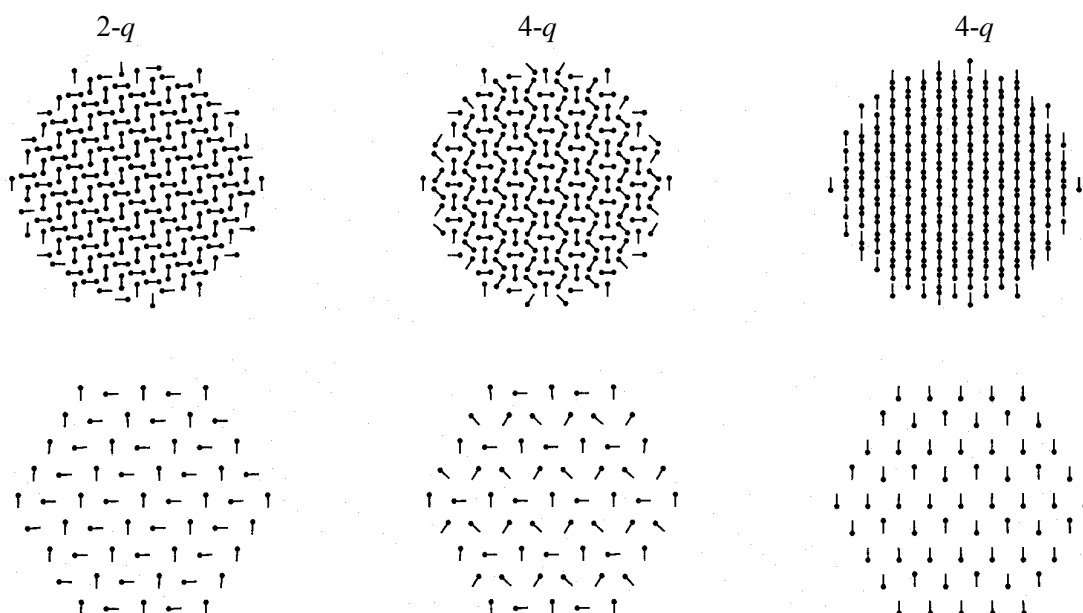
[1] R. H. Kodama and A. E. Berkowitz, Phys. Rev. **B59**, 6321 (1999).

[2] P.-A. Lindgård, Phys. Rev. Lett. **61**, 629 (1988).

[3] M. F. Hansen, F. Bødker, S. Mørup, K. Lefmann, K. N. Clausen and P.-A. Lindgård, Phys. Rev. Lett. **79**, 4910 (1997).

2.1.4. RLexact, a general program for exact diagonalisation of quantum spin systems

K. Lefmann, *Condensed Matter Physics and Chemistry Department, Risø National Laboratory, Denmark* and C. Rischel, *Department of Mathematics and Physics, Royal Veterinary and Agricultural University, Denmark.*
e-mail: kim.lefmann@risoe.dk   http://www.risoe.dk/fys/Employee/kile.htm

Few magnetic model systems have been solved quantum mechanically; even the solution of the nearest neighbour Heisenberg $s = 1/2$ chain takes a formidable effort. Thus one uses a number of approximate methods ranging from spin-wave theory to quantum field theoretical approaches. In this way, one may learn much about the essential physics of a system. For validating these calculations, one may use the method of exact diagonalization of finite-size spin clusters. By this method, quantum effects are incorporated, at the cost of introducing finite-size effects. These may be eliminated by finite-size scaling, obtaining rather accurate information about a quantum spin system.

The program RLexact performs exact diagonalisation of systems of interacting $s = 1/2$ spins. The crystal geometry and the spin interactions are determined from user input. Possible interactions terms are anisotropic exchange ($J^x s_i^x s_j^x + J^y s_i^y s_j^y + J^z s_i^z s_j^z$), dipolar, and Zeeman terms. As the dimension of the quantum mechanical subspace is $(2s+1)^N$, the possible number of spins, N, is rather limited. This limit may be pushed somewhat by incorporating various symmetries of the Hamiltonian. RLexact supports geometrical symmetries like rotation and translation, as well as time reversal ($\mathbf{s}_i \rightarrow -\mathbf{s}_i$). It also utilizes good quantum numbers, like the magnetisation in the Heisenberg model. The diagonalization may be performed by matrix methods, yielding information about all eigenstates, or by the Lanczos algorithm, obtaining the ground state and the lowest excited states. RLexact is able to calculate various observables of the system, like the energy, polarisation, and the static and dynamic structure factors. The program is rather versatile and has already been used for various purposes[1].

As an example, we show diagonalization results from the next-nearest neighbour Heisenberg model on the *fcc* lattice for N=32 for opposite signs of the two interaction constants, $-J_2 = J_1$ where the ground state structure is antiferromagnetic of type-I (ordering vectors $\mathbf{Q}=\{100\}$). At applied fields, a quantum driven transition has been predicted to occur at a magnetisation of $m=0.41$ from a spin-flop-like state to a state where three of each four spins point in the general direction of the magnetic field[2], see Fig. 1. This effect has been investigated by calculating the longitudinal and transverse static structure factors, $S^{zz}(\mathbf{Q})$ and $S^{xx}(\mathbf{Q})$, of the classical model and compare with the RLexact data, see Fig. 2. The overall agreement is rather good, and the transition happens (within the resolution) at the correct value of m. The structure factors of the diagonalization data are somewhat too high. This effect is caused by the finite size of the spin cluster.
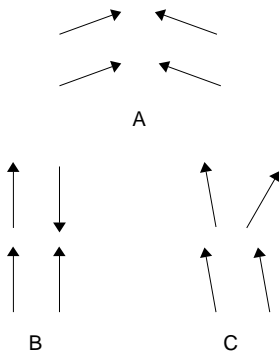
Fig. 1. Predicted structures of AF-I order on the fcc lattice at low m (A), at m=1/2 (B), and at large m (C).[2]
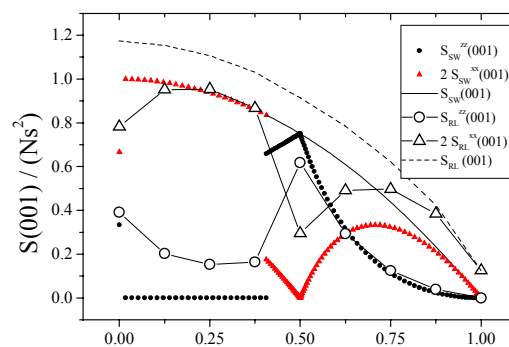
Fig. 2. Longitudinal and transverse structure factors for the classical spin structure of Fig. 1 (small symbols) and for the quantum mechanical ground state found by diagonalisation (large symbols) as a function of magnetisation, m. Solid and dashed lines represent the sum of the two structure factors.

[1] K. Lefmann and C. Rischel, Phys. Rev. **B54**, 6340-50 (1996); C. Rischel and K. Lefmann, J. Magn. Magn. Mat. **177-181**, 775 (1998); K. Lefmann, J. Ipsen and F. B. Rasmussen. To appear in Physica B.
[2] M. T. Heinilä and A. S. Oja, Phys. Rev. **B48**, 7227 (1993).

2.1.5. Mesoscopic simulation of polymers

P. Sommer-Larsen and P.-O. Åstrand, *Condensed Matter Physics and Chemistry Department, Risø National Laboratory, Denmark*

e-mail: peter.sommer.larsen@risoe.dk   http://www.risoe.dk/fys/Employee/pela.htm

Mesoscale models represent matter using larger fundamental units than molecular models. For example, polymers are represented as connected beads on the mesoscale. Simulations to determine structure, properties and dynamics of such models can be performed on today's UNIX workstations for systems containing ten thousands of beads and for long time scales. Typically, micrometer sized volumes are simulated for times exceeding microseconds. Mesoscale models link atomistic simulations with macroscopic simulations as illustrated in the table.

Table 1. Scales of polymer models

Model	Atomistic	Mesoscale	Macroscopic
Char. length	~1nm (<< R_g)	~50 nm (~R_g)	~1 mm (>> R_g)
Unit	molecule	bead / density	finite element
Times	ns	ms	s

Dissipative particle dynamics (DPD)[1] is an off-lattice Flory-Huggins type model where polymers are described as beads connected with springs. Particles follow Brownian motion but the method includes a dissipative term that conserves momentum. Thus, DPD preserves hydrodynamic interactions. This influences the dynamics of polymer solutions, hence the method results in a Zimm's like dynamics of polymers. Also, the ability of the method to simulate (micro-) phase separation in multi-component systems is strongly enhanced compared to Brownian dynamics - a comparable method that does not preserve hydrodynamics. Hydrodynamic interactions are long ranged - following inverse distance dependence - although they are mediated by short ranged forces. Effectively, the effects of a strong density upconcentration of one component at one position in the system are mediated to the whole system and these areas develop in a correlated manner to form homogenous phases. In a model without long-ranged effective interaction, density fluctuations will have to diffuse randomly without the guaranty of ever forming a homogenous phase.

Two examples are given below. Fig. 1 illustrates the up-concentration of a polymer surfactant on a water-oil interface. Fig. 2 is a hexagonal phase of a block-copolymer formed after a short simulation.
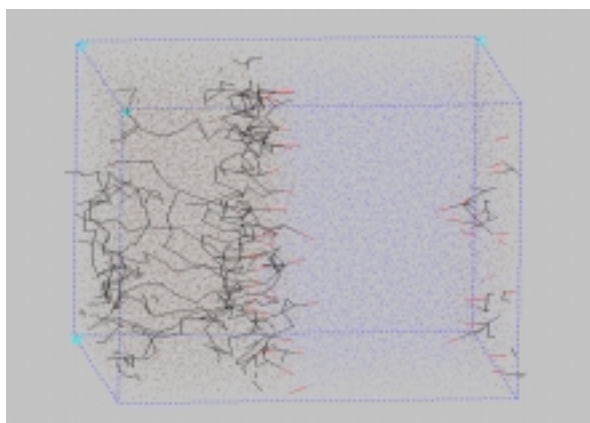
Fig. 1. 24.000 Particles. A polymer surfactant at an oil (brown particles)/ water (blue) interface. Hydrophilic headgroups on the surfactant are red:
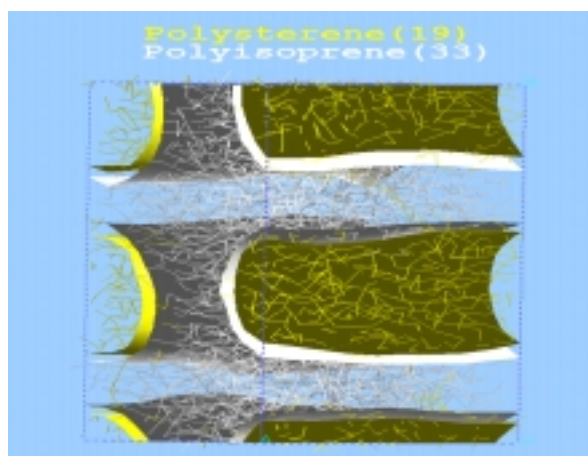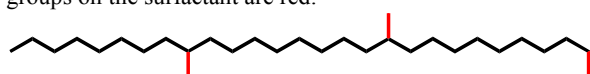
Fig. 2. 8.000 Particles. Block-copolymer. Hexagonal phase formed after 10 minutes simulation starting from randomly distributed molecules. Simulation performed on an IBM RS6000 SP Power III computer.

---

[1] R. D. Groot and P. B. Warren, J. Chem. Phys. **107,** 4423 (1997).

2.1.6. Simple model for the anomalous large volume expansion of polypyrrole

P.-A. Lindgård, *Condensed Matter Physics and Chemistry Department, Risø National Laboratory, Denmark*

e-mail: p.a.lindgard@risoe.dk   http://www.risoe.dk/fys/Employee/peli.htm

Polypyrrole (PPy) is a conjugated polymer with large electrical conductivity. The conducting state depends on the doping with the electrolyte anion, which is potential dependent. A PPy film can be switched reversible between a conducting (oxidised) and an insulating (reduced) state as a function of the potential. The large interest in PPy rest on the fact that the transition is accompanied by a change in linear dimension of about 3%. Hence it is a material of interest as a basis for micro actuators. Studies of PPy films using AFM technique[1] disclosed surprisingly that the expansion perpendicular to the silicon wafer on which it was attached (presumably with a fixed basis) could be much larger, ~ 40%. This could make PPy even more interesting for actuator or artificial muscle applications.

To offer an explanation for the large volume change a simple "sponge" model was proposed. Suppose a PPy film (as a result of the synthesis from a micellar suspension) is highly porous, which in fact would be helpful for increasing the mobility for the anions during the oxidation. Further suppose the voids in the reduced state are essentially collapsed in the film plane, with the walls of the voids being relatively flat and stiff. During the oxidation a small linear expansion of the walls of only 3% is then able to give a very large perpendicular (vertical) expansion. Take for simplicity an array of rhombohedral voids with side length ℓ. An extension $\Delta\ell/\ell = \delta\%$ upon going to the oxydized state (during the applied potential of typically 1 V) would give a vertical high increase relative to ℓ, $\Delta\ell/\ell \approx \sqrt{2\delta}$. This means a 3% linear expansion may result in a 25% vertical expansion relative to ℓ, and much more relative to the film thickness. As a test a simple 2D Monte Carlo simulation (corresponding to a vertical cut) was performed. The walls are stiff, but elastically compressible. By expanding the walls by 3% the network is allowed to relax by expanding outwards, whereas the base is fixed. The obtained expansion depends strongly in the aspect ratio of the rhombohedral diagonals. For the case shown below it was chosen as 1:10 in the reduced state of the film, shown as spheres. The expanded state is shown as the relaxed rhombohedral array. The resulting vertical expansion relative to the height is 289\% in the middle of the film, whereas the corners behave differently (notice the different vertical and horizontal length scales). The resulting profile is rather similar to that observed in the AFM experiment. It was found that if the aspect ratio was chosen too small (in order to get an even larger expansion) the opposite could happen, namely that the voids collapsed in some regions and eliminated a large-scale expansion.

The sponge model offers an idea for obtaining large expansions by simple self-organized structures, here in the form of the array of flat voids on a mesoscale; even if it is not the full explanation of the observed polypyrrole behaviour, the model might be used to get yet higher performance.

---
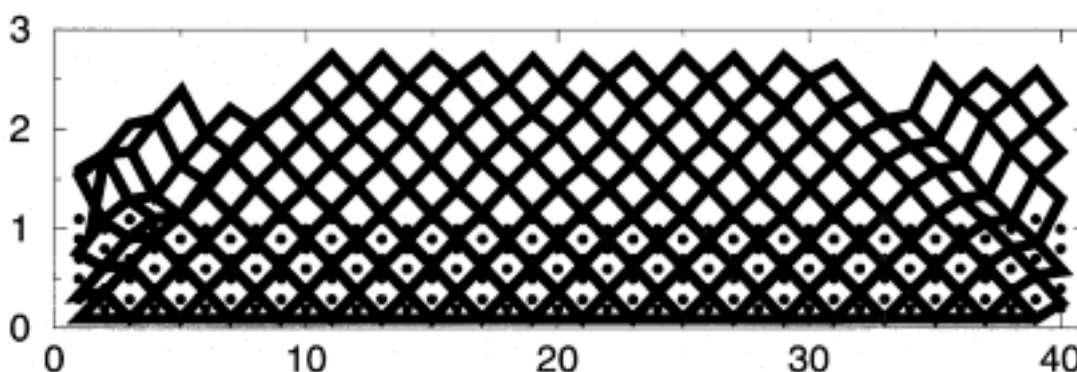
[1] E. Smela and N. Gadegaard, Adv. Mater. **11**, 953 (1999).

2.1.7. Tuning the laser wavelength in azobenzene-based data storage materials by *ab initio* quantum chemical calculations

P.-O. Åstrand, S. Hvilsted, *Condensed Matter Physics and Chemistry Department, Risø National Laboratory, Denmark,* P. S. Ramanujam, *Optics and Fluid Dynamics Department, Risø National Laboratory, Denmark,* K. L. Bak*, UNI-C, Århus, Denmark* and S. P. A. Sauer, *Chemistry Laboratory IV, University of Copenhagen, Denmark*
 e-mail: per-olof.aastrand@risoe.dk   http://www.risoe.dk/fys/Employee/peas.htm

Azobenzene dyes linked to side-chains of polymers and oligomers have been exploited for storage of information in thin films of these materials. Fast optical recording in a permanent manner with high read-out efficiencies has been demonstrated and total erasure of the inscribed information as well as multiple reuse of the material have also been achieved.[1]

Briefly, the principle of the storage process is that the *trans*-conformation of the azobenzene dyes (**1**) are excited from the electronic ground state into a singlet excited state by polarised light. In its excited state, the dye is isomerized to the *cis*-conformation, and then it relaxes back to the *trans*-conformation in a new arbitrary orientation. Since polarised light is employed, the dyes with a transition dipole moment orthogonal to the external field will not be excited. Thus, if the process is carried out repeatedly, the azobenzene dyes will be aligned. Another laser can be used to measure the diffraction pattern of the material, which will be different for the part of the material where the molecules are aligned.

One crucial aspect of the process is the wavelength of the laser used to excite the azo dyes. The $\pi \rightarrow \pi^*$ transition of the azobenzene molecule is located at 320 nm, but often it is preferred to use lasers with wavelengths in the red or infrared region (>600 nm) since cheap and compact semiconductor diode lasers are available in this region. For example, longer wavelengths can be achieved by modifying the functional groups, R_n, or by replacing one of the phenyl groups by for example a thiazole unit (**2**).

Ab initio quantum chemical calculations are useful for designing molecular components at an atomistic scale. For small molecules, they provide high accuracy and furthermore, *ab initio* methods can be used for predictive purposes since they are non-empirical. We have used a recent version of the SOPPA method[2] to calculate the excitation energies for various azobenzene dyes.[3] Calculations on azobenzenes (**1**) have been compared to experimental data and an agreement within 15 nm was found. Here, some results are presented for the $\pi \rightarrow \pi^*$ transition of azo dyes with a thiazole unit (**2**).

R_1	R_3	R_4	ΔE (nm)
H	H	H	351
OH	H	H	359
OCH_3	H	H	385
OCH_2CH_3	H	H	387
NH_2	H	H	417
$N(CH_3)_2$	H	H	488
NH_2	CN	H	455
NH_2	$CH=CH_2$	H	437
NH_2	$CH=C(CN)_2$	H	484
NH_2	CHO	Cl	470

First of all, the large impact of some of the functional groups is noted. If R_1 is assumed to be connected to the polymer side-chain, it is noted that $-N(CH_3)_2$ is the preferred choice over $-OCH_3$. Obviously, many possibilities exist for R_3 and R_4 and further investigations are required, but it has been demonstrated that it is possible to tune the laser wavelength by *ab initio* calculations. It should, however, be noted that these calculations are computer demanding, and the capacity of current computers sets a limit for the size of the molecule.

---

[1] S. Hvilsted, F. Andruzzi and P. S. Ramanujam, Optics Lett. **17**, 1234, 1992; R. H. Berg, S. Hvilsted and P. S. Ramanujam, Nature **383**, 505 (1996).
[2] K. L. Bak, H. Koch, J. Oddershede, O. Christiansen and S. P. A. Sauer, J. Chem. Phys. **112,** 4173 (2000).
[3] P.-O. Åstrand, P. S. Ramanujam, S. Hvilsted, K. L. Bak and S. P. A. Sauer. J. Am. Chem. Soc. Accepted for publication.

2.1.8. Optical properties of large molecules as calculated by an electrostatic interaction model

L. Jensen, *Chemistry Laboratory III, University of Copenhagen, Denmark* P.-O. Åstrand, *Condensed Matter Physics and Chemistry Department, Risø National Laboratory, Denmark,* K.O. Sylvester-Hvid, *Department of Electromagnetic Systems, Danish Technical University, Denmark* and K.V. Mikkelsen, *Chemistry Laboratory III, University of Copenhagen, Denmark*
e-mail: per-olof.aastrand@risoe.dk   http://www.risoe.dk/fys/Employee/peas.htm

Photonic and conducting devices based on organic and polymer materials are evidently becoming important in information distribution where data is transferred by electromagnetic waves. Furthermore, the limit for increasing the density of transistors in traditional silicon-based electronic devices will be reached in a near future.[1]

New organic functional materials are designed on an atomistic scale by modifying components at the molecular level. *Ab initio* quantum chemical methods would be an ideal tool for studying the electronic structure of molecules by theoretical means, but accurate quantum chemical calculations are restricted to rather small molecules.[2] An alternative approach is to regard a molecule as consisting of a set of point polarizabilities that interact according to classical. This is the approach outlined here.

It is well known that the molecular polarizability may be described by additive and transferable atomic polarizabilities and we have demonstrated that the frequency-dependent polarizability tensor of aromatic molecules can be calculated as a sum of atom-type polarizability tensor contributions.[3]

In an interaction model, the molecule is regarded as consisting of a set of spherically symmetric polarizabilities that interact with each other according to classical electrostatics. We have parameterised such a model for the elements H, C, N, O, F, and Cl from quantum chemical calculations of the frequency-dependent polarizability, $\alpha(\omega)$, for 115 aromatic and aliphatic molecules.[4] Three parameters have been used for each element: the atomic polarizability, a parameter describing the damping of the electric fields which is due to that the electron distribution is smeared out, and a parameter modelling the frequency-dependence in the region well below any electronic excitations. This model has been used to calculate $\alpha(\omega)$ for carbon nanotubes.[5] As seen in the figure, the interaction model gives the same trends for the static polarizability as quantum chemical methods. Furthermore, the strong frequency-dependence is noted and then especially along the tube.
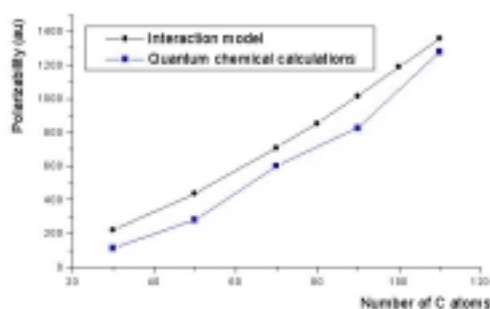
Static polarizability of (5,5) nanotubes as a function of the number of carbon atoms
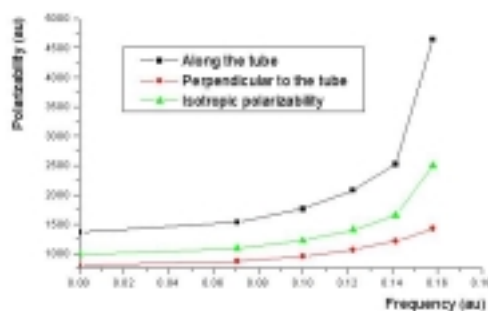
Frequency-dependent polarizability of the (5,5) nanotube with 110 atoms

---

[1] P. Ball, Made to Measure. New Materials for the 21st century. Princeton University Press, Princeton, New Jersey, 1997; D. A. Muller et al, *Nature*, **399**, 758 (1999).
[2] See e.g. 2.1.7. in this report.
[3] K. O. Sylvester-Hvid, P.-O. Åstrand, M. A. Ratner and K. V. Mikkelsen, J. Phys. Chem. A **103**, 1818 (1999).
[4] L. Jensen, P.-O. Åstrand, K. O. Sylvester-Hvid and K. V. Mikkelsen, J. Phys. Chem A **104,** 1563 (2000).
[5] L. Jensen, O. H. Schmidt, P.-O. Åstrand and K. V. Mikkelsen. Submitted to J. Phys. Chem.

2.1.9. Accurate intermolecular potentials: Bridging the gap between quantum chemistry and molecular simulations

P.-O. Åstrand, *Condensed Matter Physics and Chemistry Department, Risø National Laboratory, Denmark,* O. Engkvist, *J. Hevrovský Institute of Physical Chemistry, Academy of Sciences of the Czech Republic, Prague, Czech Republic,* S. Brdarski and G. Karlström, *Department of Theoretical Chemistry, University of Lund, Sweden*

 e-mail: per-olof.aastrand@risoe.dk   http://www.risoe.dk/fys/Employee/peas.htm

Forces between molecules govern the properties of condensed phases consisting of molecular entities such as liquids, solutions and molecular crystals. Thus, intermolecular interactions to a large extent determine for example the properties of polymers in solution, the conformations of peptides and proteins, and interactions of molecules at surfaces. The molecular geometry and the electronic structure determine these forces, and that they can be calculated if the molecular wave functions are known. However, normally empirical force fields are adopted. They are parameterised from experimental data and can only be used to model systems at conditions similar to those for which the data used in the parameterisation process were obtained. Thus, they have in principle only a limited predictive capacity.

We have developed a method termed NEMO for calculating force-field parameters based on quantum mechanical perturbation theory, and these parameters have been used in molecular dynamics simulations of liquids and solutions. The NEMO approach is thus an example of a bridge between a more detailed representation in terms of molecular wave functions and an averaged description of the electronic motion in terms of intermolecular potentials that can be used to model an assembly of many molecules.

The NEMO approach serves as a platform for studies in various parts of condensed matter theory. So far, it has been used for studies of molecular clusters, interactions of molecules at surfaces, macroscopic properties of liquids and solutions, intramolecular interactions in flexible molecules, and solvent effects on molecular properties.[1] Intermolecular potentials based on quantum chemical calculations are unbiased with respect to the experimental conditions and can thus be used for predictive studies at conditions where experiments are difficult to perform.

Adopting perturbation theory for evaluating interaction parameters provides a second-order induction term that can be represented by atomic polarizabilities. Thus, the most important many-body interaction contributions have been included in a straightforward manner. Many-body interactions are important in inhomogeneous environments as for example interactions with charged species and interactions at surfaces.

Recent developments of the NEMO approach include a new model for the repulsion energy. It implies that the expansion centres are not the same as the atomic centres, which has been implemented in the molecular simulation program MOLSIM.[2] For small changes of the repulsion parameters of the water molecule, it has been demonstrated that the structure and especially the dynamics of liquid water have been changed drastically.[3] For example, the diffusion coefficient varies with more than a factor three for the different potentials.

Furthermore, the importance of including electron correlation in the calculation of force fields has been considered.[4] By including electron correlation, the molecular dipole moment is reduced and the molecular polarizability is increased, or in other words, the electrostatic energy decreases whereas the induction energy increases. These effects have been investigated for the formamide dimer and in molecular dynamics simulations of liquid formamide. It is found that the energy minimum of the dimer is hardly affected by electron correlation whereas the total potential energy of liquid formamide is decreased drastically. The importance of including many-body effects is thus demonstrated.

---

[1] O. Engkvist, P.-O. Åstrand and G. Karlström. Submitted to Chem. Rev.
[2] MOLSIM version 2.8, P. Linse, A. Wallqvist, P.-O. Åstrand, T. M. Nymand and V. Lobaskin, Lund University (1999).
[3] S. Brdarski, P.-O. Åstrand and G. Karlström. Submitted to Chem. Phys. Lett.
[4] S. Brdarski, P.-O. Åstrand and G. Karlström. Submitted to Mol. Phys.

2.1.10. Molecular dynamics simulation of incoherent neutron scattering experiments of water near macromolecules

T. M. Nymand, *Department of Chemistry, Aarhus University, Denmark*, P-O. Åstrand and P.-A. Lindgård, *Condensed Matter Physics and Chemistry Department, Risø National Laboratory, Denmark*
e-mail: per-olof.aastrand@risoe.dk   http://www.risoe.dk/fys/Employee/peas.htm

Macromolecule's relation to water, the so-called *hydrophilic* or *hydrophobic* forces, is highly important in polymer science and biophysics, and yet very poorly understood. They are expected to play a dominant role in protein folding, a project receiving the greatest attention and recently used to motivate the construction of the next 500-fold leap in supercomputer power.[1]

The 'force' is not a regular physical force, but predominantly given by a change in entropy in the interphase. Describing it requires, hence, a detailed knowledge of the water dynamics around the macromolecule. Recently, the dynamics of the hydration shell around the plastocyanin protein has been elucidated in a combined experimental and simulation study of the incoherent part of the dynamical structure factor, $S_{inc}(q,\omega)$.[2]

Water molecules in a hydration shell around a macromolecule are normally less mobile than water molecules in the bulk liquid. These 'frozen' water molecules might show the same behaviour as the supercooled bulk liquid. It is known that water itself has many anomalous properties, in particular the density maximum at 277 K and the many ice structures. By careful studies of liquid water in the supercooled region, which includes also studies of the dynamic structure factor, $S(q,\omega)$,[3] some of these anomalies have to some extent been explained. A good understanding of this region is a prerequisite for modelling interactions of water with other molecules.

Neutron scattering measurements of $S_{inc}(q,\omega)$ provide information about the dynamics of hydrogen in the individual molecules in a sample, because of hydrogens large incoherent scattering length. The technique is especially suitable since it is possible to exchange a selected part of the hydrogens by deuteriums, which have a small incoherent scattering length.

We have implemented the calculation of the corresponding time-correlation function, $S_{self}(q,t)$, in the molecular dynamics simulation program MOLSIM.[4] Initial simulations have been carried out for liquid water, and $S_{self}(q,t)$ has been calculated for various temperatures and for different intermolecular potentials. It is well established that none of the existing water potentials can describe liquid water over a wide temperature and pressure range, and the dynamics of a liquid, in particular, is much more sensitive to the potential than static properties.[5] Some results of the simulations are presented.

The further aim is to model experiments where water interacts with other objects such as proteins and polymers. The method is suitable both for studying specific interactions, as in particular hydrogen bonding, as well as entropy-driven processes, as for example interactions at a hydrophobic surface.
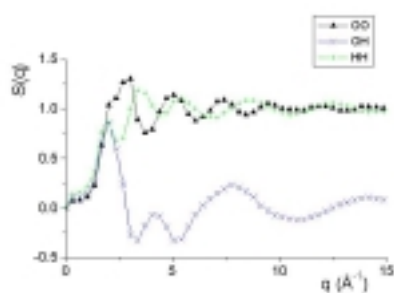
Static structure factors
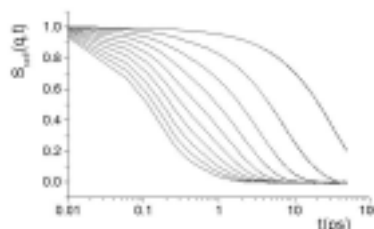
Time-dependent structure factor for hydrogen. From top to bottom: q=0.4n Å^{-1}, n=1,2,..,10

---

[1] "IBM promises scientists 500-fold leap in supercomputing power...", Nature **402**, 705 (1999).

[2] A. Paciarano, A. R. Bizzarri and S. Cannistraro, Phys. Rev. **E57**, R6277, 1998; **60**, R2476, (1999).

[3] P. Gallo, F. Sciortino, P. Tartaglia and S.-H. Chen, Phys. Rev. Lett. **76**, 2730 (1996); F. Sciortino, P. Gallo, P. Tartaglia and S.-H. Chen, Phys. Rev**. E54**, 6331 (1996).

[4] MOLSIM 2.8, P. Linse, A. Wallqvist, P.-O. Åstrand, T. M. Nymand and V. Lobaskin, Lund University (1999).

[5] O. Engkvist, P.-O. Åstrand and G. Karlström. Submitted to Chem. Rev.

2.1.11. Modelling scattering experiments of polymers by the Kratky-Porod model

P.-O. Åstrand, J. S. Pedersen, *Condensed Matter Physics and Chemistry Department, Risø National Laboratory, Denmark* and M. Ballauff*, Polymer-Institut, Universität Karlsruhe, Germany*
 e-mail: per-olof.aastrand@risoe.dk   http://www.risoe.dk/fys/Employee/peas.htm

Scattering methods like small-angle neutron scattering, small-angle X-ray scattering, and static light scattering may provide a detailed characterisation of, for example, polymers in solution and worm-like micelles. From a theoretical or modelling point of view, a polymer may be represented by a number of beads along the chain where the interaction potential between the beads is considered. Furthermore, an averaging is carried out over the solvent, which leads to modified interaction parameters. The interaction between two beads is often regarded as a Lennard-Jones potential, but it may be further approximated as excluded volume interactions or even totally neglected.

In the Kratky-Porod model, the polymer is regarded as a continuously bent thread (worm-like chain) and it is characterised by the contour length, L, and the Kuhn length, b, where b describes the stiffness of the chain. For an infinitely thin chain (no interactions between the beads) analytical theories exist for the Kratky-Porod model. Monte Carlo simulations are useful to test various analytical theories and provide results that are comparable directly to experiments. In Monte Carlo simulations, a discretized form of the Kratky-Porod model is used. We have extended previous simulations[1] of the scattering function of infinitely thin Kratky-Porod chains. A detailed comparison of available analytical theories to simulation results has been carried out, and it is demonstrated that only a few of the analytical models can be applied for comparison to scattering experiments.[2]

We have also considered birefringence experiments. The birefringence induced by magnetic fields (the Cotton-Mouton effect) probes the quantity

$$CM = \langle \sum_{i,j} \frac{3\cos^2 \theta_{ij} - 1}{2} \rangle$$

in contrast to the radius of gyration, R_G, that probes $\cos \theta_{ij}$. The Cotton-Mouton effect is sensitive to small deviations from a linear chain and should allow for the determination of the Kuhn length of stiff chains. Furthermore it has been argued that the *CM* is only to a small extent affected by excluded volume interactions. This ansatz has been tested by Monte Carlo simulations with and without excluded volume interactions and the results have been compared to an analytical expression for infinitely thin chains.[3] Results are shown in the figure for *CM* and R_G, respectively. It is demonstrated that *CM* is insensitive to excluded volume interactions within the small statistical uncertainties of around 1%, whereas R_G is clearly affected by excluded volume interactions. The analytic form is valid for continuous chains and the presented simulation have been performed for discretizations fine enough for not affecting the results. It is thus concluded that the Cotton-Mouton effect in principle is suitable for determining the Kuhn length of polymers.
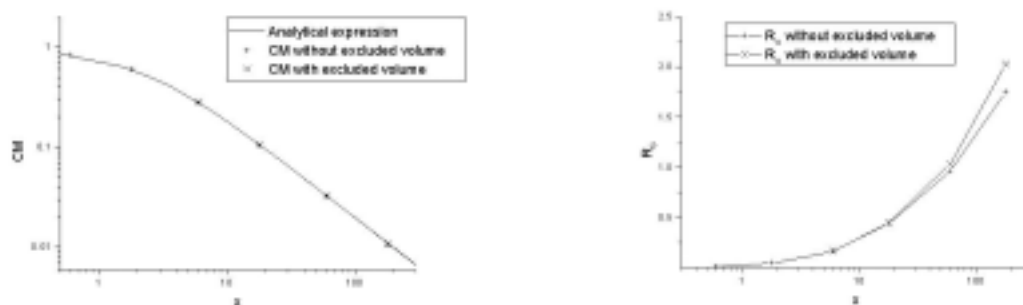
The Cotton-Mouton effect (left) and R_G (right) as a function of *x*, where *x=6L/b*.

[1] J. S. Pedersen and P. Schurtenberger, Macromolecules **29** 7602 (1996).
[2] D. Pötschke, P. Hickl, M. Ballauff, P.-O. Åstrand and J. S. Pedersen, Macromol. Chem. Theory Simul. Accepted for publication.
[3] M. Ballauff, P.-O. Åstrand and J. S. Pedersen. In preparation.

2.1.12.   Lattice models for protein folding

G. Tiana, *Niels Bohr Institute and Condensed Matter Physics and Chemistry Department, Risø National Laboratory, Denmark* and R. A. Broglia, *Universita' di Milano, Milano, Italy and Niels Bohr Institute, University of Copenhagen, Denmark.*
e-mail: tiana@nbi.dk   http://alf.nbi.dk/~tiana/

Protein conformamtions are characterized by an elevated degree of designability, that is the number of sequences which can fold fast on them. Making use of lattice models, this number could have been calculated only for sequences composed of two kinds of residues, sequences which display non-physical features. In the case of realistic sequences made of twenty kinds of residues it is possible to give an estimate of proteins designability through the knowledge of their stability. This analysis permits not only to calculate the approximate, in general very high degree of designability, by also to understand its physical origin.

Furthermore, we investigate the energy landscape in the space of designed good-folder sequences. Low-energy sequences form clusters, interconnected via neutral networks, in the space of sequences. Residues, which play a key role in the foldability of the chain and in the stability of the native state, are highly conserved, even among the chains belonging to different clusters. If, according to the interaction matrix, some strong attractive interactions are almost degenerate (i.e. they can be realized by more than one type of aminoacid contacts) sequence clusters group into a few super-clusters. Sequences belonging to different super-clusters are dissimilar, displaying very small (approx 10%) similarity, and residues in key-sites are, as a rule, not conserved. Similar behavior is observed in the analysis of real protein sequences.

2.1.13.   Secondary structures from hydrogen bonds in polymer folding

J. Borg, *Niels Bohr Institute and Condensed Matter Physics and Chemistry Department, Risø National Laboratory, University of Copenhagen, Denmark*
e-mail: borg@filine.nbi.dk   http://alf.nbi.dk/~borg/

We introduce a new model for hydrogen bonds in polymer and protein folding. By considering polymers made of monomers which have both hydrogen acceptors and hydrogen donors in specific relative orientations we demonstrate that these easily fold to secondary structures in the form of helices and sheets.

This is quantified by a structure index, and is studied as function of relative strength between the standard Van der Walls interaction and the hydrogen binding.
When these two interactions are of the same order a spin glass transition is observed at low temperatures.

Furthermore, we have developed a new method to sample the space of conformations at very low temperatures based on a combination of simulated tempering and histogram reweighting techniques.

2.2.   Magnetisme

2.2.1.   Neutron scattering study of the field-induced soliton lattice in CuGeO₃

H. M. Rønnow, D. F. McMorrow, *Condensed Matter Physics and Chemistry Department, Risø National Laboratory, Denmark,* M. Enderle, *Universität des Saarlandes, Germany,* L. P. Regnault, *CENG, Grenoble, France,* G. Dhalenne and A. Revcolevschi, *Université de Paris Sud, France,* A. Hoser, K. Prokes, P. Vorderwisch and H. Schneider, *BENSC, Berlin, Germany*
e-mail: henrik.roennow@risoe.dk   http://www.risoe.dk/fys/Employee/hero.htm

The spin-Peierls materials provide an interesting example of a non-trivial coherent quantum ground state. The magneto-elastic coupling to the 3D lattice allows an *S*=1/2 chain to form a non-magnetic ground state of dimerized spin singlets. This is the case in CuGeO₃, where below T_{sp}=14 K the S=1/2 Cu ions dimerize along the crystallographic *c*-direction, producing satellite reflections at (1/2,1,1/2)-type reflections. Though most of the predictions for a spin-Peierls material have been verified experimental, the exact form of the microscopic model in terms of phonon-interactions and second neighbour and inter-chain magnetic interactions[1].

This makes it interesting to investigate the high-field phase, for which the predictions depend only on the spin-wave velocity v_s and spin-excitation gap Δ_0, both of which can be determined experimentally without assumptions about the microscopic model. The high field phase at H_c=12.5 T is reached when the magnetic field becomes strong enough to break a dimer-bond. The two S=1/2 spins of a broken dimer will be smeared and repel each other to form an incommensurate soliton lattice.

At HMI, Germany, we have performed neutron scattering studies of the magnetic soliton structure in CuGeO₃, using a 14.5 T cryomagnet. The incommensurability is in perfect agreement with the soliton theory[2] (Fig. 1). The occurrence of odd and even harmonics (Fig. 2) enabled us to test the analytic solution for the soliton structure (Fig. 3). The amplitudes m_u=0.097(3) and m_s=0.019(3) of respectively the uniform and the staggered components agree with theory[3]. The rapid decrease of the soliton width Γ just above H_c (insert of Fig. 1) is not contained in the theory, but the minimum value $\Gamma^{..}$=9.2c is consistent with theory, and the slow increase at higher fields has been observed in density matrix calculations[4].
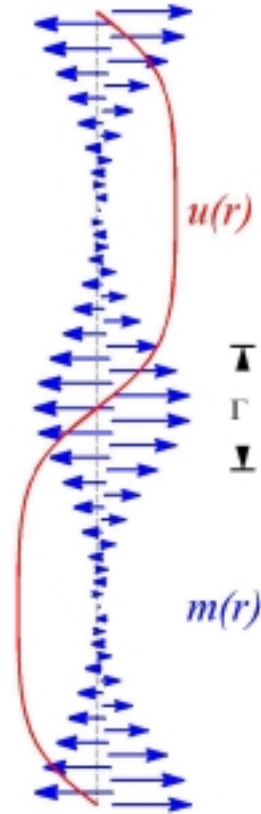
Fig. 3. The magnetic soliton structure $m(r)$ and structural distortion $u(r)$.
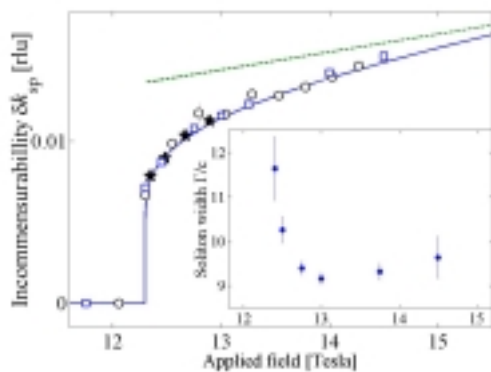
Fig. 1. The incommensurability δk_{sp} compared to the prediction from soliton theory. Insert shows the soliton width obtained from the 3rd harmonics.
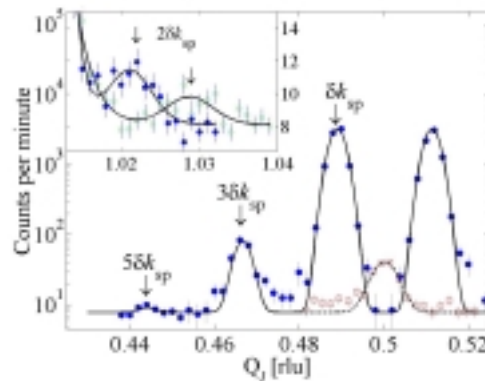
Fig. 2. The odd harmonics around (1/2,1,1/2) at 0 T and 13 T, and the second harmonics (0,0,1+2δk_{sp}) at 13 T and 14.5 T.

[1] J. P. Boucher and L. P. Regnault, J. Phys. I France **6**, 1939 (1996).
[2] A. I. Buzdin, M. L. Kulic and V. V. Tugushev, Solid State Comm. **48**, 483 (1983).
[3] J. Zang, S. Chakravarty and A. R. Bishop, Phys. Rev. **B55**, R14705 (1997).
[4] G. S. Uhrig, F. Schönfeld and J. P. Boucher and M. Horvatic, Phys. Rev. **B60**, 9468 (1999).

2.2.2. Neutron scattering study of the excitation spectrum in the high-field phase of CuGeO₃

H. M. Rønnow and D. F. McMorrow, *Condensed Matter Physics and Chemistry Department, Risø National Laboratory, Denmark,* M. Enderle, *Univ. des Saarlandes, Germany,* L. P. Regnault, *CENG, Grenoble, France,* G. Dhalenne and A. Revcolevschi, *Univ. de Paris Sud, France,* A. Hoser, K. Prokes, P. Vorderwisch, P. Smeibidl, M. Meiβner and H. Schneider, *BENSC, Berlin, Germany*
e-mail: des.mcmorrow@risoe.dk   http://www.risoe.dk/fys/Employee/demc.htm

We have recently determined the magnetic structure of the high-field phase in the spin-Peierls compound CuGeO₃[1]. For the static structure, we obtained good agreement with the prediction from soliton theory. This provides a good foundation for going beyond the current theoretical development and investigates experimentally the excitation spectrum of the high field phase.

Inelastic neutron scattering measurements were performed at the V2 cold triple axis spectrometer at HMI, Germany. In the spin-Peierls phase, the first excited states are the triplet modes, which split by $g\mu_B H$ in an applied magnetic field[2]. The two lowest of these can be seen in Fig.1 which also shows their disappearance at the critical field H_c=12.5 T. Above H_c, two new modes appear. The lowest increases slightly with field while the upper remains fairly constant at 1.6 meV. It has been argued that the high-field phase should host two modes corresponding to the flipping of a soliton[3], but a quantitative treatment hereof remains.

As seen in the energy scan at 13 T (Fig. 2), there are in addition to the two resolutions limited modes a broad remainder of the middle triplet mode. At 14.5 T this remainder has almost completely disappeared.

Concomitant with the formation of a static magnetic structure, it is expected that there should be excitations that become soft at the incommensurate positions. Such an incommensurate excitation has been found and is shown in Fig. 3. While absent at the commensurate position (1/2,1,1/2), the mode develops to maximum intensity and minimum intensity at the incommensurate position (1/2,1,1/2+δk_{sp}). The incomplete softening is believed to be related to the inter-chain interactions and the staggered *g*-tensor present in CuGeO₃.
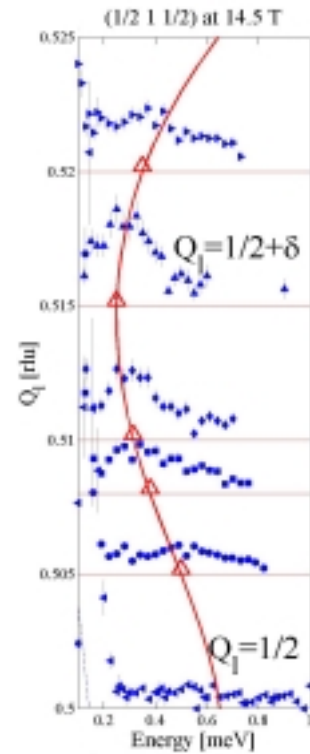
Fig. 3. The low-energy incommensurate mode at (1/2,1,1/2+δk_{sp}).
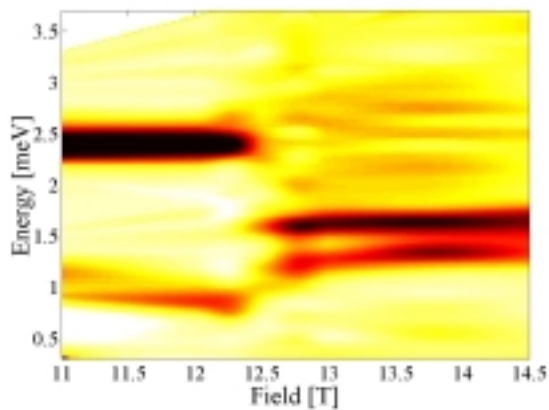
Fig. 1. Excitation spectrum at q=(1/2,1,1/2) as a function of the magnetic field. At Hc=12.5 T the triplet modes are replaced by two new modes.
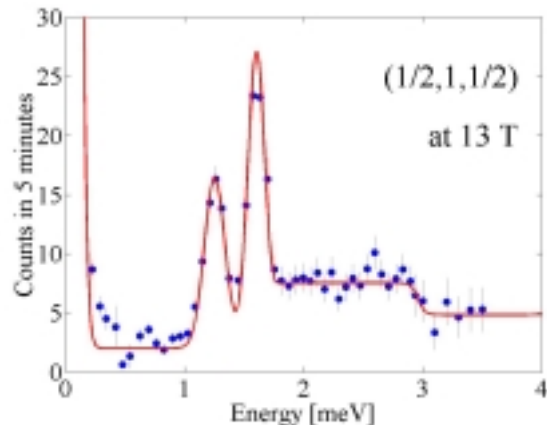
Fig. 2. The excitation spectrum at 13 T shows the two resolution limited modes. Above these peaks, the broad remainder of the middle triplet mode is visible..

[1] See 2.2.1. of this report.
[2] L. P. Regnault, M. Aïn, B. Henvien, G. Dhalenne and A. Revcolevschi, Phys. Rev. **B53**, 5579 (1996).
[3] G. S. Uhrig and F. Schönfeld and J. P. Boucher, Europhys. Lett. **41**, 431 (1998).

2.2.3. Finite temperature excitation spectrum of the 2D S=1/2 Heisenberg antiferromagnet CFTD

H. M. Rønnow, D. F. McMorrow, *Condensed Matter Physics and Chemistry Department, Risø National Laboratory, Denmark,* A. Harrison, *Department of Chemistry, University of Edinburgh, UK,* R. Coldea, T. G. Perring, *ISIS, Rutherford Appleton Laboratory, UK* and G. Aeppli, *NEC, New Jersey, USA*
e-mail: henrik.roennow@risoe.dk   http://www.risoe.dk/fys/Employee/hero.htm

During the last ten years, considerable interest has been devoted to the 2D *S*=1/2 Heisenberg antiferromagnet on a square lattice (2DQHAFSL) with nearest neighbour coupling constant *J*. At zero temperature, the system exhibits long ranged order albeit with the size of the staggered moment reduced by quantum fluctuations. At finite temperatures the system still show strong correlations characterised by a temperature dependent correlation length $\xi(T)$. In Cu(DCOO)$_2$·4D$_2$O (CFTD), which is a good physical realisation of the 2DQHAFSL, we have recently measured $\xi(T)$ for $J/5<T<J$ and obtained good agreement with the joined prediction from analytic calculations in the limits of low and high temperatures and quantum Monte Carlo calculations[1]. Also for higher values of the spin, a good understanding of the time independent properties like $\xi(T)$ has been reached.

It is therefore of great interest to look at the dynamic properties, where we sense a need for experimental data to stimulate a convergence of the theoretical results. Using the HET time of flight spectrometer at ISIS, UK, we have measured the excitation spectrum of CFTD for temperatures up to *J*/2. Below the 3D ordering temperature, we observe a resolution limited spin-wave dispersion (see Fig. 1), from which the coupling parameter *J*=6.3 meV can be extracted. An interesting feature is the energy difference at the two zone boundary points $(0,\pi)$ and $(\pi/2,\pi/2)$. This effect is correctly explained in a series expansion around the Ising limit[2] and is an example of a non-uniform quantum renormalisation beyond second order spin-wave theory.

In the 2D phase $(T > T_N)$ the spin waves are damped due to scattering against other thermally excited spin waves and due to the limited extend, $\xi(T)$, of the ordered regions. Being unable to address quantitatively the *q*-dependence of the spin-wave damping, $\Gamma(T)$, we show in Fig. 2 the average values as a function of temperature. Our result is compared to a scaling prediction[3] and quantum Monte Carlo results[4] which are shown as areas bounded by the limiting *q*=(0,0) and *q*=($\pi/2,\pi/2$) values.

The good degree of consistency between the predictions and these first data provide promising prospects for further development of the understanding of the dynamics of the 2DQHAFSL based on a convergence of the analytical results, extended Monte Carlo calculations and better experiments probing also the *q*-dependence of the damping and the softening of the excitations spectrum.
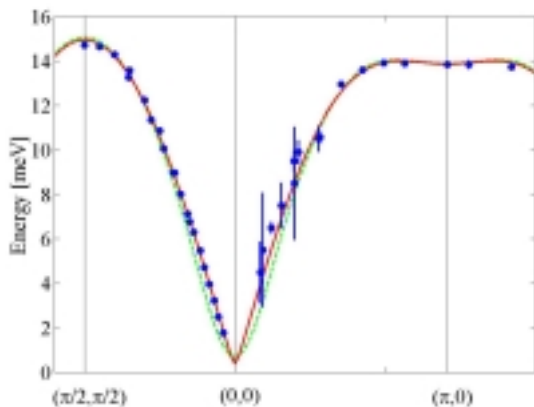
Fig. 1. Dispersion relation along two directions in reciprocal space. The zone boundary dispersion is due to quantum corrections.
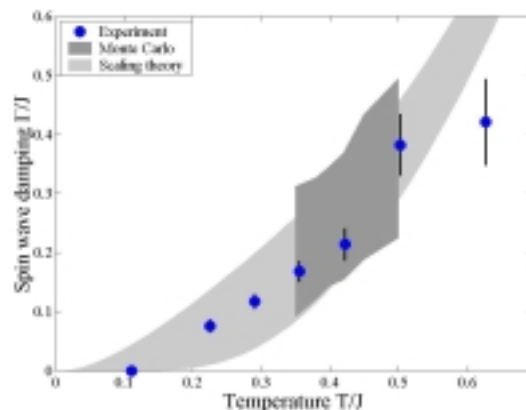
Fig. 2. Spin wave damping (●) compared to scaling prediction (light grey) and quantum Monte Carlo calculations (dark grey).

[1] H. M. Rønnow, D. F. McMorrow and A. Harrison, Phys. Rev. Lett. **82**, 3152 (1999).
[2] R. R. R. Singh and M. P. Gelfand, Phys. Rev. **B52**, R15695 (1995).
[3] S. Tyc, B. I. Halperin and S. Chakravarty, Phys. Rev. Lett. **62**, 835 (1989).
[4] M. Makivic and M. Jarrell, Phys. Rev. Lett. **68**, 1770 (1992).

2.2.4. Magnetic ordering in HoD$_{2+x}$ thin films

E. J. Grier, S. Hemon, R. A. Cowley, R. C. C .Ward, M. R. Wells, *Oxford Physics, UK*, J. P. Goff, *University of Liverpool, UK* and H. M. Rønnow, *Condensed Matter Physics and Chemistry Department, Risø National Laboratory, Denmark*
e-mail: henrik.roennow@risoe.dk   http://www.risoe.dk/fys/Employee/hero.htm

The rare-earth dideuterides adopt a simple crystal structure, the fcc fluorite structure, but they are found to exhibit surprisingly rich magnetic phase diagrams. Powder neutron diffraction studies of RD$_2$ systems with R = Tb, Dy, Ho and Er show that they order with incommensurate magnetic structures just below T$_N$, before transforming at lower temperature to a commensurate structure with the low-symmetry magnetic modulation vector ¼(113). In the case of HoD$_2$ unusual short-range magnetic order is observed above T$_N$. The fluorites have a relatively open lattice and they are able to accommodate a large concentration of excess deuterium on the octahedral interstitial sites. At low temperatures these form ordered superstructures that radically alter the electronic and magnetic properties.
In order to understand the rather complicated magnetism of these systems high-resolution single-crystal magnetic diffraction techniques have some advantages over powder methods. For example, it is easier to determine the incommensurate ordering wave vectors, to distinguish between overlapping incommensurate and commensurate phases and the presence of short-range magnetic order, and to gain information on the magnetic correlation lengths. Single-crystal films of Ho have been grown using molecular beam epitaxy. The films are of modest thickness, about 5000 Å, and it is possible to form deuterides of controlled and uniform composition. The neutron magnetic diffraction was measured using the triple-axis spectrometer TAS1.

Figure 1 shows the magnetic scattering observed at $T \sim 2$ K close to ¼(331) in scans of wave-vector transfer along ($h,h,h/3$) for pure ($x \sim 0$) and hyperstoichiometric ($x \sim 0.2$) HoD$_{2+x}$. For HoD$_2$ it is possible to resolve a large incommensurate peak as well as a weaker commensurate contribution at (0.75,0.75,0.25). The relative proportion of the two components differs markedly from the bulk, which is predominantly in the commensurate phase at low temperature. The different behaviour in the thin film may be due to epitaxial strain. The addition of deuterium interstitials has a dramatic effect on the magnetic ordering for HoD$_{2.2}$. The magnetic modulation wave vector changes, and the broadening of the diffraction peak suggests a decrease in the magnetic correlation length.
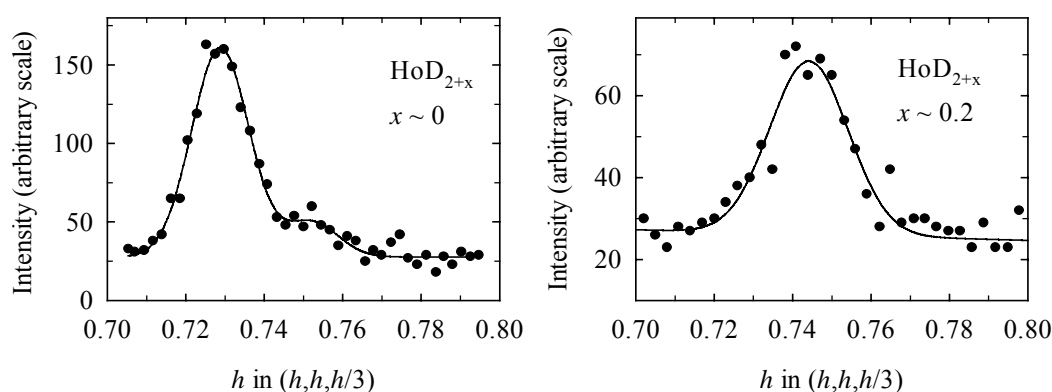
Fig. 1. Magnetic scattering close to ¼(331) at T=2 K for pure ($x \sim 0$) and hyperstoichiometric ($x \sim 0.2$) HoD$_{2+x}$.

2.2.5.   Magnetic ordering of TbRu$_2$Si$_2$ at low temperatures

S. Kawano, *Research Reactor Institute, Kyoto University, Osaka, Japan*, B. Lebech, *Condensed Matter Physics and Chemistry Department, Risø National Laboratory, Denmark*, T. Shigeoka and N. Iwata, *Faculty of Science, Yamaguchi University, Yamaguchi, Japan*
e-mail: bente.lebech@risoe.dk   http://www.risoe.dk/fys/Employee/bele.htm

The ternary rare-earth compound, TbRu$_2$Si$_2$ crystallises in the ThCr$_2$Si$_2$ type structure (I4/mmm). The compound shows various magnetic phenomena, such as successive magnetic transitions with temperature and multi-step metamagnetic transitions in applied magnetic fields. These transitions are caused by the competition between crystalline field effects and long-range RKKY exchange interactions[1]. Magnetic susceptibility and specific heat data have revealed three antiferromagnetic phases in zero magnetic field: with transition temperatures of T_N = 56 K, T_1 = 5 K and T_2 = 4.2[2]. The antiferromagnetic structure may be described by a fundamental propagation vector Q = (3/13 0 0). Odd harmonic satellites are observed at lines parallel to the basal plane reciprocal lattice vectors a* and b* in all ordered phases[3]. In the intermediate phase satellites on the h = 1, h = 1-3/13 and h = 3/13 lines[4] are evidence of a two-dimensional magnetic modulation (see Fig. 1, left).
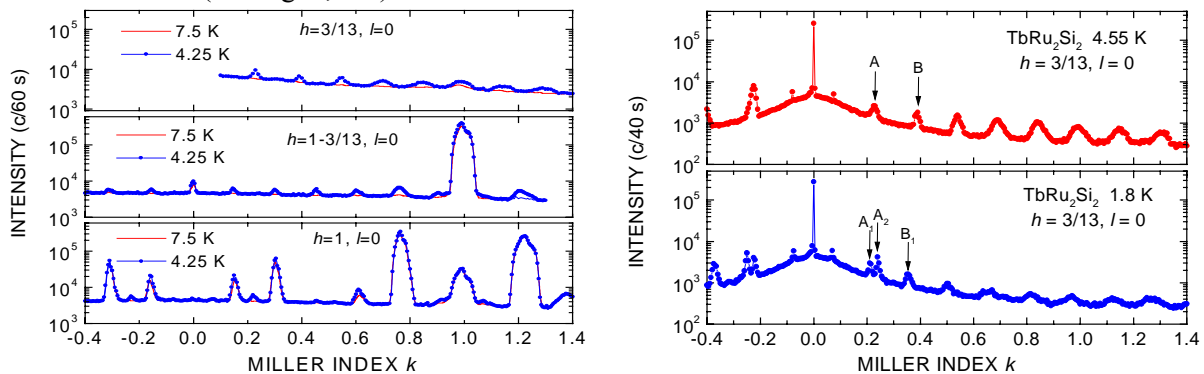
Fig. 1. Diffraction patterns from TbRu$_2$Si$_2$ obtained for scans parallel to the k−direction. In the left-hand panel for h = 3/13, 1-3/13 and 1 at 4.25 K and 7.5 K and in the right hand panel for h=3/13 at 4.55 K and 1.8 K.

Figure 1 (right) shows similar diffraction patterns (with slightly reduced background) at lower temperatures. The scans are parallel to the k−direction for h = 3/13 along at 1.8 K (low temperature phase) and 4.55 K (intermediate temperature phase). The (3/13 3/13 0) reflection (A) in the intermediate phase splits at low temperature. In addition, the position of the (3/13 5/13 0) reflection shifts slightly. The temperature dependencies of these reflections are illustrated in Fig. 2. Although the diffraction patterns in the intermediate and low temperature phases have been known for some time, the detailed magnetic structures are still unclear. Salgueiro da Silva et al.[5] have proposed a magnetic modulation creating paramagnetic (1 0 0) planes for the high temperature phase of TbRu$_2$Si$_2$. This model neither compatible with the data shown in Figs. 1 and 2 nor with the well-known magnetic behaviour of Tb and other heavy rare earth metals.
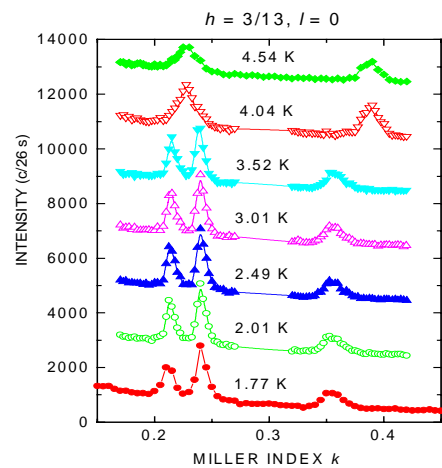
Fig. 2. Temperature dependence of the A and B satellites (T > 4.04 K) and A$_1$, A$_2$ and B$_1$ satellites (T < 3.52 K) shown in Fig. 1 (right).

[1] A. Garnier, D. Gignoux, D. Schmitt and T. Shigeoka, Physica B **212**, 343 (1995).

[2] T. Kawae, H. Sakita, M. Hitaka, K. Takeda, T. Shigeoka and N. Iwata, J. Magn. Magn. Mater. **177-178,** 795 (1998).

[3] T. Shigeoka, M. Eguchi, S. Kawano and N. Iwata, Physica B **213 & 214**, 315 (1995).

[4] S. Kawano, B. Lebech and T. Shigeoka, Risø-R-**1014**, 22 (1998).

[5] M. A. Salgueiro da Silva, J. B. Sousa, B. Chevalier, J. Etourneau, E. Gmelin and W. Schnelle, Phys. Rev. **B52,** 12846 (1995).

2.2.6. Magnetic fluctuations in maghemite nano-particles

K. Lefmann, S. N. Klausen, K. N. Clausen and P.-A. Lindgård, *Condensed Matter Physics and Chemistry Department, Risø National Laboratory, Denmark,* F. Bødker, S. Mørup and M. F. Hansen, *Department of Physics, Technical University of Denmark, Denmark*
e-mail: stine.nyborg.klausen@risoe.dk   http://www.risoe.dk/fys/Employee/stkl4768.htm

From a fundamental point of view, magnetic nano-particles are interesting because several phenomena can be studied, *e.g.* reversal of magnetisation direction along an easy axis (superparamagnetic relaxation), transverse fluctuations of the magnetisation direction near an easy direction of magnetisation (collective magnetic excitations), and ordering phenomena in systems of interacting particles. From a technological point of view, magnetic nano-particles are important because of their applications in *e.g.* magnetic storage media, ferrofluids, catalysts, and because of their possible medical applications as targetable drug delivering objects. Previously, we have presented the first neutron scattering measurements of magnetic fluctuations in nano-particles of hematite (α-Fe$_2$O$_3$).[1] Both the superparamagnetic relaxation and the precession modes were observed. Also inelastic neutron diffraction on antiferromagnetic NiO and ferromagnetic α-Fe nano-particles have revealed magnetic dynamics.[2]

Our present work concentrates on nano-particles of maghemite (γ-Fe$_2$O$_3$), which in bulk form is a simple ferrimagnet. Our sample consists of 5 nm particles in the form of a coated powder, *i.e.* magnetic interactions between the particles are not expected. At the antiferromagnetic *q*-value, $Q = 1.31$ Å^{-1}, we have observed a broad magnetic powder line. In applied magnetic fields 1-4 T at 300 K, we observe for the first time a clear signal from collective magnetic excitations, see fig. 1. At high fields, the position of the peaks is linear with field, as expected from freely precessing particle moments. A quasielastic signal is clearly observed rising between 10 and 100 K, being almost constant up to 300 K. The inelastic data, see fig. 2, can be fitted to a sum of a damped harmonic oscillator form expected for the precession mode and a Lorentzian for the quasielastic signal, all convoluted with the resolution function.
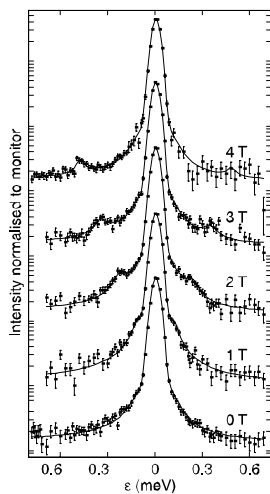
Fig. 1. Inelastic neutron data for maghemite in an applied magnetic field of 1-4 T at a temperature of 300 K shown on logarithmic scale.
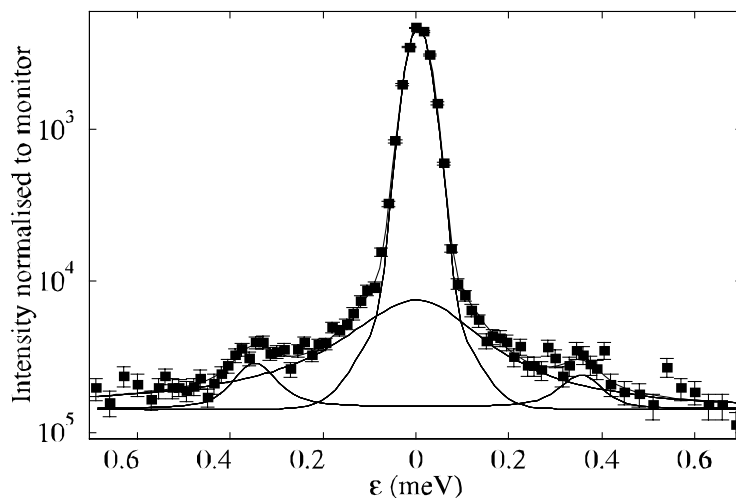
Fig. 2. Inelastic neutron data at 3 T on logarithmic scale. Each component of the fit is shown explicitly. The components are a damped harmonic oscillator contribution, a Lorentzian and the Gaussian central incoherent peak. For comparison a uniform background is added to all contributions.

[1] M. F. Hansen, F. Bødker, S. Mørup, K. Lefmann, K. N. Clausen and P.-A. Lindgård, Phys. Rev. Lett. **79**, 4910 (1997).

[2] K. Lefmann, B. Bødker, M. F. Hansen, H. Vázques, N. B. Christensen, P.-A. Lindgård, K. N. Clausen and S. Mørup, Europ. Phys. J. D **9**, 491-494 (1999); M. F. Hansen, F. Bødker, S. Mørup, K. Lefmann, K. N. Clausen and P.-A. Lindgård,. To appear in J. Magn. Magn. Mat. (2000); H. Casalta, P. Schleger, C. Bellovard, M. Hennion, I. Mirebeau, G. Ehlers, B. Farago, J.-L. Dormann, M. Kelsch, M. Linde and F. Philipp., Phys. Rev. Lett. **82**, 1301 (1999).

2.2.7. Small angle neutron scattering from cubic α-Fe nanoparticles

L. Theil Kuhn[1], K. Lefmann, J. S. Pedersen and K. N. Clausen, *Condensed Matter Physics and Chemistry Department, Risø National Laboratory, Denmark*
e-mail: kim.lefmann@risoe.dk   http://www.risoe.dk/fys/Employee/kile.htm

We have calculated and measured the magnetic neutron scattering cross section for a powder of bcc Fe nanoparticles in the size range between perfect single domain and multi domain particles. Single particle magnetisation measurements have indicated the presence of a vortex like configuration of the spins in cubic Fe nanoparticles in this size range[2]. We have numerically evaluated the cross sections for the bcc structure and various magnetic configurations in a cubic Fe nanoparticle. Special for this system is the finite size of the nanoparticles, requiring modifications of the expressions for the scattering cross sections given in[3]. The model includes a powder average taking into account the random orientation of the nanoparticles in the sample. The effects of an oxide surface layer, a size distribution, and correlations between the nanoparticles are not included.

The vortex like spin configuration is easily distinguishable from both the nuclear spectrum and the spectra for an antiferromagnetic or ferromagnetic configuration. A characteristic feature is that it appears in the spectrum as a giant antiferromagnetic unit cell with twice the size of the nanoparticle.

Small angle neutron scattering (SANS) is perfect for probing long wavelength magnetic order. The SANS experiments were performed at DR3 at Risø National Laboratory. We have performed the first SANS measurements on a powder of the cubic Fe nanoparticles. They are single crystalline and of cubic shape in the size range 5 nm to 50 nm. The nanoparticles were deposited in a per-deuterated branched hydro-carbon oil (PEP-D, synthesized for SANS by F. Krebs) in order to reduce interparticle correlations. The SANS spectra were recorded at 2 K and with an external magnetic field of up to 4.7 T applied parallel to the neutron beam.

The figures 1, 2 and 3 show the preliminary processing of the SANS data. The data recorded at 0 T has been subtracted from all the data sets, i.e. the figures show the change induced by spin order due to the applied magnetic field. For Q_1=0.009 Å and Q_2=0.05 Å corresponding to the characteristic lengths d_1=$2\pi/Q_1$=700 Å and d_2=$2\pi/Q_2$=126 Å we find a significant difference. In the predicted vortex configuration, we expect the spins forming the vortex to gradually align with the field direction upon increasing field. This will reduce the SANS signal with applied field. The decrease and saturation of the signal at Q_1 shows this behaviour, but the magnitude of d_1 shows that it is rather a vortex formed by several nanoparticles, i.e. despite the presence of the oil, d_1 is the magnetic length over which the nanoparticles are interacting. The signal at Q_2 is positioned at the correct value for a single particle vortex configuration, but the increasing signal with applied magnetic field shows that it is merely a gradual polarisation of the spins, i.e. d_2 corresponds to the interparticle correlation distance.

The Fe nanoparticles were produced in the hollow cathode sputter cluster source at the Ørsted Laboratory, Niels Bohr Institute fAPG, Denmark.
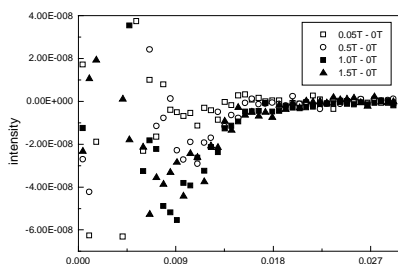
Fig. 1. The difference between SANS spectra at low fields and a reference spectrum at zero field, shown at low *q*.
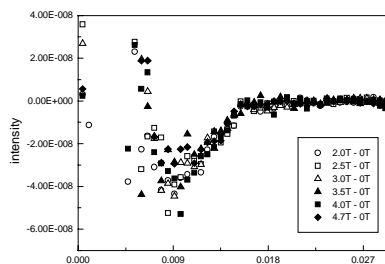
Fig. 2. The difference between SANS spectra at high fields and a reference spectrum at zero field, shown at low *q*.
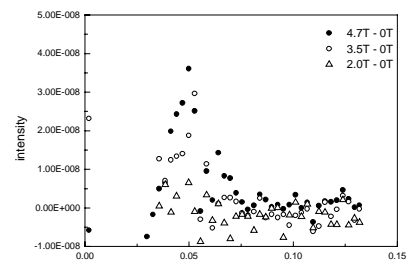
Fig. 3. The difference between SANS spectra at high fields and a reference spectrum at zero field, shown at high *q*.

[1] Present address: Lab. of Solid State Physics and Magnetism, Katholieke University, Leuven, Belgium.
[2] L. Theil Kuhn, Ph.D. thesis, University of Copenhagen (1999).
[3] G. L. Squires, Introduction to the theory of thermal neutron scattering, Cambridge University (1996).

2.2.8. Powder neutron diffraction studies of UAl_3C_3

B. Lebech, *Condensed Matter Physics and Chemistry Department, Risø National Laboratory, Denmark*,
A. P. Gonçalves, L. Pereira, M. Kuznietz[1] and M. Almeida, *Departamento de Quimica, Instituto Tecnológico e Nuclear, Sacavém, Portugal*
e-mail: bente.lebech@risoe.dk   http://www.risoe.dk/fys/Employee/bele.htm

In an ongoing effort of synthesis and physical characterisation of new uranium-poor intermetallic phases, the ternary compound UAl_3C_3 has been prepared at Sacavém by arc melting the constituting elements under an argon atmosphere followed by long term annealing. The structural aspects of the compound was initially studied be Gesing et al.[2] and recently detailed studies of the magnetic properties of UAl_3C_3 have been reported by A. P. Gonçalves et al.[3].

X-ray powder diffraction data obtained on selected single crystals confirmed the hexagonal $ScAl_3C_3$ crystal structure[1] with the U−atoms at the $2a$ sites, the Al1−, Al2− and C2−atoms at $4f$ sites with z = 0.1346, 0.75004 and 0.594, respectively and the C2−atoms at the $2c$ sites. For the compounds made in Sacavém the lattice parameters of the $P6_3/mmc$ space group were a = 3.3884(8) Å and c = 17.406(4) Å[3]. Powder x-ray diffraction data indicated[3] a well-characterised material with negligible amounts (up to 7%) of secondary phases. However, it was concluded[3] these secondary phases do not affect the magnetic properties because bulk magnetic measurements performed on samples with variable amounts of such phases led to similar results. The bulk data showed a transition at ~15 K to an antiferromagnetic phase at ambient applied magnetic field and a ferrimagnetic phase for fields above 1.6 T at the lowest temperatures[3]. A neutron diffraction study was therefore initiated with the aim to study the low temperature magnetic order in UAl_3C_3. A sample produced at Sacavém was crushed to a powder immediately before being sealed in a vanadium container with helium exchange gas and used for neutron diffraction studies. Neutron diffraction data collected using an Orange cryostat at the TAS3/POW multi-detector powder diffractometer did not show any evidence of magnetic order down to 1.5 K. However, unfortunately the diffraction data revealed amounts of secondary phases which are larger than found in the previously investigated samples made at Sacavém. Figure 1 shows the observed and calculated diffraction pattern and their difference.
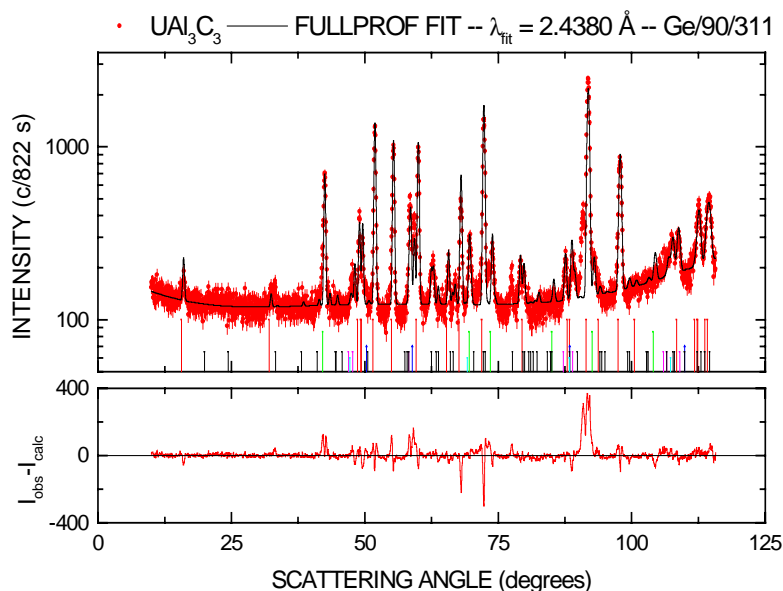
Fig. 1. Observed and calculated neutron powder diffraction patterns of UAl_3C_3. The experimental data was obtained at ambient temperature and without cryostat. The solid curve in the upper panel is the result of a profile refinement using FullProf.98[4]. The model structure included UAl_3C_3 and seven secondary phases. However, not all observed Bragg peaks are explained by this model. The secondary phases are (in order of decreasing importance) graphite, UC, UC_2, U_2C_3, Al_4C_3, UAl_4, UAl_3, UAl_2 and Al. The vertical bars indicate the two-theta positions of the expected reflections for UAl_3C_3 and the most pronounced secondary phases, which are graphite, UC, UC_2, UAl_4 and UAl_3.

---

[1] On leave from the Nuclear Research Centre − Negev, Beer Sheva, Israel.
[2] T.-M. Gesing, R. Pöttgen, W. Jeitchko and U. Wortmann, J. Alloys Compounds **186**, 321 (1992).
[3] A. P. Gonçalves, L. Pereira, M. Kuznietz and M. Almeida,. In the "Proceedings of the 29iemes Journées des Actinides, 14-17 May 1999, Luso, Portugal (1999).
[4] J. Rodriguez- Carvajal, http://www-llb.cea.fr/fullweb/fullprof98/fp98.htm.

2.3. Superconducting materials and phenomena

2.3.1. Anomalous tetragonal symmetry of a superconducting YBa$_2$Cu$_3$O$_{6.62}$ single crystal:
I: Magneto-optic studies of superconductivity

T. Frello, N. H. Andersen, *Condensed Matter Physics and Chemistry Department, Risø National Laboratory, Denmark,* M. Baziljevich, T. H. Johansen, *University of Oslo, Norway*, R. Liang, P. Dosanjh and W. N. Hardy, *The University of British Columbia, Vancouver, Canada*
e-mail: thomas.frello@risoe.dk   http://www.risoe.dk/fys/Employee/thfr.htm

For oxygen concentrations *x*>0.35 the high-*T$_c$* superconductor YBa$_2$Cu$_3$O$_{6+x}$ (YBCO) undergoes a transition from a tetragonal insulating to an orthorhombic superconducting state. During a systematic study of the orthorhombic phase diagram of YBCO a single crystal, prepared with oxygen composition *x*=0.62, turned out to have an anomalous tetragonal symmetry (see Table 1)[1]. The oxygen concentration, *x*=0.62, was established by a high-precision gasvolumetric method, and another simultaneously prepared YBCO crystal was clearly orthorhombic.

	This study	**Topnikov *et al.*[2]**	***x*=0.62 (normal)**	***x*=0.30 (normal)**
***a* (Å)**	3.8652	3.869	3.825	3.855
***b* (Å)**	3.8652	3.869	3.880	3.855
***c* (Å)**	11.7289	11.723	11.70	11.79

Table 1. Lattice parameters for anomalous tetragonal *x*=0.62 YBCO samples compared to "normal" sample values. First and second columns are this study and Topnikov *et al.*[2], respectively. Third and fourth columns are generally accepted values for orthorhombic YBCO with *x*=0.62 and for tetragonal YBCO with *x*=0.30. The latter data apply, if the crystal for some reason had not been properly oxidised.

From AC susceptibility measurements it turned out that the tetragonal sample has two critical superconducting transition temperatures: a minor volume with *T$_c$* = 43K and a larger one with *T$_c$* = 27 K. To determine whether the crystal was bulk superconducting or if the superconductivity originates from a minor orthorhombic part of the crystal it was investigated by magneto-optical (MO) imaging. By this technique the magnetic field at the sample surface can be imaged, utilising the Faraday rotation in Bi-doped yttrium-iron garnets. Due to the superconducting shielding currents there is a strong spatial modulation of the magnetic field distribution in and around a superconductor, and from this the path of the supercurrents can be determined. An example of a MO image is given in Fig. 1b. In a sample containing superconducting weak links the flux will first penetrate along the defects, and this is immediately seen as bright areas in the MO images. It is evident from Fig. 1b that the sample is bulk superconducting and that it is divided into three parts that shield off the applied field as separate domains. The elongated edge domain at the top has *T$_c$* = 43 K, the two larger domains have *T$_c$* =27 K, consistent with the AC susceptibility measurements.
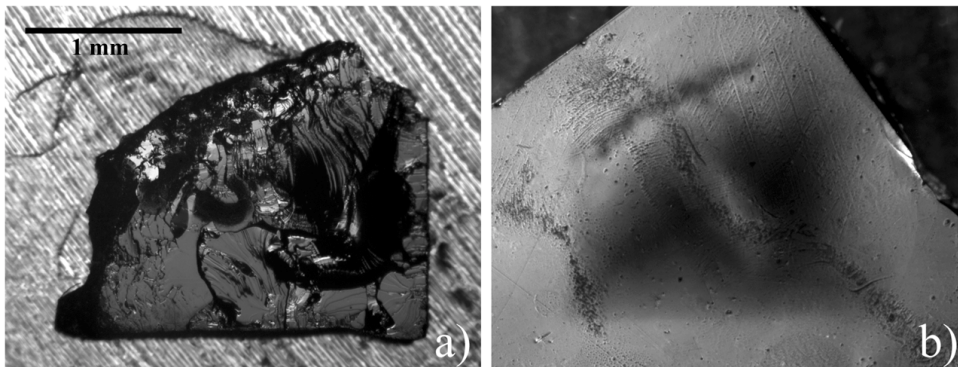
Fig. 1. Direct image a) and MO image b) of the tetragonal YBa$_2$Cu$_3$O$_{6.62}$ crystal in a field of 10 mT at 17K. In b) bright and dark areas correspond to high and low magnetic flux, respectively. The *c*-axis is normal to the plane.

---

[1] More details of the tetragonal structure are presented section 2.3.2. of this report.
[2] V.N. Topnikov, V. I. Simonov, L. A. Muradyan, V. N. Molchanov, A. V. Zvarykina, V. N. Laukhin, L. P. Rozenberg, R. P. Shibaeva and É B Yagubskii
JETP Lett. **46**, 577 (1988).

2.3.2. Anomalous tetragonal symmetry of a superconducting YBa$_2$Cu$_3$O$_{6.62}$ single crystal: II: Studies of the tetragonal structure

T. Frello, N. H. Andersen, *Condensed Matter Physics and Chemistry Department, Risø National Laboratory, Denmark,* M. von Zimmermann, T. Niemöller, J. R. Schneider, *HASYLAB at DESY, Germany*, R. Liang, P. Dosanjh and W. N. Hardy, *The University of British Columbia, Canada*
e-mail: thomas.frello@risoe.dk   http://www.risoe.dk/fys/Employee/thfr.htm

The different superconducting domains of the tetragonal YBa$_2$Cu$_3$O$_{6.62}$ (YBCO) crystal, observed by magneto-optic technique,[1] were studied in horizontal Laue geometry by hard x-ray diffraction at the BW5 beamline at HASYLAB, using a photon energy of 100 keV. A setup with optimum resolution was chosen. Perfect Si crystals were used as monochromator and analyzer. The Si (2 2 0) reflection was chosen to investigate the (0 2 0) reflection of the tetragonal YBCO crystal, as there is a close lattice match for these reflections. Thus, we were close to the nondispersive setting that offers maximum resolution. According to Bouchard *et al.*[2] in the non-dispersive setting we should be able to detect an orthorhombic splitting of $\Delta h \approx 10^{-5}$ Å^{-1} ($\approx 0.05''$) and $\Delta k \approx 1.4 \cdot 10^{-4}$ Å^{-1} ($\approx 0.55''$). The size of the incoming beam was reduced to 0.4×0.4 mm^2 by a slit and the crystal was mounted with the *ab*-plane horizontally in the scattering plane. In this way we could probe the 27K domains and the 43K domain separately (see Ref. 1). Grid scans were performed for the (0 2 0) reflection, and the results are shown in Fig. 1.

The peak shape was Lorentzian squared and the width of the 27K domain was $\Delta k = 4 \cdot 10^{-4}$ Å^{-1} longitudinally and $\Delta h = 4 \cdot 10^{-4}$ Å^{-1} in the transverse direction. For the 43K domain $\Delta k = 7 \cdot 10^{-4}$ Å^{-1} and $\Delta h = 8 \cdot 10^{-4}$ Å^{-1}. For the 27K domains Δk is essentially resolution limited, while Δh is governed by the mosaicity. In comparison the 43K domain is broadened considerably, both transversely and longitudinally, which may be a sign of a very weak orthorhombic splitting. By orienting the sample with the *ac*-plane horizontally and scanning the sample itself through the monochromatic beam while monitoring the (2 0 0) reflection it became clear that near the center of the sample there was a local variation in the mosaicity distribution of 20'' in the *ac*-plane. Thus, the superconducting weak link boundary separating the two 27K domains seen in Fig. 1b of Ref. 1 is due to local variations in the mosaic distribution.

Superconductivity in a tetragonal YBa$_2$Cu$_{2.862}$O$_{6.62}$ crystal with $T_c \approx 50$K has been observed by Topnikov *et al.* (*cf.* Ref. 1). Their data compare well with ours but both data sets deviate significantly from the generally accepted values for the orthorhombic state with $x = 0.62$ as well as for the tetragonal underdoped one at $x = 0.30$. It is generally accepted that the Cu-O chain structures leading to the orthorhombic state are necessary for superconductivity. Despite careful search we have not been able to detect any orthorhombic splitting beyond the broadening shown in Fig. 1b).
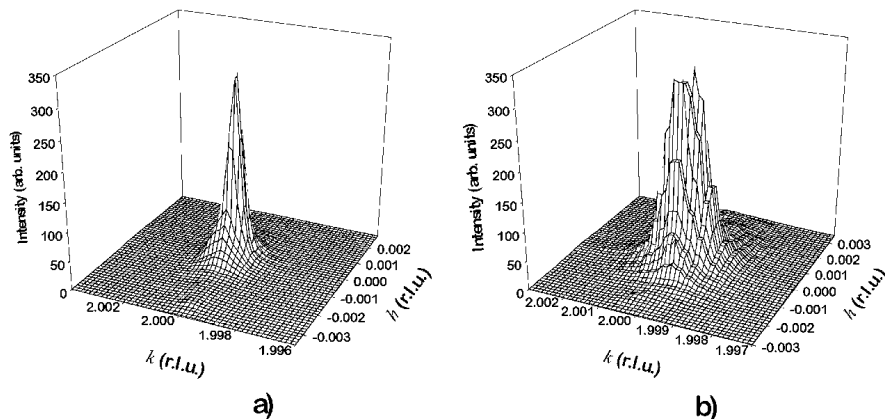
Fig. 1. Grid scan of the (0 2 0) reflection for a) the 27K domain and b) the 43K edge domain.

---

[1] The magneto-optic studies are presented in the section 2.3.2. of this report.

[2] R. Bouchard, D. Hupfeld, T. Lippmann, J. Neufeind, H.-B. Neumann, H. F. Poulsen, U. Rütt, T. Schmidt, J. R. Schneider, J. Süssenbach and M. von Zimmermann., J. Synchrotron Rad. **5**, 90 (1998).

2.3.3. Charge density studies of $YBa_2Cu_3O_{6.98}$

T. Lippmann, *GKSS, Geesthacht, Germany*, N. H. Andersen, *Condensed Matter Physics and Chemistry Department, Risø National Laboratory, Denmark*, Th. Wolf, *Forschungszentrum Karlsruhe, IPT, Karlsruhe, Germany* and J. R. Schneider, *HASYLAB at DESY, Hamburg, Germany*
e-mail: niels.hessel@risoe.dk   http://www.risoe.dk/fys/Employee/nihe.htm

X-ray and neutron diffraction has been extensively used for structural studies of the high-T_c superconductors, because the charge transfer leading to superconductivity depends strongly on details of the structural ordering. Thus, in $YBa_2Cu_3O_{6+x}$ the formation and ordering of copper-oxide chains on the Cu(1) and O(1) sites with depletion of the O(5) site l (see Fig. 1) lead to a weak orthorhombic distortion and charge transfer. So far focus has been on the atomic positions, and the charge transfer has been determined indirectly by bond valence calculations. Recently, it has been shown that x-ray crystallography using high energy (~100keV) synchrotron radiation is an excellent method for charge density studies because absorption is negligible in most cases, and extinction is small. [1]

A high quality mono-domain single crystal (slice: ~0.2×0.15×0.03 mm³) of $YBa_2Cu_3O_{6.98}$ has been investigated on the Triple-Axis Diffractometer at beam-line BW5, and 2052 reflections were recorded in two octants. After Lorentz- and polarisation corrections the data were averaged to 1026 unique reflections with internal consistency of $R_{int} = 0.0064$. An absorption correction was tested but gave no significant changes of the refined data. Conventional refinements of atomic positions (*i.e.* the z-coordinates) were carried out with spherical charge distributions and anisotropic displacement factors. Anisotropic extinction corrections were included but gave no significant changes ($Y_{ext} = 0.96$ for the strongest reflection). The oxygen occupancy numbers and the z-coordinates were found in close agreement with expectations for a fully oxygenated crystal, and with results obtained from neutron diffraction, [2] but the anisotropic displacement factors deviate somewhat. However, the neutron data were measured on a significantly larger twinned crystal, which impose constraints in the refinements that are not necessary in the analysis of the synchrotron data.

Although the agreement index ($R(F) = 0.0072$) indicates that the data are well refined, the residual density maps show additional features that are not properly described by the spherical atom model. Hence refinements with multipole expansion of the charge distributions were carried out. Fig. 1 shows the deformation density maps, *i.e.* the aspherical part of the charge distributions,[3,4] in the x-y-planes at $z=0$ (left) and $z=0.366$ (right). No significant charge density was found at the O(5) positions. Surprisingly we find that the density at the O(3) site shows considerable deformation whereas the O(2) distribution is nearly spherically. The high quality of the agreement index ($R(F)=0.0049$) and low residual density maps show the high quality of our experimental data and the model. Negative lobes, found in all the contour maps between neighbouring ions, indicate charge depletion, *i.e.* mainly ionic bonding. Further refinements and topological analyses are currently in progress.
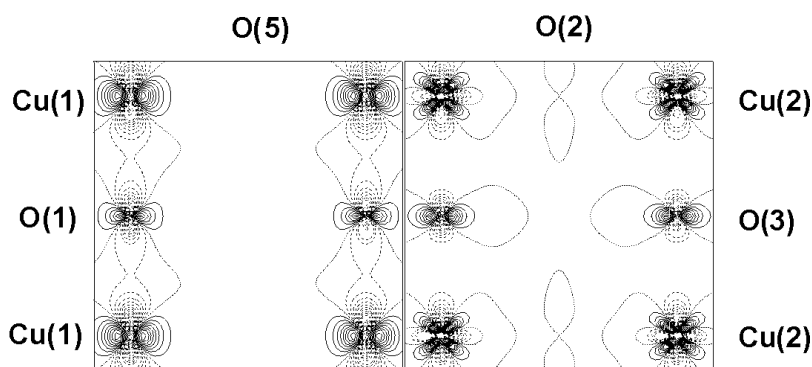
Fig. 1. Charge deformation density map in the x-y-plane at left: $z=0$ (the basal plane), and right: at $z=0.366$ (a cut between oxygen and copper in the superconducting plane). Contours are at every 0.2 e$Å^3$. Full and dashed lines indicate additional and reduced electron densities compared to the spherical distributions, respectively.

[1] T. Lippmann and J. R. Schneider, J. Appl. Cryst. **55** (1999). In the press.
[2] H. Casalta P. Schleger, P. Harris, B. Lebech, N. H. Andersen, R. Liang, P. Dosanjh amd W. Hardy, Physica **C 258**, 321 (1996).
[3] R. F. Stewart and M .A. Spackman, VALRAY Users Manual, Carnegie-Mellon Univ. Pittsburg, USA (1993).
[4] XD Users Manual, Berlin (1999).

2.3.4. Spin dynamics of PrBa$_2$Cu$_3$O$_{6.2}$

S. J. S. Lister, A. T. Boothroyd, *Department of Physics, Oxford University, Oxford, UK*, B. H. Larsen, N. H. Andersen, *Condensed Matter Physics and Chemistry Department, Risø National Laboratory, Denmark*, A. A. Zhokhov, *Russian Academy of Sciences, Institute of Solid State Physics, Russia*, A. N. Christensen, *University of Aarhus, Denmark* and A. Wildes, *Institut Laue Langevin, Grenoble, France*
e-mail: britt.h.larsen@risoe.dk   http://www.risoe.dk/fys/Employee/brla.htm

One of the outstanding problems associated with the layered cuprate superconductors is to explain the absence of superconductivity in PrBa$_2$Cu$_3$O$_{6+x}$. Substitution of Pr for Y in YBa$_2$Cu$_3$O$_{6+x}$ evidently has a strong effect on the charge carriers, and Pr $4f$ – O $2p$ hybridisation is likely to be important. Such changes will influence the magnetic couplings within the Pr and Cu sublattices, and so studies of the magnetic structure and dynamics may lead us to a better understanding of the electronic structure.

Diffraction experiments at Risø and at synchrotron x-ray sources have revealed a complex magnetic behaviour when the Pr and Cu sublattices order concurrently below $T_{Pr} = 10 - 20$ K. This phase is characterised by an incommensurate ordering vector[1,2] and a non-collinear arrangement of Cu spins[3]. Following these findings we embarked on a study of the magnetic dynamics in a single crystal of PrBa$_2$Cu$_3$O$_{6.2}$. Measurements of the low energy (<10 meV) excitations were made on the TAS 6 (RITA) spectrometer at Risø, and these data were extended up to 90 meV on the IN8 spectrometer at the Institut Laue Langevin. The simplest view of the excitation spectrum is one of localized Pr crystal field excitations and highly dispersive Cu spin waves. On more careful inspection, however, we find clear evidence in the spectrum for both Pr–Pr and Pr–Cu coupling. On RITA we studied in detail a peak centered at 1.7 meV. Fig. 1 shows the q dependence of the peak energy and intensity in the (h, 0, 0) direction[4]. There is a weak dispersion both in the energy and intensity, and evidence for a more rapid variation near $h = 0.5$ and 1.5. We have modeled the excitations using a pseudo-boson method, and the lines in Fig. 1.1 represent the calculated results for the lowest energy Pr excitation. The agreement is generally good, and we believe that the deviations near $h = 0.5$ and 1.5 are due to mixing of the Pr and Cu excitations which was neglected in the calculation. Measurements of the Cu antiferromagnetic spin waves on IN8 revealed one striking difference to those of YBa$_2$Cu$_3$O$_6$. We found that the optic mode gap at $\mathbf{q} = (\pi,\pi)$ was ~52 meV, corresponding to an interplanar exchange a factor of 2 smaller than in YBa$_2$Cu$_3$O$_6$. This surprising result, together with the other exchange constants derived from our model, needs to be analysed in connection with models for the electronic structure of PrBa$_2$Cu$_3$O$_{6+x}$.
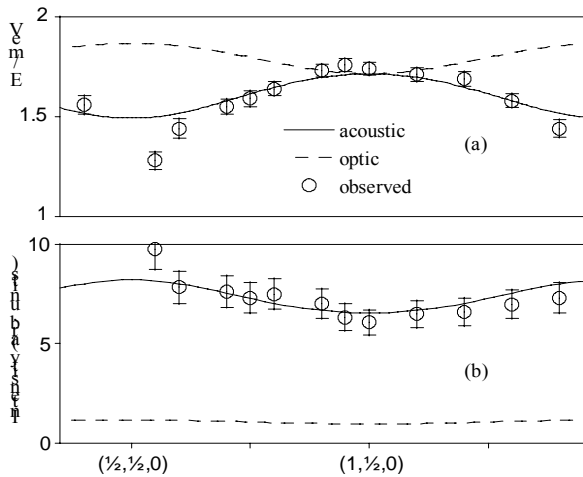
Fig. 1. **q** variation in the (h, 0, 0) direction of the 1.7 meV peak in PrBa$_2$Cu$_3$O$_{6.2}$. This mode is essentially a magnetic excitation of the Pr ions. The observed dispersion reflects a small Pr–Pr exchange coupling.

[1] J. P. Hill, A. T. Boothroyd, N. H. Andersen, E. Brecht and Th. Wolf, Phys. Rev. **B58** 11211 (1998).
[2] A. T. Boothroyd, J. P. Hill, D. F. McMorrow, N. H. Andersen, A. Stunault, C. Vittier and Th. Wolf, Physica C **317–318,** 292 (1999).
[3] A. T. Boothroyd, A. Longmore, N. H. Andersen, E. Brecht and Th. Wolf, Phys. Rev. Lett. **78** , 130 (1997).
[4] S. J. S. Lister, A. T. Boothroyd, N. H. Andersen, A. A. Zhokhov, A. N. Christensen and Th. Wolf, Physica C **317–318,** 572 (1999).

2.3.5. Two coexisting oxygen configurations in non-superconducting NdBa$_2$Cu$_3$O$_{6.5}$

T. Frello and N. H. Andersen, *Condensed Matter Physics and Chemistry Department, Risø National Laboratory, Denmark*
e-mail: thomas.frello@risoe.dk   http://www.risoe.dk/fys/Employee/thfr.htm

A new type of oxygen ordering was found by hard x-ray diffraction in non-superconducting tetragonal NdBa$_2$Cu$_3$O$_{6.5}$. The experimental results and a discussion of the influence of oxygen ordering on the superconducting properties are mentioned in Ref.[1]. It was found experimentally that the superstructure peaks are described by three ordering vectors Q_1=±(½ ½ ½), Q_2=±(¼ ¾ n/2) and Q_3=±(¼ ¼ n/2) with n integer. Unlike the orthorhombic oxygen superstructures in YBa$_2$Cu$_3$O$_{6.5}$ no reflections were found along the principal axes. The smallest unit cell describing the superstructure reflections is of the type $2\sqrt{2}a{\times}2\sqrt{2}b{\times}2c$. This unit cell is rotated 45° with respect to the basal unit cell, it contains two basal planes and has 32 available oxygen sites. Assuming an oxygen occupancy of exactly x=0.5 each plane in the superstructure unit cell will be occupied by four oxygen atoms, in total eight oxygen atoms. From symmetry considerations we can define that the first site in the first plane is always occupied. This gives 455 possible combinations in the first plane of the unit cell and 1820 in the second, in total 828100 configurations. The limited number of combinations makes is feasible to systematically calculate the scattering structure factor for all the oxygen configurations and discard any configuration not complying with the experimentally observed diffraction pattern. Discarding all combinations that give reflections on the principal axes we find that there exist no single oxygen configuration that can give different l dependencies for ordering vectors Q_1 and Q_2,Q_3, meaning that there is more than one single oxygen configuration present in the sample. We also find that no configuration can give the Q_3 reflections alone, thus, the Q_2 and Q_3 ordering vectors are locked to each other. Taking this into account we find that only two unique oxygen configurations (shown in Fig. 1) exist that in combination give the right diffraction pattern. Both configurations are unlikely to lead to any charge transfer as no chains longer than two consecutive oxygen atoms are formed. This explains the suppression of superconductivity at x=0.5 for NdBa$_2$Cu$_3$O$_x$.

a)   b)
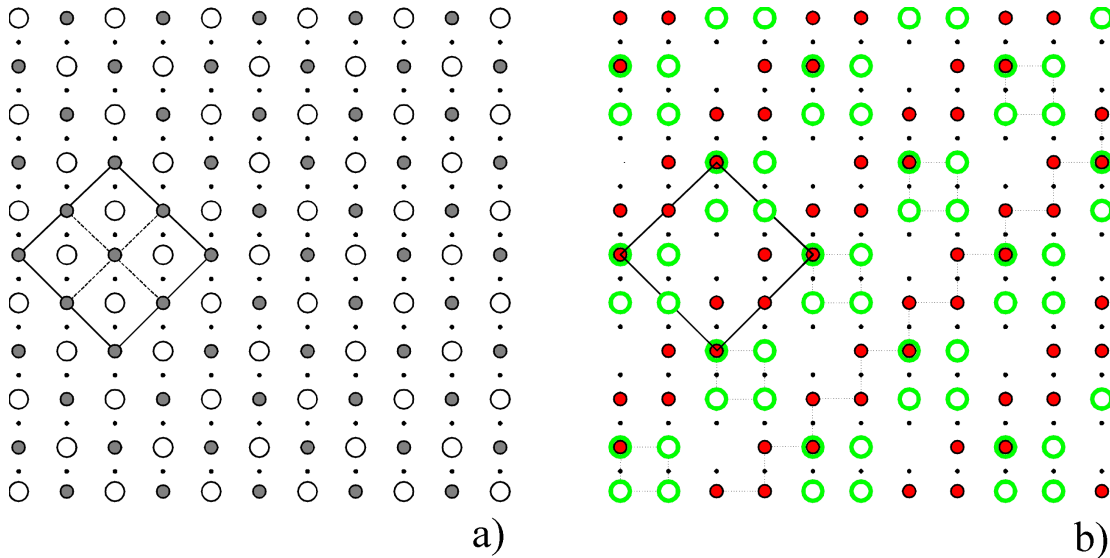
Fig. 1. The two coexisting oxygen configurations in NdBa$_2$Cu$_3$O$_{6.5}$. Small filled circles are Cu atoms, large circles are occupied oxygen sites. Open and filled circles are shifted along the c-axis by one unit cell with respect to each other. The Q_1 ordering vector arise from the configuration shown in a) and the alternate stacking of the "ragged stripes" (filled circles) and "small squares" (open circles) configurations shown in b) gives the Q_2 and Q_3 vectors, respectively. Solid lines indicate the superstructure unit cell in the ab-plane. For a) the cell can be subdivided further as indicated by the dashed lines.

[1] Risø-R-1014(EN). Editors M. Nielsen, K. Bechgaard, K.N. Clausen, R. Feidenhans'l and I. Johansen, 42 (1998).

2.3.6. Flux line lattice reorientation transition in LuNi$_2$B$_2$C with $H \parallel a$

M. R. Eskildsen[1], A. B. Abrahamsen, N. H. Andersen, K. Mortensen, *Condensed Matter Physics and Chemistry Department, Risø National Laboratory, Denmark*, D. Lopez, P. L. Gammel, D. J. Bishop, *Bell Laboratories, Lucent Technologies, New Jersey, USA* and P. C. Canfield, *Ames Laboratory and Iowa State University, Ames, Iowa, USA*
e-mail: morten.eskildsen@physics.unige.ch   http://www.risoe.dk/fys/Employee/moes.htm

Using small angle neutron scattering we have studied the magnetic flux line lattice (FLL) in LuNi$_2$B$_2$C induced by an applied magnetic field along the crystalline *a*-axis. For this field direction we observe a first order reorientation transition of the flux line lattice at 3 kOe. At fields below the transition the flux line lattice is aligned with the nearest neighbour direction parallel to the crystalline *b*-axis, and above the transition it is parallel to the *c*-axis. For both orientations the flux line lattice is found to be hexagonal, slightly distorted by the *ac*-anisotropy in LuNi$_2$B$_2$C. The reorientation transition is found to be largely independent of temperature. These results are in disagreement with the currently accepted model for the FLL symmetry and orientation.
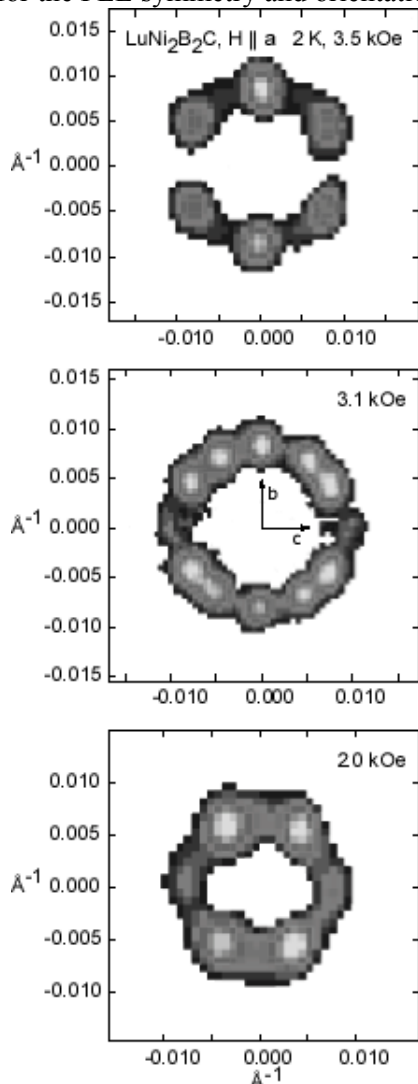
Fig. 1. False color images of the FLL diffraction patterns in LuNi$_2$B$_2$C at 2 K and 3 different fields.

In Fig. 1. we show FLL diffraction patterns obtained at 2 K for three values of applied field going from 2 to 3.5 kOe. The data are obtained by a summation of a full rocking curve, rotating the sample around the vertical axis. This figure shows the FLL undergoing a transition between two discrete orientations. In both cases the FLL is hexagonal only slightly distorted by the effective mass anisotropy in the plane perpendicular to the field. The orientation of the FLL with respect to the crystalline axes is shown in the middle panel, where one must remember that the FLL in real and reciprocal space is related by a simple 90° rotation. Hence, at low fields the FLL is oriented with the nearest neighbour direction parallel to the crystalline *b*-axis, and at high fields with the nearest neighbour direction parallel to the *c*-direction. The diffraction pattern at 3.1 kOe shows clearly resolved domains of the two FLL orientations coexisting, proving that the reorientation does not proceed continuously but is in fact a first order transition. Taking the exact transition field to be where the ratio between the reflectivity of the two domain orientations is equal to one, we find $H_{trans.} = 2.95$ kOe at 2 K.

Measurements at higher temperatures, although less detailed, revealed that the reorientation was nearly independent of *T*, with a possible small upwards shift before reaching H_{c2}.

Using non-local corrections to the London model and incorporating the symmetry of the screening current plane obtained from band structure calculations, V. G. Kogan *et al*. were able to describe the smooth FLL square to hexagonal symmetry transition found in the borocarbides for $H \parallel c$[1]. In the present geometry with $H \parallel a$, the model predicts a qualitative similar behaviour, with a slight shift in the transition field and a distortion of the FLL due to the effective mass anisotropy in the *ac*-plane. It is therefore clear that the results reported above are not contained in the Kogan mode, and at present it is not possible to argue what mechanisms drives this new FLL reorientation transition.

---

[1] Present address: Département de Physique de la Matière Condensée, Université de Genève, 24 Quai E.-Ansermet, CH-1211 Genève 4, Schwitzerland

2.3.7. Magnetic structures in the superconducting state of $TmNi_2B_2C$

K. Nørgaard, M. R. Eskildsen, N. H. Andersen, K. Lefmann, *Condensed Matter Physics and Chemistry Department, Risø National Laboratory, Denmark*, S. N. Klausen, J. Jensen, P. Hedegård, *Ørsted Laboratory, Niels Bohr Institute fAPG, Denmark* and P. C. Canfield, *Ames National Laboratory and Iowa State University, USA*

e-mail: katrine.noergaard@riso.dk   http://www.risoe.dk/fys/Employee/moes.htm

$TmNi_2B_2C$ is a superconductor, with T_c = 11 K, and Tm^{3+} is magnetically ordered, with a long wavelength antiferromagnetic spin density wave, Q_F = (0.094,0.094,0) below T_N = 1.5 K. This long wavelength structure is unique among the borocarbides, and one question that immediately arises and which we believe is important for the understanding of the interaction between magnetism and superconductivity, is why it is found only in $TmNi_2B_2C$. Our assumption was that it was induced by the superconducting state which, compared to the magnetic state (T_c/T_N ~7), is particularly strong in $TmNi_2B_2C$. The idea of the experiment was to study the magnetic order of $TmNi_2B_2C$ when superconductivity is suppressed, which is possible because the magnetic system is Ising like with alignment along the *c*-axis. The critical in-plane field of the magnetic system is 3.3 T, while the superconducting critical field is only 2 T. Hence, we are able to suppress superconductivity while the Ising-like magnetic system remains ordered when applying an in-plane magnetic field.

At a magnetic field of approx. 1 T in the *a*-direction, a new antiferromagnetic structure emerges with a scattering vector of Q_A = (0.48,0,0), see the insert in figure 1. In figure 1 is shown the intensity of the Q_A peak versus temperature at different fields. At low temperatures the intensity is saturated, between 0.5-2 K it decreases linearly, but at app. 2 K is rounds of, and has a low intensity tail at temperatures as high as 6 K. The origin of this low intensity tail is unknown. Figure 2 summarises the experimental data, and shows a phase diagram calculated theoretically. The calculations show that two effects are important: A suppression of the ferromagnetic component of the RKKY interaction due to the superconducting phase, and a reduction of the superconducting condensation energy due to the periodic modulation at the wave vector Q_A: the superzone effect.
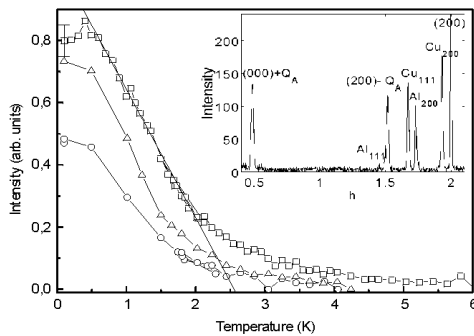
Fig. 1. Normalised integrated intensities versus temperature of the field-induced magnetic peaks at 1.2 T ($\circ$), 1.4 T ($\triangle$) and 1.8 T ($\square$). The linear fit to the 1.8 T data shows the determination of $T_N(B)$. Inset: Scan along the [*h*00] direction at 100 mK and 1.8 T, showing the field-induced satellite peaks at Q_A = (0.48,0,0) around the (000) and (200) nuclear reflections. The peak intensity of the (200) reflection is 800.

[1] V. G. Kogan, M. Bullock, B. Harmon, P. Miranović, Lj. Dobrosavljević-Grujić, P. L. Gammel and D. J. Bishop, Phys. Rev. **B55**, R8693 (1997).
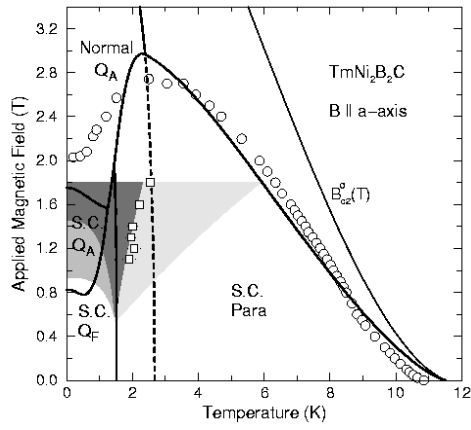
Fig. 2. Experimental and theoretical phase diagram of TmNi$_2$B$_2$C in a magnetic field along [100]. The medium-grey area denotes the region where both the Q_A and the Q_F reflections are present. In the dark-grey area only the Q_A reflections were observed, up to the maximum field of 1.8 T. The light-grey area denotes the region where the long tail of low intensity scattering at Q_A is observed. The squares denote the extrapolated phase boundary between the Q_A phase and the paramagnetic one, $T_N(B)$. The circles denote the upper critical field determined by transport measurements[1]. The solid lines are the theoretical phase boundaries. The dashed line is the calculated Néel temperature of the Q_A phase had the metal stayed in the normal state. The thin line labelled $B^0_{c2}(T)$ is the estimated upper critical field if the magnetic subsystem is neglected.

---

[1] D. G. Naugle, K. D. D. Rathnayaka, K. Clark and P. C. Canfield, Int. J. Mod. Phys. B. Submitted for publication.

2.3.8. Characterisation of BiSCCO/Ag superconducting tapes

L. G. Andersen, J.-C. Grivel, H. F. Poulsen, *Materials Research Department, Risø National Laboratory, Denmark,* A. B. Abrahamsen, B. H. Larsen, B. A. Jacobsen, N. H. Andersen, *Condensed Matter Physics and Chemistry Department, Risø National Laboratory, Denmark,* T. Tschentscher and L. Wcislak, *HASYLAB at DESY, Hamburg, Germany*

e-mail: niels.hessel@risoe.dk   http://www.risoe.dk/fys/Employee/nihe.htm

In collaboration with Nordic Superconducting Technologies and the Technical University in Denmark, Risø is pursuing the development of multifilament superconducting tapes. These contain a precursor powder within an Ag sheet, which by annealing is converted to $(Bi,Pb)_2Sr_2Ca_2Cu_3O_x$ (2223). During the last 4 years we have investigated ~500 tapes with 80-100 keV x-rays at the BW5 beamline at HASYLAB. Uniquely, the hard x-rays penetrate the Silver, allowing *in-situ* structural characterisation during annealing (1-3 days). Using a CCD the variations in texture, phase composition and stoichiometry is monitored with a time resolution of 1-5 minutes[1]. In 1999 focus was on the phase and texture development in 8% oxygen, the generation of the 3321 phase during cooling, the role of filament geometry and the use of additives such as CaF_2 for increasing the flux pinning properties.

A summary of the project includes 1) Models for the texturing taking place (grain growth caused by the instability of Pb-rich 2212 and governed by filament geometry)[2,3], for the phase conversion to 2223 (fast and non-simultaneous nucleation and growth)[2], and for the decomposition processes taking place during cooling (two-step model)[4]. 2) In-situ studies of the equilibrium phase diagram in air[2,3] and at 8% oxygen partial pressure, with direct observation of the concentration of the partial liquid. High-temperature cycling providing information on eutectics[3]. 3) For use in optimisation: the speed of conversion as function of partial pressure[1,2], tape geometry (number of filaments, their density and thickness), additives (Ag, CaF_2 fluxes) and composition of pre-cursor powder. Correlation of time-evolution with micro-structure (SEM) and electro-magnetic properties[5].

Ultimo 1999, the structural variables directly connected with the synchrotron work are well optimised. The mis-alignment of the *c*-axis of the 2223 grains from the tape normal is 14°, and the phase purity – as measured with x-rays – is 98%. Other variables, such as the powder quality and the flux pinning have become bottlenecks for the superconducting critical current. The manufacturing process have reached the stage where a full-scale field test of a 30 m cable for power transport, supplying the inner part of Copenhagen, is planned for year 2000.

---

[1] H .F. Poulsen, T. Frello, N. H. Andersen and M. von Zimmermann, Physica C **298**, 265 (1998).

[2] T. Frello, H. F. Poulsen, L. G. Andersen, N. H. Andersen, M D. Bentzon, and J. Schmidberger, Supercon. Sci. Technol. **12**, 293 (1999).

[3] H. F. Poulsen, L. G. Andersen, T. Frello, S. Prantontep, N. H. Andersen, S. Garbe, J. Madsen, A. Abrahamsen, M. D. Bentzon and M. von Zimmermann, Physica C **315**, 254 (1999).

[4] L. G. Andersen, H. F. Poulsen, T. Frello, N. H. Andersen and M. von Zimmermann, Proc. of Appl. Supercond. Conf. September 1998, Palm Desert , California.

[5] Y. L. Liu, W . G. Wang, H . F. Poulsen and P.Vase, supercond. Sci. Technol. **12**, 376 (1999).

2.3.9. In-situ study of individual grains in superconducting BSCCO/Ag tapes using the 3D XRD microscope

L. Gottschalck Andersen, H. F. Poulsen, *Materials Research Department, Risø National Laboratory, Denmark*, N. H. Andersen, *Condensed Matter Physics and Chemistry Department, Risø National Laboratory, Denmark* and U. Lienert, *ESRF, Grenoble, France*
e-mail: niels.hessel@risoe.dk   http://www.risoe.dk/fys/Employee/nihe.htm

The properties of Ag-clad BSCCO High-T_c superconducting tapes have been studied in detail using hard x-ray powder diffraction at HASYLAB (cf. contribution in this annual report). As a result the **average** stoichiometry and orientation of the grains belonging to the major phases are known as function of process parameters. However, with powder data one cannot directly test models of the texture and transformation mechanisms, due to the fact that transformation rates etc. vary with grain size, grain stoichiometry and grain orientation. With the 3DXRD microscope at ESRF we aimed at following the kinetics of the **individual** embedded grains inside the Ag-clad during heating and 12 hours of annealing at 838 $^{\circ}$C.

An 80 keV beam was focused to a 5 μm horizontal line, and limited horizontally to 40 μm by a slit. The diffracted beam from a single filament green tape was monitored by a CCD camera while oscillating the tape by 0.5°. Reflections from individual grains of the main phases: 2212 ($Bi_{2-x}Pb_xSr_2CaCu_2O_y$) and 2223 ($Bi_{2-x}Pb_xSr_2Ca_2Cu_3O_y$) are clearly visible as dots on the detector, as shown in Fig. 1. The grain volume is proportional to the integrated intensity of the dots and the grain stoichiometry related to the 2θ angle. Due to identical a/b- axes the transformation of 2212 to 2223 will give rise to spots appearing with identical azimuthal angle in the images, if and only if the grain orientation is conserved. In this way essential information on the transformation mechanism should be available ("intercalation" versus "growth on top" versus "random nucleation"). At the beginning of the annealing the diffraction pattern consisted of segmented Debye-Scherrer powder rings. At 825 $^{\circ}$C the diffraction spots from grains appeared. Validation tests were made continuously to test whether the fully integrated intensity was monitored. Due to an unfortunate setting most grains "rotated out" of the volume as function of time. The kinetics of a few constantly valid diffraction spots is being analysed.

The prospect arising from this experiment leads beyond high-T_c superconductivity. With the 3DXRD microscope it will in general be feasible to perform statistics on the volumes, strains, stoichiometry and orientation of the embedded grains in a powder, provided the grain volumes are ~1 μm^3.
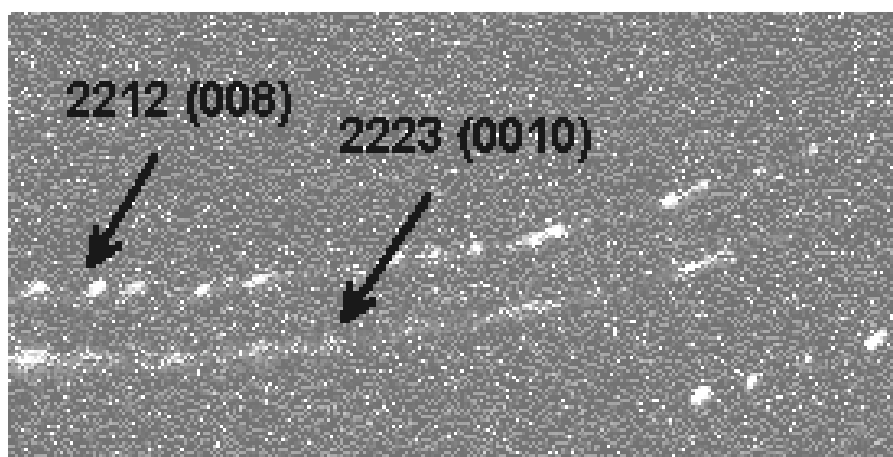
Fig. 1. Detail of image acquired after 8 hours of annealing at 838 $^{\circ}$C in air. Dots appearing on the (0 0 8) and (0 0 10) Debye Scherrer rings associated with the 2212 and 2223 phases, reflect the transformation from 2212 to 2223.

2.3.10. Magneto-optical investigations of multifilamentary Bi-2223 tapes

M. R. Koblischka[1], B. H. Larsen, N. H. Andersen, *Condensed Matter Physics and Chemistry Department, Risø National Laboratory, Denmark,* T. H. Johansen, *Department of Physics, University of Oslo, Norway,* H. Wu, P. Skov-Hansen, M. Bentzon and P. Vase, *Nordic Superconductor Technologies (NST) A/S, Brøndby, Denmark*
e-mail: britt.h.larsen@risoe.dk   http://www.risoe.dk/fys/Employee/brla.htm

For the development of long Bi-2223 tapes, it is essential to study the defects caused in production. To measure the quality of kilometre-length tapes, NST operates a so-called "tape-recorder" which measures the maximum remanent field with a resolution of about 1 cm and a speed of 150 m/h. To further elucidate the obstacles in the current flow found by the tape recorder, we employ magneto-optic (MO) imaging, which provides a spatial resolution of about 1 μm.

In Fig. 1, we present MO images at 15 K and a field of 50 mT, taken on tapes with 14 (a), 19 (b), and 37 filaments (c). The dark stripes in the images correspond to the filament centers; the bright regions are due to the field distribution around and inside the filaments. Filament bridging and twisting may lead to a "widening" of the observed stripes. The images clearly reveal that under DC conditions and low temperatures the filaments are not coupled together. This may change with temperature as discussed recently. In all tapes, the number of filaments in the top layer of the tapes can be resolved; this is 5 (a), 6 (b), and 9 (c). The tapes with 19 and 37 filaments also show that the improved deformation technique leads to homogeneous filaments; the tape with 14 filaments stems from an early production stage. Note the extremely bright stripes in (c), which are due to a well-defined filament stacking and good shielding. Further, we also analyze for the first time flux patterns of cross-sections of tapes; enabling the study of filament quality as function of position, and to obtain information about the filament coupling in an intact tape. Fig. 2 presents flux patterns of a cross-section of a tape with 37 filaments. In this case the field is oriented parallel to the filaments. In this view, we see several dark areas along the Ag sheath; these dark areas are shielding filaments. Note that only a minor number of filaments contribute to the shielding of the sample.
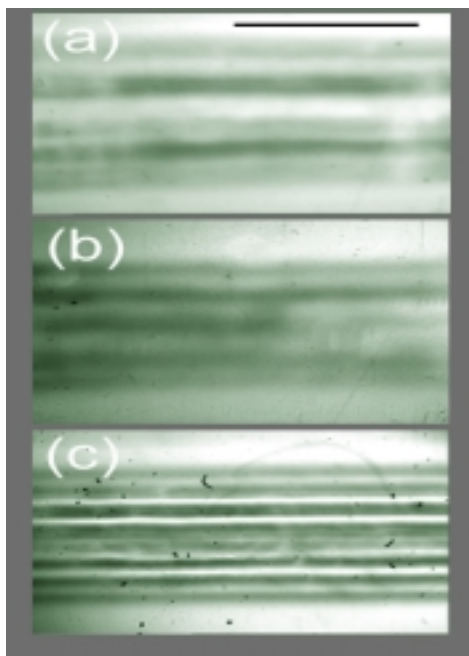
Fig. 1. Flux patterns of Bi-2223 tapes with 14 (a), 19 (b), and 37 filaments (c) at 15 K and 80 mT. Marker = 1 mm.
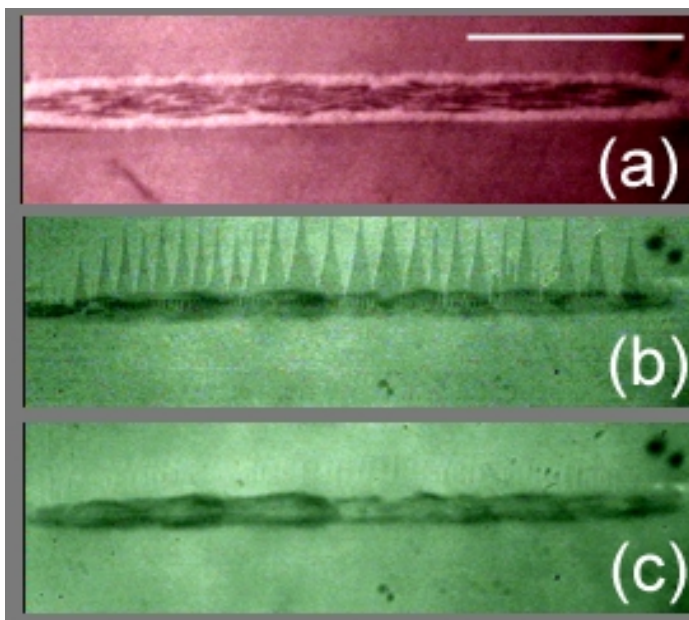
Fig. 2. Flux patterns of a cross-section of a 37 filament Bi-2223 tape, T = 7 K and field applied parallel to the filaments. (a) – polarization image, 20 mT (b), and 50 mT (c). Marker = 1 mm.

---

[1] Also at Nordic Superconductor Technologies (NST) A/S, Brøndby, Denmark.

2.4. Structure and defects

2.4.1. Evaluation of the solid state dipole moment and pyroelectric coefficient of phosphangulene by multipolar modelling of x-ray structure factors

G. K. H. Madsen, F. K. Larsen, *Department of Chemistry, University of Aarhus, Denmark,* F. C. Krebs and B. Lebech, *Condensed Matter Physics and Chemistry Department, Risø National Laboratory, Denmark*
e-mail: frederik.krebs@risoe.dk   http://www.risoe.dk/fys/Employee/frkr.htm

The electron density distribution of the molecular pyroelectric material phosphangulene has been studied by multipolar modelling of X-ray diffraction data. The "in-crystal" molecular dipole moment has been evaluated to 4.7 D corresponding to a 40% dipole moment enhancement compared to the dipole moment measured in chloroform solution. It is substantiated that the estimated standard deviation of the dipole moment is about 0.8 D.The s.u. of the derived dipole moment has been derived by splitting the dataset into three independent datasets. A novel method for obtaining pyroelectric coefficients has been introduced by combining the derived dipole moment with temperature dependent measurements of the unit cell volume. The derived pyroelectric coefficient of 3.8(7) $\mu C \ m^{-2} \ K^{-1}$ is in very good agreement with the measured pyroelectric coefficient of 3(1) $\mu C \ m^{-2} \ K^{-1}$. This method for obtaining the pyroelectric coefficient uses information from the X-ray diffraction experiment alone and can be applied too much smaller crystals than traditional methods:
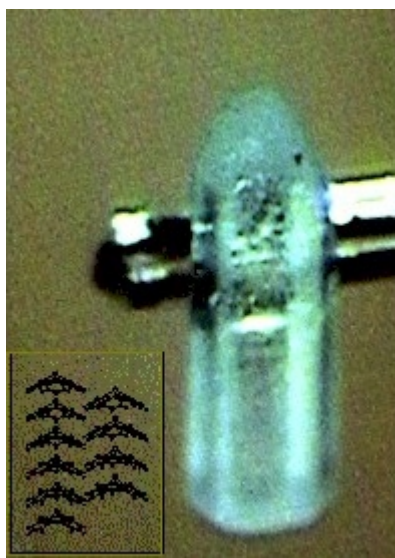
Fig. 1. A picture of a typical phosphangulene crystal along with an illustration of the orientation of the molecules with respect to the crystal morphology.

2.4.2. The structure of Zn₂F(PO₄) − A neutron powder diffraction study

K.-I. Taasti, A. N. Christensen, *Department of Inorganic Chemistry, University of Aarhus, Denmark* and B. Lebech, *Condensed Matter and Chemistry Department, Risø National Laboratory, Denmark*
e-mail: bente.lebech@risoe.dk   http://www.risoe.dk/fys/Employee/bele.htm

Microporous compounds with open framework structures as zeolites and aluminophosphates are often made in hydrothermal or organothermal synthesis and are in many cases only obtained as powders. Investigations have shown that Al^{3+} in the ALPO₄−framework can be substituted by Me^{2+}−ions and this has an improving effect on the catalytic properties of the microporous compounds. Recent investigations on the synthesis of Zn^{2+}− and Co^{2+}−substituted aluminophosphates were reported using hydrofluoric acid as a mineraliser[1]. With the use of this mineraliser it is possible to synthesise large crystals of microporous compounds[2]. Hydrofluoric acid was used as mineraliser in the synthesis of Zn^{2+}−substituted ZnAPO−35. Zincphosphates have structural similarities with aluminophosphates, and it was tested if a zinc analogue to APO−35 could be made. This turned out not to be the case, but the compound $Zn_2F(PO_4)$ was formed.

The structure of $Zn_2F(PO_4)$ was solved from synchrotron X-ray single crystal data[3]. It turned out that the fluoron atoms showed some disorder that could be due to a partial substitution of F^--ions with OH^--ions. To solve this problem $Zn_2F(PO_4)$ was prepared using D_2O as the solvent and a neutron diffraction powder pattern was measured at TAS3/POW using incident neutrons of wavelength 1.540 Å. A profile refinement[4] indicated no substitution of F^-−ions with OD^-−ions. Figure 1 displays the observed and calculated diffraction patterns for $Zn_2F(PO_4)$ and their difference.
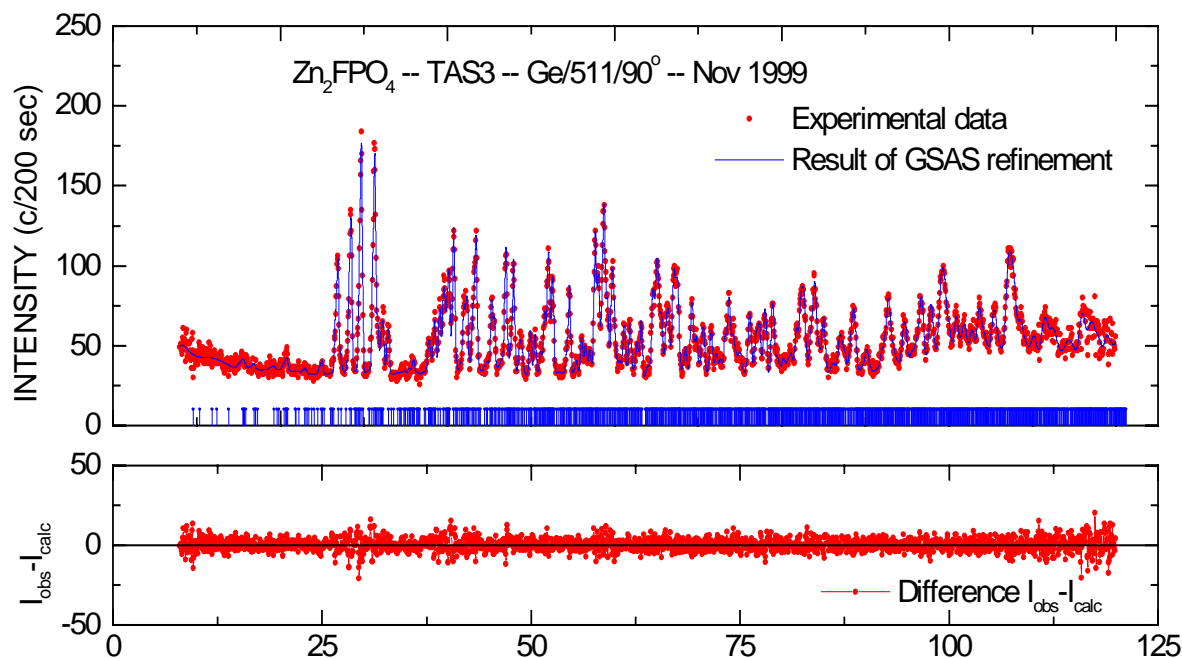
Fig. 1. Observed and calculated neutron powder diffraction patterns of $Zn_2F(PO_4)$. The vertical bars indicate the two-theta positions of the expected reflections.

---

[1] A. N. Christensen and R. G. Hazell, Acta. Chem. Scand. **53**, 403 (1999).
[2] A. Kupermann, S. Nadimi, S. Oliver, G. A. Ozin, J. M. Garcés and M. M. Olken, Nature (London) **365**, 239 (1993).
[3] K.-I. Taasti, A. N. Christensen, P. Norby, J. C. Hanzon and B. Lebech, Dalton Transactions. In preparation.
[4] A. C. Larson and R. B. von Dreele, GSAS, General Structure Analysis System, LANSCE, MS-H805, Los Alamos National Laboratory, NM 87545 (1994).

2.4.3. Zinc substitution in ZnAPO−35 − A neutron powder diffraction study

K.-I. Taasti, A. N. Christensen, *Department of Inorganic Chemistry, University of Aarhus, Denmark*, and B. Lebech, *Condensed Matter and Chemistry Department, Risø National Laboratory, Denmark*
e-mail: bente.lebech@risoe.dk   http://www.risoe.dk/fys/Employee/bele.htm

Microporous aluminophosphates with open framework structures are made in hydrothermal synthesis with organic templates as structure directing compounds. The size of the organic molecule determines the pore size in the aluminophosphates. The Al^{3+}−ions in the $AlPO_4$ framework can be substituted by Me^{2+}−ions and this has an improving effect on the catalytic properties of the microporous compounds. The template 1,4−diazabicyclo[2.2.2] octane, $N_2C_6H_{12}$ (DABCO), was used to make the Zn^{2+}−substituted aluminophosphate ZnAPO−35.

The template molecules in the microporous compounds can be removed by calcination. Thermogravimetric analysis of ZnAPO−35 showed a loss in weight of 2% at 525°C, which was assumed to reflect loss of water and template molecule. After this treatment an X−ray powder diffraction pattern showed that the sample still had the ZnAPO−35 structure. In order to determine the degree of Zn^{2+}−substitution a sample of ZnAPO−35 was calcinated at 525°C for 20 hours to reduce the hydrogen content in the sample. After this treatment, a neutron diffraction powder pattern was measured at 25°C at TAS3/POW using incident neutrons of wavelength 1.540 Å.

X-ray powder diffraction investigations showed that ZnAPO−35 in the calcinated form had decomposed to a mixture of two phases of $Zn_3(PO_4)_2$[1,2] and $AlPO_4$[3]. A preliminary analysis of the data[4] gave a Zn^{2+}/Al^{3+} ratio of 14/86 for the prepared sample.

[1] C. Calvo, J. Phys. Chem. Solids **24,** 141 (1963).

[2] Natl. Bur. Stand. (US), Monogr. **25,** 16, 80 (1979).

[3] A. F. Wright, A. J. Leadbetter, Phil. Mag. **31**, 1391 (1975).

[4] A. C. Larson and R. B. von Dreele, GSAS, General Structure Analysis System, LANSCE, MS-H805, Los Alamos National Laboratory, NM 87545 (1994).

2.4.4. Strontium oxalate hydrate − A neutron powder diffraction study

R. B. Nielsen, A. N. Christensen, *Department of Inorganic Chemistry, University of Aarhus, Denmark*, and B. Lebech, *Condensed Matter and Chemistry Department, Risø National Laboratory, Denmark*
e-mail: bente.lebech@risoe.dk   http://www.risoe.dk/fys/Employee/bele.htm

Strontium oxalate can be made as a monohydrate, $SrC_2O_4 \cdot H_2O$, and as a dihydrate, $SrC_2O_4 \cdot 2H_2O$. In addition, it is also known as an anhydrous compound, SrC_2O_4. The dihydrate may contain additional water so that the formula should be $SrC_2O_4 \cdot (2+x)H_2O$. Thermogravimetric investigation of the dehydration of strontium oxalate hydrates indicates that dehydration is complete at $300°C$ and that decomposition to strontium carbonate takes place at $485°C$[1]. An *in-situ* investigation by neutron powder diffraction of the dehydration of strontium oxalate hydrates has been made in the temperature range $50-350°C$[2]. In order to get an accurate determination of the water content of the sample, a neutron diffraction powder pattern of $SrC_2O_4 \cdot xD_2O$ at $25°C$ was measured at TAS3/POW using incident neutrons of wavelength 1.540 Å. The profile refinement of this data[3] indicated that the sample was a mixture of $SrC_2O_4 \cdot D_2O$ and $SrC_2O_4 \cdot 2D_2O$ and contained ~10% of $SrC_2O_4 \cdot D_2O$. Figure 1 displays the observed and calculated diffraction patterns and their difference.
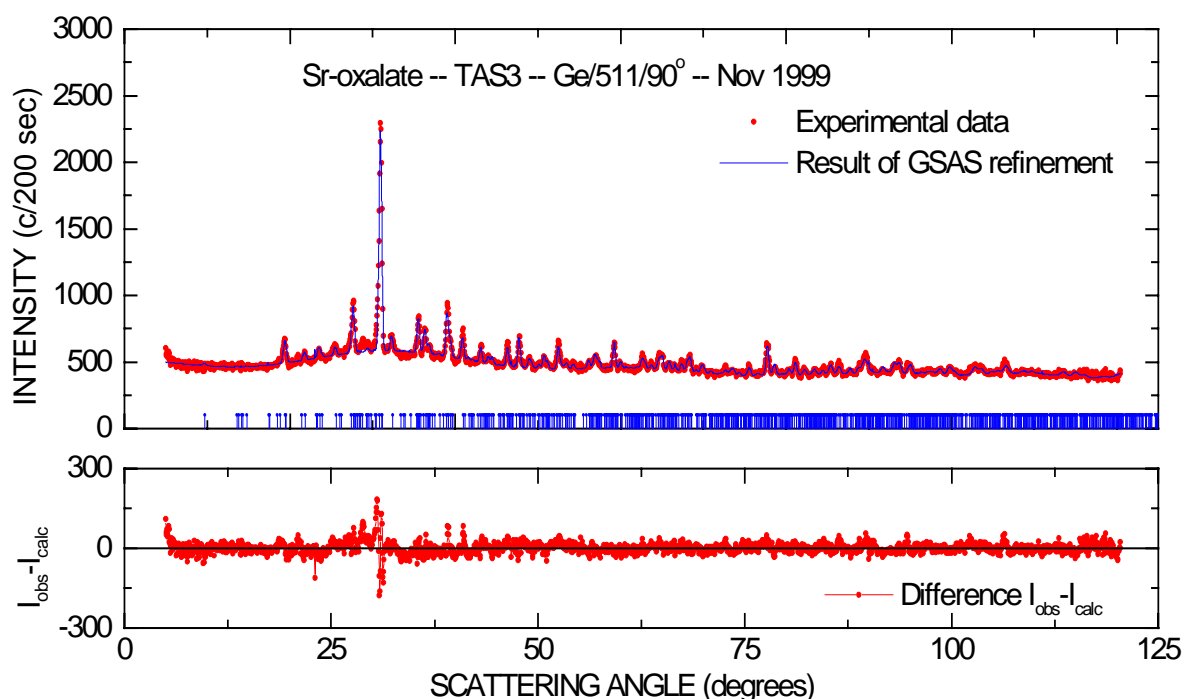
Fig. 1. Observed and calculated neutron powder diffraction patterns of $SrC_2O_4 \cdot 2D_2O$ with an ~10% impurity of $SrC_2O_4 \cdot D_2O$. The vertical bars indicate the two-theta positions of the expected reflections.

---

[1] A. N. Christensen and R. G. Hazell. Acta Chem. Scand. **52**, 508 (1998).
[2] R. B. Nielsen, P. Norby and A. N. Christensen. Experimental Report HMI (1999).
[3] A. C. Larson and R. B. von Dreele, GSAS, General Structure Analysis System, LANSCE, MS-H805, Los Alamos National Laboratory, NM 87545 (1994).

2.4.5. The structural role of iron in tetrahedrite $Cu_{12-x}Fe_xSb_4S_{13}$ and tennatite $Cu_{12-x}Fe_xAs_4S_{13}$ by means of neutron diffraction

E. Makovicky, J. Wenzel Andreasen, *Geological Institute, University of Copenhagen, Denmark* and B. Lebech, *Condensed Matter and Chemistry Department, Risø National Laboratory, Denmark*
 e-mail: bente.lebech@risoe.dk   http://www.risoe.dk/fys/Employee/bele.htm

Iron can replace copper in tetrahedrite $Cu_{12-x}Fe_xSb_4S_{13}$ and tennatite $Cu_{12-x}Fe_xAs_4S_{13}$ up to two atoms per formula unit in the I-43m cubic structure. Between $x = 0$ to 1, iron enters as Fe^{3+}, at larger x as Fe^{2+}. When the substitution proceeds from $x = 1$ to $x = 2$ there is a progressive change of all Fe-atoms in both compounds into Fe^{2+}. The structural role of this iron has been interpreted variously in the literature and either assigned to the tetrahedral or to the trigonal-planar co-ordination sites initially occupied by copper atoms in the ratio 1:1. This problem is difficult to resolve from x-ray diffraction data. However, it may be feasible from neutron diffraction data because of the difference in the neutron scattering amplitudes of Cu and Fe. Therefore, we have prepared tetrahedrite and tennatite powder charges with $x = 0.5$, 1.0, 1.5 and 2.0 by means of dry synthesis from the pure elements at 450°C and initiated a neutron scattering study. The neutron diffraction data were collected at ambient temperature in the angular range of 5° to 120° in steps of 0.05288° using the neutron powder multi-detector diffractometer (TAS3/POW). The incident wavelengths (~1.55 Å and ~2.44 Å) were obtained using the (511) and (311) reflections at a scattering angle of 90° from a germanium composite wafer monochromator. Profile refinements using GSAS[1] or FullProf.98[2] turned out to be difficult because the samples are not pure single phase as intended. So far a multiphase model can explain all peaks observed in the Cu10.5Fe1.5As4S13 sample and most peaks in the $Cu_{11}Fe_1As_4S_{13}$ sample (Fig. 1, logarithmic intensity scale). We assumed a model structure, which contained two phases of the same form of tennatite (**T1** and **T2** with different lattice parameters), and one phase of chalcopyrite ($CuFeS_2$, **C**). Inclusions of other impurity phases like Cu, Fe and bornite have so far failed. The same is true for inclusions enargite and famatinite impurity phases in the structure models for the tennatite and tetrahedrite samples, respectively. The refinements were made using the nominal stoichiometry, fixing the Fe-atoms at the 12d Cu atom sites and assuming half occupancy of the remaining Cu atoms at the 24g sites. The two phases of tennatite have lattice parameters that differ by about 2%.
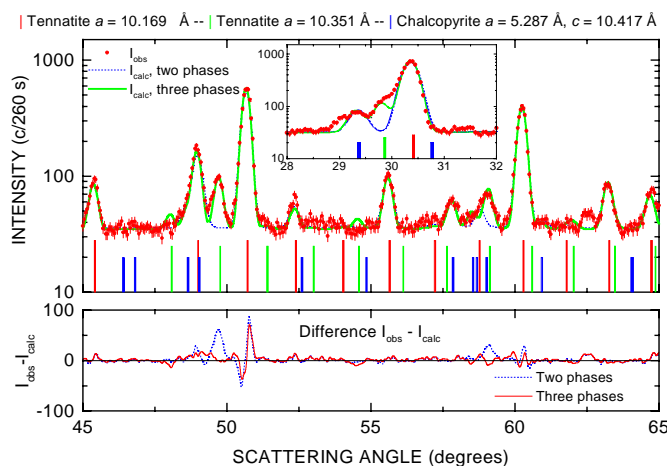
Fig. 1. Illustrative sections of the neutron diffraction pattern of the $Cu_{11}Fe_1As_4S_{13}$ sample with the results of the FullProf.98 analysis including one tennatite and one chalcopyrite phases (dashed) and two tennatite and one chalcopyrite phases (full). The vertical bars indicate peak positions for the **T1**, **T2** and **C** phases (long, medium and short bars, respectively). The incident wavelength is 1.54 Å. The overall B has been fixed to 1 for all atoms.

With the present model the ratios (**T1**:**T2**:**C**) between the scale factors of three phases are about 1:24:0.05 and 1:24:0.1 for $Cu_{10.5}Fe_{1.5}As_4S_{13}$ and $Cu_{11}Fe_1As_4S_{13}$, respectively. Inclusions of the second phase of tennatite improved the chi-squared of the FullProf.98 profile analysis from 2.6 to 1.5 for both tennatite samples. Figure 1 shows sections of the profile analysis of the $Cu_{11}Fe_1As_4S_{13}$ sample with at least one of the unexplained Bragg peak at a scattering angle of ~62.5°. In order to proceed with the attempts to discern the site occupancy of the Fe-atoms it is obvious that phase identification is essential and that the possibility for making phase pure samples needs to be explored.

---

[1] A. C. Larson and R. B. von Dreele, GSAS, General Structure Analysis System, LANSCE, MS-H805, Los Alamos National Laboratory, NM 87545 (1994).
[2] J. Rodriguez-Carvajal, http://www-llb.cea.fr/fullweb/fullprof.98/fp98.htm

2.4.6. X-ray powder diffraction on cubic Fe nanoparticles

L. Theil Kuhn[1], M. M. Nielsen, K. Lefmann and K. N. Clausen, *Condensed Matter Physics and Chemistry Department, Risø National Laboratory, Denmark*
e-mail: kim.lefmann@risoe.dk   http://www.risoe.dk/fys/Employee/kile.htm

We have studied the crystal structure of cubic Fe nanoparticles produced in the hollow cathode sputter cluster source at the Ørsted Laboratory, Niels Bohr Institute fAPG, Denmark[2]. The nanoparticles were softly deposited on a plastic substrate, transferred to the X-ray facility at Risø (Rigaku rotating anode, Cu Kα radiation, λ=1.542 Å), and powder diffraction patterns were recorded, using an analyser crystal set-up for suppressing the Fe fluorescence. The figure shows the X-ray powder diffraction pattern after subtraction of the background from the plastic substrate, and the numerically determined powder patterns for bcc Fe, spinel Fe_3O_4, and spinel γ-Fe_2O_3. The bcc Fe indexed peaks fall exactly on the largest and narrowest peaks in the pattern, whereas the positions of the spinel γ-Fe_2O_3 peaks fall on the smaller and broader peaks. There is only a minor trace of the spinel Fe_3O_4 present, and no α-Fe_2O_3 is found. The bcc Fe has the bulk lattice constant, but the γ-Fe_2O_3 has a 3% expansion in one direction as compared to the bulk structure. By use of the Debye-Scherrer equation[3] we have determined the weighted average size of the nanoparticles. For bcc Fe the peaks are best fitted by a Lorentzian, the size is approximately 25 nm. For the γ-Fe_2O_3 the peak widths give different sizes. The width of the peak with the lowest indices (220) gives the size 2.7 nm and that of the (440) peak gives the size 4.7 nm, indicative of strain in the system. The other peaks give sizes in the same range. Combined with previous transmission electron micrographs showing that the nanoparticles have the shape of a truncated cube and consist of a dark (i.e. heavy) core and a thin light shell[2], we can conclude that each nanoparticle has a pure bcc Fe core of average size (weighted) 25 nm and is surrounded by an oxide surface layer of strained γ-Fe_2O_3 nanocrystallites of maximum size 4 nm. The crystalline oxide shell is stable on the time scale of months, and therefore it protects the nanoparticle against further oxidation.

This structural information will be used in the interpretation of measurements of the magnetic properties of the nanoparticles.

---
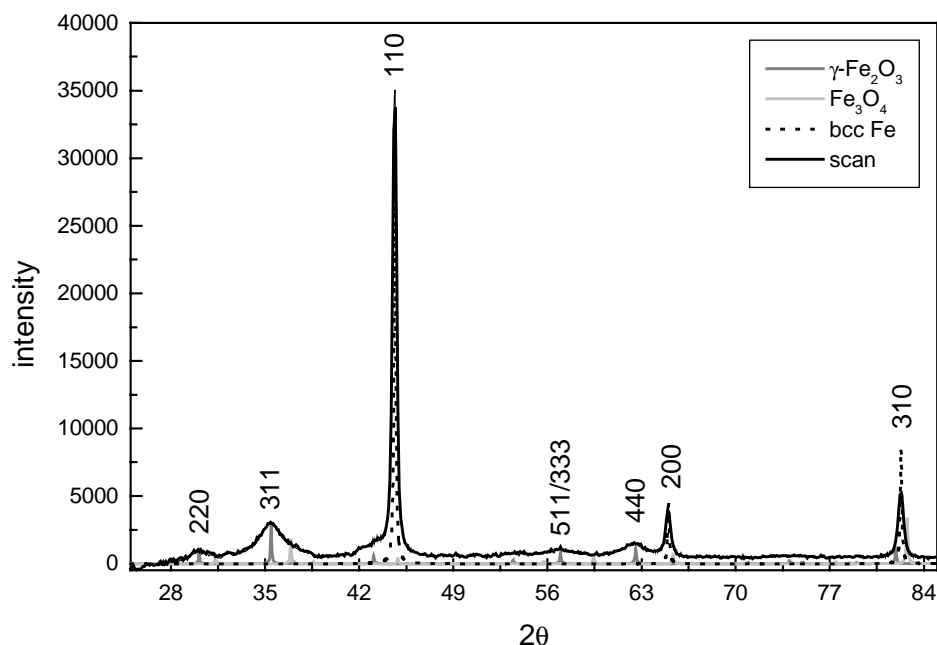
[1] Present address: Laboratory of Solid State Physics and Magnetism, Katholieke Universiteit Leuven, Belgium
[2] L. Theil Kuhn, Ph.D. thesis, University of Copenhagen (1999).
[3] B. E. Warren, X-ray diffraction, Dover Publications (1990).

2.5. Structure and interfaces

2.5.1. X-ray reflectivity measurements on plasma activated bonded wafers

M. Poulsen, R. Feidenhans'l, M. Nielsen, C. Kumpf, *Condensed Matter Physics and Chemistry Department, Risø National Laboratory, Denmark,* S. Weichel and F. Grey, *Mikroelektronik Centret, The Technical University of Denmark, Denmark.*
e-mail: robert.feidenhansl@risoe.dk   http://www.risoe.dk/fys/Employee/rofe.htm

Bonding is a process where adhesion between two clean Si wafers can be achieved by pressing them together. The bonding will normally only be the Van der Waals type and heating is necessary to get strong bonds. However if the surfaces have been pre-treated by plasma activation it is possible to achieve bonding between two Si wafers at room temperature.

The process behind the plasma bonding is an unknown process. To solve this puzzle it is necessary to characterize the interface between the bonded wafers. We have made X-ray reflectivity measurements on two differently prepared plasma-bonded samples. For both samples we use 4 inch. Si(100) wafers. At sample one we first use a standard RIE (Reactive Ion Etching) treatment, (300mTorr oxygen, 200W, 60sec) on both wafers. Then the wafers where rinsed in water for 3 min and bonded by pressing them together. For the second sample we used same plasma treatment, but the wafers were bonded without the waterdip. After bonding we waited five days for the bonding to gain proper strain, and then cut the wafers in thin strips, ~100μm , with a diamond saw. It is necessary to cut such thin strips in order to lower the absorption for the x-rays. The X-ray set-up is shown in Fig.1.

A week after bonding the first measurement where made, and then repeated 3 weeks later. We got the same result in both measurements, which indicates that the interface doesn't changes over time. The results are shown below
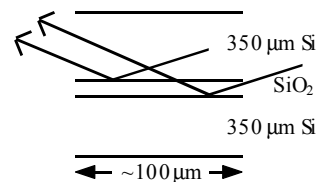
Fig. 1. X-ray set-up.
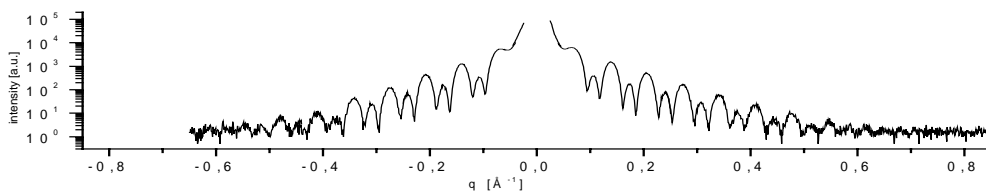
Fig. 2. Reflectivity curves for the sample with water dip
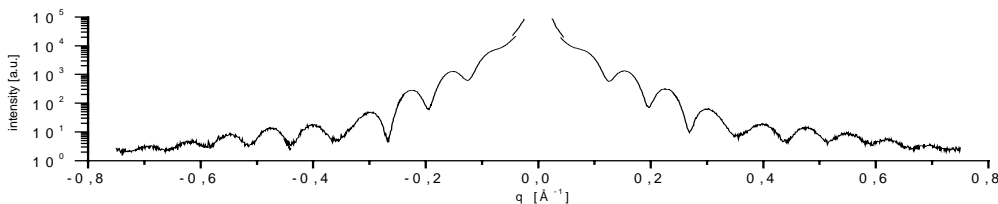
Fig. 3. Reflectivity curves for sample with no water dip.

There is a significant difference between the two-reflectivity curves, which suggest that the water remain at the interface. Due to the structure of the reflectivity data, we assume that the model that fits the data is a symmetric 5 layer model, Si /SiO$_2$/H$_2$O/SiO$_2$/Si. To obtain more information on the oxide layer, we have made reflectivity measurements on single plasma activated wafer. The model for this problem is much simpler, and by solving this problem we may get an indication of the magnitude of some the fitting parameters in the five-layer model.

2.5.2. Bonded Si wafers with small and large twist angles

M. Nielsen, R. Feidenhans'l, C. Kumpf, *Condensed Matter Physics and Chemistry Department, Risø National Laboratory, Denmark,* S. Weichel, M. Poulsen and F. Grey, *Mikroelektronik Centret, Technical University of Denmark,*

e.mail: mourits.nielsen@risoe.dk   http://www.risoe.dk/fys/Employee/moni.htm

We have extended previous measurements of interface structure of directly bonded Si(001) wafers with twist angle misorientations[1]. The twist angle θ is the relative rotation of the two lattices around their (001) surface normal. The measurements are performed at the BW2 diffractometer, HASYLAB, DESY, Hamburg and at the beamline ID32, ESRF, Grenoble, France. The interface structure of ideally bonded twist samples may be described by a square net of screw dislocations with a period $\lambda = 2a_{nn} / sin(2\theta)$ where a_{nn} is the nearest neighbour distance of the atoms in the bonding surface. The displacement field from the dislocations decays exponentially away from the interface with the 1/e length equal to $\frac{\lambda}{2\pi}$. Thus, for sufficiently small twist angles the periodic strain field extends deeply into the crystals, and eventually for a thin bonded wafer the outer surface will also be affected. We have shown that down to θ = 0.2 degree this description holds and the strain field extends several hundreds Å into the crystals, but we have not yet obtained thin enough crystals to observe the outer surface effect.

For large twist angles, we have observed x-ray reflections up to θ = 25 degree, showing that the regular displacement waves persist parallel to the interface with the same relation for the period as above, $\lambda = 2a_{nn} / sin(2\theta)$. However perpendicular to the interface the exponential decay of the displacement field becomes so steep that essentially only a pair of atomic layers are influenced. This is illustrated in the figure below showing that the thickness of the interface influenced by periodic displacements become independent of the twist angle.
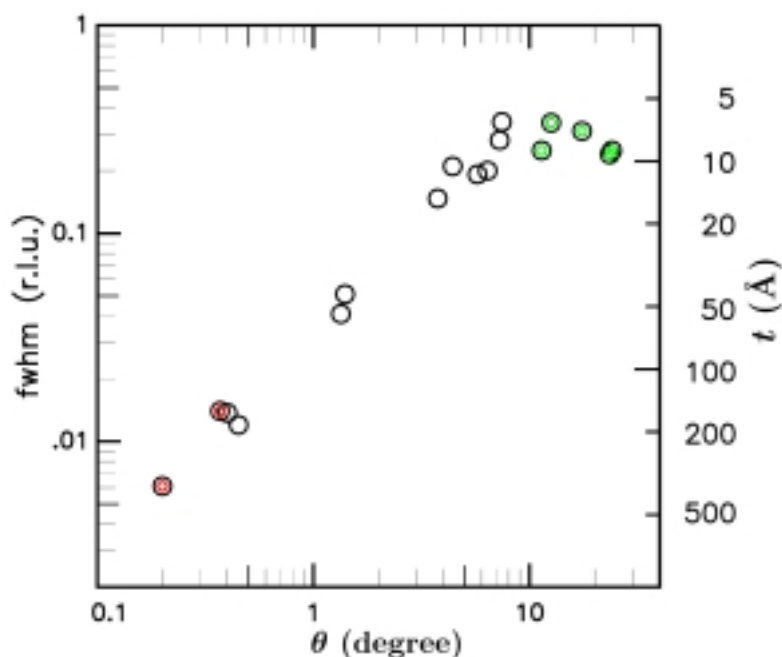
Fig. 1. The width, (fwhm), of diffraction peaks from the interface structure scanned perpendicular to the interface, as function of the twist angle θ. t(Å) is the double exponential decay length of the displacement field, deduced from the measured fwhm values.

[1] M. Nielsen, R. Feidenhans'l, P.B. Howes, J. Vedde, K. Rasmussen, M. Benamara and F. Grey, Surf.Science **442**, L898-L994 (1999).

2.5.3. The Interface of directly bonded Si wafers with a finite tilt angle

M. Nielsen, R. Feidenhans'l, C. Kumpf, *Condensed Matter Physics and Chemistry Department, Risø National Laboratory, Denmark,* S. Weichel, M. Poulsen, F. Grey, *Mikroelektronik Centret, Technical University of Denmark, Denmark* and J. Vedde, *TOPSIL Semiconductor Materials A/S, Frederikssund, Denmark*

e-mail: mourits.nielsen@risoe.dk   http://www.risoe.dk/fys/Employee/moni.htm

Silicium wafers can be directly bonded to obtain ideal covalent bonding between the atoms at the interface. Misorientation of the two crystals will introduce nets of dislocations at the interface, and the displacement field from these will extend into the two crystals. In the present study we have measured the resulting atomic structure for bonded Si wafers with varying tilt-misorientation. One of the bonded surfaces was a (001) surface, whereas the other crystal was miscut with its (001) normal vector tilted towards the (110) direction. The samples are prepared by fusion bonding of the wafers, including annealing at 1100° C[1].

X-ray measurements are performed at the BW2 diffractometer, HASYLAB, DESY, Hamburg and at the beamline ID32, ESRF, Grenoble, France and strong satellite reflections are observed around the Bragg points of either crystal with wavectors given by the periodicity of the dislocation net, as shown in the figure below.
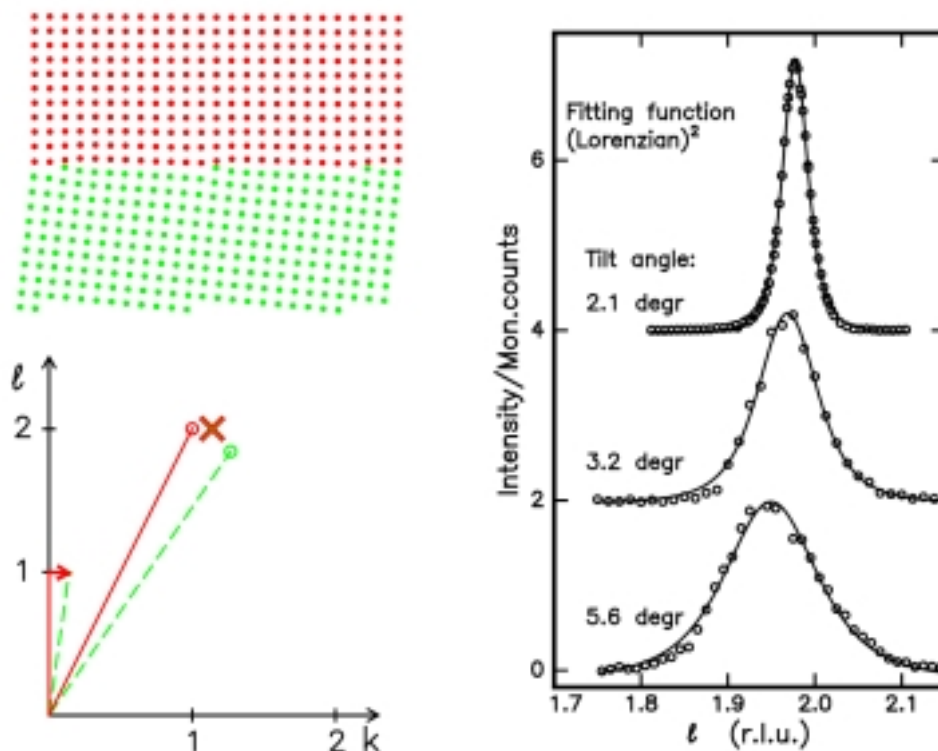
Fig. 1. The left side figures illustrate the relation between the density modulation from the row of edge dislocation and the fundamental satellite wavevector shown by the little arrow. The right hand figure shows diffraction profiles measured in scans through the satellite point given by X to the left. The data are for samples with the three tilt angles given in the figure.

---

[1] S. Weichel, F. Grey, K. Rasmussen, M. Nielsen, R. Feidenhans'l, P. B. Howes and J. Vedde. To be in published in Appl. Phys. Lett.76, January (2000).

2.5.4. Surface structures of Cu₃Au and Au₃Cu determined by surface x-ray diffraction

O. Bunk, J. H. Zeysing, Y. Su, D. A. Ehlers, R. L. Johnson, *II. Institut für Experimentalphysik, Universität Hamburg, Germany*, M. Nielsen, M. M. Nielsen, C. Kumpf, and R. Feidenhans'l *Condensed Matter Physics and Chemistry Department Risø National Laboratory, Denmark,* G.A. Eckstein, S. Maupai, A. S. Dakkouri and M. Stratmann, *Lehrstuhl für Korrosion und Oberflächentechnik (LKO), Universität Erlangen-Nürnberg, Germany*
e-mail: robert.feidenhansl@risoe.dk   http://www.risoe.dk/fys/Employee/rofe.htm

Following our investigations of the low-index Au₃Cu(111), (110) and (001) surfaces [1] in the course of studies of selected corrosion phenomena we investigated the Cu₃Au(111), (110) and (001) surface structures using surface x-ray diffraction (SXRD). The motivation for these measurements is twofold: First, it is interesting to trace back the differences in corrosion experiments to their origin in the atomic structure of the surfaces. Second, although gold and copper are isoelectronic, the change in the stoichiometry of the bulk-crystal induces significant changes of the surface structure, too. Determining the structure of the "selvedge" of the crystal is the necessary condition for an understanding of the different pathways for a minimization of the surface free energy.

A remarkable example for the structural differences is given by the (110) surfaces of these two copper-gold alloys: The Cu₃Au(110) surface undergoes a (4×1) reconstruction for which a model with double rows of gold and copper atoms has been proposed [2] . In contrast, the Au₃Cu(110) surface exhibits a (1×4) unit-cell indicating a completely different atomic structure of the surface. One reason for this difference in the surface unit-cell may be gold segregation together with differences in the lattice parameter: For geometrical reasons gold enrichment may induce more compression in the (110)-surface of (1×4) reconstruction than in the (4×1) reconstruction. Therefore for an Cu₃Au(110) crystal with a lattice parameter significantly smaller than the gold lattice parameter (3.75 Å compared to 4.08 Å a (4×1) reconstruction is much more likely than a (1×4) reconstruction. The data analysis is under way and will provide the basis for detailed theoretical investigations of these interesting systems.

In the course of this work the new technique of applying direct methods to SXRD data[3] has been evaluated. An example of electron density maps determined using L. D. Mark's fs98 code is given in the Figure. Although a fully automatic analysis of SXRD data will not be a viable option in the near future, valuable additional information can be gained using this new approach for the analysis of surface diffraction data.

Fig. 1. Possible scattering potentials derived from the SXRD in-plane data using direct methods: left, Cu₃Au(110)-(4×1) and (b) Au₃Cu(110)-(1×4). In both cases p2mm symmetry is assumed.

[1] G. A. Eckstein, S. Maupai, A. S. Dakkouri, M Stratmann, M. Nielsen, M. M. Nielsen, R. Feidenhans'l, J. H. Zeysing, O. Bunk and R. L. Johnson, Phys. Rev. **B60**, 8321, 1999.
[2] H. Over, G. Gilarowski and H. Niehus, Surf. Sci. **381**, 619 (1997).
[3] L. D. Marks, W. Sinkler and E. Landree, Acta Cryst. A **55**, 601 (1999).

2.5.5. High-index semiconductor surfaces: Structure determination of a Si(115) surface reconstruction

O. Bunk, J. H. Zeysing, D. A. Ehlers, Y. Su, R. L. Johnson, *II. Institut für Experimentalphysik, Universität Hamburg,* M. Nielsen, C. Kumpf, M. M. Nielsen, and R. Feidenhans'l, *Condensed Matter Physics and Chemistry Department, Risø National Laboratory, Denmark*
e-mail: robert.feidenhansl@risoe.dk   http://www.risoe.dk/fys/Employee/rofe.htm

In comparison to low-index surfaces the high-index semiconductor surfaces exhibit new local bonding configurations and offer new possibilities for heteroepitaxial growth and self-organization of nanostructures. The discovery of stable high-index surfaces that do not form facets and elucidating the atomic structure that stabilizes these surfaces is advancement in understanding the mechanisms that minimize the surface free energy.

One way to find stable high-index surfaces is to study the faceting of low-index surfaces. For example the adsorption of indium on the Ge(001) surface at a temperature of ~350ºC induces {103} facets[1] and the structure of both the Ge(103) surface stabilized by the adsorption of indium as well as the clean Ge(103) surface were found to form stable well ordered surface structures. Encouraged by the interesting results found for these systems we started investigations of the Si(115) surface - motivated by the partial formation of {115} facets of the Si(001) surface after gallium adsorption. It is found that both the Ga covered and the clean Si(115) surface do not facet and exhibit stable surface reconstructions. Contrary to previous results the Si(115)[2] surface was found to reconstruct with a matrixnotation unit-cell. Based on thorough scanning tunnelling microscopy (STM) investigations a structural model for this complex reconstruction has been developed (see the model in Fig. 1).

$[\bar{5}\bar{5}2]$
$\uparrow\!\!\rightarrow[\bar{1}10]$
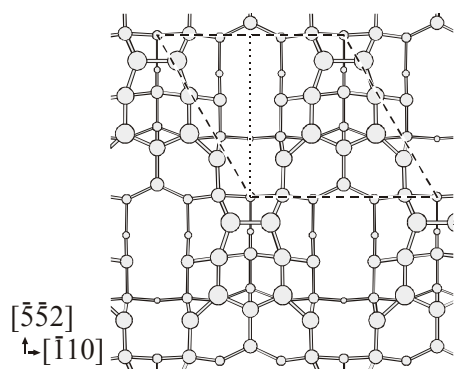
Fig. 1. Structural model for the Si(115)- surface reconstruction developed based on STM investigations. A unit-cell is indicated by a dashed line and a mirror-line is indicated by a dotted line.

It is well known that STM investigations alone are not sufficient to determine the atomic structure of the surface and surface near regions so we have performed surface x-ray diffraction (SXRD) measurements on this system. The sample was prepared in an ultra high vacuum (UHV) system equipped with reflection high-energy electron diffraction, low-energy electron diffraction and STM facilities. The sample was cleaned repeatedly by `flashing' to ~ 1150ºC for 15-20 s and slow cooling from 900ºC to room temperature in ~ 45 min. The sample was transferred in a portable UHV chamber to the wiggler beamline BW2 at HASYLAB for the x-ray diffraction measurements. The incident monochromized x-rays with an energy of 10.5 keV impinged on the sample at a grazing angle of 0.3º. In total the data set consists of 90 symmetry inequivalent reflections in-plane reflections, 35 reflections along two fractional order rods and 108 reflections along four crystal truncation rods. The model developed based on the STM investigations is used as a starting point for the SXRD data analysis and structural refinement which will be published soon.

---

[1] M. Nielsen, D.-M. Smilgies, R. Feidenhans'l, E. Landemark, G. Falkenberg, L. Lottermoser, L. Seehofer and R. L. Johnson, Surf. Sci. **352-354**, 430 (1996).
[2] A. A .Baski, S. C. Erwin and L. J. Whitman, Surf. Sci. **392**, 69 (1997).

2.5.6. Periodically arranged dislocation lines in MgO films grown on Ag(100)

J. Wollschläger, H. Goldbach, *Institut für Festkörperphysik, Universität Hannover, Germany*, R. Feidenhans'l, *Condensed Matter Physics and Chemistry Department, Risø National Laboratory, Denmark*, O. Bunk, *II Institut für Experimentalphysik, Universität Hamburg, Germany*, T. Schmidt and J. Falta, *HASYLAB at DESY, Hamburg, Germany*
e-mail: robert.feidenhansl@risoe.dk   http://www.risoe.dk/fys/Employee/rofe.htm

Oxide/metal systems are important e.g. for tunnelling barriers as in Josephson junctions, for resonant tunnelling devices in nanoelectronics and as spin valves in giant magnetic resistance devices. The growth of various metals on different oxides has been studied extensively. For instance it has been reported from Surface X-Ray Diffraction (SXRD) experiments that Ag grows in 3D islands on MgO and that dislocations with (111) glide planes are formed in the large Ag islands.

Here, we have studied the "reciprocal" system: MgO films grown on Ag(100) (lattice mismatch 2.9%). In previous studies with High-Resolution Spot Profile Analysing Low Energy Electon Diffraction (SPA-LEED) we have demonstrated that the MgO film forms mosaics at the film surface [1]. The spacing of the mosaics is quite regular as satellites approximately 3% from the fundamental LEED spots in <001> directions demonstrate. Since the mosaic tilt angle decreases with increasing film thickness we concluded that the mosaics are caused by interface dislocations with (011) glide planes. The LEED experiment, however, is not sensitive directly to the interface region where the dislocations are formed most probably. In addition, nothing is known about relaxation effects in the Ag(100) substrate which might be possible because single crystalline Ag is much softer than MgO. These problems were addressed to X-ray studies at the BW2 beam line at HASYLAB.
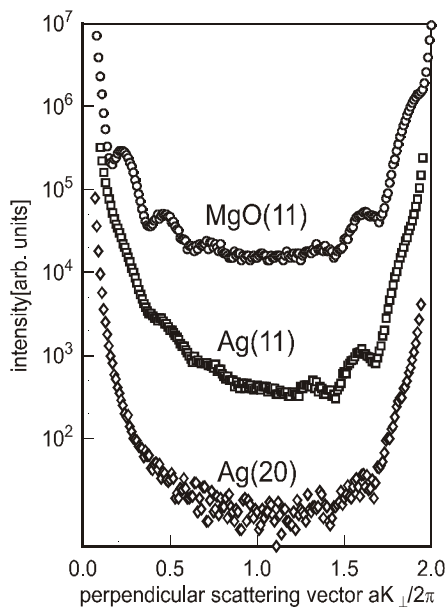
Fig. 1. Different MgO and Ag CTRs. The CTRs are scaled by different factors to distinguish them clearly. The MgO(11) CTR shows oscillations due to the finite film thickness. The oscillations of the Ag(11) CTR and the absence of the Ag(20) CTR demonstrate that periodic dislocation lines in <100> are formed at the metal/oxide interface.

In this SXRD study we investigated an 8ML MgO film grown on Ag(100) at 500K. Additional diffraction peaks were obtained beside the diffraction pattern of the Ag substrate. The MgO Crystal Truncation Rods (CTRs) spots show oscillations typical for the small film thickness. The position of the MgO rods proves that the average lattice constant of the MgO film is only 1.5% larger than the Ag lattice constant. Thus the film is only partially relaxed. Oscillations were also observed for the Ag(11)-CTR but none for the Ag(10)-CTR and the Ag(20)-CTR. The absence of oscillations for the latter two CTRs demonstrates that the dislocation network does not penetrate the Ag substrate. On the other hand the Ag(11)-CTR coincides with the first order satellite due to a regular MgO interface dislocation network. Therefore, oscillations are observed at the Ag(11)-CTR. In addition, the absence of CTR oscillations for Ag(10) and Ag(20) prove that the dislocation "network" consists of two orthogonal domains of one dimensional periodic arrangements of parallel dislocation lines.

---

[1] J. Wollschläger, D. Erdös and K. M. Schröder, Surf. Sci. **402-404**, 272 (1998).

2.5.7. Structural studies of the reconstructed Pb/InAs(001) surface

Y. Su, O. Bunk, J. H. Zeysing, D. A. Ehlers, R. L. Johnson, *II. Institut für Experimentalphysik, Universität Hamburg, Germany, J.M. Gay, B. Aufray, S. Sawaya, G. Lelay, CRMC2-CNRS, Campus de Luminy, Marseille, France,* C. Kumpf , M. Nielsen and R. Feidenhans'l, *Condensed Matter Physics and Chemistry Department, Risø National Laboratory, Denmark*
e-mail: robert.feidenhansl@risoe.dk   http://www.risoe.dk/fys/Employee/rofe.htm

InAs is a very important narrow band gap semiconductor, which exhibits some unique properties, such as high carrier densities and electron mobilities. The technically most important (100) face of InAs was found to show several complicated surface reconstructions, of which the atomic structure of the In-rich 4x2/c(8x2) reconstruction has still been in wide debate. In comparison to our recent structural investigation of the clean InAs(100)-4x2/c(8x2) surface and also in order to provide some complementary information for the structure determination of this complex reconstruction, we measured the Pb-deposited InAs(100)-1x4 surface by surface x-ray diffraction.

Upon deposition of one Pb monolayer on the clean In-rich InAs(100)-4x2/c(8x2) surface, a new (1x4) reconstruction can be obtained. One of the most intriguing features of this surface, is the formation of a strong two-dimensional electron gas in the sub-surface region, which was revealed in a recent study by synchrotron radiation photoelectron spectroscopy[1]. In particular, the single Pb 5d component used in the fit of the experimental spectra seems to indicate a single Pb adsorption site on this well-ordered surface, possibly a symmetric Pb dimer. Since no structural model so far has been provided for this surface, our x-ray structure studies are essential to clarify these interesting observations.

Adsorption of Pb ($\geq$ 1ML) on the clean In-terminated InAs(100)4x2/c(8x2) reconstructed surface at 300-350°C gave a very sharp 1x4 superstructure in LEED patterns. The sample was then transferred into a portable UHV chamber to the wiggler beamline BW2 at HASYLAB for the x-ray diffraction measurements. 83 symmetry inequivalent in-plane reflections, 322 fractional-order-rod reflections and 163 reflections along four crystal truncation rods were measured in total. The Patterson map was calculated from the in-plane fractional-order reflections, as shown in Fig. 1. Since Pb (a heavy metal atom) dominates the Patterson map, we are able to decouple the study of the Pb atom arrangement in the very top layer. In addition, the electron density maps of this surface could also be obtained through direct methods, which can provide valuable information for full structure refinements.
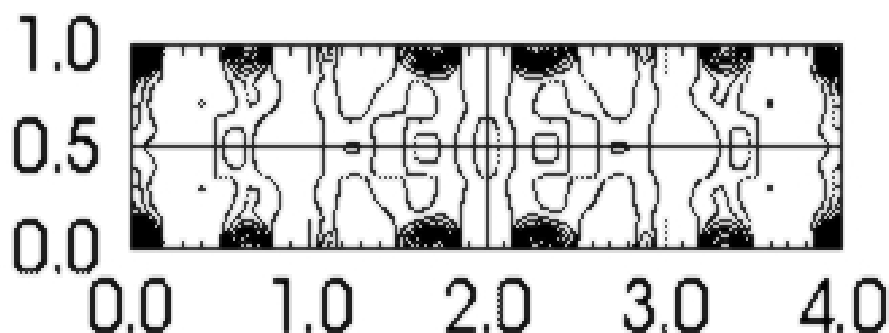
Fig. 1. The Patterson map of Pb/InAs(100)-1x4 surface obtained from all in-plane fractional-order reflections.

---

[1] J. M. Layet, M. Carrere, H. J. Kim, R. L. Johnson, R. Belkhou, V. Zhilin, V.Yu, Aristov and G. Lelay, Surface Science **402-404**, 724 (1998).

2.5.8. Nanoscale quasi-one-dimensional quantum structures induced by adsorbates: Structural study of the Si(111)-(8×2)-In low temperature reconstruction

C. Kumpf, M. M. Nielsen, M. Nielsen, R. Feidenhans'l, *Condensed Matter Physics and Chemistry Department, Risø National Laboratory, Denmark,* O. Bunk, J.H. Zeysing, Y. Su and R. L. Johnson, *II. Institut für Experimentalphysik, Universität Hamburg, Germany*
e-mail: christian.kumpf@risoe.dk   http://www.risoe.dk/fys/Employee/crku.htm

Considerable interest has focused recently on adsorbate-induced modifications of semiconductor surfaces as a technique to create nanoscale quantum structures. Indium induced reconstructions of the Si(111) surface show either semiconducting (coverage < 1 ML) or metallic (coverage > 1 ML) character. At the borderline between the two regions a (4×1) phase occurs, consisting of 1D chains of indium atoms. The chains are separated from each other by rows of silicon atoms causing a 1D metallic character of the surface. A detailed structural model obtained from surface X-ray diffraction (SXRD) has been published recently[1]. The system undergoes a phase transition to a (8×2) structure at lower temperature showing a 1D charge density wave along the indium chains[2]. To evaluate the structural changes associated with this phase transition we have investigated this low temperature phase by SXRD. The inplane data set of the (8×2) phase is shown in fig. 1. The intensity pattern of the quarter-order reflections is similar to that of the (4×1) phase, which suggests that the two structures also are similar, apart from minor relaxations. Relatively strong in-plane eighth-order reflections and flat eighth-order rods (see fig. 2) show that the relaxation has a strong lateral component and not much out-of-plane buckling. Furthermore the eighth order reflections along the $k = 0$ line are extinguished, indicating the presence of a glide line in the (8×2) phase. We propose that a similar oriented mirror line in the (4×1) structure is replaced by the glide line due to the atomic dislocations at low temperature. This would indicate strong pair-wire coupling of the dislocations in the neighbouring chains. No sharp half-order reflections are observed in the k-direction but only broad streaks showing no long-range correlation between the pairs of indium chains in [01] direction. The structure refinement for the (8×2) phase is in progress.
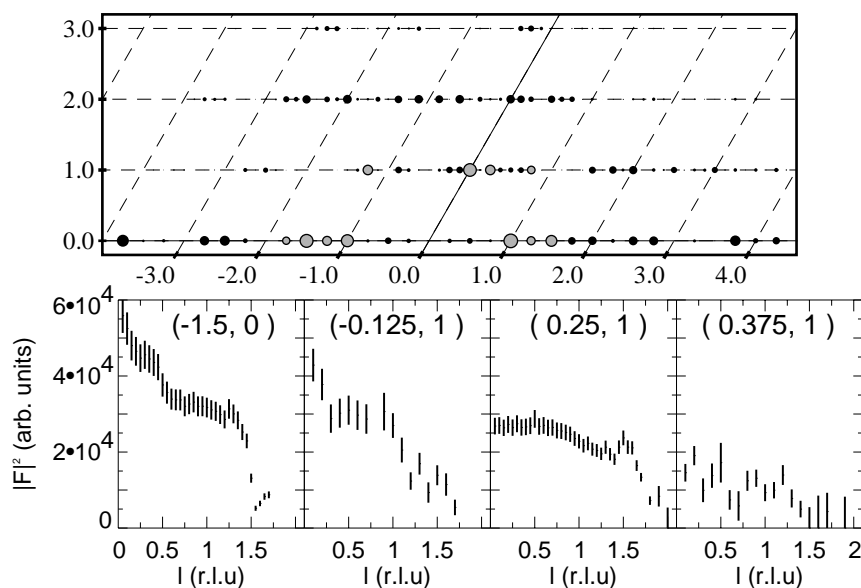
Fig. 1. Inplane data set: The areas of the circles correspond to measured intensities. Grey circles are scaled with 0.5.

Fig. 2. Some selected fractional order rods. The (-0.125, 1) and (0.375, 1) rods are scaled with a factor of 10.

[1] O. Bunk, G. Falkenberg, J. H. Zeysing, L. Lottermoser, R. L. Johnson, M. Nielsen, F. Berg-Rasmussen, J. Baker and R. Feidenhans'l, Phys. Rev. **B59**, 12228 (1999).
[2] H. W. Yeom, S. Takeda, E. Rotenberg, I. Matsuda, K. Horikoshi, J. Schaefer, C. M. Lee, S D. Kevan, T. Ohta, T. Nagao and S. Hasegawa, Phys. Rev. Lett. **82**, 4898 (1999).

2.5.9. X-ray diffraction studies on metal-rich (001) surfaces of III-V compound semiconductors

C. Kumpf, M. M. Nielsen, M. Nielsen, R. Feidenhans'l, *Condensed Matter Physics and Chemistry Department, Risø National Laboratory, Denmark,* O. Bunk, J. H. Zeysing, G. Falkenberg, Y. Su, R.L. Johnson, *II. Institut für Experimentalphysik, Universität Hamburg, Germany* and J. Zegenhagen, *ESRF, Grenoble, France*
e-mail christian.kumpf@risoe.dk   http://www.risoe.dk/fys/Employee/crku.htm

The surface reconstruction of III-V compound semiconductors has been investigated for more than two decades, but its atomic structure is still under highly controversial discussion. Despite its high technological importance, there is only very little definitive knowledge on the atomic arrangement of the various surface reconstructions. In order to clarify this unsatisfactory situation we investigated the Ga-rich GaAs(001)-c(8×2) and the In-rich InAs(001)-c(8×2) surface reconstruction using surface X-ray diffraction (SXRD). The high quality of our measured data allowed us to rule out all the models published for the (001) surface reconstruction of III-V compound semiconductors so far. In order to find some additional information on the atomic arrangement we used the technique of direct methods, which was applied to SXRD data recently by L.D. Marks[1]. Fig. 1 shows the result of his *fs98* code on the GaAs data set. Using this atomic arrangement as a starting model for the refinement of the atomic inplane positions a good fit to the inplane data set could be achieved. The data set is shown in fig. 2, demonstrating that the in-plane projected structure reproduces the data quite well. They do not differ strongly from the starting model found with the direct methods code. But strong variations in intensity in the fractional order rods demonstrate that out of plane displacements play an important role in this surface reconstruction. The development of a 3-dimensional model is still in progress. For InAs(001) we expect a very similar model, even though the direct methods code did not yield such an unequivocal result as in the case of GaAs(001). A refinement of a model for this data set is also on the way.
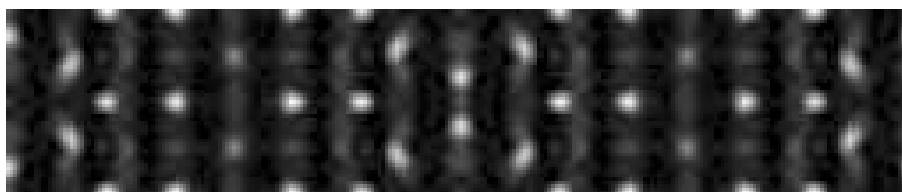
Fig. 1. (upper): Possible atomic positions in the GaAs(001)-(8×2) structure derived from the SRXD data using direct methods. One (8×2) unit cell is shown under the assumption of p2mm symmetry.
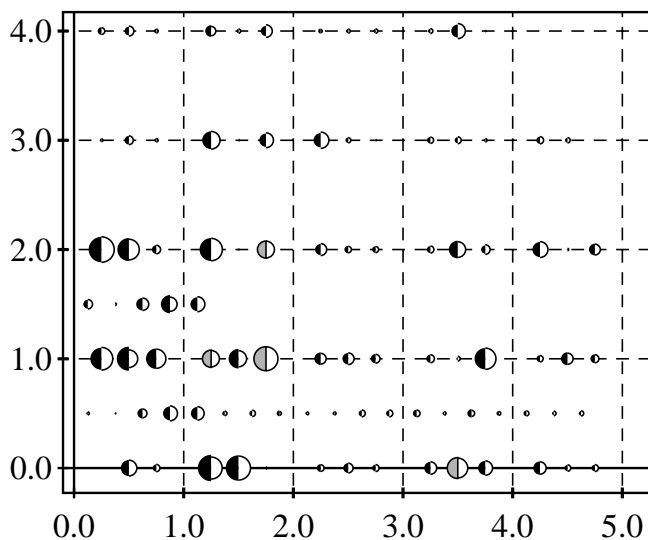
Fig. 2. (right): Inplane data set. The areas of the filled and empty semi-circles correspond to measured and calculated intensities. Grey circles are scaled with a factor of 0.5.

---

[1] L. D. Marks, W. Sinkler and E. Landree, Acta Cryst. A **55**, 601 (1999).

2.5.10. Structural study of the commensurate-incommensurate low temperature phase transition of Pb on Si(111)

C. Kumpf, M. M. Nielsen, M. Nielsen, R. Feidenhans'l, *Condensed Matter Physics and Chemistry Department, Risø National Laboratory, Denmark*, O. Bunk, J. H. Zeysing and R. L. Johnson, *II. Institut für Experimentalphysik, Universität Hamburg, Germany*
e-mail: christian.kumpf@risoe.dk   http://www.risoe.dk/fys/Employee/crku.htm

It is well known that adsorbates and impurities can induce significant reorganization of the atoms on semiconductor surfaces. Such reconstructed surfaces have been extensively investigated at room temperature in the past. Recently it has been found that a number of systems exhibit low temperature phases with unusual properties. We present the results of our investigations on the phase transition from the hexagonal incommensurate (HIC) phase of lead on silicon(111) at RT to the $\begin{pmatrix} 3 & 2 \\ -1 & 1 \end{pmatrix}$ commensurate phase at low temperature

An extended surface X-ray diffraction data set was measured at the BW2 beamline at HASYLAB at a temperature below 30 K. For solving the surface structure a starting model for the refinement was developed from the known surface reconstruction of the HIC phase. It consists of a lead overlayer with six atoms per unit cell. Refining only the positions of the lead atoms a $\chi^2 = 3.4$ was found which shows that the model contains all essential features. The fit could be improved to $\chi^2 = 2.5$ by including the positions of one double-layer of silicon atoms and anisotropic Debye Waller (DW) factors for the lead atoms in the refinement. To avoid an unrealistic high out-of-plane DW factor for atom 1 (9.9 Å^2) a split position in the z-direction was assumed for this atom. The inplane data set is shown in Fig. 1, the model in Fig. 2.

The Pb overlayer consists of a sequence of three different rows of lead atoms in the direction of **b**. One row (atoms 1/1a and 2) lies on the mirror line, indicated by the dash-dotted line in Fig. 2. The atomic positions of these two atoms are essentially similar to those in the SIC model. The zig-zag row formed by atoms 3 and 4 is mapped onto the third row (atoms 5 and 6) by the mirror line. Compared to the SIC model these atoms are shifted close to T1 on-top positions above the uppermost silicon atoms. Judging from next-neighbor distances the bonds between the lead atoms can be classified in covalent like bonds (below 3.15 Å), and metallic like bonds (between 3.30 and 3.55 Å). This is illustrated in Fig. 2 by gray and black lines between the lead atoms, indicating covalent- and metallic-like interatomic distances, respectively. Atom number 1, which is located on a hollow site, is the only one without a covalent bond to a silicon atom. This is probably the reason for the disorder in z-direction. Judging from these atomic distances all of the five silicon dangling bonds within one unit cell are saturated. The partially covalent bonds between lead adatoms and the silicon substrate atoms seem to stabilize the system and in contrast to the situation at room temperature produce a commensurate surface reconstruction at low temperature. We speculate that the formation of such "covalent bonds" might be the driving force behind the formation of the $\begin{pmatrix} 3 & 2 \\ -1 & 1 \end{pmatrix}$ phase.
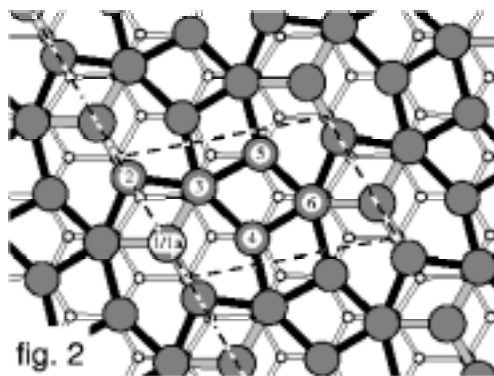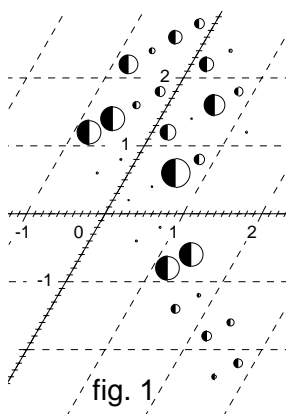
Fig. 1. Inplane data set: The areas of the filled and empty semi-circles correspond to measured and calculated intensities.

Fig. 2. The final model in top view. Lead and silicon atoms are shown as gray and white circles. The unit cell is indicated by the dashed line, the mirror line by the dash-dotted line.

2.5.11. Dehydration of aluminium hydroxides studied by in situ small and wide angle x-ray scattering

K. Johansen[1,2], F. Berg Rasmussen[1,3], A. M. Molenbroek[1], R. Feidenhans'l[3], B. S.Clausen[1] and K. Ståhl[2],
[1]Haldor Topsøe Research Laboratories, Lyngby, Denmark, [2]Department of Chemistry, Technical University of Denmark, Denmark, [3] Condensed Matter Physics and Chemistry Department, Risø National Laboratory, Denmark
 e-mail: frank.berg.rasmussen@risoe.dk og fbr@topsoe.dk   http://www.risoe.dk/fys/Employee/frbe.htm

The transition aluminas represent a group of technically important materials used in a wide variety of applications. They are obtained by thermal dehydration of aluminium-hydroxides, leaving a highly porous structure of aluminium-oxide. The dehydration of pseudo-boehmite to η-alumina was studied by simultaneous in situ X-ray powder diffraction (XRD) and small angle X-ray scattering (SAXS and US-AXS) carried out at BW4 (HASYLAB, Hamburg) and at Risø National Laboratory.

Figure 1 shows XRD diagrams measured during heating with the sample exposed to a flow of dry air. The transformation from pseudo-boehmite to η-alumina is clearly seen to take place at around 300°C. Figure 2 shows the combined SAXS and USAXS data spanning 7-8 orders of magnitude in intensity and providing information on both the primary particles and the aggregates of the particles. Upon dehydration the largest change is obtained at the primary particle level. Using a polydisperse cylinder model the pseudo-boehmite primary particles are found to be platelet-like with mean thickness around 2.0 nm and mean diameter of around 16.0 nm. During dehydration the mean thickness remains approximately constant whereas the mean diameter shrinks to around 11.0 nm at 600°C. At the aggregates level the intensity is approximately proportional to $q^{-2.8}$ through the whole dehydration series. This suggests that the primary platelet-like particles aggregate into mass-fractal objects of fractal dimension 2.8. Furthermore, it indicates that the dehydration does not involve long range restructuring but is of a topotactic nature involving rearrangement of local bonds only.
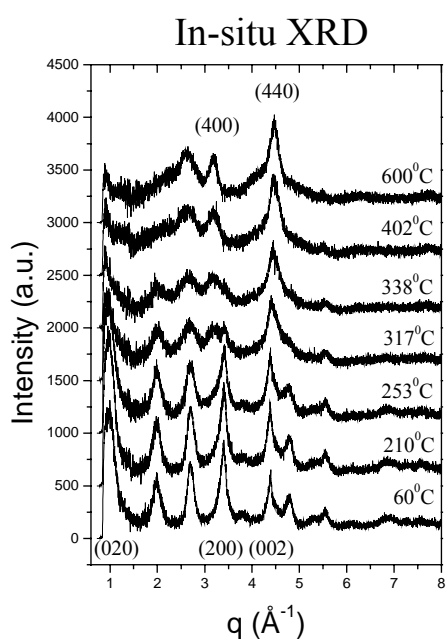
Fig 1. In situ XRD (BW4) diagrams showing the transformation of pseudo-boehmite to η-alumina.
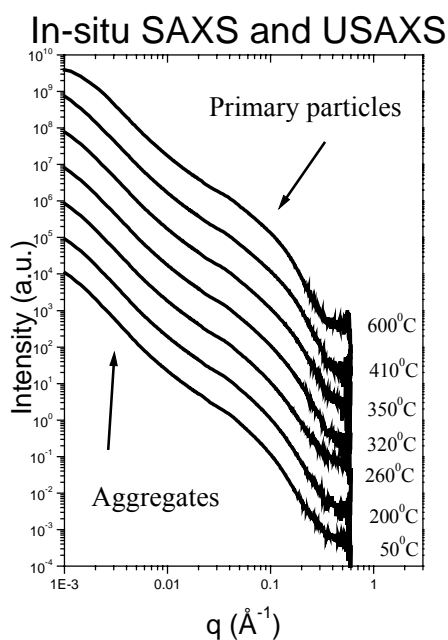
Fig. 2. Combined in situ SAXS (Risø) and USAXS (BW4) data.

2.5.12. Particle size distribution of an Ni/SiO₂ catalyst determined by ASAXS

F. Berg Rasmussen[1,2], A. M. Molenbroek[1], B. S. Clausen[1], and R. Feidenhans'l[2], [1]*Haldor Topsøe Research Laboratories, Lyngby, Denmark,* [2]*Condensed Matter Physics and Chemistry Department, Risø National Laboratory, Denmark*
e-mail: frank.berg.rasmussen@risoe.dk og fbr@topsoe.dk   http://www.risoe.dk/fys/Employee/frbe.htm

Anomalous small angle X-ray scattering (ASAXS) was used to determine the Ni particle size distribution of a 4 wt. % Ni/SiO₂ catalysts[1]. ASAXS measurements were performed at the JUSIFA ASAXS beamline at DESY-HASYLAB (Hamburg) using three different energies below the Ni K-absorption edge at 8333 eV. Figure 1 shows the normalised small angle scattering of a Ni/SiO₂ sample using an incident X-ray energy of 8290 eV and compares it to the scattering curve measured at 8326 eV. Figure 2 shows the separated ASAXS intensity obtained as the difference between the normalised SAXS data measured at 8290 eV and 8326 eV.

Assuming only that the particles are spherical a free-form determination of the particles size distribution was possible using a method published recently by Pedersen[2]. The best fit obtained is shown as the full line in figure 2. The volume weighted mean particle radius (57 Å) and specific surface area (52 m²/g) calculated from the determined particle size distribution were in good agreement with the mean crystallite size estimated by X-ray diffraction. The specific surface area determined from hydrogen chemisorption (10 m²/g) indicated that the individual particles (crystallites) observed by ASAXS and XRD aggregate into larger composite particles.
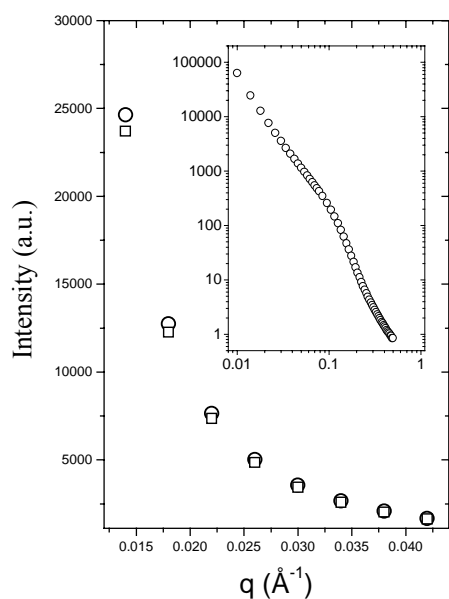
Fig. 1. A section of the small angle X-ray scattering curve (linear scales) of an Ni/SiO₂ sample measured at 8290 eV (circles) and at 8326 eV (boxes). The insert shows the full curve (log scales) measured at 8290 eV.
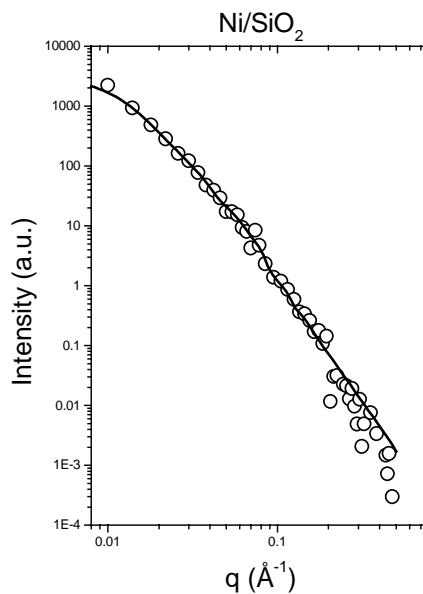
Fig. 2. Separated ASAXS data of an Ni/SiO₂ sample (open circles). The best fit obtained by a free-from distribution of spherical particles (full curve) is also shown.

---

[1] F. Berg Rasmussen, A. M. Molenbroek, B. S. Clausen and R. Feidenhans'l, J. Catal. **189** (2000). In the press.
[2] J. S. Pedersen, J. Appl. Cryst. **27**, 595 (1994).

2.5.13. Nano-dispersed NiMo/Al$_2$O$_3$ catalysts studied by ASAXS

F. Berg Rasmussen[1,2], A. M. Molenbroek[1], M. M. Nielsen[2], R. Feidenhans'l[2], B. S. Clausen[1] and G. Goerigk[3], [1]*Haldor Topsøe Research Laboratories, Lyngby, Denmark*, [2]*Condensed Matter Physics and Chemistry Department, Risø National Laboratory, Denmark*, [3]*Forschungszentrum Jülich, Germany*
e-mail: frank.berg.rasmussen@risoe.dk og fbr@topsoe.dk   http://www.risoe.dk/fys/Employee/frbe.htm

In a number of important catalytic processes petroleum streams are refined by saturation of hydrocarbons and by removal of light impurities and metals. These processes are referred to as hydrotreating. The most commonly used sulphide catalyst for hydrotreating is Mo supported on an Al$_2$O$_3$ (alumina) carrier and promoted by either Co or Ni[1]. A large effort has been put into the characterisation of the structure and morphology of the Mo species both in the calcined oxide state and in the catalytic active sulphided state.

Mo/Al$_2$O$_3$ and NiMo/Al$_2$O$_3$ catalysts were prepared in both the calcined and sulphided state and investigated by Anomalous Small Angle X-ray Scattering (ASAXS) experiments at several energies around the Mo K-edge (20.0 keV) using the JUSIFA beamline at HASYLAB (Hamburg). Figure 1 shows the separated scattering curve of a sample with 14.7 wt. % Mo on Al$_2$O$_3$ sulphided at 400°C. Figure 2 shows a similar curve for a sample with 9.8 wt. % Mo and 3.9 wt. % Ni sulphided at 600°C. Similar scattering curves were obtained on oxide (as prepared) samples. Two regions are observed in both cases.

At high q (q>0.1 Å^{-1}) the scattering intensity is approximately linear in the log-log plot with a slope of around –2.5, indicating the presence of flat MoS$_2$-particles. Assuming these particles to be flat cylindrical disks, fits to the scattering curves indicate a typical diameter of around 2 nm and a thickness below 0.7 nm for samples sulphided at 400°C. For samples sulphided at 600°C similar fits lead to a typical diameter of 4 nm and a somewhat larger thickness but still below 1 nm. These numbers are in reasonably good agreement with expectations as indicated above. The low-q scattering (q<0.1 Å^{-1}) indicates that also larger particles containing Mo are present. However, as these are not observed by e.g. transmission electron microscopy, further investigations are needed to clarify the origin of this additional scattering.
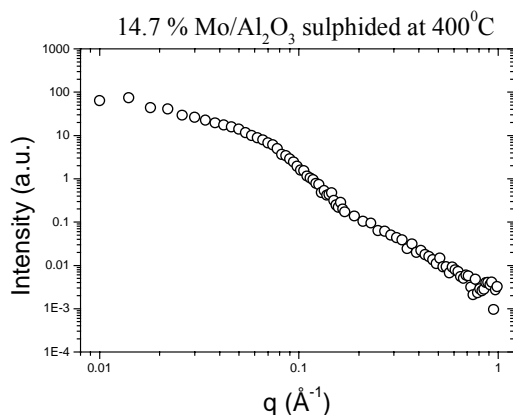
Fig. 1. Separated scattering of a Mo/Al$_2$O$_3$ catalysts sulphided at 400°C.
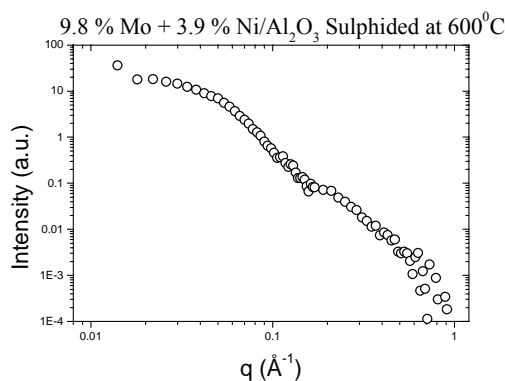
Fig. 2. Separated scattering of a NiMo/Al$_2$O$_3$ catalysts sulphided at 600°C.

---

[1]   H. Topsøe, B. S. Clausen and F. E. Massoth, 'Hydrotreating Catalysis' in Volume 11 of the series 'Catalysis, Science and Technology' ed. J. R. Anderson and M. Boudart (Springer-Verlag Berlin Heidelberg 1996) and references therein.

2.5.14. Spontaneous chiral separation on solid mineral surfaces

L. Nedelmann, I. Weissbuch, L. Leiserowitz, *Department of Materials and Interfaces, Weizmann Institute of Science, Israel*, C. Kumpf and R. Feidenhans'l, *Condensed Matter Physics and Chemistry Department, Risø National Laboratories, Denmark*
e-mail: robert.feidenhansl@risoe.dk   http://www.risoe.dk/fys/Employee/rofe.htm

The spontaneous separation of left- and right-handed molecules (i.e. enantiomers) from a racemic mixture has intrigued scientists since it was discovered by Pasteur more than a century ago. This phenomenon might have played a significant role in an abiotic process proposed to explain the transformation from a racemic chemistry to a chiral biology. On simple symmetry grounds, such a separation should be easier in two dimensions, as the symmetry element `inversion', so prevalent in 3-D crystals is absent in the 2-D counterpart (a crystal structure exhibiting inversion symmetry cannot be chiral).

We wish to achieve the 2-D separation of enantiomers on a mineral crystal surface. More specifically, we want to use naturally occurring α-amino-acids or closely-related molecules. A prime candidate for the mineral surface is the $(10\bar{1}4)$ face of calcite (which we label the (001) face according to indexing by the true cleavage rhombohedron). We choose this surface because: (a) it is a cleavage plane that yields a surface atomically flat on the micron scale; (b) this surface contains rows of calcium ions arranged in rows with a spacing of 5 Å along the $(2\bar{2}0)$ direction, a spacing also found in α-amino acids and secondary amides crystals. Various organic adsorbate systems have been tried. At present, we are concentrating our studies on N-octadecanoyl-alanine whose carboxyl acid moiety should show a strong affinity to the calcite surface and whose amide function should be spaced by 5 Å.

Measurements of the specular reflectivity performed at beamline BW2 (Hasylab) clearly indicate the presence of organic molecules on the calcite surface. The film's thickness of ~18 Å corresponds to a molecular tilt angle of 45°, which these molecules have at the air-water interface. In order to probe the lateral ordering of the adsorbate, we performed crystal truncation rod (CTR) measurements on the pure substrate as well as on calcite covered by the long chain acids. We assume the N-octadecanoyl-alanine to be in registry along the 5 Å spacing of the calcite. This is reasonable, since grazing incidence diffraction experiments (GIXD) data, measured from such a monolayer on water at the diffractometer at BW1, showed one of the lattice spacing to be 4.8 Å. Due to the molecular tilt, the contribution of the adsorbate layer to the corresponding CTR, the $(2\bar{2}2)$ rod, should be maximum for an index $L \sim 0.7$.
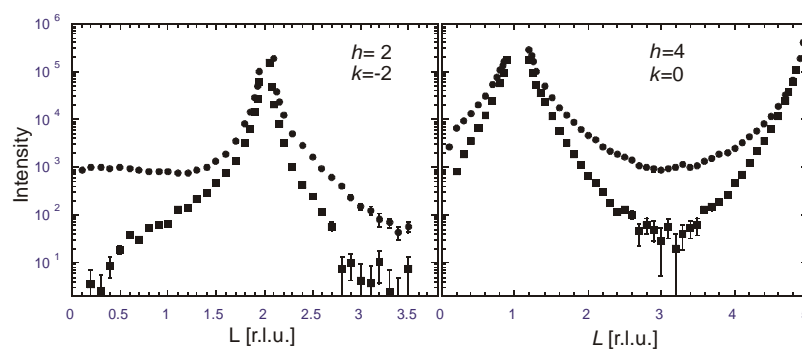
Fig 1. $(2\bar{2}L)$ and $(40L)$ crystal truncation rod of pure calcite (squares) and calcite with
a N-octadecanoyl-alanine adsorbed (circles).

Figure 1 shows a comparison between the nonspecular $(2\bar{2}L)$ and $(40L)$ CTRs of a freshly cleaved, pure calcite surface and one covered with the adsorbate. While the pure calcite's CTR is roughly symmetric around the $(2\bar{2}2)$ Bragg peak, the CTR of the adsorbate system shows a significant difference at L less than 1.2 which may arise from the adsorbate. On the other hand, the $(40L)$ CTR shows, as expected, only minor fluctuations in shape, which can be explained by a difference in surface roughness.

2.5.15. Building better plastic transistors: Study of orientation effects in self-organised domains of thin polymer films

M. M. Nielsen, K. Bechgaard, M. Nielsen and R. Feidenhans'l, *Condensed Matter Physics and Chemistry Department, Risø National Laboratory, Denmark*
e-mail: martin.m.nielsen@risoe.dk   http://www.risoe.dk/fys/Employee/mani.htm

Building logic circuits with polymers as the active, semiconducting material promises very attractive possibilities for creating cheap and flexible electronic devices of obvious technological interest. Thin films of poly-3-hexylthiophene self-organise into a lamellar-type structure with alternating planes of conjugated backbones and phase segregated hexyl side chains along the (100)-axis of an orthorhombic unit cell[1]. For thin ($\approx$70-100nm) films spin-cast on SiO2/Si FET substrates, X-ray diffraction (XRD) investigations (Fig. 1) show the orientation of the self-organised domains with respect to the substrate to be different for films of different regioregularity. Regioregularity being the percentage of stereoregular head-to-tail (HT) attachments of the hexyl side-chains of the 3-position of the thiophene rings.

The change in orientation is evident from the different intensity distributions along the (100) and (010) reflections in Fig. 1 (a, b). Samples with 95-96% HT show preferential orientation of the ordered domains with the (100)-axis normal to the film surface and the $\pi-\pi$ stacking direction, the (010)-axis, in the plane of the film (Fig. 1a). In contrast, 81% HT samples have a higher number of crystallites with the (100)-axis oriented along the film surface, while the (010)-axis is parallel to the surface normal (Fig. 1b). The measurements are made on a wide angle X-ray (WAXS) image-plate camera operated at our in-house Rigaku 18kW rotating anode. The orientation of the sample can be adjusted to select a grazing incidence angle. Detailed, quantitative information on the different orientations is obtained by grazing incidence XRD measurements made at the BW2 beamline at HASYLAB, DESY in Hamburg, as demonstrated in Fig. 1 by comparison of the in-plane (c) and pseudo-out-of-plane (d) scattering geometry (dark grey (light grey) - 96% (81%), spincoated). In addition to the spin-cast films, Fig. 1 c, d also shows the results for a drop cast 81% HT film (black curve). The widths of the diffraction peaks are similar to the results for the spin cast samples, and accordingly, the crystallite sizes are similar, but the preferential orientation is much less pronounced.

The ability to control the orientation of the ordered domains enables us to establish a direct correlation between the orientation of the $\pi-\pi$ stacking direction and the mobility μ-FET for in-plane transport in FET devices fabricated on the same substrates as used for the XRD samples[2]. Samples with HT < 91%, ((010)-axis out-of-plane), have mobilities several orders of magnitude lower than what is found for samples with the highest regioregularity ((010)-axis direction in-plane). Further the mobility of the solution-cast 81% HT film is by more than an order of magnitude higher than that of the spin-coated sample. Consequently, the strong dependence of the FET mobility on regioregularity is not caused by different degrees of disorder. It is a measure of the large anisotropy of the mobility induced by the two different orientations of ordered domains[2].
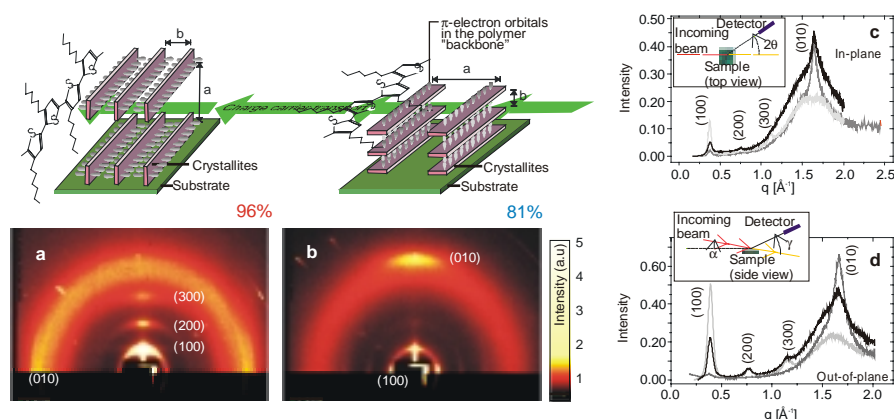
Figure 1

---

1 See e.g. E. J. Samuelsen and J. Mårdalen in Handbook of Organic Conductive Molecules and Polymers, edited by H.S. Nalwa (Wiley, New York, 1997)

2 H. Sirringhaus, P. J. Brown, R. H. Friend, M.M. Nielsen, K. Bechgaard, B. M. W. Langeveld-Voss, A. J. H. Spiering, R. A. J. Janssen, E. W. Meijer, P. Herwig and D. M. de Leeuw, Nature **401**, 685 (1999).

2.5.16. Our new versatile TOF-SIMS instrument

K. Norrman, N. B. Larsen and R. Feidenhans'l, *Condensed Matter Physics and Chemistry Department, Risø National Laboratory, Denmark*
e-mail: kion.norrman@risoe.dk

Our department recently acquired a TOF-SIMS (Time Of Flight-Secondary Ions Mass Spectrometry) instrument, a TOF-SIMS IV from CAMECA/ION-TOF. The technique is primarily used for chemical surface characterization. It is a qualitative method, which analyses the outermost atomic layer of a surface. The instrument can be operated in static or dynamic mode; perform imaging (including SEM); and perform depth profiling. First and foremost non-volatile compounds can be analyzed, but a cold finger arrangement makes volatile compound analysis possible. A temperature-regulated device can regulate the sample temperature between –130 °C and 600 °C with 1 °C precision. The maximum sample size is approximately 10x10x2 cm. The instrument is equipped with two different ion guns, a Ga gun and an EI gun for various gasses, which makes it highly versatile. The pulsed ion gun can produce an ion pulse between 0.6 ns and 100 ns each 50 to 300 µs. The energy of the primary ion beam can be varied between 5 and 25 keV. The primary ion beam can raster an area of up to 0.5x0.5 mm. With the mechanical stage the raster area can be increased to approximately 10x10 cm. The primary ion beam can be focused to a width between 30 µm and 50 nm. Depth profiling can be performed to a depth of approximately 100 nm, with a depth resolution of approximately 1 nm. The TOF analyzer is equipped with a reflectron, which gives a high mass resolution as well as a high ion transmission. The length of flight is 2 m. The mass resolution ($M/\Delta M$) is up to approximately 15000 and the mass precision is between 10 and 1 ppm. For most compounds the detection limit is in the ppm range. The versatility of this instrument makes it applicable for a variety of applications on almost all known materials, for example metals, ceramics, inorganic salts, polymers, organic and biological material, pharmaceutical materials, and electronics. Figure 1 A to D displays illustrative applications.
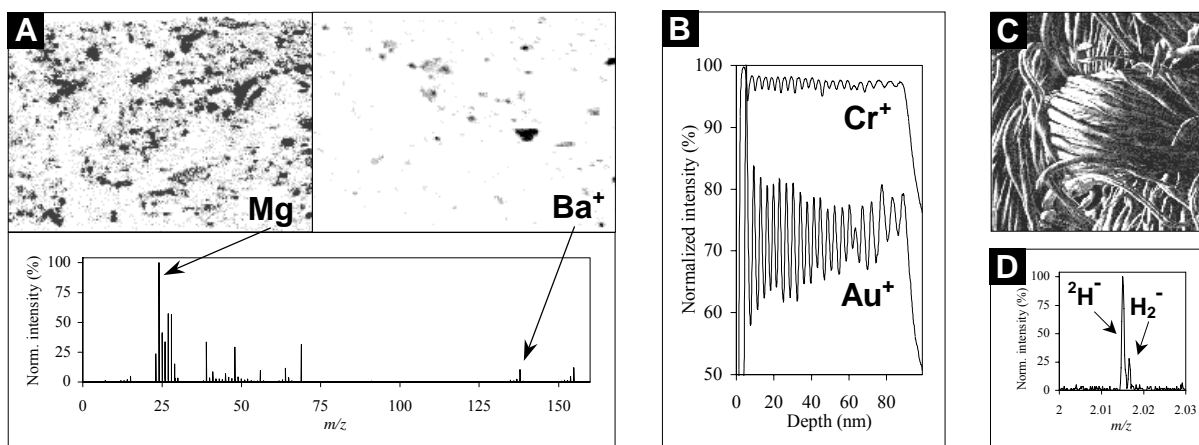
Fig. 1. TOF-SIMS analysis results of various types of samples. **A)** Cross-section of a paint floe (90x125 µm) analyzed with imaging and spectrometry. The ion images shows the distribution of some of the pigments in the bulk material. **B)** Depth profiling (1 keV SF_5^+) of epitaxial multi layers of metals (Cr/Au). The excellent depth resolution demonstrates how powerful SF_5^+ is as a molecular sputter ion. **C)** Total ion image (500x500 µm) of a woven textile sample. This illustrates the applicability on samples having a highly corrugated surface. **D)** Mass spectrum illustrating the excellent mass resolution of the TOF analyzer. At the lowest mass to charge ratios the optimal mass resolution is approximately 3000, and at higher mass to charge ratios the mass resolution approach approximately 15000. The two ions are separated by only 1.6 mg/mol.

2.5.17. Plasma oxidation of silicones

N. B. Larsen, *Condensed Matter Physics and Chemistry Department, Risø National Laboratory, Denmark,* E. M. Lauridsen, *Materials Research Department, Risø National Laboratory, Denmark* and R. Feidenhans'l, *Condensed Matter Physics and Chemistry Department, Risø National Laboratory, Denmark*
e-mail: niels.b.larsen@risoe.dk   http://www.risoe.dk/fys/Employee/nila.htm

Polydimethylsiloxane (PDMS) containing polymers are widely used as industrial elastomers. A major obstacle to the use of PDMS is its highly inert surface chemistry of very low surface energy. Both factors complicate subsequent gluing and painting of molded objects. Surface activation of the PDMS surface by oxidation of the silicone to more reactive silica (amorphous silicon dioxide) is consequently of general interest. The activation may be accomplished either by wet chemistry (oxidizing acids) or by dry methods based on gas ionization (flame, corona or cold plasma treatment). We have investigated the chemical changes occurring in the surface region of PDMS exposed to an oxygen containing plasma (20% O_2 / 80% Ar) for prolonged periods of time.

Flat silicone thin films of thickness 200 nm resulted from spin coating a 21000 g/mol PDMS oil (Dow Corning DC360) onto a cured optical adhesive (Norland NOA 81). Atomic Force Microscopy of the substrate before spin coating showed a RMS roughness of 0.5 nm. The surfaces of the silicone thin films were exposed for varying times (5 or 10 minutes) using three different plasma powers (20W, 40W or 80W). The resulting silica like layers was analyzed by x-ray reflectometry, x-ray photoelectron spectroscopy (XPS) and secondary ion mass spectrometry (SIMS) depth profiling (Fig. 1). The combined analysis shows that the type and extent of surface modification is largely invariant to the exposure times and plasma powers investigated. All sets of exposure conditions result in a 1-2 nm thick silica layer on top of a 10-20 nm layer of gradually less oxidized silicone.

Our studies indicate that plasma oxidation of silicones is a fast self-passivating process where the nanometer thick layer of amorphous silicon oxide initially formed acts as a very effective barrier towards subsequent reactive oxygen ions impinging on the surface from the plasma. Consequently, the creation of thicker oxidized surface layers on silicones is probably not possible by standard plasma oxidation procedures
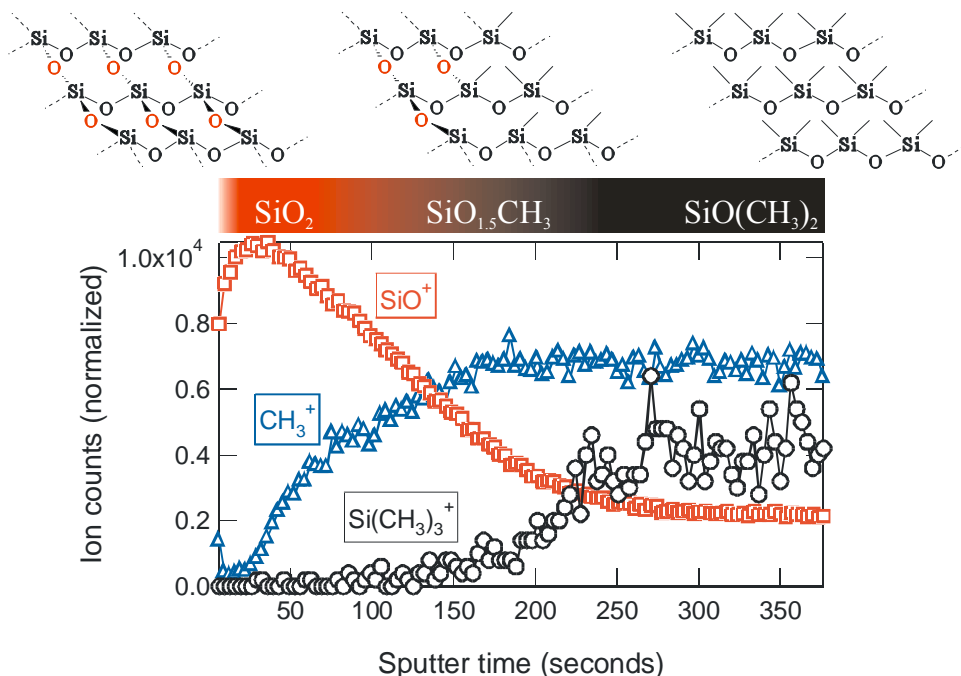
Fig. 1. SIMS depth profiling probes the detailed surface chemistry with sub-nanometer vertical resolution. The three ion concentrations displayed probe silica (SiO^+), partly oxidized and non-oxidized silicone (CH_3^+), and non-oxidized silicone ($Si(CH_3)_3^+$), respectively.

2.5.18. Wet cleaning of silicon wafers

S. Mentzel, N. B. Larsen, *Condensed Matter Physics and Chemistry Department, Risø National Laboratory, Denmark* and K. Schaumburg, *CISMI, Chemistry Department, University of Copenhagen, Denmark*
e-mail: soeren.mentzel@risoe.dk   http://www.risoe.dk/fys/Employee/sme.htm

The contamination of silicon wafers can be divided into 1. organic (hydrocarbons from the air and the oil used for polishing the wafer), 2. ionic (from solutions), 3. atomic (mostly metals that adhere to the silicon) and 4. silicon particle contamination from the backside of the wafer.

The classic way of cleaning silicon wafers is by oxidation of the contamination with hot acidic or basic solutions of H_2O_2 and by etching with diluted solutions of HF (ca. 0,05%). In large scale cleaning one would like to avoid large amounts of waste chemicals and alternative methods are used, e.g. megasonication (1MHz) and oxidation with ozone solutions[1, 2].

The purpose of this work was to establish a fast, efficient and preferably low cost routine of cleaning silicon wafers in small scale. Since exotic methods like megasonication and ozone oxidation were not available and the decision of not using HF routinely was made, different combinations of standard wet cleaning techniques were investigated. XPS was used to measure the level of carbon and other relevant elements on the silicon wafer surface and darkfield microscopy coupled with particle counting software was used to investigate the removal of particles.

The different cleaning methods investigated were:
Piranha: H_2SO_4/H_2O_2 4:1 for 10min at 120-150°C; SC1: $NH_4OH/H_2O_2/H_2O$ 0,05:1:5 for 10min at 80-90°C; SC2: $HCl/H_2O_2/H_2O$ 1:1:5 for 10min at 80-90°C and ultrasound for 10min at 60°C, between two treatments and in the end of every treatment cycle the wafer was flushed with large amounts of ultra pure water (UPW).

A complete removal of the carbon contamination could not be achieved (see Fig. 1), but this is probably due to new contamination deposited on the samples while they were being transferred from the clean room spinner to the XPS. The removal of particles was very effective (see Fig. 2).
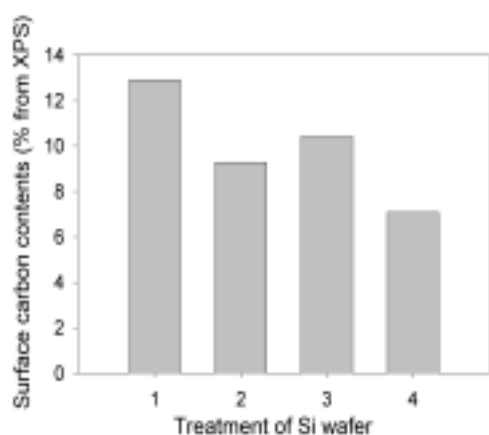
Fig. 1. Effect of carbon removal
1: Fresh Si wafer
2: Piranha treated Si wafer
3: Piranha and SC1 treated Si wafer
4: Piranha, SC1 and SC2 treated Si wafer
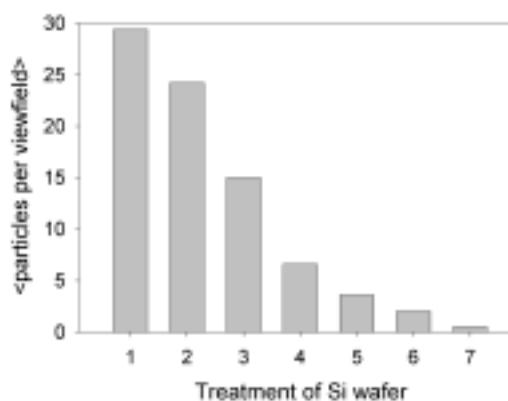
Fig. 2. Effect of particle removal
1: Fresh Si wafer
2: Upw treated Si wafer
3: Upw and ultrasound treated Si wafer
4: Piranha treated Si wafer
5: Piranha, SC1 and SC2 treated Si wafer
6: Piranha and ultrasound treated Si wafer
7: Piranha, SC1, SC2 and ultrasound treated Si wafer

[1] W. Kern and D.A. Panotien, RCA Review, June 1970, 187.
[2] S. C. O'Brien, Chemical Society Reviews, 393 (1996).

2.5.19. Surface morphology of PS-PDMS diblock copolymer films

T. H. Andersen, S. Tougaard, *Physics Department, Odense University, SDU, Denmark*, N. B. Larsen, L. Hubert, K. Almdal and I. Johannsen, *Condensed Matter Physics and Chemistry Department, Risø National Laboratory, Denmark*
e-mail: niels.b.larsen@risoe.dk   http://www.risoe.dk/fys/Employee/nila.htm

The surface behavior of a diblock copolymer, consisting of 25 kg/mol poly(styrene) (PS) and 25 kg/mol poly(dimethylsiloxane) (PDMS), is investigated here. The polymer surfaces are probed by X-ray photoelectron spectroscopy (XPS). The extent of PDMS surface segregation is quantified by analysis of the detailed XPS peak shape and background. This technique allows determination of the surface morphology of the films in terms of the surface coverage and thickness. The equilibrium morphology of this symmetrical diblock copolymer is a lamellar structure of which the top layer of PDMS is investigated.

The polymer solutions, made from 10 mg/ml chloroform, are spin-coated as thin films on silicon wafers at 4000 rpm. The films are annealed for varying times at 90°C and 130°C before analysis, corresponding to temperatures below and above the glass temperature of PS. The XPS spectra are analyzed with the Tougaard method. This method takes the inelastically scattered electrons from the uppermost hundreds of angstroms into account. As seen in figure 1, the background on the low kinetic energy (high binding energy) side of the main peaks changes during annealing. These changes are attributed to different surface morphologies. The XPS spectra are analyzed with respect to reference spectra obtained from spin-coated PS and PDMS films. The structures are modelled by visual fitting to the best agreement between the calculated and reference curves.

The surface morphology is determined before and after annealing. At room temperature, a partial top layer of PDMS is formed, with a thickness of 5-7 Å and a coverage of ~80%. Below this layer the PDMS contents is approximately 35%. Annealing at 90°C, i.e. below the glass transition temperature T_g, results in a small increase of both the thickness and the coverage of the top PDMS layer independent of the annealing time up to 20 hours. Increasing the annealing temperature to 130°C, i.e. above T_g, for up to 3 hours causes the formation of a more dense PDMS layer. The variation in thickness is large, however (figure 2). Extended annealing at 130°C for 20 hours results in the reproducible formation of a dense 65 Å thick PDMS layer with a variation between samples of less than 10 Å. These results point to the very slow dynamics involved in approaching the equilibrium morphology of larger block copolymers even at temperatures significantly above the glass transitions of both blocks.
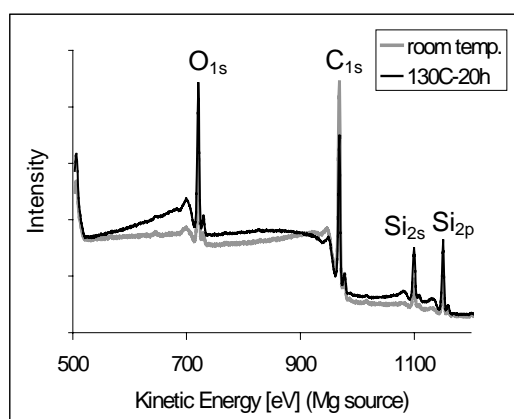
Fig.1. The XPS spectra show pronounced changes in the peak shape background after annealing.
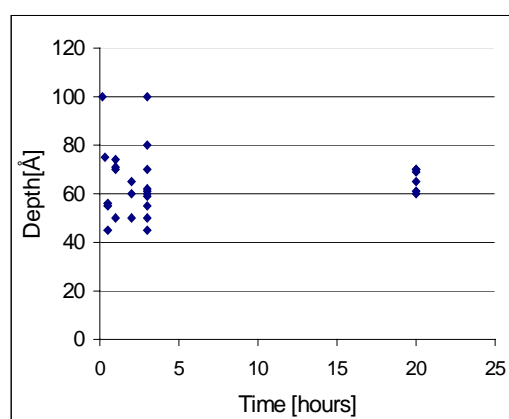
Fig. 2. Annealing at 130°C cause formation of a PDMS surface layer of reproducible thickness.

2.5.20. Injection moulding nanostructures

N. Gadegaard, N. B. Larsen, *Condensed Matter Physics and Chemistry Department, Risø National Laboratory, Denmark* and S. Mosler*, Fraunhofer-Institute for Interfacial Engeneering and Biotechnology, Stuttgart, Germany.*

e-mail: nikolaj.gadegaard@risoe.dk   http://www.risoe.dk/fys/Employee/niga.htm

Previous studies[1] have demonstrated that surface topography on the nanometer scale influences cell behaviour, e.g. adhesion, proliferation and differentiation. Most of these investigations have used model structures of non-biological origin made by lithographic techniques in inorganic materials such as silicon, glass and titanium. We have taken the approach of mimicking the important connective tissue protein collagen I in polymeric materials. Our method is based on CD production technology, where a polymeric material is injection moulded in a nickel master carrying the negative structure of the original. Injection moulding is a very inexpensive and fast method for mass production.

The collagen networks were self-assembled *in vitro* in a phosphate buffer containing purified collagen I monomers. They were incubated at 37°C for 15 h and then sedimented on a suitable substrate by dehydration in the presence of propanol. After gentle rinsing the surface was sputter coated with a 200 nm thin conducting layer. This layer acted as a cathode in the galvanic process, where the total thickness of ca. 0.3 mm was reached. The nickel master was separated from the substrate and cleaned by sonication in a 1:1 mixture of ethanol and milli-Q water.

Collagen assembles into a very distinct fibrillar structure with a characteristic 65 nm periodic cross-striation. This cross-striation is clearly seen in Fig. 1A. It was the aim to transfer this characteristic feature from the original to the all-polymer replicate, and as is seen in Figure 1B the 65 nm cross-striation is clearly visible in the replica. The cleft in the cross-striations is 3-5 nm deep. A range of commercially available polymers ranging from transparent to fibre re-enforced, were tested. However, only a few grades were able to transfer not only the fibrous structure (200 – 500 nm) but also the cross-striation (65 nm).
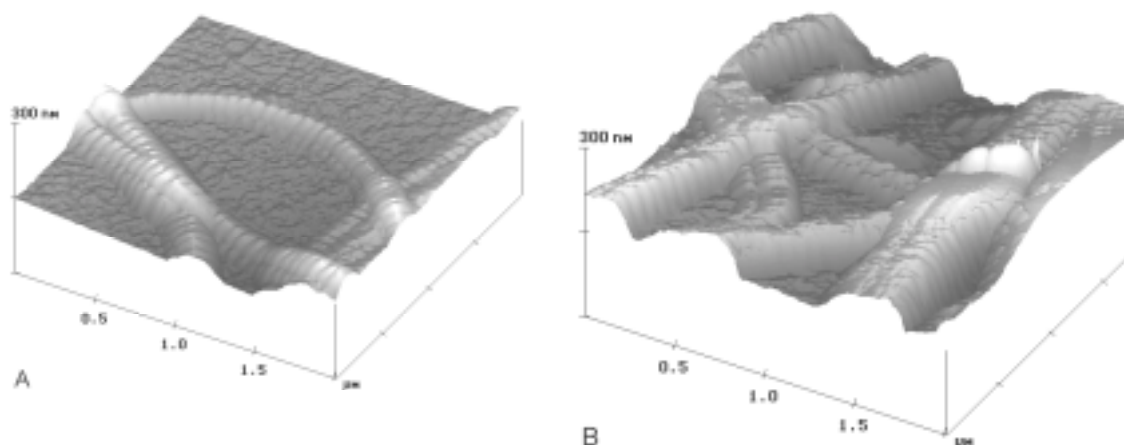
Fig. 1. 2x2 μm^2 AFM images of fibrillar collagen sedimented on a silicon wafer A) and the corresponding all-polymer replicate B).

---

[1] R G. Flemming, C. J. Murphy, G. A. Abrams, S. L. Goodman and P. F. Nealey, Biomaterials **20,** 573 (1999).

2.5.21. Monitoring protein adsorption kinetics by *In-Situ* ellipsometry

V. Thom, N. B. Larsen and I. Johannsen, *Condensed Matter Physics and Chemistry Department, Risø National Laboratory, Denmark*
e-mail: niels.b.larsen@risoe.dk   http://www.risoe.dk/fys/Employee/nila.htm

Ellipsometry is an extremely accurate optical technique for the measurement of the optical constants of reflecting surfaces or for the measurement of thickness and refractive index of very thin films deposited onto surfaces. The method can detect changes in the thickness of films as small as 0,1 nm, and changes in the refractive index of approximately 0,002. In combination with an automated set-up, it is a powerful technique for monitoring *in situ* the adsorption of macromolecules at a solid/liquid interface.

Ellipsometry involves analysis of the change in the state of the polarized light that accompanies reflection from a surface. The state of polarization is defined by the phase and amplitude relationships between the two component plane waves into which the electric field oscillation is resolved, i.e. the wave in the plane of incidence and the wave normal to the plane of incidence. In general, reflection causes a change of these component waves in their relative phases and amplitudes.

One way of determining the ellipsometric angles is to use the concept of null-ellipsometry, where the angles Δ and Ψ, are determined from the polarizer and analyzer settings that result in a minimum of the detected light intensity. In order to determine the numeric values of the thickness and the refractive index of the adsorbed film an iteration procedure is applied that presupposes a physically sensible positive and real value for the obtained film thickness. Underlying assumptions for this calculation are that the reflecting surface is perfectly smooth, and that the adsorbing film is homogeneous and of uniform thickness. The fact that these requirements can hardly be satisfied, especially in the case of adsorbed proteins, indicates that the values obtained for the refractive index and the thickness of the film should be considered as effective values only. However, the adsorbed amount can be calculated from these values, if some properties of the adsorbed film are known, as e.g. its refractive-index increment, or the partial specific volume together with the ratio of the molecular weight and the molar refractivity.

In the present study we were interested in characterizing the adsorption of proteins and other solutes preceeding bacterial adhesion to surfaces found in food processing equipment. To understand better the formation of these so called *conditioning films* and their impact on the consecutive adhesion of bacteria could help to design superior material surfaces, i.e. surfaces which can inhibit bacterial adhesion and biofilm formation. The figure shows long term adsorption kinetics of soy hydrolysate (TSB) to different surfaces. Note the increased adsorption to methylated (hydrophobic) silicon in comparison to stainless steel or etched (hydrohilic) silicon probably caused by the main driving force of protein adsorption, i.e. the so called hydrophobic interaction.
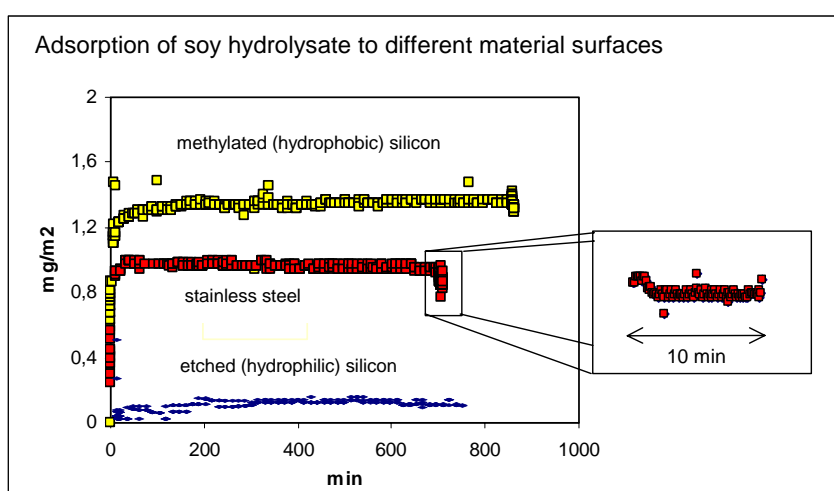
2.5.22. Protein repellent surface modification of silicon and PDMS

A. Papra and N. B. Larsen, *Condensed Matter Physics and Chemistry Department, Risø National Laboratory, Denmark*

e-mail: alexander.papra@risoe.dk   http://www.risoe.dk/fys/Employee/ALPA.htm

Due to a strong need for protein repellent surfaces (e.g. in biotechnology and medical applications) our work was aimed at a general and simple scheme to provide an efficient coating for silicon and polymeric (PDMS) surfaces. We took advantage of known coupling strategies that have been adjusted to our needs. Commercially available poly-(ethyleneglycol)-silanes (PEG-silanes) with 6-9 PEG units have been grafted onto silicon and PDMS.

First, both of the materials were oxidized to yield silanol groups. This has been achieved by applying piranha solution (silicon) or plasma oxidation (PDMS). The PEG-silane has been grafted to the respective surface out of 0.1 to 100mM solutions from toluene or ether. This led to a complete coverage of the surfaces with non-visible layers of protein repellent PEG-chains.

According to XPS measurements the grafting density do not depend on the concentration of the PEG-silanes within the range from 1 to 100mM. The typical composition of the surface (C: 23%, O: 30%, Si: 47%) indicates a very thin layer clearly below 10nm. Figure 1 shows the development of the water contact angle with time for a silicon wafer. For the modified sample there is hardly any change in the contact angle within two weeks after the modification (stored in air). In contrast to that the blank sample (just oxidized with piranha) loses its hydrophilic character while stored in air due the loss of silanol groups. Figure 2 shows the same graph for the grafting of PEG-silanes to PDMS. The blank sample loses its hydrophilicity even faster (within minutes) due to reorganization of the very flexible polymer chains. The PEG covered surfaces yielded a similar advancing angle like the silicon surfaces but with somewhat poorer reproducibility (see error bars). The receding angle is lower than for the silicon surfaces leading to a higher hysteresis. Adsorption experiments with bovine serum albumin (BSA) showed that the PEG covered silicon surfaces repel proteins even if huge concentrations were applied (0.1-10%). Thus, it can be concluded that even short-chained PEG's are capable of acting as powerful protein repellents.

Two completely different material surfaces can be modified by this procedure yielding similar surface properties towards hydrophilicity and protein rejection.
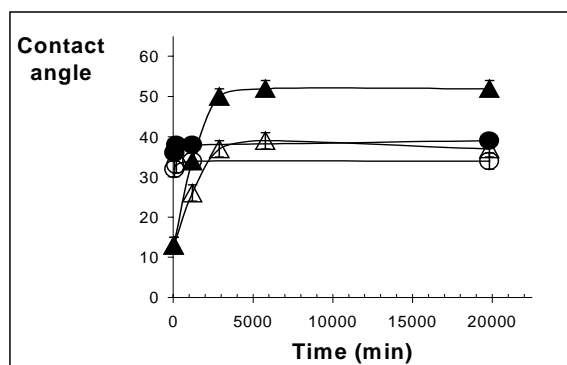
Fig. 1. Evolution of contact angles with time of a silicon wafer hydrophilized with piranha solution (filled triangles: advancing; open triangles: receding) and of a wafer grafted with PEG (circles).
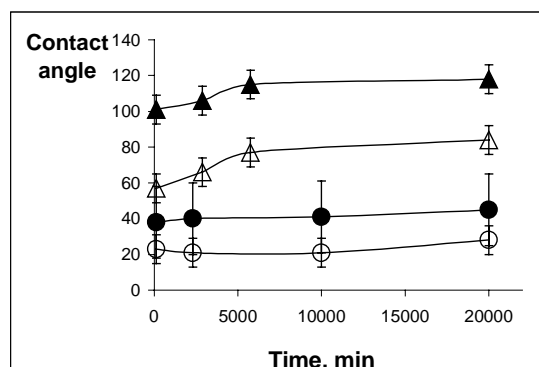
Fig. 2. Evolution of contact angles with time of PDMS hydrophilized with an oxygen-based plasma (filled triangles: advancing contact angles; open triangles: receding contact angles) and of PDMS grafted with PEG (circles).

2.6. Langmuir films

2.6.1. Structure of Langmuir films of conjugated disk-like molecules studied by synchrotron X-ray diffraction

N. Reitzel, T. Bjørnholm, *CISMI, Laboratory for Materials Science, Department of Chemistry, University of Copenhagen, Denmark,* A. Fechtenkötter, J. D. Brand, S. Ito, K. Müllen, *Max-Planck-Institut für Polymerforschung, Mainz, Germany,* K. Kjær, P. B. Howes and T. R. Jensen, *Condensed Matter Physics and Chemistry Department, Risø National Laboratory, Denmark*
e-mail: kristian.kjaer@risoe.dk   http://www.risoe.dk/fys/Employee/krkj.htm

The disk-like molecules hexa-benzo-coronene (HBC) substituted with alkyl chains or long chains terminated with carboxylic acids (Fig. 1) assemble in discotic 2-D structures at the air/water interface. The structure of the Langmuir films have been investigated by grazing-incidence synchrotron X-ray diffraction and synchrotron X-ray reflectivity measurements at beamline BW1. Depending on the substituents and the surface pressure applied to the Langmuir films, various distinct phases are observed. Here, only data from the monoacid substituted hexa-benzocoronene (1) are presented. The compression isotherm (Fig. 2) of the hexa-benzocoronene molecule 1 shows a transition between two distinct crystallographic phases. In the low-pressure phase a rectangular 2-D unit cell is seen with $a = 22.95$ Å and $b = 4.94$ Å (Fig. 3A), the tilted aromatic cores forming a coherent π-stack. As pressure is increased, only diffraction from the alkyl chains is seen and coherence in the π-stack is lost. Due to the limited number of Bragg reflections, the unit cell parameters cannot be uniquely identified but two possibilities are shown in Fig. 3B. In the high-pressure phase, the π-π distance is *increased*. The two phases can be thought of as a pressure induced switch such that, in the low-pressure phase, the π-π interactions are "on" and when pressure is increased they are turned "off".
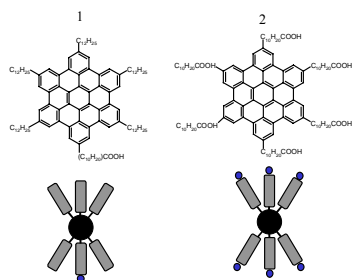
Fig. 1.
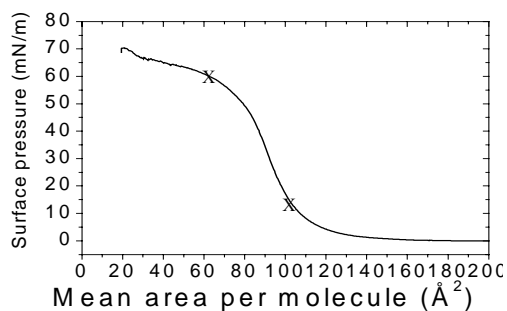
Fig. 2.
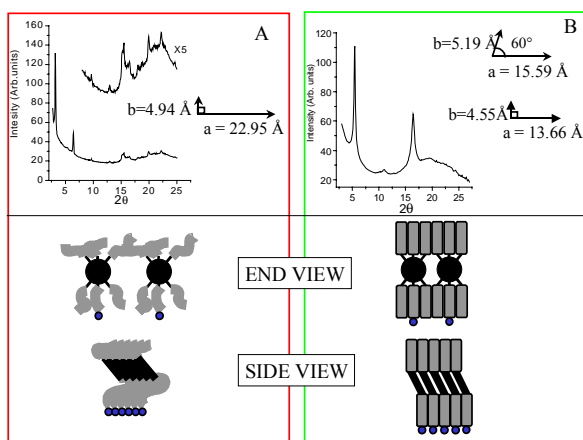
Fig. 3.

2.6.2. Langmuir films of self-complementary hydrogen bonded disk molecules

T. Bjørnholm, N. Reitzel, *CISMI, Laboratory for Materials Science, Department of Chemistry, University of Copenhagen, Denmark,* E. W. Meijer, J. H. K. K. Hirschberg and R. P. Sijbesma, *Laboratory of Organic Chemistry, Eindhoven University of Technology, The Netherlands,* T. R. Jensen and K. Kjær, *Condensed Matter Physics and Chemistry Department, Risø National Laboratory, Denmark*
e-mail: kristian.kjaer@risoe.dk   http://www.risoe.dk/fys/Employee/krkj.htm

Self-complementary hydrogen bonded disk-shaped molecules, illustrated in Fig. 1, can be manipulated to form hydrogen bonded polymers[1] and discotic phases typically in non-polar organic solvents or in the bulk. This is a step wise process; first the two complementary half-disks assemble into a full disk by hydrogen bonding. Next the full disks organize in larger supramolecular aggregates such as polymers or columns depending on the detailed molecular structure of the monomer (Fig. 1). In this way molecular recognition through hydrogen bonding is directly coupled to the co-operative assembly of molecular nanoscale architectures as illustrated in Fig. 1.
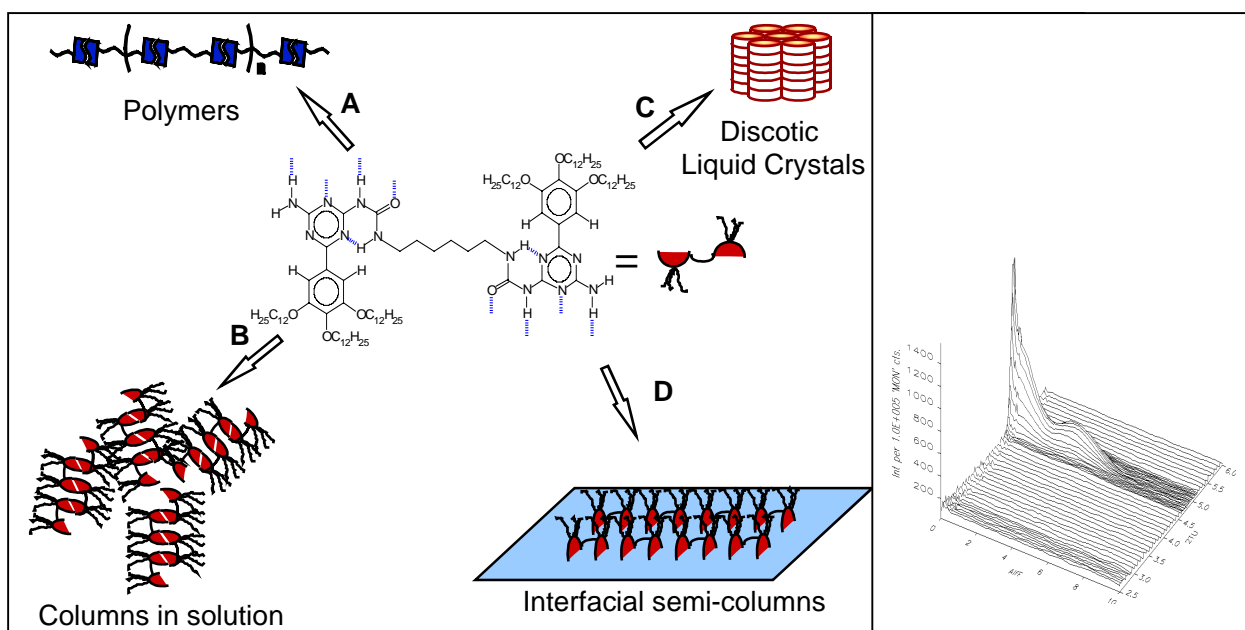
Fig. 1. Left: Schematic representation of various aggregation phenomena of self-complementary hydrogen bonded half disks (shown in middle). Right: Bragg rod of semi-columns assembled at the air-water interface.

We have extended the study of the organization of these systems to interfaces. By X-ray diffraction and specular reflectivity studies of Langmuir films of these molecules we have shown that highly ordered "semi-columnar" lamellae form at the air-water interface (Fig. 1 D). By Langmuir-Blodgett multi-layer deposition the half-disk bound to the water surface are allowed to reassemble into "full disks" resulting in the layer by layer deposition of re-assembled columns. Multi-layer films possess optical properties which indicate the formation of a new supramolecular arrangement which presently is being studied by XRD.

---

[1] R. P. Sijbesma, F. H. Beiher, L. Brunsveld, B. J. B. Folmer, J. H. K. K. Hirschberg, R. F. M. Lange, J. K. L. Lowe and E. W. Meijer, Science **278**, 1601 (1997).

2.6.3. GIXD Investigation of a Conjugated Cyclomer at the Air-Water Interface

J. Majewski, G. Smith, J. Roberts, *Los Alamos National Laboratory, LANSCE-12, Los Alamos NM 87545, USA,* K. Kjær, *Condensed Matter Physics and Chemistry Department, Risø National Laboratory, DK-4000 Roskilde, Denmark*

e-mail: kristian.kjaer@risoe.dk   http://www.risoe.dk/fys/Employee/krkj.htm

By grazing-incidence x-ray diffraction (GIXD) at beamline BW1, we have investigated the in-plane structure, at the air–water interface in a Langmuir trough at 10°C, of an amphiphilic charge-transfer cyclomeric compound (Fig. 1) which is of interest for possible non-linear optics applications. Only upon compression to 30mN/m did we observe one in-plane diffraction peak: at $q_{xy} \cong 1.03\text{Å}^{-1}$, corresponding to $d = 6.1\text{Å}$, (Fig. 2). The FWHM(q_{xy}) of this peak is 0.076Å^{-1} which indicates an in-plane coherence length of approximately 75Å.
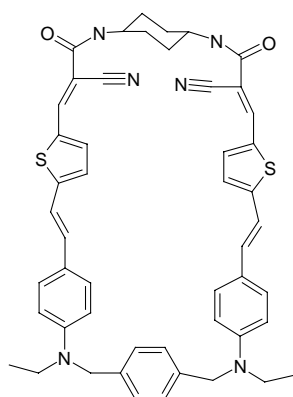
Fig. 1.
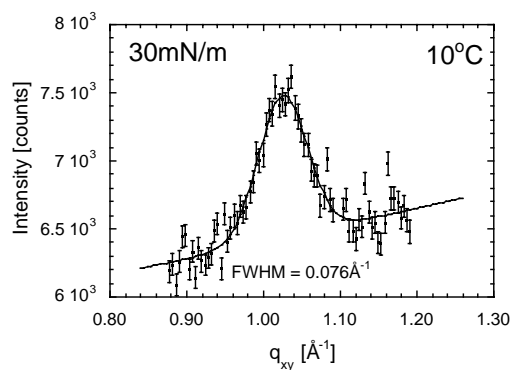
Fig. 2. Bragg peak at $q_{xy} \cong 1.03\text{Å}^{-1}$. The solid line is a Gaussian fit to the intensity distribution.

The corresponding q_z-resolved intensity distribution (Bragg rod) is shown in Fig. 3. A Gaussian fit to it gave FWHM(q_z) = 0.62Å^{-1}, which indicates that the coherently scattering portion of the cyclomer molecule is about 10Å high. The electron density distribution in the cyclomer molecule can be approximated by an ellipsoidal shape 10 x 20 x (4-6) Å^3. With the d-spacing of 6.1 Å this suggest that the cyclomer molecules lie edge-on on the water surface, with the longer edge in contact with the subphase. The intensity distribution of the Bragg rod (Fig. 3) has its maximum at $q_z \approx 0\text{Å}^{-1}$, implying that the molecular planes are approximately perpendicular to the water surface. In conclusion, our results suggest that at 30mN/m the cyclomer molecules are arranged in the monolayer with the longer edge in contact with the water subphase (Fig. 4.), stacked plane-parallel along the interface and with approximately 12 molecules in positional registry.

Fig. 4. Model of the proposed packing arrangement.

Fig. 3. Bragg rod intensity distribution of the diffraction peak at $q_{xy} \cong 1.03\text{Å}^{-1}$. The solid line is a Gaussian fit to the data.

2.6.4. Lipase adsorption at the air/water interface and the crystallographic phase problem for X-ray reflectivity

T. R. Jensen, K. Kjær, P. B. Howes, *Condensed Matter Physics and Chemistry Department, Risø National Laboratory, Denmark,* K. Balashev, N. Reitzel, T. Bjørnholm, *CISMI, Laboratory for Materials Science, Chemistry Department, University of Copenhagen, Denmark,* M. Ø. Jensen, G. H. Peters, *Department of Chemistry, The Technical University of Denmark, Denmark* and A. Svendsen, *Enzyme Design, Novo Nordisk A/S, Denmark*
e-mail: torben.rene.jensen@risoe.dk   http://www.risoe.dk/fys/Employee/toreje.htm

Specular X-ray reflectometry is a powerful method for the characterisation of interfaces. The laterally averaged electron density profile, $\rho(z)$, can be extracted, on an absolute scale, from the measured reflectivity data, $R(q_z)$[1]. A model-independent method for data inversion[2] can be valuable. However, the phase problem of crystallography can lead to non-unique $\rho(z)$ profiles when physico-chemical knowledge (bond lengths and angles, etc.) is not available to constrain the solutions. Using the liquid surface diffractometer at beamline BW1 we have investigated the microbial lipase *HLL* produced by Novo Nordisk A/S, Copenhagen (Lipolase™). Figure 1 shows the measured normalised *reflectivity $R(q_z)/RF(q_z)$* (points) for lipase adsorbed at the air-water interface. Figure 2 shows three $\rho(z)$ profiles (preliminarily extracted by a model-independent method[2]) which are all consistent with observation for $q_z < 0.65$ Å^{-1}, as seen from the three corresponding calculated reflectivity curves shown in figure 1. Profile (A) in Fig. 2. is chosen as the most realistic by comparison with $\rho(z)$ calculated by molecular dynamics. A profile similar to (A) can be constructed with a single slab of constant density but with different roughness at the two interfaces. Small angle X-ray diffraction from the adsorbed lipase film suggests hexagonal packing with lattice parameter, $a = 53$ Å.
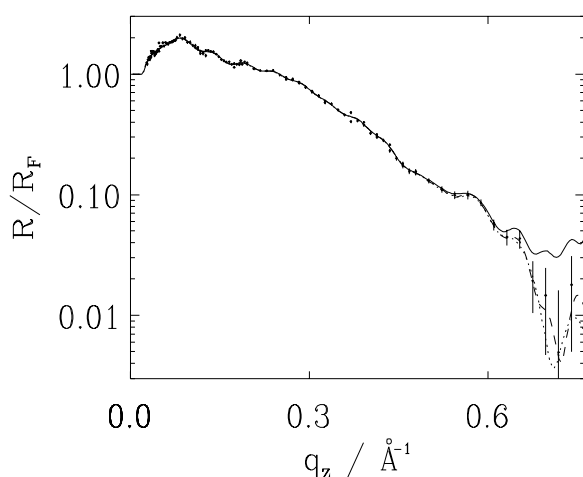
Fig. 1. Observed reflectivity (points) and three fitted curves for lipase at the air/water interface.
A: ——— , B:- - - , C:· · · · ·.
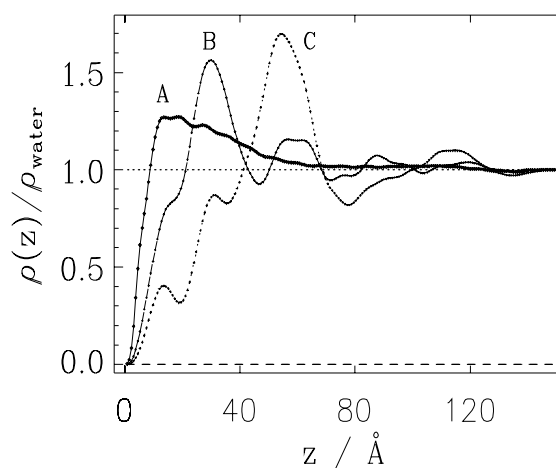
Fig. 2. Three-electron density models for lipase adsorbed at the air/water interface

---

[1] J. Als-Nielsen, D. Jacquemain, K. Kjær, F. Leveiller, M. Lahav and L. Leiserowitz, Phys. Rep**. 246**, 251 (1994).
[2] J. S. Pedersen and I. W. Hamley, J. Appl. Crystallogr. **27**, 36 (1994).

2.6.5. Lipid-lipase interactions investigated using synchrotron x-ray scattering

T. R. Jensen, K. Kjær, P. B. Howes, *Condensed Matter Physics and Chemistry Department, Risø National Laboratory, Denmark,* A. Svendsen, *Enzyme Design, Novo Nordisk A/S, Denmark,* K. Balashev, N. Reitzel and T. Bjørnholm, *CISMI, Laboratory for Materials Science, Chemistry Department, University of Copenhagen, Denmark*
e-mail: torben.rene.jensen@risoe.dk   http://www.risoe.dk/fys/Employee/toreje.htm

Lipases and other enzymes are of increasing importance within a broad range of fields, *e.g.* organic synthesis and the detergent industry. We have investigated the lipase *HLL* produced by Novo Nordisk A/S, Copenhagen and utilised in washing powder (Lipolase™). Detailed knowledge of lipase adsorption and hydrolysis of lipid layers is crucial for the improvement of the catalytic efficiency by protein engineering. Specular X-ray reflectometry of a monomolecular layer at the air/water interface is a powerful method[1] which we have utilised at the liquid surface diffractometer at beamline BW1[2] for investigation of lipid-lipase interactions. Initially a monomolecular layer of lipid is characterised by X-ray scattering; then lipase is injected under the monolayer. Two classes of glycerolipids were investigated: 2D-'crystalline' lipids, *e.g.* dipalmitoylglycerol (DPG) having saturated hydrocarbon moieties, and glycerolipids which form amorphous monolayers, *e.g.*, monooleoylglycerol (MOG) with a *cis* double bond.

The measured specular reflectivity, $R(q_z)$, from a monolayer of MOG (triangles) is shown in figure 1 along with the reflectivity measured 2.5 hours after injection of lipase under the MOG monolayer (diamonds). A dramatic change of the reflectivity is observed, presumably due to adsorption of lipase. Additional modulations of the reflectivity curve (marked by dashed lines) can be used to give a first estimate of the layer thickness, using $L_z \approx 2\pi/\Delta q_z \approx 80$ Å. Further data analysis is required in order to interpret this layer thickness in terms of one or more full lipase layers adsorbed under the lipid monolayer: An electron density profile has to be extracted and visualised as a molecular model. grazing-incidence X-ray diffraction[1] was used as well for characterising the crystalline monolayers before and after lipase adsorption.
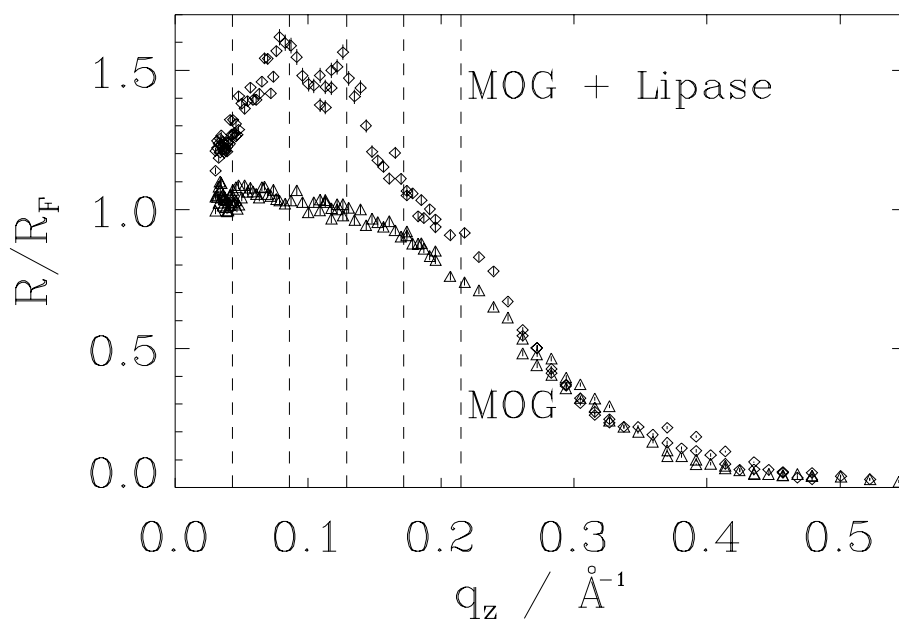
Fig. 1. Normalised specular reflectivity, $R(q_z)/R_F(q_z)$, for a monolayer of MOG before (triangles) and 2.5 hours after injection of lipase under the MOG monolayer (diamonds).

---

[1] J. Als-Nielsen, D. Jacquemain, K. Kjær, F. Leveiller, M. Lahav and L. Leiserowitz, Phys. Rep. **246**, 251 (1994).
[2] In Hasylab at DESY, Hmaburg, Germany

2.6.6. Monolayer structures of triple-chain phosphatidylcholines as substrates for phospholipases

U. Dahmen-Levison, G. Brezesinski, H. Möhwald, *Max-Planck-Institute of Colloids and Interfaces, Golm/Potsdam, Germany,* T. R. Jensen and K. Kjær, *Condensed Matter Physics and Chemistry Department, Risø National Laboratory, Denmark*
e-mail: kristian.kjaer@risoe.dk   http://www.risoe.dk/fys/Employee/krkj.htm

This study is performed as a part of investigations on the enzymatic hydrolysis of phospholipids by phospholipase A_2 (PLA_2). It is known that the activity of PLA_2 depends on the properties of the lipid substrate, such as thermodynamical state, crystallographic and chemical structure. The study of phospholipids with well-defined chemical modifications should help to understand the mechanism of hydrolysis by PLA_2 and to find potential inhibitors. Branched-chain phospholipids have been used as substrates for PLA_2 and were found to be resistant to hydrolysis[1]. In order to elucidate the competitive interactions between the hydrophilic headgroup and the hydrophobic chain regions, a number of molecular properties (chain length, linkage to the glycerol, branching) were varied. Film-balance pressure/area isotherms and grazing-incidence X-ray diffraction (GIXD) experiments, using the liquid surface diffractometer at the undulator beamline BW1[2], were utilized in the present study.

At higher lateral pressures, monolayer structures of all triple-chain compounds investigated show hexagonal packing of the hydrophobic chains. Differences are observable at lower lateral pressures. Components substituted (branched) at the 2-position result in monolayers consisting of rectangular unit cells with tilted chains.
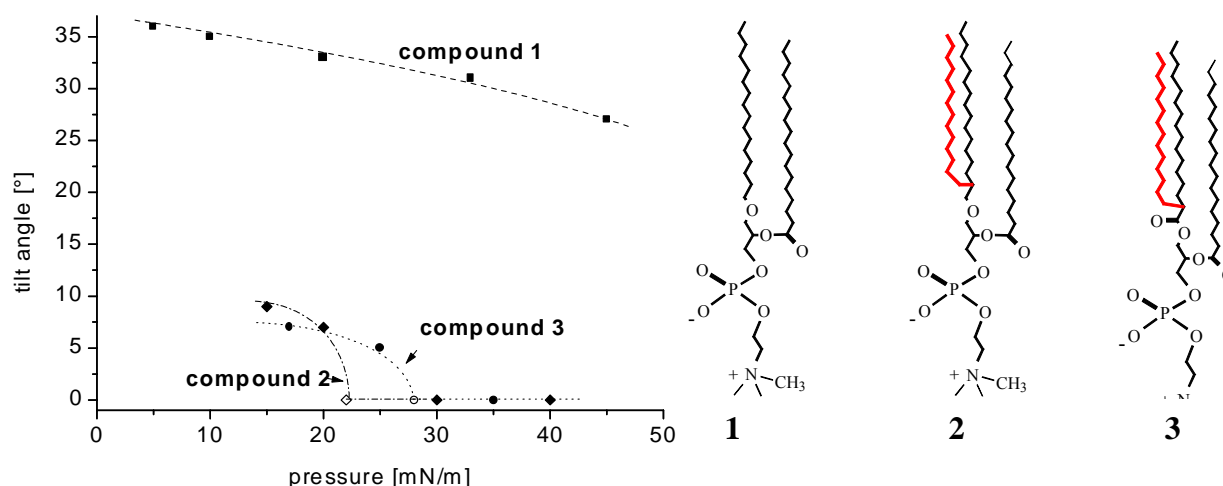
Fig. 1. *Left*: Tilt angles of compounds **1** (■), **2** (◆) and **3** (●) as a function of pressure. Open symbols represent the pressure of the tilting transition determined from the pressure/area isotherms. *Right*: Chemical structures of compounds **1** (1-O-hexadecyl-2-stearoyl-phosphatidylcholine), **2** (1-O-(2-tetradecyl-hexadecyl)-2-stearoyl-phosphatidylcholine) and **3** (1-(2-tetradecyl-palmitoyl)-2-stearoyl-phosphatidyl-choline).

Figure 1 compares the tilt angles of the unbranched with those of two branched-chain compounds The replacement of an ether (-O-CH$_2$-) in compound **2** by an ester linkage (-O-CO-) in compound **3** does not change the polymorphism. At low lateral pressure, the tilt angle is slightly reduced compared to the ether compound. The pressure of the tilting transition (determined from the kink in the isotherm) is shifted to larger values. Branching at the 4-position (not shown) reduces the stiffness of the molecules, acting as a hydrophobic spacer. Therefore 4-substituted branched components exhibit hexagonal packing of upright-oriented chains already at lower pressures. The cross-sectional chain area of the branched compounds is rather large (*ca.* 20.8 Å^2).

[1] F. M. Menger and M. G. Wood, Angew. Chem. **101**, 1277 (1989).
[2] In Hasylab at DESY, Hmaburg, Germany

2.6.7. Cardiolipin: A four-chain phospholipid coupled to the charged polyelectrolyte PDADMAC

C. Symietz, G. Brezesinski, H. Möhwald, *Max-Planck-Institute of Colloids and Interfaces, Golm/Potsdam, Germany,* K. Kjær, T. R. Jensen, *Condensed Matter Physics and Chemistry Department, Risø National Laboratory, Denmark*
 e-mail: kristian.kjaer@risoe.dk   http://www.risoe.dk/fys/Employee/krkj.htm

Charged polyelectrolyte chains dissolved in water do not tend to adsorb at the air/water interface. However in the presence of an oppositely charged monolayer of surface active substances a strong electrostatic interaction can result in the formation of coupled double layers. They represent a well ordered combination of self organized lipids, similar to biological membranes, and the mechanically stabilizing polymer chains. It is difficult to characterize the polyelectrolyte layer directly, but the observation of structure changes in the lipid layer allows some conclusions about the layer formation. Extensive studies by de Meijere[1,2] on 1,2-dipalmitoyl phosphatidic acid (DPPA) coupled to polydiallyldimethyl-ammonium chloride (PDADMAC) resulted in a model of rod shaped, horizontally streched PDADMAC molecules coupled in a one to one stoichiometry to the DPPA monolayer. A correspondence was found between the calculated distance of the positive binding sites on PDADMAC with the lattice parameters of DPPA. The grazing-incidence X-Ray Diffraction (GIXD) measurements were performed at the liquid surface diffractometer on the undulator beamline BW1 at HASYLAB, DESY in Hamburg, Germany. GIXD from the quadruple-chain phospholipid cardiolipin on water shows a rectangular NN-tilted chain lattice at lower surface pressure. After a phase transition above $\pi = 12$ mN/m (pressure area isotherm Fig.1) the tilt angle of the chains is reduced to zero and a hexagonal chain packing is observed, indicated by a single diffraction peak which for 30 mN/m is shown in Fig. 2. (top). Its position at $Q_{xy} = 1.494$ Å^{-1} gives a lattice parameter of 4.86 Å and an area per molecule of 82 Å^2. The FWHM $= 0.015$ Å^{-1} corresponds to a positional coherence length of $L=470$ Å using the Scherrer equation. On binding of PDADMAC this well ordered hexagonal lattice is expanded and disturbed. A broad peak of very low intensity at $Q_{xy} = 1.398$ Å^{-1} yields an area per chain of 23.3 Å^2 under the assumption of a hexagonal-like lattice. The FWHM $= 0.245$ Å^{-1} gives a coherence length of only 23 Å, leading to the idea of clusters of tens of cardiolipin molecules kept apart by the binding to relatively stiff PDADMAC chains. A comparable broad peak is observed on water at $T = 25$ °C in the liquid expanded phase just below the transition pressure to the LE/LC coexistence region. Thus one can assume a weak interaction between the four chains of a single molecule that results in a poorly correlated structure which consequently can also be detected after the coupling of PDADMAC. The chains are in a fluid-like state with a molecular area typical for liquid-crystalline L_α-phases in lipid/water dispersions.
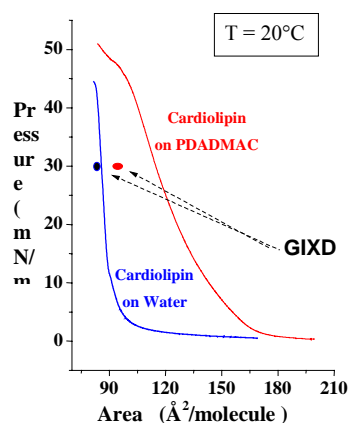
Fig. 1. (*left*): Pressure area isotherms of Cardiolipin on water and on PDADMAC (c = 10^{-3} mol/l) with the marked values of area per molecule from the GIXD measurements.

Fig. 2. (*right*): GIXD peaks of DPPA integrated over Q_z measured at $\pi = 30$ mN/m on water (top) and on PDADMAC (bottom).
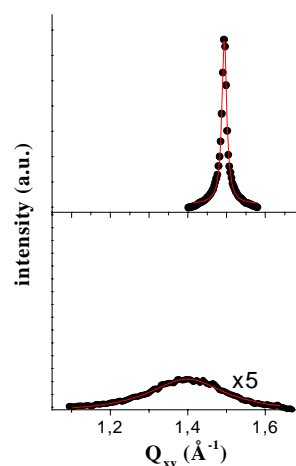
[1] K. de Meijere, G. Brezesinski and H. Möhwald, Macromolecules **30**, 2337 (1997).
[2] K. de Meijere, PhD thesis, University of Potsdam, Germany (1998).

2.6.8. X-ray and neutron reflectivity from surface monolayers of a lipopolymer

A. Wurlitzer, P. Krüger, M. Weygand, M. Lösche, *Institute of Experimental Physics I, University of Leipzig, Germany,* E. Politsch, G. Cevc, *Institute of Medical Biophysics, Technical University Munich, Germany* and K. Kjær, *Condensed Matter Physics and Chemistry Department, Risø National Laboratory, Denmark*
e-mail: kristian.kjaer@risoe.dk   http://www.risoe.dk/fys/Employee/krkj.htm

A lipopolymer with a polyoxazoline headgroup (1,2-dioctadecanyl-*sn*-glycero-3-poly(2-methyl-2-oxazoline), PMO), designed for application as a pharmaceutical drug carrier, has been characterized in monolayers at the air-water interface. Using X-ray and neutron reflectometry, the molecular conformations of the lipopolymer at the liquid surface were investigated as a function of lateral area per molecule, particularly with respect to the plateau observed in the isotherm. Conceptually, such a plateau may be caused by a first order transition either within the polymer (mushroom-to-brush)[1,2] or within the lipid hydrocarbon chains[3]. In order to warrant compatibility of the data sets for a simultaneous evaluation we have studied the same lipopolymer – patterned by isotopic (H/D) substitution on the polyoxazoline moiety – both in neutron and X-ray measurements. Reflectivity data were obtained below and above the phase transition (at lateral pressures π = 17.5 mN/m and 30.0 mN/m) at T = 15°C on H_2O and D_2O for neutrons and on H_2O for X-rays. For evaluation, a novel approach to data inversion was applied that utilizes an Evolution Strategy (ES) based algorithm[4] acting on ensemble conformations of the polymers. This procedure provides a realistic impression of the (averaged) organization of the molecules at the interface. From the optimized ensemble configurations, the resulting volume density (Φ) distributions have been deduced (Fig. 1). We observe that the hydrophilic polymers are similarly organized on both sides of the phase transition, and even at high π, the molecules are not completely elongated. The alkyl chains, by contrast, change their average organization at the interface qualitatively: The model suggests they are confined to the hydrophilic/hydrophobic interface at the lower pressure, whereas they may protrude more deeply into the subphase above the phase transition, similar to the situation observed with PEG lipopolymers[5]. From these result we conclude, that the plateau in the investigated pressure range should not be assigned to a mushroom-to-brush transition of the hydrophilic polymer but must be attributed to a transition of the hydrocarbon chains.
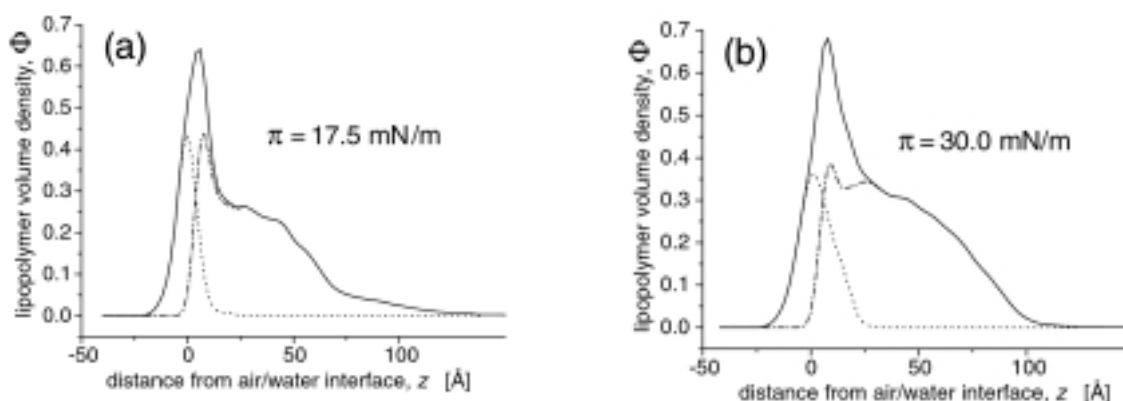
Fig. 1. Volume density distribution, $\Phi = \Phi(z)$, of the lipopolymer across the interface at two lateral pressures, (a) π = 17.5 mN/m and (b) π = 30.0 mN/m. Shown are partial volumes of the hydrophilic headgroups (dash-dotted lines) and of the alkyl chains (dotted lines) as well as total molecular volumes of the lipopolymer (continuous lines). $z > 0$ indicates the aqueous subphase. $z < 0$ corresponds to the air half-space.

[1] S. Alexander, J. Phys. **38**, 983 (1977).
[2] P.G. de Gennes, Adv. Colloid Interf. Sci. **27**, 189 (1987).
[3] T. R. Baekmark, T. Wiesenthal, P. Kuhn, T. M. Bayerl, O. Nuyken and R. Merkel, Langmuir **13**, 5521 (1997).
[4] H.-P. Schwefel, Evolution and Optimum Seeking, J. Wiley & Sons, New York (1995).
[5] T. L. Kuhl, J. Majewski, P. B. Howes, K. Kjær, A. von Nahmen, K. Y. C Lee, B. Ocko, J. N. Israelachvili and G. S. Smith, J. Am. Chem. Soc. **121**, 7682 (1999).

2.6.9. Phospholipid headgroup organization of DMPA in Langmuir monolayers

M. Schalke, P. Krüger, M. Weygand, M. Lösche, *Institute of Experimental Physics I, University of Leipzig, Germany* and K. Kjær, *Condensed Matter Physics and Chemistry Department, Risø National Laboratory, Denmark*

e-mail: kristian.kjaer@risoe.dk   http://www.risoe.dk/fys/Employee/krkj.htm

A new approach to the data refinement of reflectivity measurements from lipid surface monolayers at high momentum transfer, q_z – applied to DMPA[*] on pure water – has revealed the structural organization of the lipid in unprecedented detail and provided new insights into headgroup conformation and hydration as a function of lateral pressure π. While conventional box models are incapable of satisfactorily modelling the experimental data at high momentum transfer, a quasimolecular composition-space refinement approach using distribution functions to map the spatial organization of submolecular headgroup fragments yields a much better description and overcomes inherent difficulties of box models[1]. Space filling in this approach is achieved by using volumetric information – from molecular dynamics simulations[2] – as constraints in the least-square fitting.

We find that the conformation of the lipid headgroups – as assessed by their average inclination angle α from the surface normal – is tightly coupled to the ordering of the acyl chains. The spread of the headgroup fragment distribution is considerably larger than the global interface roughness and increases with compression. In distinction to earlier work on DMPE[*] using the two-box approach[3], we find that the phosphate hydration stays essentially constant along the entire isotherm. For DMPA monolayers on subphases containing divalent cations – Ba^{2+} or Ca^{2+} – this approach to data refinement suggest[4] that stochoimetric binding of cations, $DMPA^-:Cat^{2+} = 2:1$, occurs only at exceedingly low areas per molecule, A. At $> 41.5 \text{ Å}^2$, both cations *and* anions are incorporated into the headgroups in significant amounts. They are continuously squeezed out of the headgroup region upon compression. Surprisingly, not even ion binding to the headgroup affects phosphate hydration significantly within the confidence limits of the measurements: The number of water molecules per phosphate, n_W is found in a narrow corridor between 5 and 6, with an experimental uncertainty of $+1/–2$. To accommodate for the extra space upon ion binding, headgroups on subphases containing Ba^{2+} are tilted away from the surface by ~ 10° further than headgroups on pure water at comparable values of A.

[*]abbreviations:

DMPA – dimyristoylphosphatidic acid; DMPE – dimyristoylphosphatidylethanolamine
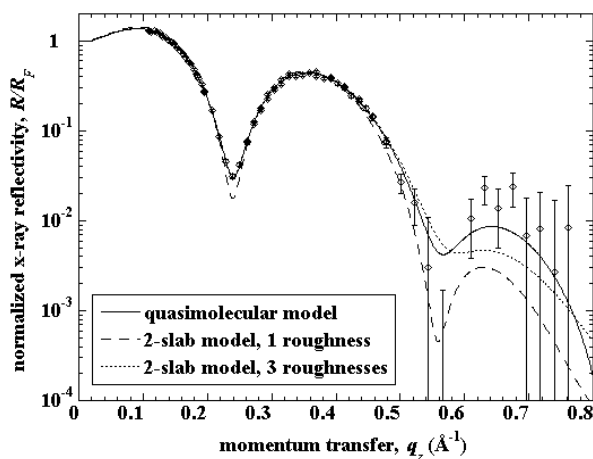
Fig. 1. Data refinement of X-ray reflectivity measurements from a DMPA monolayer on water ($T = 27°C$, π = 45 mN/m). The conventional box models are clearly incapable of describing the data satisfactorily, whereas the quasimolecular approach to data modelling describes the data reasonably well.

[1] M. Schalke, P. Krüger, M. Weygand and M. Lösche., Biochim. Biophys. Acta. In the press.
[2] R. S. Armen, O. D. Uitto and S. E. Feller, Biophys. J. **75**, 734 (1998).
[3] C. A. Helm, P. Tippmann-Krayer, H. Möhwald, J. Als-Nielsen and K. Kjær, Biophys. J. **60**, 1457 (1991).
[4] M. Schalke and M. Lösche, Adv. Colloid Interf. Sci. Submitted for publication.

2.6.10. Bacterial S-layer protein coupling to lipids: Combination of x-ray and neutron reflectivity measurements for a detailed assessment of the protein/lipid interface

M. Weygand, M. Lösche, *Institute of Experimental Physics I, University of Leipzig, Leipzig, Germany,* B. Wetzer, D. Pum, U. B. Sleytr, *Ultrastructure Research, University for Agricultural Sciences, Vienna, Austria,* P. B. Howes and K. Kjær, *Condensed Matter Physics and Chemistry Department, Risø National Laboratory, Denmark*
e-mail: kristian.kjaer@risoe.dk   http://www.risoe.dk/fys/Employee/krkj.htm

We have recently studied the coupling of bacterial surface (S)-layer proteins in monomolecular sheet crystals to lipid model membranes with x-ray reflectivity and grazing-incidence diffraction (GIXD)[1,2]. Upon protein recrystallization at DPPE[*] surface monolayers, a broadening of the lipid headgroup distribution along the surface normal, z, was revealed by high resolution ($q_z^{max} \sim 0.8$ Å^{-1}) reflectivity measurements. At the same time, a slight increase of the scattering length in the headgroup region was observed, indicating that protein material inserts into this region[1]. By contrast, both X-ray reflectivity and grazing-incidence diffraction showed that the lipid chains are not affected by protein adsorption and crystallization. More recently, we have performed complementary neutron reflectometry measurements on the same system to particularly assess the protein/lipid interface in detail. For the protein from *Bacillus sphaericus* CCM2177, the electron density profile suggests a thickness of the reconstituted S-layer of $\sim$ 90 Å and the presence of water-filled cavities near the center of this layer. A detailed analysis reveals that underneath the primary protein sheet crystal a partial secondary layer is formed in which the protein orientation is upside down with respect to the primary layer (*cf.* Fig. 1). With respect to the lipid/protein interface, the simultaneous analysis of x-ray data and neutron data suggests that on average less than one amino group ($\sim$ 65 electrons) per lipid penetrates the headgroup region and yields the water distribution in that region (Fig. 1).

Similar X-ray measurements performed with the S-layer protein from *B. coagulans* E38–66 reveal a similar overall picture of the coupling of a monomolecular protein sheet crystal to a phospholipid monolayer[2].

[*]abbreviation: DPPE – dipalmitoylphosphatidylethanolamine
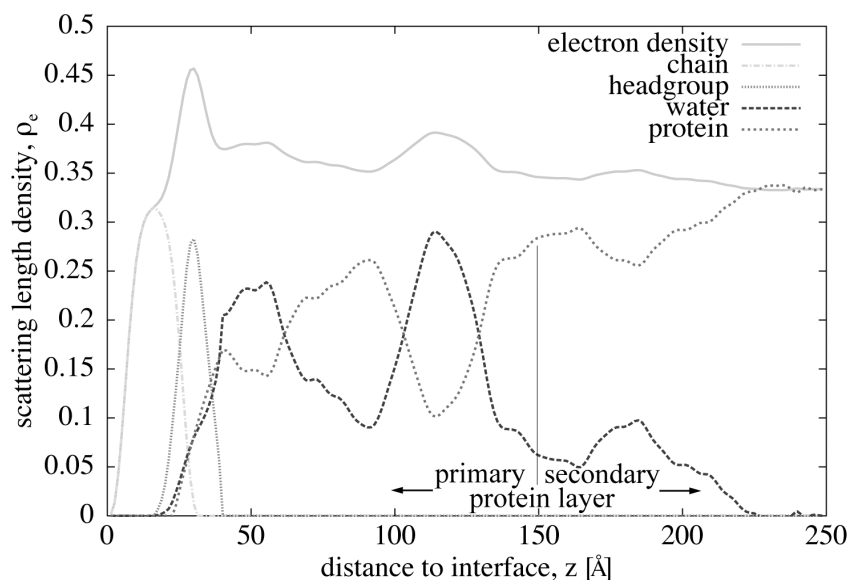
Fig. 1. Chemical model of the DPPE/CCM2177 layer system derived from X-ray and neutron reflectometry. Shown is the electron density profile which describes the X-ray data with high fidelity.[1] Using the neutron data, this profile has been decomposed into the individual contributions of the system components: Protein, water and lipid headgroups and chains. Note the contribution of the secondary protein layer, most prominent around z = 180 Å, which mirrors the contribution of the primary protein sheet crystal around z = 120 Å.

[1] M. Weygand, B. Wetzer, D. Pum, U. B. Sleytr, N. Cuvillier, K. Kjær, P. B. Howes and M. Lösche, Biophys. J. **76**, 458 (1999).
[2] M. Weygand, M. Schalke, P.B. Howes, K. Kjær, J. Friedmann, B. Wetzer, D. Pum, U. B. Sleytr and M. Lösche, J. Mater. Chem. In the press.

2.6.11. Towards spontaneous generation of enantiomerically pure peptides *via* polycondensation of racemic precursors at the air-water interface

I. Weissbuch, L. Leiserowitz, M. Lahav, *Department of Materials and Interfaces, Weizmann Institute of Science, Israel*, J. Als-Nielsen, *Ørsted Laboratory, University of Copenhagen, Denmark*, T. R. Jensen and K. Kjær, *Condensed Matter Physics and Chemistry Department, Risø National Laboratory, Denmark*
e-mail: kristian.kjaer@risoe.dk   http://www.risoe.dk/fys/Employee/krkj.htm

Recently we have reported on the spontaneous separation, in two-dimensions, of racemic long-chain derivatives of α-amino acids spread as Langmuir monolayers at the air-water interface[1]. These amphiphiles self-assemble into enantiomorphous crystalline domains containing molecules of single handedness when they contain an amide group within the alkyl chain. The amide groups promote molecular packing *via* translation symmetry by virtue of their tendency to hydrogen-bond along a 5 Å axis. Based on this concept, we have initiated a study of the surface polycondensation reaction of N-carboxyanhydrides (NCA) of the above amphiphiles to generate homochiral peptides, a question related to the origin of life. We expect that the racemic NCA derivative N^{ϵ}-stearoyl-lysine (NCA-*lys*), when spread on water, will spontaneously separate into domains containing molecules of single handedness, which, by reaction within single domains, should lead to peptides containing *lys* residues of a single handedness. Figures a-c show Grazing-Incidence X-ray Diffraction (GIXD) patterns measured from (a) (S)-NCA-*lys* self-assembled on pure water, (b) in "polymerized" form on a solution containing Ni^{2+} catalyst and (c) from the racemic amphiphile on either water or solution. Indeed, the three GIXD patterns exhibit three Bragg peaks consistent with packing in an oblique 2-D cell, the molecules being related by translation symmetry. Figures d-f show the corresponding GIXD patterns measured from NCA-γ-stearyl-glutamate (NCA-*glu*), an amphiphile without an amide group. Although the GIXD pattern of the optically pure NCA-*glu* on water (Figure d) displays three Bragg peaks consistent with an oblique unit cell, the pattern measured from the polymerized form (Figure e) exhibits only two peaks, presumably indicative of a centered rectangular unit cell with molecules related *via* translation. It is not yet clear whether the pattern measured for the racemic NCA-*glu* (Figure f) indicates a herring-bone packing of the chains or a translational packing as in the polymerized form of the optically pure amphiphile.

---
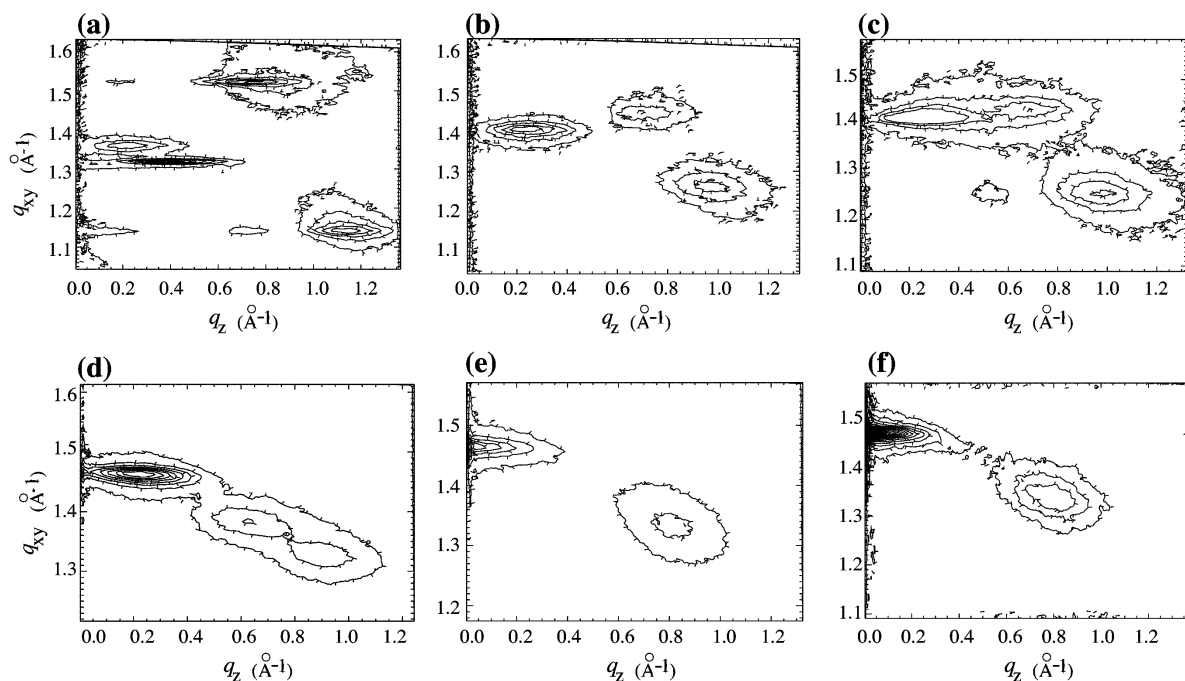
[1] I. Weissbuch, M. Berfeld, W. Bouwman, K. Kjær, J. Als-Nielsen, M. Lahav and L. Leiserowitz., J. Am. Chem. Soc., **119**, 933, (1997).

2.6.12. 2D-crystalline films of Cd^{2+} and Pb^{2+} salts of rigid-rod molecular wires aligned parallel to the air-water interface

I. Weissbuch, V. Hensel, L. Leiserowitz, M. Lahav, *Department of Materials and Interfaces, Weizmann Institute of Science, Israel,* J. Als-Nielsen, *Ørsted Laboratoru, University of Copenhagen, Denmark,* T. R. Jensen and K. Kjær, *Condensed Matter Physics and Chemistry Department, Risø National Laboratory, Denmark*
e-mail: kristian.kjaer@risoe.dk   http://www.risoe.dk/fys/Employee/krkj.htm

Organometallic salts involving monodisperse aromatic rigid rod molecular wires in the form of poly-*p*-phenyleneethynylene-dicarboxylic acids were designed to form oriented crystalline films to be converted into organized inorganic nano-size particles/organic composites. Two compounds, **1** and **2,** differing in the number of *p*-phenyleneethynylene units, were synthesized and spread, as chloroform solutions, over aqueous solutions containing Pb^{2+} or Cd^{2+} ions to yield oriented thin films of the corresponding dicarboxylic acid salts. The formation of oriented insoluble films, of layer structure with *d*-spacings of 33.7Å for **1** and 41.8Å for **2** consistent with the long rigid molecules being aligned parallel to the solution surface, was detected by grazing-incidence X-ray diffraction (GIXD), performed *in-situ* at the air-solution interface.
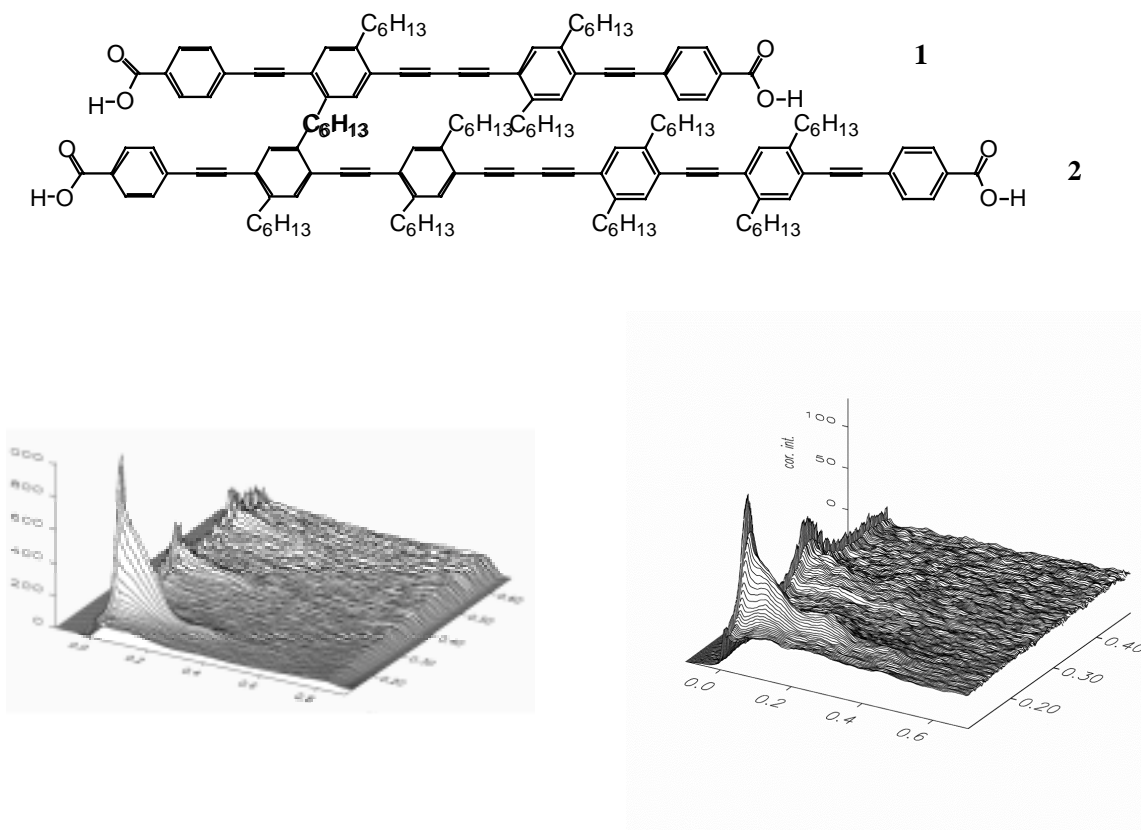
Fig. 1. GIXD patterns (*I vs. Q$_z$* and *Q$_{xy}$*) from the Cd^{2+} salt of **1** (left) and the Pb^{2+} salt of **2** (right)

2.6.13. Self-assembly into 2D-crystalline monolayers of molecules adopting an m-shape on the surface of water

I. Weissbuch, M. Lahav, L. Leiserowitz, *Department of Materials and Interfaces, Weizmann Institute of Science, Israel,* K. Lederer, A. Godt, G. Wegner, *Max-Planck-Institut für Polymerforschung, Mainz, Germany,* J. Als-Nielsen, *Ørsted Laboratory, University of Copenhagen, Denmark,* P. B. Howes and K. Kjær, *Condensed Matter Physics and Chemistry Department, Risø National Laboratory, Denmark*
e-mail: kristian.kjaer@risoe.dk   http://www.risoe.dk/fys/Employee/krkj.htm

Molecules containing four linear alkyl chains separated by three 1,3-bis(ethynylene)benzene units, designed to fold three times into an M-shape **1** as promoted by the affinity of the two hydrophilic OH end-groups to the water, were found to self-assemble, at the air-water interface, into crystalline monolayers. Such molecules self-assemble on water at a surface coverage as low as 30% to yield a grazing-incidence X-ray diffraction (GIXD) pattern with two Bragg peaks corresponding to a centered, rectangular subcell of dimensions $a_s = 5.0$ Å, $b_s = 8.7$ Å and molecules tilted along the a_s axis by 25° with respect to the surface normal. These cell dimensions and the tilt direction of the chains appear to be fingerprint evidence for the packing of all the molecules containing the 1,3-bis(ethynylene)benzene unit as a spacer and which are aligned in ribbons parallel to the b_s axis. In this arrangement, the chains of one molecule are separated by an average distance of ~8.7 Å. Consequently, b_s is a subcell dimension and must be multiplied by four to give the true unit cell repeat as $b = 34.8$ Å, whereas along a axis the unit cell repeat is $a = a_s = 5.0$ Å.

The crystalline film thickness of about 14 Å, as determined from the FWHM(q_z) of the two Bragg rods, indicates that chains of a length of 12 to 13 CH_2-groups contribute to the diffraction signal. X-ray structure factor calculations using an atomic coordinate molecular model yielded a good fit to the measured Bragg rods when chains of only 12 CH_2-groups were considered, indicating crystalline registry of only the central 12 CH_2-groups of the chains of the molecule. The packing arrangement is shown in Fig.1 as viewed parallel to the water surface (a) and along the chains molecular axes (b).

1
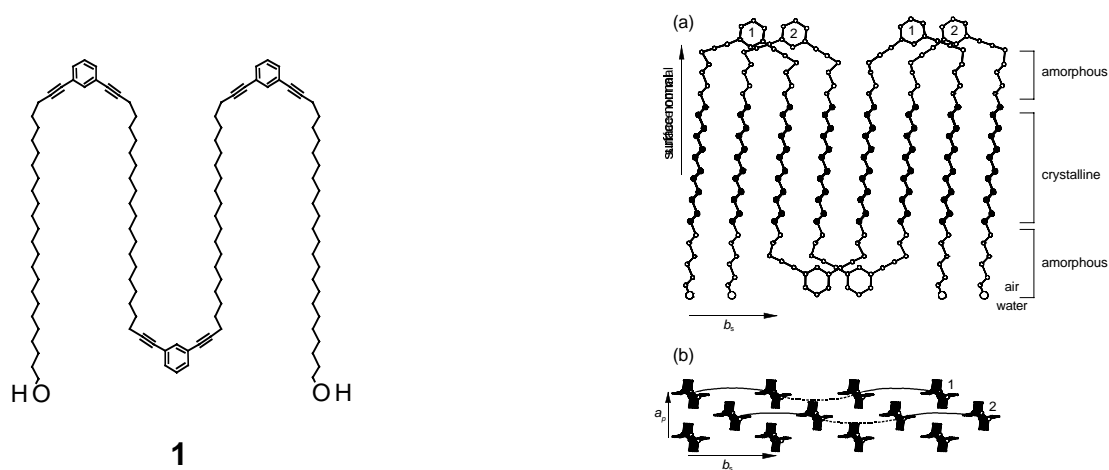
Fig. 1.

2.6.14. Self-assembled monolayers of folded molecules on the surface of water

I. Weissbuch, M. Lahav, L. Leiserowitz, *Department of Materials and Interfaces, Weizmann Institute of Science, Israel,* K. Lederer, A. Godt, G. Wegner, *Max Planck Institut für Polymerforschung, Mainz, Germany,* J. Als-Nielsen*, Ørsted Laboratory*, *University of Copenhagen, Denmark,* P. B. Howes and K. Kjær, *Condensed Matter Physics and Chemistry Department, Risø National Laboratory, Denmark*
e-mail: kristian.kjaer@risoe.dk   http://www.risoe.dk/fys/Employee/krkj.htm

Insertion of the 1,3-bis(ethynylene)benzene unit (Scheme 1) as a rigid spacer into a linear alkyl chain, thus separating the two resulting stems by 9Å, induces chain folding of molecules in monolayers at the air-water interface. Such folded molecules self-assemble into crystalline monolayers at the interface and are aligned with the plane of the folding unit almost perpendicular to the water surface, as determined by synchrotron grazing-incidence X-ray diffraction. Two molecular shapes of the type U and inverted U were obtained in the two-dimensional crystalline state, depending upon the number and position of the hydrophilic groups in the molecule (molecules **1-3**). A similar molecule but with a spacer unit imposing a 5Å separation between alkyl chains yields the conventional herring-bone arrangement (molecule **4**). The grazing-incidence X-ray Diffraction (GIXD) patterns of the monolayers of **1** and **4** are shown in Fig. 1 left and right as contour plots of the scattered intensity I(q_{xy},q_z). The analysis of all the GIXD patterns led to similar crystalline packing arrangements for the monolayers of **1-3**, with the intramolecular alkyl chains, separated by 8.7Å, forming molecular ribbons stabilised by intermolecular van der Waals contacts. The packing arrangement of **4** consists of intramolecular chains separated by 5 Å, equivalent to a conventional two-chain amphiphile.
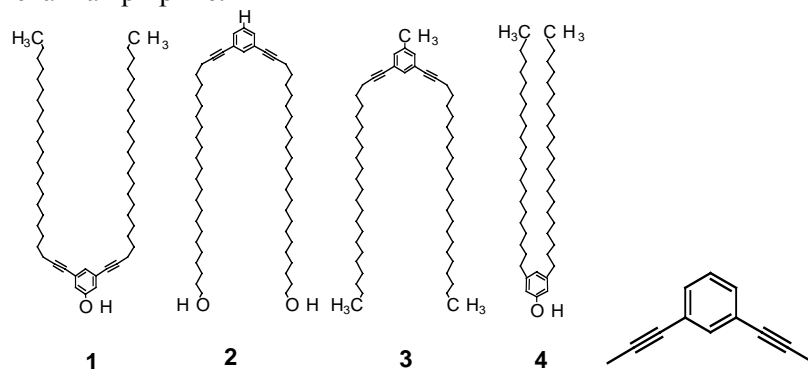
Scheme 1
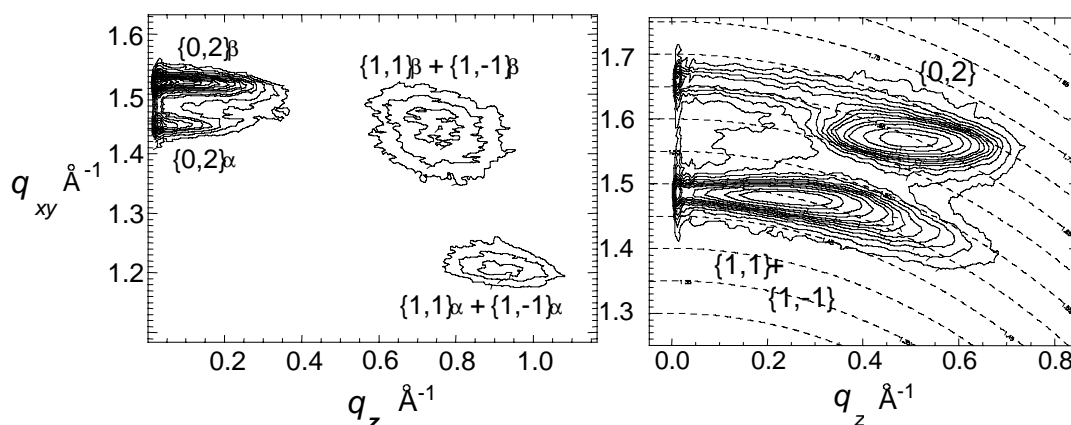
Fig. 1. Contour plots of the GIXD intensity measured for molecule **1** (left) and **4** (right).

2.7. Microemulsions, surfactants and biological systems

2.7.1. Interaction of β-lactoglobulin and aggregates of phosphorlipids

T. Ishøy, J. S. Pedersen, K. Mortensen, *Condensed Matter Physics and Chemistry Department, Risø National Laboratory, Denmark*, R. Bauer, *Institute for Mathematics and Physics, Royal Veterinary and Agricultural University, Denmark* and T. Nylander and J. Khakhar, *Physical Chemistry 1, Lund University, Sweden*
e-mail: torben.ishoy@risoe.dk   http://www.risoe.dk/fys/Employee/torish.htm

In the search of understanding the specific interactions between β-lactoglobulin (BLG) and bilayer stacks of phosphorlipids, small-angle x-ray and neutron scattering experiments have been made. Because of the flexibly nature of the phosphorlipid double layers and lack of perfect lattice structure, it is problematic to derive the structural information from scattering spectra from for example a multilayer system of swollen phosphorlipid bilayers. Theoretically the structural analysis has been restricted to only the dimension normal to the bilayer. Under most physiological conditions the pseudo two dimensional lipid bilayer is in a fluid (liquid crystalline) phase (the L_α phase). This L_α phase is a pseudo two-dimensional liquid with translational disorder and with a high degree of lipid acyl chain disorder. At a temperature below the main transition temperature T_m, the lipid bilayer is in a solid gel phase. In this gel phase the lipids-acyl-chains are highly ordered, and the bilayer is a pseudo two-dimensional crystalline solid.

For analysis of the collected SANS or SAXS spectra, there are basically two theories that have been applied for the derivation of an expression for the scattering function. The two theories are the Caillé- theory[1] and a paracrystalline theory[2]. The Caillé theory takes into account thermal disorder, i.e. oscillation of molecular positions around well defined sites within the unit-cell (disorder of first kind), as well as lattice disorder, i.e. lack of long-rang order and/or lack of a uniform unit-cell (disorder of second kind). In contrast paracrystalline theory takes into account only the disorder of second kind. In the analysis of the experimental data we have expanded a theoretical model based on a one dimensional paracrystalline theory parameterised in terms of a strip model[3] with a methyl layer in the middle of the lipid bilayer (Fig. 1). The reason for expanding the model with the methyl layer originates in published results on the absolute electron density of fully hydrated dipalmitoylphosphatidylcholine (DPPC) in the gel phase[4]. Further on we will, using the same strip type of model, derive an expression for the scattering function based on Caillé theory.
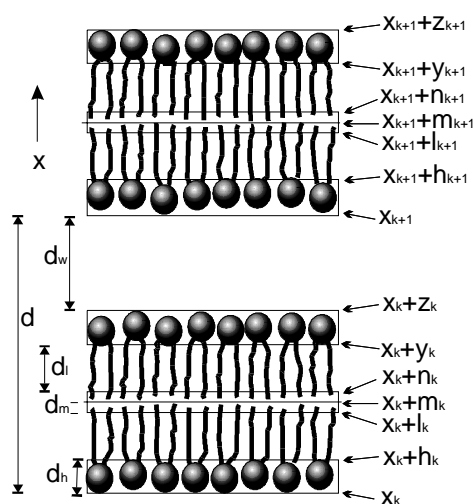
Fig. 1. Schematic illustration of a multi-lamellar array of lipid bilayers. The repeat distance of the system is d, d_h is the thickness of the headgroup, d_l is the thickness of the CH_2 and CH part of the lipid acyl chains, d_m is the thickness of the methyl layer, and the water layer between two neighbouring bilayers has the thickness d_w. The repeat distance d is equal to $2d_m+2d_l+2d_h+d_w$, the hydrophobic thickness of the bilayer is equal to $2d_m+2d_l$ and the hydrophilic thickness of the bilayer is equal to $2d_h+d_w$.

[1] A. Caillé, C. R. Acad. Sci Ser. B **274,** 891 (1972).
[2] R. Hossemann and S. N. Bacchi, Direct analyse of Diffraction by Matter (Noth-Holland, Amsterdam, 1962) p. 408.
[3] J. Lemmich, K. Mortensen, J. Hjort-Ipsen, T. Hønger, R. Bauer and O. G. Mouritsen. Phys. Rev. **E53**, (5) 5169 (1996).
[4] M. C. Wiener, R. M. Suterm and J. F. Nagle, Biophys. Jour. **55**, 315 (1989).

2.7.2. Solutions with a crystallization agent investigated by the SANS technique

T. Sørensen, *Norwegian University of Science and Technology, Department of Chemical Engineering, Trondheim, Norway,* J. Samseth, *SINTEF Energy Research, Department of Themal Energy, Trondheim, Norway and* K. Mortensen, *Danish Polymer Centre, Condensed Matter Physics and Chemistry Department, Risø National Laboratory, Denmark*
e-mail: kell.mortensen@risoe.dk   http://www.risoe.dk/fys/Employee/kemo.htm

Crystallization from solutions is an important process in the industry. One of the many problems with this technique is reproducibility, and another one is the fact that the theory of the crystallization process is still incomplete. Most crystallisation theories of molecular solutions postulate the existence of clusters in the stable liquid state. These clusters may or may not induce the crystallisation in supersaturated solutions. Small-angle neutron scattering experiments were performed with the aim to confirm the existence of clusters in molecular solutions of this type, and to investigate if there is a correlation between temperature and thermal history of cluster size and form. Two previous studies of such systems have been made applying SANS: a study of ND_4Cl in water (Gago-Duport), and a study of vanillin (3-methoxy-4-hydroxybenzaldehyde) in 20% 2-propanol with D_2O (Hussain). In the present study, different concentrations of vanillin and ethyl-vanillin (3-ethoxy-4-hydroxybenzaldehyde) (2-30 volume percent) solved in different concentrations of ethanol and 2-propanol in D_2O, and DTPA-BMA (Diethylenetriamine-pentaaceitc acid - Bismethylamin) in D_2O. Only two of the systems gave valuable scattering-data: vanillin in 20% ethanol and vanillin in 20% 2-propanol, both with saturation temperature $T_s=30^o$C. All the other samples except DTPA-BMA gave indications of cluster sizes of vanillin outside the resolution of the SANS-instrument. The DTPA-BMA sample gave no neutron scattering, which is in agreement with earlier light scattering experiments.

The scattering data was fitted to several functions. The best fit was obtained for ellipsoidal-formed aggregates. Typical SANS-data with fitted curves are given in fig. 1 for one of the samples. The resulting volume of the fitted ellipsoids is given in fig. 2. The experiments and their interpretation indicate that there is no hysteresis effect of thermal history, and that the volume of the clusters is proportional to the exponential of the sample temperature. No Porod region was found, but the experimental data fitted nicely to an exponential function with exponent in the range –1.35 to –1.55 for scattering vector larger than 0.1 Å^{-1}.
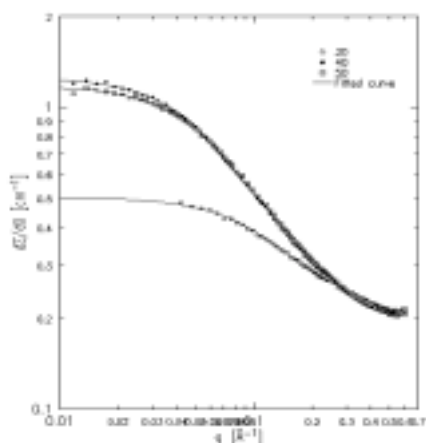
Fig. 1. SANS data of vanilin in as obtained at 30, 40 and 50°C.
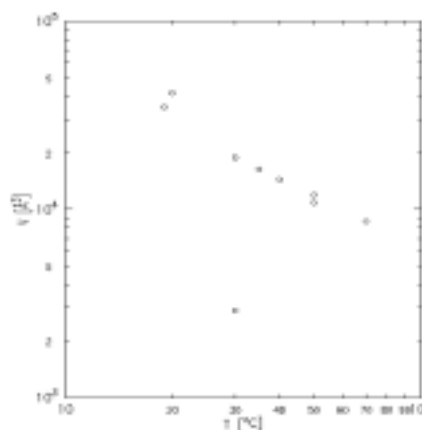
Fig. 2. Resulting volume of vanilin clusters, versus temperature

2.7.3. Droplet polydispersity and shape fluctutions in AOT microemulsions studied by contrast variation small-angle neutron scattering

L. Arleth and J. S. Pedersen, *Condensed Matter Physics and Chemistry Department, Risø National Laboratory, Denmark*
e-mail: lise.arleth@risoe.dk   http://www.risoe.dk/fys/Employee/liar.htm

Microemulsions consisting of AOT (bis(2-ethylhexyl)sulfosuccinate sodium salt), water and respectively, decane and iso-octane are studied in the region of the phase diagram where surfactant covered water droplets are formed. The aim of the study is to determine and compare the polydispersity and shape fluctuations of the microemulsion droplets in the two different alkane types. Conductivity measurements show that there is a severe temperature dependence of the microemulsion behaviour on the type of alkane used. In both cases the microemulsion droplets start to form larger aggregates when the temperature increases. But in the system with decane this aggregation temperature occurs at a temperature about 10 degrees lower than in the similar system with iso-octane. The aggregation phenomena are avoided and the two systems are at approximately the same reduced temperature with respect to this aggregation temperature, when the temperature of the AOT/D_2O/decane microemulsion is 10°C and the temperature of the AOT/D_2O/iso-octane is 20°C. Contrast variation SANS measurements are performed at these temperatures on systems with volume fractions of 5% D_2O+AOT by varying the scattering length density of the alkane. The small-angle scattering for eleven different contrasts evenly distributed around the match points were studied for each sample. The scattering data of the AOT/D_2O/decane system are shown in Fig.1.

The lowermost spectrum is with pure deuterated decane (shell-contrast), as one moves upward the volume fraction of protonated decane increases and the uppermost spectrum is for 1/3 deuterated and 2/3 protonated decane. The scattering data for the different contrasts are analysed using a molecular constrained model for ellipsoidal droplets of water covered by AOT, interacting as polydisperse hard-spheres. All contrasts are fitted simultaneously by taking the different contrast factors into account. These fits are also shown in fig.1. The analysis show that at the same reduced temperature with respect to the aggregation temperature both droplet size, polydispersity index and the size of the shape fluctuations are only slightly different in the two systems. A polydispersity index (σ/R of the Gaussian size distribution) of 18.0% and an average axis ratio of the droplets of 1.6 is found in the AOT/D_2O/decane microemulsion, whereas in AOT/D_2O/iso-octane the polydispersity index is 17.4% and the axis ratio is 1.74. The bending elastic constant κ and the Gaussian bending constant $\overline{\kappa}$, can be estimated from these numbers. For AOT/D_2O/decane we find $\kappa = 2.7$ kT and $\overline{\kappa} = -5.1$ kT and for AOT/D_2O/iso-octane we find $\kappa = 2.1$ kT and $\overline{\kappa} = -3.4$ kT where k is the Boltzmann constant and T is the absolute temperature.
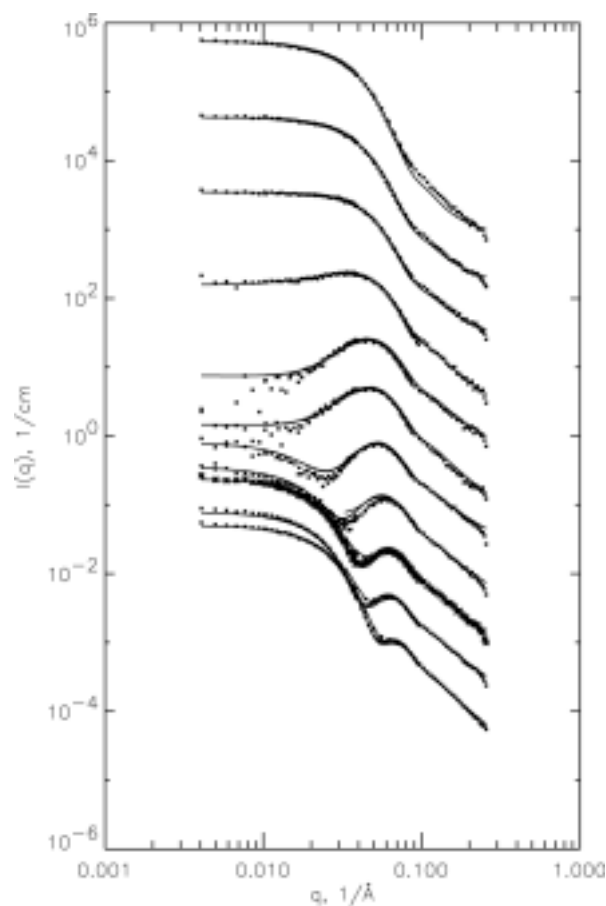
Fig. 1. Contrast variation SANS measurements on AOT/D_2O/decane. Each data set is shifted by a factor of 5. The full lines are the model fits.

2.7.4. A small-angle neutron scattering (SANS) study of surfactant aggregates formed in aqueous mixtures of sodium dodecyl sulfate (SDS) and didodecyldimethylammonium bromide (DDAB)

M. Bergström, *Department of Chemistry, Surface Chemistry, Royal Institute of Technology, Sweden* and J. S. Pedersen, *Condensed Matter Physics and Chemistry Department, Risø National Laboratory, Denmark*

e-mail: jan.skov.pedersen@risoe.dk   http://www.risoe.dk/fys/Employee/jask.htm

The structure of aggregates formed in aqueous mixtures of a single-chain anionic surfactant (SDS) and a double-chain cationic surfactant (DDAB) has been investigated at 38 ° C using small-angle neutron scattering (SANS). Several overall surfactant concentrations [SDS] + [DDAB] between 0.1 - 5 wt % were measured at the two SDS-rich compositions [SDS]:[DDAB] = 90:10 and 95:5. Samples with a concentration above about [SDS] + [DDAB] = 1 wt % at [SDS]:[DDAB] = 95:5 contained only somewhat elongated tablet-shaped micelles (tri-axial ellipsoids) with typical values of the half axes a (related to the thickness) = 14 Å, b (related to the width) = 23 Å and c (related to the length) = 27 Å. When a sample at [SDS]:[DDAB] = 95:5 is further diluted below about [SDS] + [DDAB] = 1 wt %, an increasing amount of small unilamellar vesicles forms and in the samples below about 0.2 wt % only vesicles are observed. The average radius of the vesicles $\langle R \rangle$ increases from about 90 Å at 0.3 wt % to 110 Å 0.1 wt %. The transition from micelles to vesicles with decreasing surfactant concentration was also observed in the samples at [SDS]:[DDAB] = 90:10 in which, however, an additional amount of bilayer sheets was seen to be always present. Compared with the micelles at [SDS]:[DDAB] = 95:5, the micelles formed at [SDS]:[DDAB] = 90:10 were considerably longer ($c \approx 40$ Å), but with similar cross-section dimensions, and the vesicles formed were seen to be somewhat larger than the corresponding aggregates at 95:5. The relative standard deviation $\sigma_R/\langle R \rangle$ of the (number-weighted) vesicle size distributions were seen to be in the range $0.2 < \sigma_R/\langle R \rangle < 0.3$.
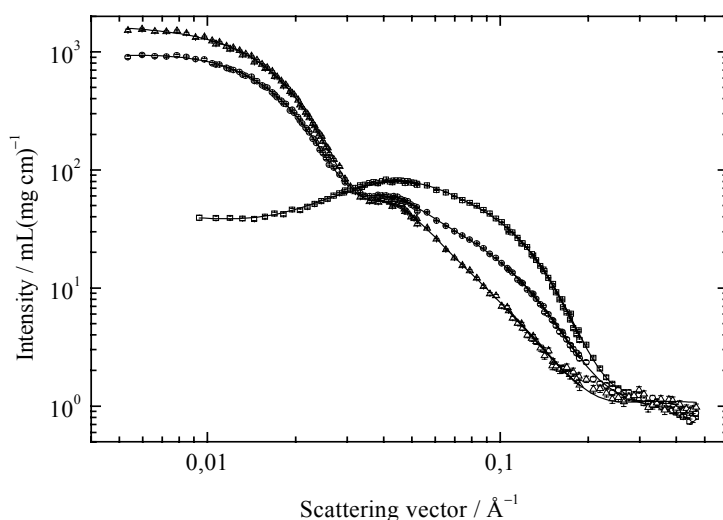
Fig. 1. Normalized scattering intensity as a function of the scattering vector q for samples with an overall surfactant concentration [SDS] + [DDAB] = 0.20 wt % (triangular symbols), 0.31 wt % (circular symbols) and 0.72 wt % (squared symbols), respectively, at a given surfactant molar ratio [SDS]:[DDAB] = 95:5. Individual symbols represent SANS data obtained with different combinations of neutron wavelength and sample-detector distance. The lines are the fits with a model for spherical bilayer shells (vesicles, triangles), a model for tri-axial ellipsoids (micelles, squares) and a model for coexisting micelles and vesicles (circles). The agreements of these fits as measured by χ^2 are 4.0 (triangles), 1.6 (circles) and 2.2 (squares), respectively.

2.7.5. A small-angle neutron scattering (SANS) study of surfactant micelles formed in aqueous mixtures of sodium dodecyl sulfate (SDS) and tetraethylenoxidedodecylamid (TEDAD)

M. Bergström, M. Kjellin, *Department of Chemistry, Surface Chemistry, Royal Institute of Technology, Sweden* and J. S. Pedersen, *Condensed Matter Physics and Chemistry Department, Risø National Laboratory, Denmark*
e-mail: jan.skov.pedersen@risoe.dk   http://www.risoe.dk/fys/Employee/jask.htm

Mixtures of the anionic surfactant sodium dodecyl sulfate (SDS) and the non-ionic surfactant tetra-ethylenoxidedodecylamid (TEDAD) in D_2O have been investigated at 22 and 40 ° C using small- angle neutron scattering (SANS). Pure SDS and TEDAD in D_2O as well as mixtures with surfactant mass ratios 75:25, 50:50 and 25:75 were measured at the three overall surfactant concentrations [SDS] + [TE-DAD] = 0.25, 0.50 and 1.0 wt %. The scattering data for the samples containing pure SDS have the best agreement with a model for rather small oblate ellipsoids of revolution with half axes $a \approx 13$ Å and $b \approx$ 20 - 21 Å. The pure SDS micelles at 22 ° C appeared to be somewhat larger, i.e. $b = 21$ Å rather than $b =$ 20 Å at 40 ° C. Pure TEDAD was observed to form rather elongated rigid rods at 22 ° C, the average length of which is growing from 260 to 440 Å when the surfactant concentration is raised from 0.25 to 1.0 wt %. At 40 ° C the TEDAD micelles appeared to be considerably longer, the average length is growing form 670 to 990 Å between 0.25 and 1.0 wt %, and the data of the corresponding samples could only be fitted assuming the micelles to be somewhat flexible rather than rigid. The cross-section of the elongated TEDAD micelles appeared to be slightly elliptical ($1 < b/a < 1.4$). The mixed micelles were best fitted with a model for tri-axial ellipsoids with half axes a (related to the thickness) $< b$ (related to the width) $< c$ (related to the length of the micelles). The half axis related to the thickness of the micelles increases from about $a = 13$ Å to $a = 16$ Å with increasing mole fraction of TEDAD while the corresponding values for the width and the length of the micelles are $20 < b < 26$ Å and $22 < c < 30$ Å. No significant change in the size of the mixed micelles between the two temperatures could be observed. At 22 ° C the mixed micelles appeared to be shaped as oblate ellipsoids of revolution ($b = c$) at all overall compositions at 0.25 wt % whereas they were seen to become somewhat elongated (tablets) at higher surfactant concentrations. On the other hand, at 40 ° C the structure of the mixed micelles appeared to be rather independent on overall surfactant concentration but dependent on the overall composition: The micelles were seen to be shaped as oblates at [SDS]:[TEDAD] = 75:25 but as elongated tablets at [SDS]:[TEDAD] = 50:50 and 25:75. The effective surface charge density in the mixed micelles was seen to significantly decrease with increasing surfactant concentration at both 22 and 40 ° C indicating that the fraction of SDS in the micelles decreases with [SDS] + [TEDAD] at a given [SDS]:[TEDAD].
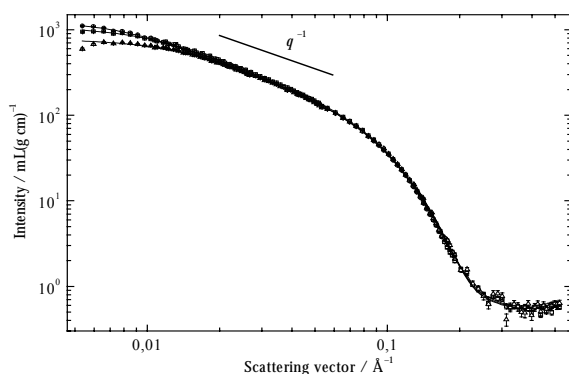
Fig. 1. Normalized scattering intensity as a function of the scattering vector q for samples with a concentration of tetraethylenoxidedode-cylamid [TEDAD] = 0.25 wt % (triangular symbols), 0.50 wt % (squared symbols) and 1.0 wt % (circular symbols), respectively, at 22 ° C. Individual symbols represent SANS data obtained with different combinations of neutron wavelength and sample-detector distance. The lines are the fits with a (two-shell) model for elongated polydisperse rigid rods with elliptical cross-sections. The agreements of these fits as measured by χ^2 are 3.6 (triangles), 5.3 (squares) and 5.9 (circles), respectively.

2.7.6.   SANS Study of semi-dilute salt water solutions of polymer-like micelles of TDAO

V. M. Garamus, *GKSS Research Centre, Geesthacht, Germany*, J. S. Pedersen, *Condensed Matter Physics and Chemistry Department, Risø National Laboratory, Denmark*, H. Kawasaki and H. Maeda, *Department of Chemistry, Kyushu University, Fukuoka, Japan*
e-mail: jan.skov.pedersen@risoe.dk   http://www.risoe.dk/fys/Employee/jask.htm

Aqueous solutions of alkylmethyleamine oxide are suitable model systems for studies of polymer-like micelles. A specific property of these surfactants is that it is quite easy to change the electrical charge density of the micelles. Alkylmethyleamine oxide exists as either a nonionic or cationic (protonated form) species depending on the pH of the aqueous solutions and thus the solution properties vary with pH. It has been found that the aggregation number of dodecyldimethylamine oxide exhibits a maximum around the half-ionized state and that salt addition initiate elongated micelle formation.

Aqueous solutions of tetradecyldimethylamine oxide varying surfactant concentration, degree of ionization of surfactant molecules (pH variation) and concentration of added salt (NaCl) were studied by small-angle neutron scattering. The scattering data demonstrate the presence of worm-like micelles in the solution with high salt concentration (0.1 M). The data were successfully analysed using polymer theory and the results from Monte Carlo simulation. A concentration dependence of the growth of the micelles was obtained from analysis of the forward scattering and it was found to be in agreement with mean-field theory. A modified random phase approximation expression was applied for analysis of the scattering data in the full range of measured scattering vector and it gives an excellent agreement (Figure). The fits demonstrate that cross-section of the micelles is elliptical. The variation of degree of ionization of surfactant molecules from 0 to 0.2 does not influence to the local structure of micelles. Small differences are present at low q which is due to a variation of the overall size of the micelles. The micelles are largest for the highest degree of ionization.
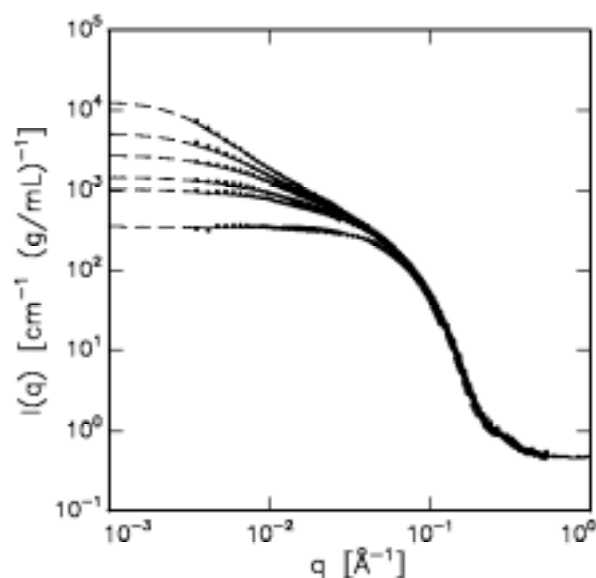
Fig. 1. SANS data versus scattering vector q for different concentrations of half-ionized TDAO (TDAO concentration from top to bottom of scattering curves 2.88, 8.51, 14.7, 23.7, 29.8 and 62 mg/ml, respectively) in a 0.1 M NaCl heavy water solution and corresponding model fits using the modified random phase approximation expression (solid lines).

2.7.7. Charged worm-like micelles as model systems for polyelectrolytes: Single chain properties investigated by light and neutron scattering and Monte Carlo simulations

P. Schurtenberger, C. Sommer, *Physics Department, University of Fribourg, Switzerland*, L. Cannavacciuolo, *ETH Zürich, Switzerland*, S. U. Egelhaaf, *University of Edinburgh, UK and* J. S. Pedersen, *Condensed Matter Physics and Chemistry Department, Risø National Laboratory, Denmark*
e-mail: jan.skov.pedersen@risoe.dk   http://www.risoe.dk/fys/Employee/jask.htm

We conducted a systematic study of the effect of charges and ionic strength on the micellar properties of non-ionic polymerlike micelles doped with a small amount of ionic surfactants. We investigated the effect of ionic strength and linear charge density on the apparent molar mass M_{app} and the radius of gyration $R_{g,app}$ using static light scattering and on the micellar flexibility expressed as the Kuhn length b by SANS for three different charge densities (i.e., weight ratio $[C_{16}SO_3Na]/[C_{16}E_6] = 0.03, 0.06, 0.09$). Figures 1(a) and (b) summarize the light scattering results obtained at 3 different ionic strengths and a doping level of 3% (weight ratio $[C_{16}SO_3Na]/[C_{16}E_6] = 0.03$). At low concentrations, the dramatic increase of the apparent molar mass M_{app} with increasing values of the concentration primarily reflects the pronounced concentration-induced micellar growth. The resulting micelles are extremely large, and no measurable ionic strength dependence can be observed for M_{app}. The results for the concentration dependence of the apparent radius of gyration $R_{g,app}$ shown in figure 1(b) exhibit a similar trend. However, in contrast to M_{app}, in the dilute regime and at fixed total surfactant concentration, $R_{g,app}$ as a measure of the micellar size strongly increases as the ionic strength decreases. Together with the finding that M_{app} is independent of the ionic strength, this indicates that the micellar flexibility decreases as a result of intra-micellar electro-static interactions. This is in quantitative agreement with the SANS measurements, that give direct access to structural properties on the length scale of b, and single chain Monte Carlo simulations of polyelectrolyte chains.
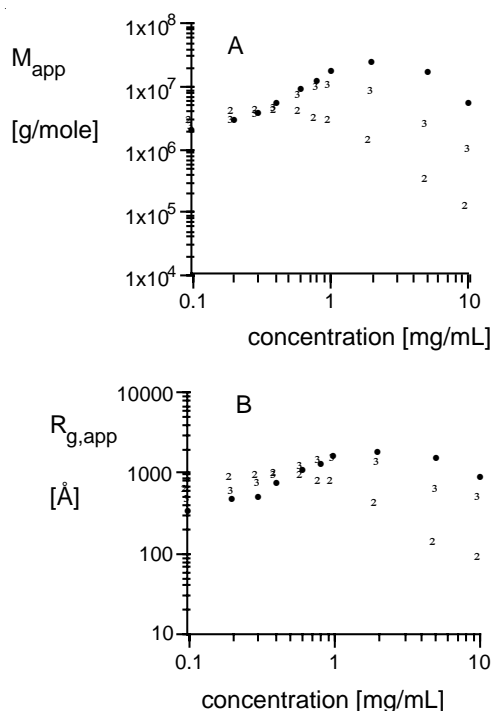
Fig. 1. M_{app} (a) and $R_{g,app}$ (b) versus total surfactant concentration for a 3% doping level (weight ratio $[C_{16}SO_3Na]/[C_{16}E_6] = 0.03$).

2.7.8. Dynamics and structure of giant worm-like micelles near the nematic phase

K. Mortensen, *Danish Polymer Centre, Condensed Matter Physics and Chemistry Department, Risø National Laboratory, Denmark*, U. Olsson, *Center for Chemistry and Chemical Engineering, Lund University, Lund, Sweden*, R. Angelico, A. Ceglie, *DISTAM, University of Molise, Campobasso, Italy* and G. Palazzo, *Department of Chemistry, University of Bari, Bari, Italy*
e-mail: kell.mortensen@risoe.dk   http://www.risoe.dk/fys/Employee/kemo.htm

Several surfactant and lipids self-assembly in solutions into very long worm-like micelles with spectacular viscoelastic properties. There have been considerable attentions to their flow behavior, where banded flow has been observed and interpreted as a shear induced transition from the isotropic solution (L) to a nematic (N) phase. In the present study we have focused on the structural relaxation of a sample from the shear induced nematic state back to the disordered liquid. The sample is made of biological lecithin, which form giant polymer-like reversed micelles in cyclohexane in the presence of small amounts of water. The scattering data clearly shows the formation of nematic order upon shear, as shown in Fig.1. The structure is characterized by the nematic order parameter

$$P_2 = 1 - 3/2 \cdot \int \left[\sin^2 \phi + \sin \phi \cos^2 \phi \cdot \ln((1 + \sin \phi)/\cos \phi) \right] I(\phi) d\phi \Big/ \int I(\phi) d\phi$$

where ϕ is the azimuthal angle. The analysis is carried out in a small narrow q-range around the structure factor peak, as illustrated in Fig.1. By recording the scattering pattern for periods down to 2 sec after shear has been turned off, the relaxation of the order was followed. The resulting, time dependent order-parameter P_2 relaxes exponentially with a relaxation time τ that depends critically on the temperature, approaching infinite at T_N. From the initial order parameter $P_2(0)$, one can estimate the micellar persistence length λ_p, using the Schoot-Cates theory:

$$P_2 \approx 1 - 3 \left(\sqrt{\pi} d / 8 \lambda_p \phi \right)^{2/3}$$

With the micellar diameter equal d=50Å, and the experimental P_2-value equal 0.41 this gives λ_p=500Å[1]. A similar value of λ_p has been obtained from lecithin self-diffusion.
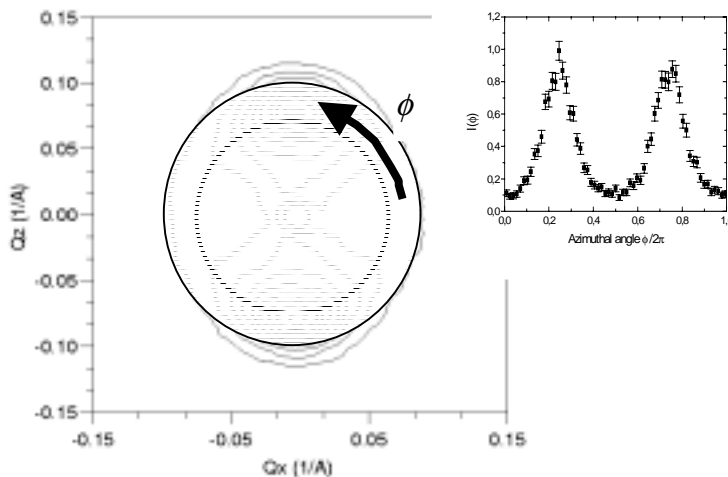
Fig. 1. Two-dimensional plot of SANS data of shear induced nematic state of worm-like lecithin micelles. The circles and arrow illustrates how the $I(\phi)$-data is obtained. The order parameter P_2 is calculated on the basis of this $I(\phi)$-function.

---

[1] R. Angelico, U. Olsson, K. Mortensen, G. Palazzo and A. Ceglie. Europhys. Lett. In the press.

2.7.9. Charged worm-like micelles as model systems for polyelectrolytes: Semi-dilute solutions investigated by SANS and Monte Carlo simulations

P. Schurtenberger, C. Sommer, *Physics Department, University of Fribourg, Switzerland*, L. Cannavacciuolo, *ETH Zürich, Switzerland*, S. U. Egelhaaf, *University of Edinburgh, UK* and J. S. Pedersen*, Condensed Matter Physics and Chemistry Department, Risø National Laboratory, Denmark*
e-mail: jan.skov.pedersen@risoe.dk   http://www.risoe.dk/fys/Employee/wape.htm

We have previously demonstrated the close analogy between polyelectrolytes and polymerlike micelles doped with a small amount of ionic surfactants[1]. While we initially concentrated on the effect of charges on the micellar flexibility and thus worked at very low surfactant concentrations, we have now started to extend our experiments to higher concentrations. Solutions were prepared at a fixed charge density (constant weight ratio $[C_{16}SO_3Na]/[C_{16}E_6]$ = 0.03, 0.06 and 0.09, respectively). The SANS experiments were performed at the instrument D22 of the ILL in Grenoble, France (dilute solutions), and at the SANS instrument at PSI, Switzerland (semi-dilute solutions). At a salt concentration of 10^{-3} M NaCl, we clearly see the appearance of a well-defined structure factor peak at a finite scattering vector value $q*$ factor for surfactant concentrations c > 5 mg/ml. It becomes more pronounced and shifts to higher values of q at higher surfactant concentrations (Figure 1(a)). This peak completely disappears at higher salt concentrations, where the electrostatic interactions are efficiently screened by the salt and the solution exhibits classical polymer behavior. In Figure 1(b) we have plotted the location of the peak $q*$ versus the surfactant concentration for different doping levels. We find that $q*$ follows a power law of the form $q* \sim c^{1/2}$, i.e., we observe exactly the same behavior as reported for classical polyelectrolytes. We currently compare these data with results from a systematic Monte Carlo simulation of many chain polyelectrolytes under comparable conditions. In the simulations we use a semi-flexible chain model with fixed valence angle and free rotation around the bonds. The interaction potential consists of a hard-sphere part and a screened electrostatic potential. The simulations are rather time consuming and we are currently running series of simulations. Although the data is not analysed in any detail, the scattering functions qualitatively agree with those observed experimentally in the sense that a structure factor peak is observed for the same range of volume fractions, charge densities and ionic strength where it is observed experimentally.
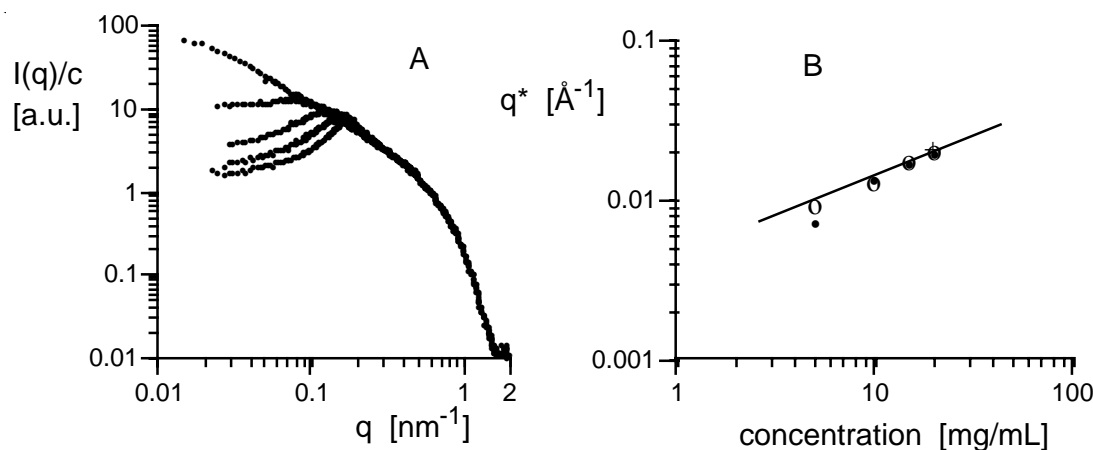
Fig. 1. (a) Formation of a peak in $I(q)$ at low salt ([NaCl] = 0.001 M) for doped non-ionic polymer-like micelles at different concentrations c = 0.4, 5, 10, 15, and 20 mg/ml and (b) location $q*$ of the structure factor peak vs. surfactant concentration for different doping levels $[C_{16}SO_3Na]/[C_{16}E_6]$ = 0.03 (•) , 0.06 (o) and 0.09 (+). Also shown as the solid line is a power law of the form $c^{1/2}$.

[1] G. Jerke, J. S. Pedersen, S. U. Egelhaaf and P. Schurtenberger, Langmuir **14**, 6013 (1998).

2.7.10. Evidence of the lamellar to vesicle transition by SANS experiments under shear

J. I. Escalante, M. Gradzielski, H. Hoffmann, *Universität Bayreuth, Physikalische Chemie I, Bayreuth, Germany* and K. Mortensen, *Danish Polymer Centre, Condensed Matter Physics and Chemistry Department, Risø National Laboratory, Denmark*
e-mail: kell.mortensen@risoe.dk   http://www.risoe.dk/fys/Employee/kemo.htm

Small angle neutron scattering studies were performed in the ternary system: tetradecyldimethylamineoxide C_{14}DMAO /Hexanol/D_2O for phases that form bilayer structures. We started from a sponge phase (L_3) to which a corresponding amount of diethyl oxalate was added and the sample was immediately transferred into the Couette cell. By a hydrolysis reaction the bilayer of this L_3-phase becomes charged. This renders the L_3-phase unstable and, in the absence of shear, it is transformed into a classical lamellar phase of stacked bilayers (with the advantage that this preparation process yields a lamellar phase that has not been exposed to any shear). After the hydrolysis reaction was complete, a constant shear rate was applied and the structural changes were monitored in the radial configuration of the Couette cell. Previous rheological and conductivity experiments[1] indicated that a structural transition takes place in the course of time where the critical parameter is the deformation of the sample during shear. In the SANS experiment one finds that before the shear is turned on a preferential orientation of the lamellae along the vorticity axis is observed. Immediately after turning on the shear two pronounced peaks in e-direction are observed (Fig. 1a). Evidently the lamellae are now oriented perpendicular, i. e. along the plane of flow and shear gradient. Depending on the chosen shear rate the degree of orientation goes through a maximum, but decreases always again with passing time. After long times (Fig. 1c) still a preferential orientation along the e-axis is observed but in general the scattering pattern becomes relatively isotropic. This scattering pattern then is in agreement with the formation of large multi-lamellar vesicles where the number of shells depends on the shear rate employed. A very interesting point revealed in these SANS experiments is that before the transition from lamellae to vesicles the lamellae always go through a perpendicular orientation. Such a perpendicular orientation can be explained on theoretical ground[2], but so far no satisfactory explanation has been given for the subsequent transition to vesicles. The SANS shear experiments have proven that a well-defined vesicle phase can be prepared by starting from a well-defined lamellar phase and applying a corresponding shear rate.

| (a) | (b) | (c) |
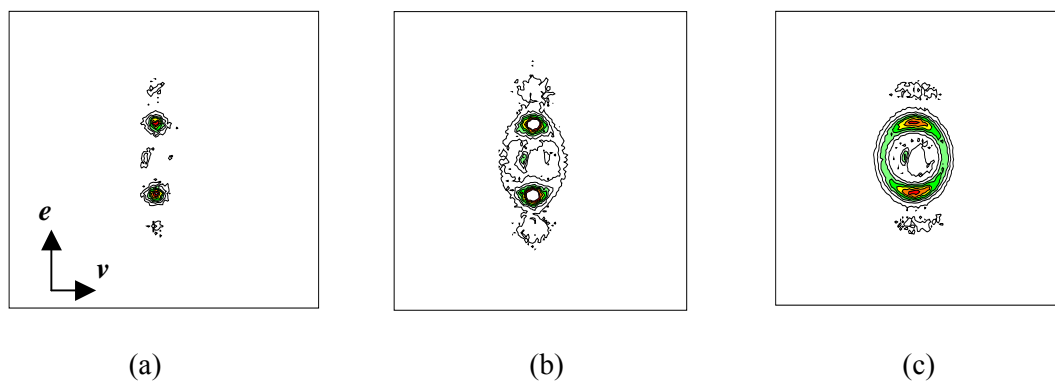
Fig. 1. SANS curves for a sample of 100 mM C_{14}DMAO/10 mM diethyl oxalate/250 mM hexanol/ D_2O in the Couette cell at constant shear rate of 10 s^{-1}. a) after 30 s, b) after 150 s and c) after 1 hour.

[1] J. I. Escalante and H. Hoffmann, Rheol Acta. In the press. (1999).
[2] M. Cates and S. F. Milner, Phys. Rev. Lett. **62**, 1865 (1989).

2.7.11. Modeling entropic contributions in biophysical force measurements

H. Flyvbjerg, *Condensed Matter Physics and Chemistry Department, Risø National Laboratory, Denmark*

e-mail: henrik.flyvbjerg@risoe.dk and   http://www.risoe.dk/fys/Employee/hefy.htm
      flyvbj@delbruck.nbi.dk   www.nbi.dk/~biophys/

Four related problems are under investigation. The role of configurational entropy is at the core of all of them. Three of them are relevant for the interpretation of force measurements in biological physics, done with optical tweezers, AFM, or other means.

1) Nano- and pico-forces measured with micro-spheres:

The potential energy landscape experienced by a micro-sphere in a liquid can be measured by monitoring the sphere's position during its Brownian motion. This is a popular way of finding the force exerted on the sphere by an optical tweezer, or a tether, or both. We investigate contributions from configurational entropy in various situations to forces measured in this manner.

2) Force-extension curves for some bio-polymers:

AFM measurements of titin's and dextrose's force-extension curves find a saw-tooth shaped curve which contains information about the folding potential of those parts of the molecule which unfold under the force. We consider the statistics of force-induced unfolding of identical folders coupled in series in an attempt to better understand the experimental data.

3) Worm-like chain model for DNA:

Experimental force-extension curves for DNA are modelled with the worm-like chain model for a somewhat flexible polymer. The model has been solved numerically, and for analytical purposes an interpolation formula exists which is based on lowest order perturbation theory. The model is mathematically equivalent to the non-linear sigma-model in an external field. Thus, non-perturbative methods from field theory might yield a more interesting analytical solution. This possibility is investigated.

4) Steric depletion factors of some non-spherical macromolecules:

Large molecules in narrow spaces occur in shape-dependent concentrations. We consider the information about macro-molecules in solution that can be gleaned from this effect.

2.8.   Polymers

2.8.1.   Synthesis of small molar mass perdeuterated polyethylpropylene (d-PEP) as an auxiliary for neutron studies

F. C. Krebs, M. Jørgensen, B. Lebech, K. Almdal and W. B. Pedersen, *Condensed Matter Physics and Chemistry Department, Risø National Laboratory, Denmark*
e-mail: frederik.krebs@risoe.dk   http://www.risoe.dk/fys/Employee/frkr.htm

An inert non-crystalline cryoprotectant oil was needed as a non-incoherent scattering matrix for neutron studies of solvent containing crystalline materials. This led us to prepare perdeuterated polyethylpropylene (PEP) with a molar mass around 1100 g/mol. On route to this material an improved method for the preparation of isoprene-d_8 starting from calcium carbide and acetone-d_6 was devised. Subsequent anionic polymerisation using t-butyl lithium as initiator resulted in an oligomeric perdeuterated polyisoprene (PI) with an average chain length of approx. 15 monomer units and Mw/Mn: 1.1. This polymer was deuterated with D_2 and Pd/C (10%) in cyclohexane to yield the desired perdeutero polymer (PEP-d). The polymer fulfils the important properties that it does not crystallize at low temperature and that it has a low neutron scattering efficiency.
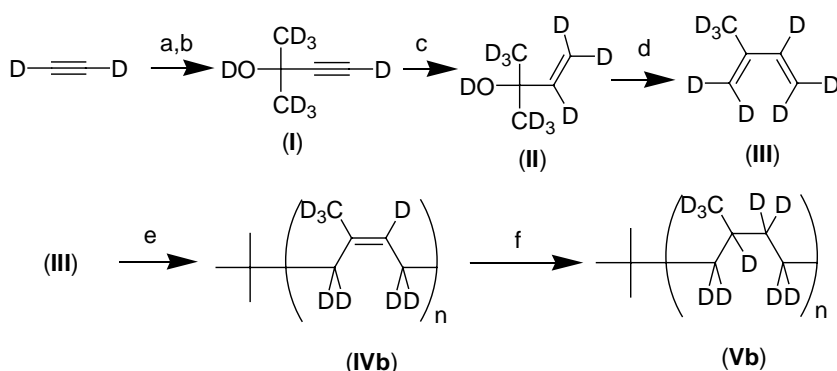
Fig. 1. a: n-BuLi, b: acetone-d_6, c: D_2 Pd/C, d: Al_2O_3 Δ, e: t-BuLi, f: D_2 Pd/C.
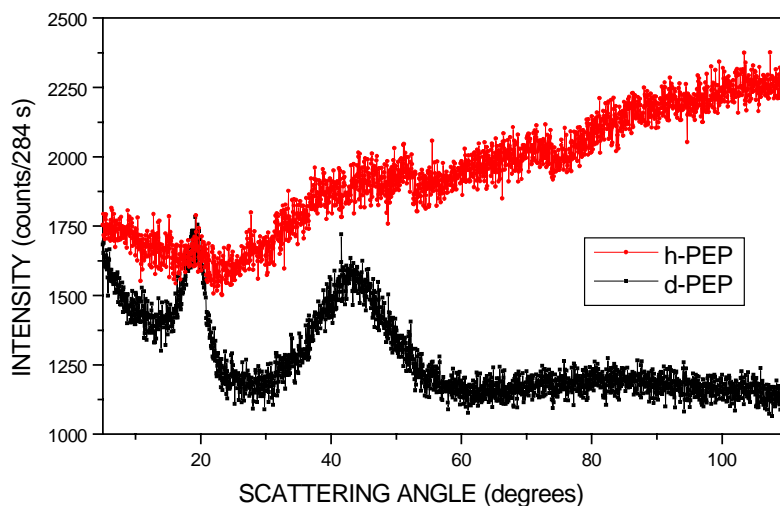
Fig. 2. Neutron scattering data for the hydrogenated or deuterated PEP oils **Va** and **Vb**.
Incident wavelength 1.55 Å.

An account of this work has been accepted for publication[1] while further work on the usage of this new polymer is in progress.

---

[1] F. C. Krebs, M. Jørgensen, B. Lebech, K. Almdal, and W.B. Pedersen, Polymer Bulletin. Accepted for publication.

2.8.2. Dielectric spectroscopy of a polyurethane

P. Sommer-Larsen and C. Wang, *Condensed Matter Physics and Chemistry Department, Risø National Laboratory, Denmark*

e-mail: peter.sommer.larsen@risoe.dk   http://www.risoe.dk/fys/Employee/pela.htm

Segmented polyurethanes (PU) are thermoplastic elastomers. The thermal and electric properties of a commercial PU (Dow 2103-80AE) have been investigated. The polymer is a block-copolymer of hard urethane segments capable of crystallising (Bis-[4-isocyanat-phenyl]methan and 1,4-butandiol) and soft polyether segments (poly(oxytetramethylene)). The complex dielectric constant has been measured for frequencies between 10^{-3} Hz and 10^6 Hz and temperatures between 173 K and 423 K. The dispersion curves was fitted to an expression including dielectric relaxation terms (Havriliak- Negami functions), intrinsic conductivity and the effect of blocking electrodes.

Two dielectric relaxations were identified as α- and β-relaxations connected to the mobility of the poly-ether chain. The temperature dependence of the α-relaxation follows a Vogel-Fulcher-Tammann-Hesse (VFTH) equation (see fig 1. For parameters) whereas the β-relaxation is Arrhenius like (Fig. 1). The Vogel temperature found for the α-relaxation is 5 degrees below T_g for poly(oxytetramethylene).

The conductivity likewise follows VFTH temperature dependence with almost the same parameters as the α-relaxation (Fig. 1). The differences are insignificant because of the low number of data points. The Vogel temperature found for the conductivity is 25 degrees below T_g for poly(oxytetramethylene). Presumably, the conductivity is ionic in nature, takes place in the amorphous polyether phase and is allowed by - or coupled to - the chains movements.
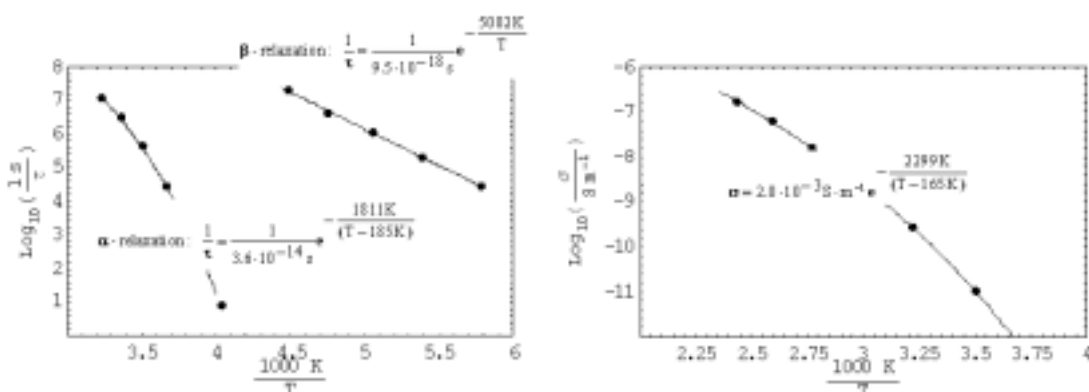
Fig. 1. Temperature dependence of relaxation times for dielectric relaxations (left) and temperature dependence of intrinsic conductivity (right). The VFTH equations with fitted parameters are given.

The elastic properties of the PU are due to the micro-phase separation of the hard and soft segments. The nature of the hard segment phase is strongly dependent on the thermal treatment of the polymer. Films cast from a solution of the PU in THF or films heat pressed from pellets show no crystallinity. After annealing at 145^OC for days, DSC traces show a melting endotherm at $170\,^O$C - a clear indications of a crystalline phase (Fig. 2).

Fig. 2. Differential Scanning Calorimetry (DSC) traces of a heat pressed PU film. The upper trace is for a sample annealed at 145^OC for 1 week. The lower trace is for an unannealed sample. The two curves are displaced for visualisation.
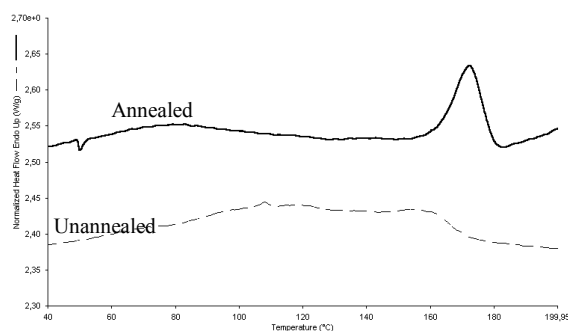
2.8.3. Dielectric property of rubber with graphite

G. Kofod, A. Faldt and P. Sommer-Larsen, *Condensed Matter Physics and Chemistry Department, Risø National Laboratory, Denmark*

e-mail: guggi.kofod@risoe.dk   http://www.risoe.dk/fys/Employee/pela.htm

The mixture of polydimethylsiloxane (PDMS) rubber and graphite (carbon black) exhibits percolative behaviour, a property found in many systems. Here the properties of interest are the dielectricity and the conductivity of the whole mixture. These properties can be measured very accurately with the Novocontrol Dielectric Analyzer, situated in the Artificial Muscles laboratory. A capacitor is prepared with the sample under study placed between the capacitor electrodes. Then the analyser applies an AC current with a certain amplitude and frequency, and measures the resulting current through the sample capacitor, and converts it to impedance, from which the complex conductivity and dielectricity of the sample material may be deduced. The frequency can be scanned from $3\cdot10^{-5}$ to $2\cdot10^{7}$ Hz, but a typical dielectric spectrum $\varepsilon^*(\omega)$ is obtained from 10^{-2} to 10^{7}, which takes about 45 minutes.

The carbon black particles are very small and conducting, while the PDMS rubber is insulating and fills the space between particles. When the amount of carbon black (p, volume percentage) is low, the dielectricity and conductivity of the mixture is small. The conductivity of the mixture is determined from the current running in the carbon particles, and tunnelling from particle to particle through the PDMS. The particles are separate, and the dielectricity and conductivity are scarcely affected as the carbon black content, p, is increased, both ε' and $\sigma'(\omega=0)$ increasing a tiny amount. As the amount of carbon particles increases, particles begin to lie next to each other in larger and larger clusters, until at least one path exists between carbon particles that stretch from one electrode to the other. The conductivity of this path is orders of magnitude higher than the same mixture without the path thus the conductivity of the mixture increases very rapidly. This dramatic increase is critical, so the point at which the conductivity shoots up is known as the percolation threshold, pc. The DC conductivity (σ_0, at zero frequency) is well described by $\sigma_0 \propto |p-p_c|^t$, where t is a critical exponent.
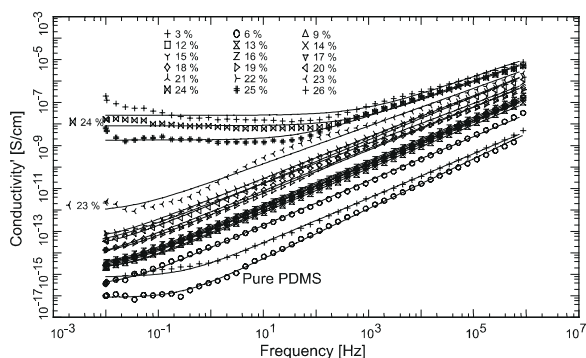
Fig. 1. Conductivity traces. At the percolation threshold the conductivity jumps five orders of magnitude.
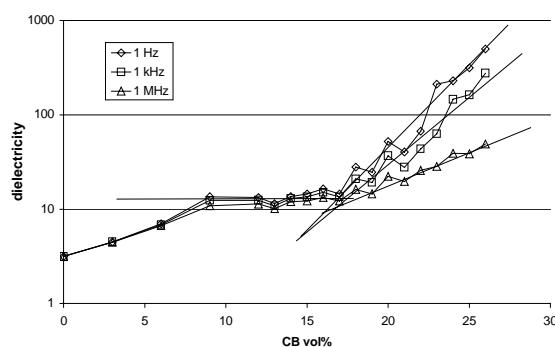
Fig. 2. Dielectricity vs. carbon black content measured at different frequencies. Up to some value (17%) it is practically constant, then it shoots up.

The σ' spectrums for samples with increasing carbon black content are shown in fig. 1. For low carbon black content, the spectra follow a typical behaviour for perfect capacitors. At some value of the carbon black content (~23%), suddenly a leaking current shows up as a conductivity plateau, this is ordinary conduction through carbon particles. The threshold value is seen better in the dielectric spectrum. Here the values of ε' have been extracted for different frequencies, 1Hz, 1kHz and 1Mhz. At low carbon black content, the dielectricity is practically constant, while suddenly for a value of 17%; the dielectricity starts to increase with increasing carbon black content.

The system of carbon black in PDMS rubber shows high versatility. Low content of carbon black yields insulating, low dielectricity mixtures, while a high content of carbon black yields conducting samples. In between the dielectricity is high while the conductivity is still low. These are excellent properties for the manufacture of dielectric artificial muscles: the conducting carbon black rich mixtures may be used for stretchable rubber electrodes, while mixtures with a content of ~17% have a high dielectricity and a low conductivity, excellent properties for the active medium in an artificial muscle.

2.8.4. Conducting polymer actuators

K. West, S.V. Skaarup, L. Bay, *Department of Chemistry, The Technical University of* Denmark, Denmark, M. M. Nielsen, E. Smela, I. Johannsen, J. Hooker, O. Jørgensen, T. Mazur and P. Sommer-Larsen, *Condensed Matter Physics and Chemistry Department, Risø National Laboratory, Denmark*
e-mail: keld.west@risoe.dk   http://www.risoe.dk/fys/Employee/kelw.htm

Polypyrrole (PPy) films formed by electrochemical polymerisation of pyrrole in a sodium dodecylbenzenesulphonate (DBS) solution are electromechanical active, i.e. they change volume upon oxidation and reduction. The DBS anions are incorporated as immobile counterions surrounding the positively charged PPy chains. PPyDBS can be used as actuator material.

Commercially available DBS is a technical grade. A GPC analysis indicates that it is a mixture of isomers as well as benzenesulphonates with C_{10} to C_{13} chains. Furthermore, microanalysis shows the commercial DBS to contain large amounts of sodiumsulphate. Use of a well-characterised DBS as immobile counterion has a pronounced influence on the properties of PPyDBS. We have synthesised three isomers of DBS (see fig.1), in short they are denoted (1D)BS, (2D)BS, (6D)BS.

Fig. 1. (1D)BS
4-(1-dodecyl)-benzenesulphonate

(2D)BS
4-(2-dodecyl)-benzenesulphonate

(6D)BS
4-(6-dodecyl)-benzenesulphonate
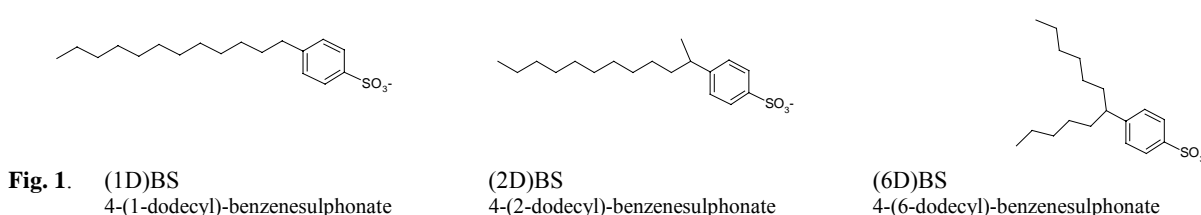
Using the pure DBS, PPyDBS forms layered structures as shown by their X-ray diffraction pattern. (fig. 2). The repeat distance in the layers correlates with the chain lengths of DBS.

PPy(1D)BS d=39.2 Å   PPy(2D)BS d=31.7   PPy(6D)BS d=24.2 Å
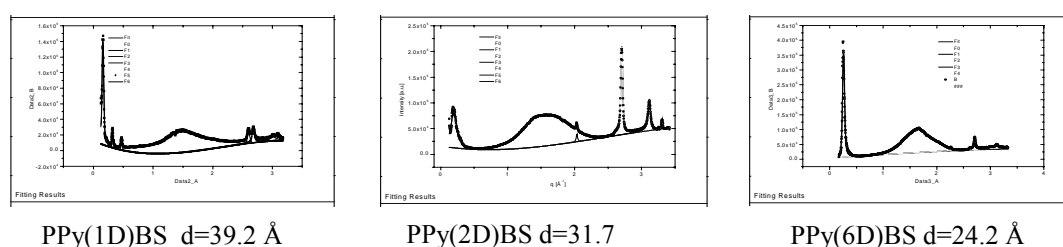
Fig. 2. Gracing incidence wide angle X-ray diffraction patterns for PPyDBS synthesised with the three different anions. The diffraction peak at lowest angle corresponds to the layer repeat distances given below each figure. The broad amorphous peak corresponds to nearest neighbour distances in PPy and between dodecyl chains (~ 4 Å). The high angle diffraction is from the underlying gold substrate.

From electrochemical measurements, it is found that PPyDBS has the average stoichiometric composition of 3 pyrroles per anion. If all anions are DBS, this corresponds to an average molecular mass per electron removed from pyrrole during polymerisation of 75.3 g mol^{-1}. This quantity can also be found by tracing the mass increase during polymerisation with an electrochemical quartz crystal microbalance and at the same time measure the charge removed during polymerisation.

For PPy polymerised with technical grade DBS this number varies between 61 and 72 g mol^{-1}, indicating that anions lighter than DBS, i.e. sulphate, are also incorporated. For PPy(6D)BS the number is 77.7 g mol^{-1} in good agreement with the number given above.

Figure 3 shows the maximum force produced by a bimorph actuator when the PPy is activated from fully reduced to fully oxidised. The bimorph consists of PPy grown on gold-coated kapton® (1 mil). The forces measured for different PPy film thickness is shown. The various curves correspond to films grown in solutions of different anions.

PPy(6D)BS shows the highest force measured!
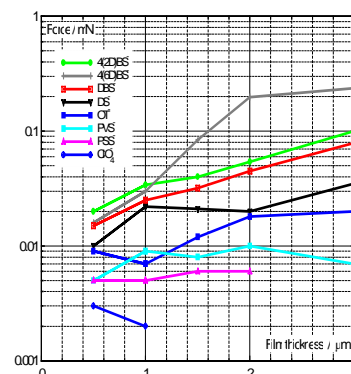
2.8.5. Monitoring volume expansion in PPy(DBS) with AFM: Effects of DBS isomers

J. C. Hooker and I. Johannsen, *Condensed Matter Physics and Chemistry Department, Risø National Laboratory, Denmark* and E. Smela, *Santa Fe Science and Technology, Santa Fe, New Mexico, USA*
e-mail: jacob.hooker@risoe.dk   http://www.risoe.dk/fys/Employee/jach.htm

Conducting polymers such as polypyrrole (PPy) have been shown to be potential materials for actuation devices, in particular for micromechanics[1]. By incorporating a large anion such as dodecylbenzenesulfonate (DBS) as a dopant, large out-of-plane expansion of up to 35% has been observed[2] in aqueous solution using atomic force microscopy (AFM). In this case, by changing the potential applied to the system (app.1 volt) cation molecules and their solvation cage are inserted/ejected upon reduction/oxidation causing an anisotropic expansion/contraction (see Fig. 1). Conversely, if small anions are incorporated, the anions are inserted and ejected upon reduction and oxidation, respectively. This is represented by equations 1 and 2 (left side of equations, oxidised - right, reduced):

$$P^+(A^-) + C^+ + e^- \leftrightarrow P^o(AC), \qquad \text{large anion (A)} \qquad (1)$$
$$P^+(A^-) + C^+ + e^- \leftrightarrow P^o + A^- + C^+, \qquad \text{small anion} \qquad (2)$$
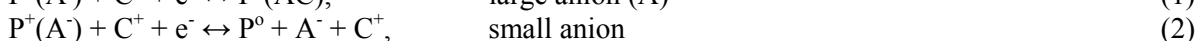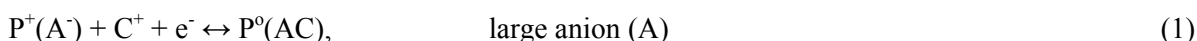
In order to use PPy(DBS) as an actuator material, a better understanding of the factors, which influence this expansion, is necessary. However, it was recently discovered[3] that the sodium DBS (Na m-DBS) used in this system consisted of a large assortment of isomers and other contaminants that produced samples giving inconsistent results. To avoid these shortcomings, well-defined isomers were synthesised that included sodium salts of 4-(2-dodecyl)-benzenesulphonate [4(2D)BS] and 4-(6-dodecyl)-benzenesulphonate [4(6D)BS].[4]

Figure 2 shows the results of the out-of-plane expansion for PPy(DBS) films electrochemically polymerised under galvanostatic conditions (0.05M Py, 0.05M NaDBS, 1 mA/cm² vs. Ag/AgCl ref.) using various DBS's as a function of film thickness. As is evident, the 4(2D)BS isomer shows the smallest expansion, whereas the behaviour between m-DBS and 4(6D)BS are almost identical. Also, it is interesting to note that the maximum out-of-plane expansion is observed for a film thickness around 2 microns. This suggests that to optimise both expansion and force[4], 4(6D)BS isomer should be used.
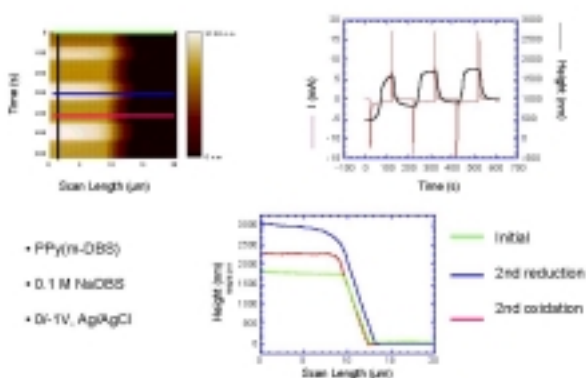
Fig. 1. AFM images and electrochemical behaviour obtained simultaneously for a PPy(m-DBS) film during potential stepping between O and −1V (vs. Ag/AgCl ref.) in 0.1 M NaDBS solution.
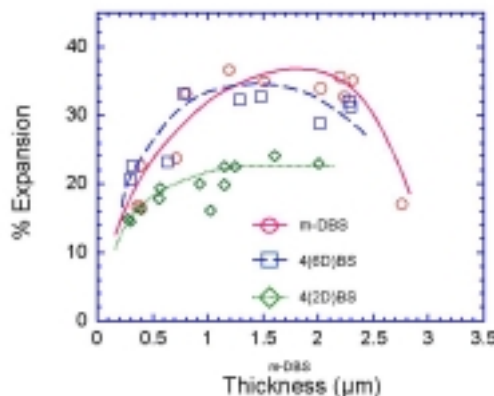
Fig. 2. % out-of-plane expansion of PPy(DBS) films for various DBS isomers as a function of film thickness. Conditions similar to those used in Figure 1.

[1] E. Smela, O. Inganäs and I. Lundström, Science, 268, 1735 (1995).
[2] E. Smela and N. Gadegård, Adv. Mater., 11, 953 (1999).
[3] K. West and S. Skaarup, K. Vidanapathirana, M. Benslimane, P. Graversen and I. Johannsen, 4th Workshop Multifunc. & Smart Polym. Sys., Dublin, Ireland, Sept. 1999.
[4] See 2.8.4. in this report.

2.8.6. Instant holography

P. S. Ramanujam, *Optics and Fluid Dynamics Department, Risø National Laboratory, Denmark,* M. Pedersen, *Nunc A/S, Denmark* and S. Hvilsted, *Condensed Matter Physics and Chemistry Department, Risø National Laboratory, Denmark*
e-mail: s.hvilsted@risoe.dk   http://www.risoe.dk/fys/Employee/sohv.htm

Optical storage in azobenzene containing polymers is believed to take place due to the statistical reorientation of azobenzene chromophores perpendicular to the electric field vector of the incident polarized light. Since this involves many pumping cycles of the chromophore between the *trans* and *cis* state, a steady-state macroscopic birefringence from the orientation of a large number of chromophores is intuitively expected to arise after several seconds to minutes even though the individual *trans-cis* isomerizations takes place in a few picoseconds. Several groups have shown recently that a surface relief arises when two polarized laser beams are allowed to overlap on a thin azobenzene containing polymer film. We have previously shown that the formation of the surface relief is strongly polarization dependent and that the presence of the anisotropy and the surface relief are concomitant.

Instant holography, epitomized by Polariod films is characterized by the rapid appearance of an image after exposure. We have exploited[1,2] thin films of new amorphous cyanoazobenzene side-chain polyester with a glass transition temperature at 63°C and a low molecular mass, and a conventional two-beam set-up for polarization holography. A frequency doubled yttrium-aluminum-garnett (YAG) laser operating at 532 nm and capable of producing Q-switched pulses of 5-7 ns duration at a 20 Hz rate was used. After just one pulse from the YAG laser, 11 diffracted orders from the film are seen by HeNe laser readout with maximum diffraction efficiency in the first order exceeding 4% at a spatial frequency of 160 lines/mm. However, the recording of spatial frequencies of greater than 900 lines/mm with a single pulse is possible, indicating the attainable spatial resolution. After the exposure, the film is scanned in an atomic force microscope (AFM) resulting in the surface relief shown in Fig. 1.

The surface relief is stable at room temperature but can be erased after heating the films to 80°C. This paves the way for a cheap, mass replication of the surface relief employing a micromolding technique. Thus, by pouring a heat curable liquid polysiloxane on top of the relief surface and let it cure at elevated temperature a polysiloxane rubber replica with the same diffraction properties can easily be manufactured.
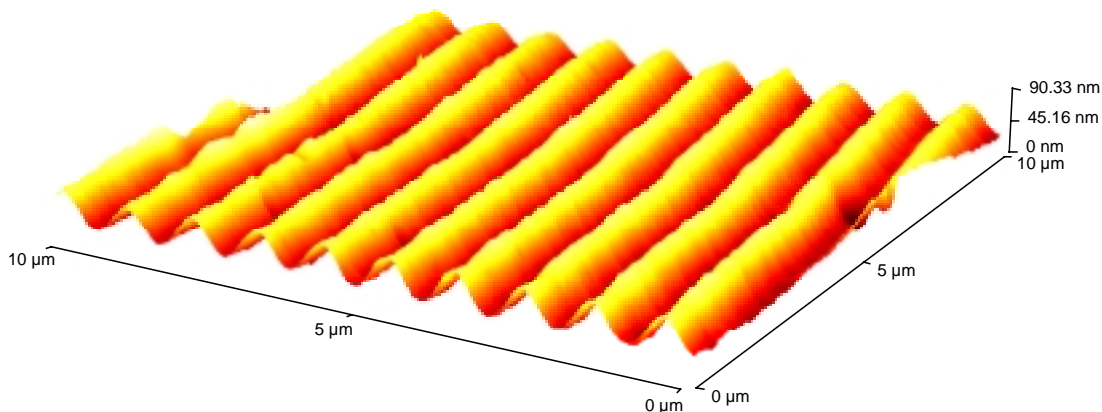
Fig. 1. AFM scan of 10 □ m by 10 □ m area of the polyester film exposed to two laser beams. The surface relief with a maximum roughness of 90 nm is observed after one 5 ns pulse. The interbeam angle between the recording beams is 28°, resulting in a spatial frequency of 900 lines/mm.

---

[1] P. S. Ramanujam, M. Pedersen and S. Hvilsted, Appl. Phys. Lett., **74,** 3227 (1999).
[2] P. S. Ramanujam and S. Hvilsted, Holography, SPIE's Int. Tech. Group Newsletter, **10** (2), 1 (1999).

2.8.7. Synthesis and characterization of azobenzene functionalized dendritic macromolecules for holographic storage applications

P. Busson, A. Hult, *Department of Polymer Technology, Royal Institute of Technology, Stockholm, Sweden,* S. Hvilsted, *Condensed Matter Physics and Chemistry Department, Risø National Laboratory, Denmark* and P. S. Ramanujam*, Optics and Fluid Dynamics Department, Risø National Laboratory, Denmark*
e-mail: s.hvilsted@risoe.dk   http://www.risoe.dk/fys/Employee/sohv.htm

Dendritic macromolecules, comprising dendrimers and hyperbranched polymers constitute a novel class of highly branched polymers with a multitude of end-groups. Whereas dendrimers are described by a well-defined, monodisperse structure, the related family of hyperbranched polymers is less well-defined, polydisperse molecules. The Stockholm group has been focusing on the development of hydroxy-functional dendritic and hyperbranched aliphatic polyesters based on 2,2-bis(hydroxy-methyl)propionic acid (bis-MPA).[1] The hydroxy surface of these dendrimers and hyperbranched polymers has been successfully functionalized with different end-groups.[2] Recently, poly(propylene imine) dendrimers have been end-capped with azobenzene groups in order to get materials for holographic storage.[3]

In this study, dendrimers of generation 1 to 3 and a hyperbranched polymer of generation 3 were functionalized with azobenzene groups giving dendritic macromolecules bearing 6, 12, 24, and 32 chromophores, respectively. Different chromophoric units based on the cyanoazobenzene moiety substituted with alkoxy ω-carboxylic acid were coupled to the dendritic matrix by use of an acid chloride reaction as illustrated in Fig. 1 for the second generation with one methylene spacer.

Investigations of these new materials' thermal and optical properties have demonstrated that no LC phase could be observed when the spacer length n is < 5 methylenes, whereas T_g decreases when n increases. When n = 5 or 10 a LC phase was observed. However, with the same n the broadness of the LC phase increases with increasing size of dendrimer generation. Permanent anisotropy on the order of 0.2 rad could be induced in thin film materials with laser light at 488 nm. Investigations by AFM have demonstrated surface relief on the order of 1 μm in these films. The preliminary results have demonstrated that the spacer linking the chromophore to the dendritic core has a dramatic influence on the optical properties and is more important than the size of the dendritic core.
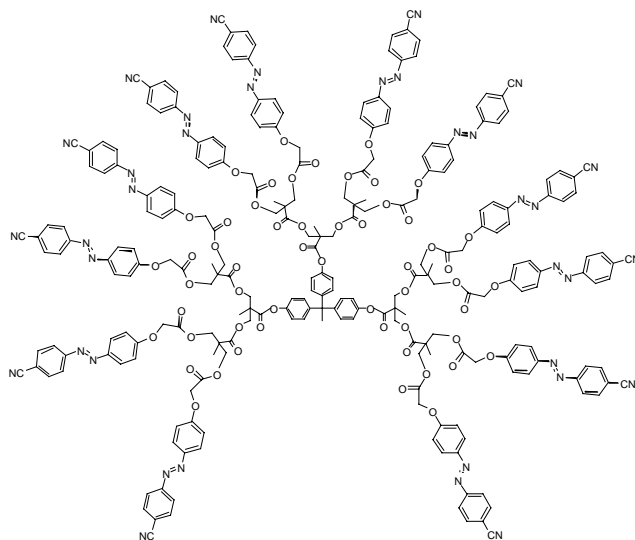
Fig. 1. Azobenzene dendrimer with a second generation aliphatic polyester scaffold and the cyanoazobenzene chromophore with one methylene in the spacer.

[1] E. Malmström, M. Johansson and A. Hult, Macromolecules, **28**, 1698 (1995).
[2] P. Busson, P. Ihre and A. Hult, J. Am. Chem. Soc., **120**, 9070 (1998).
[3] A. Archut, F. Vögtle, L. De Cola, G. C. Azzelinni, V. Balzani, P. S. Ramanujam and R. H. Berg, Chem. Eur. J. **4,** 699 (1998).

2.8.8.   Structure of poly(benzylether) dendrimers in solution

R. Kleppinger, *FOM Institure for Atomic and Molecular Physics, Amsterdam, The Netherlands,* B. Forier, W. Dehaen, *Laboratory for Organic Synthesis, Catholic University Leuven, Heverlee, Belgium,* H. Reynaers, *Laboratory for Molecular Structural Chemistry, Catholic University Leuven, Heverlee, Belgium* and K. Mortensen, *Danish Polymer Centre, Condensed Matter Physics and Chemistry Department, Risø National Laboratory, Denmark*

e-mail: kell.mortensen@risoe.dk   http://www.risoe.dk/fys/Employee/kemo.htm

Dendrimers are well-characterised macromolecules consisting of branched subunits that grow step-wise from a central core. A crucial aspect in view of their potential application as molecular carriers of highly reactive catalysts, is the distribution of the large number of end-groups. Several models have been proposed to account for these distributions. Most well known is the *dense shell model*, proposed by de Gennes and Herves, suggesting an increasing density of the sub-units toward the periphery (see Fig.1). In contrast, the *dense core model* proposed by Mathukumar and Lescanec, predicts a density maximum in the molecular core caused by backfolding of the sub-units. Both simulations[1,2] and experimental studies[2,3] on model dendrimers seem to agree in a relatively homogeneous mass distribution within the dendrimer molecules. Most of the experimental systems that have been studied are, however, polyelectrolytes, where the charges to more or less extend might influence the structure. For this reason, the poly(benzylether)-dendrimers was investigated, where the structure are determined by the conformation of the branched aromatic sub-unints only. In the attempt to further rule out the influence of the solvent, the experiments were performed in both a moderate (tetrahydrofuran, THF and THF-d_4) and a highly polar solvent (dimethylsulfoxide, DMSO and DMSO-d_4). Using contrast variation by mixing the deuterated and non-deuterated solvents, rather detailed structural insight was gained.

The small-angle neutron scattering results shows, that in spite of the significant difference in chemical structure, the dimensions and overall structure of the poly(benzylether)-dendrimers is quite similar to that of both poly(amidoamine) and poly(propyleneimine) systems. The dendrimer size seems also rather unaffected by solvent quality, a result, which differ from that of linear polymers. The molecular parameters shows that the subsegments are relatively homogeneous distributed throughout the polymer, and that the dendrimer-molecule include a significant amount of solvent molecules.
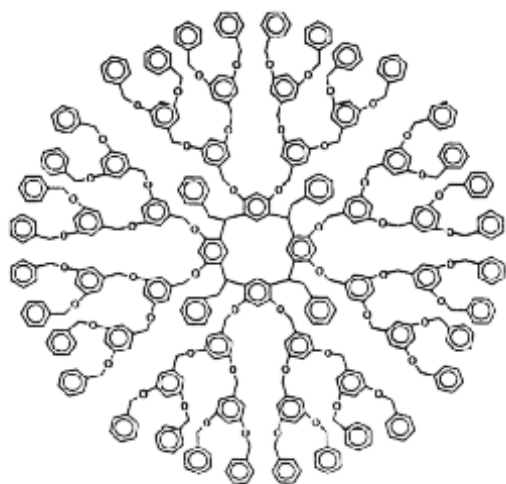
Fig.1. The typical imagination of a perfect dendrimer molecule. This *dense shell model* seems far from the true structure. Scattering data on both polyelectrolyte and neutral dendrimers indicate rather homogeneous mass distribution throughout the dendrimer polymer, caused by major backfolding of the sub-units.

[1] M. Murat and G.S. Grest, Macromolecules **29**, 1278 (1996).

[2] R. Scherrenberg, B. Coussens, P. van Vliet, G. Edouard, J. Brackman, E. Brarander and K. Mortensen, Macromolecules **31**, 342 (1998).

[3] J. Prosa, B. Bauer, E. Amis, D. Tornalia and R. Scherrenberg. J. Pol. Sci. Pol. Phys. **35**, 2913 (1997).

2.8.9. Structural studies of hyperbranched polyesteramides

B. Godaris and R. Sherrenberg, *DSM Research, Geleen, The Netherlands* and K. Mortensen, *Danish Polymer Centre, Condensed Matter Physics and Chemistry Department, Risø National Laboratory, Denmark*

e-mail: kell.mortensen@risoe.dk   http://www.risoe.dk/fys/Employee/kemo.htm

The structures of three different hyperbranched polyesteramides dissolved in THF (1% m/m in deuterated THF) were studied using small-angle neutron scattering (SANS). The SANS-scattering data were analyzed to yield the polymer radius of gyration (R_g) and the polymer fractal dimension (d_f).

The first series consists of five base resins of increasing molar mass, M_w. These are reaction products of a cyclic carboxylic anhydride with di-isopropanolamine. The value of R_g increases with increasing M_w, where the value M_w is based on independent SEC results. For the polymers of lowest M_w, the fractal dimension d_f is close to 1, indicating elongated, rod like structure. With increasing M_w, the d_f-value gradually shifts to 5/3, which is the value characteristic for swollen polymer chains in a good solvent (Figure 1). In the second series, lauric acid was added during the synthesis with the aim to have a 100% fatty acid functionalized resin, while in the third series lower amounts of lauric acid were added to yield products with varying degrees of fatty acid functionalization. The structure of these latter two series did not show fractal characteristics. This is likely to reflect the appending long aliphatic chains. The radius of gyration of these molecules, R_g , as obtained from the SANS data, follow a power law with respect to molar mass, as shown in Fig. 2.
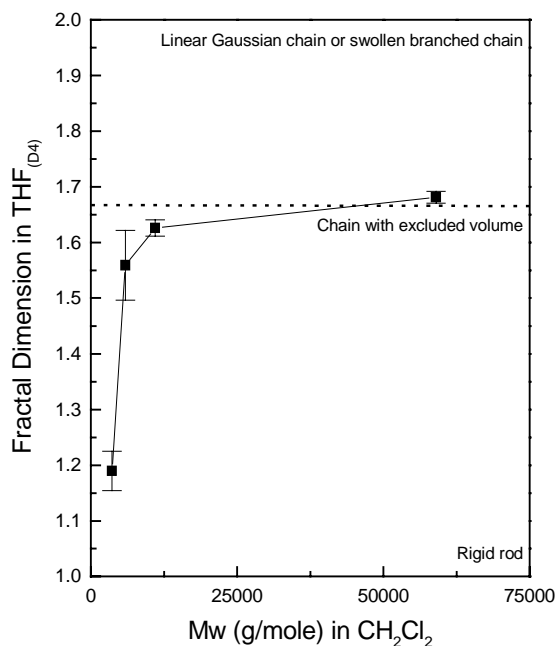
Fig. 1. Illustration of the fractal dimension as a function of M_w for the base resin series: an evolution from rod like particles to swollen polymer coils is observed (chain with excluded volume).
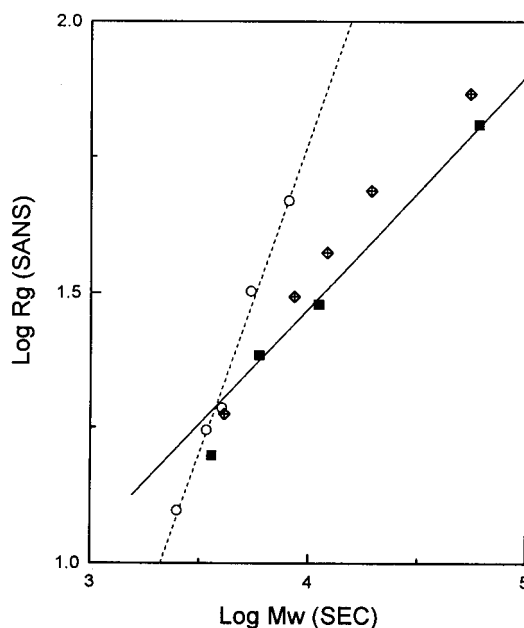
Fig. 2. Double logarithmic presentation of R_g(Å) vs. M_w (g/mole). The slope corresponding to the base resin series equals 0.43 (full squares and full line) and that of the 100% functionalized samples equals 1.16 (open circles and dashed line). The data of the partially functionalized samples are intermediate and not fitted to a linear curve (crossed diamonds*).*

2.8.10. Association of disc-shaped chiral molecules in solution

A. Ramzi, L. Brunsveld, R. Sijbesma, B. Meijer, *Eindhoven University of Technology, Department of Chemistry, Eindhoven, The Netherlands* and K. Mortensen, *Danish Polymer Centre, Condensed Matter Physics and Chemistry Department, Risø National Laboratory, Denmark*
 e-mail: kell.mortensen@risoe.dk   http://www.risoe.dk/fys/Employee/kemo.htm

SANS experiments were performed with the aim to investigate the properties and the conformation of the self-assembled structures in aqueous solutions. The investigated systems are based on C3-symmetrically extended core discotic molecules provided with alkyl chains, or with chiral ethylene oxide side chains to ensure solvatation in water[1]. The association behaviour of related molecules, with chiral alkyl chain, has been studied extensively in hexane with circular Dichroism (CD) and fluorescence spectroscopy.[1] The ethyleneglycol derivatives have been studied with the same techniques in chloroform, butanol and water. The intense CD signals of aqueous solutions, changes sign when the temperature is increased from room temperature to 80°C. This phenomenon indicates profound changes in aggregate structure in this temperature range, probably related to the presence of an LCST of the poly(ethyleneglycol)-like periphery of the structure. At lower temperatures, hydrophobic interactions of the core dominate the aggregation process, while at higher temperatures, the side chains become less soluble in water. In butanol solutions, the CD effect is lost upon heating at a lower temperature than the transition in fluorescence is observed. This indicates that the helical order of the stacks is lost before dissociation takes place. We have studied the morphology of the aggregates in different solvents at different temperatures. Figure 1 shows the scattering intensities at temperature T=20°C for concentrations varying between 0.05 wt% and 2 wt%. The scattering curves are similar and independent on the concentration, leading to the form factor of the aggregates. In "Holtzer plot" ($Q \cdot I(Q)$ vs. Q), the scattering intensities are constant at large Q values ($I(Q) \sim Q^{-1}$), reflecting that the aggregates are rodlike rather than flexible. Dissociation of the aggregates has been also observed in chloroform resulting in a very low aggregation number. By increasing the temperature, the scattering intensity at $Q \rightarrow 0$ decreases, as shown in Fig. 2, due to the dissociation of the aggregates.
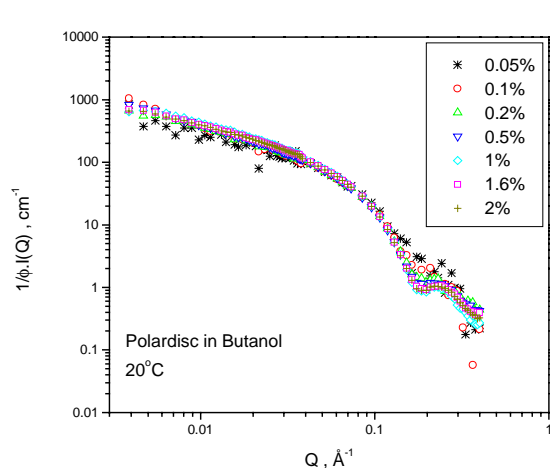
Fig. 1. Scattering intensity of discotic molecules in Butanol for different concentrations varying between 0.05 wt% and 2 wt%. The intensities are normalized by concentration.
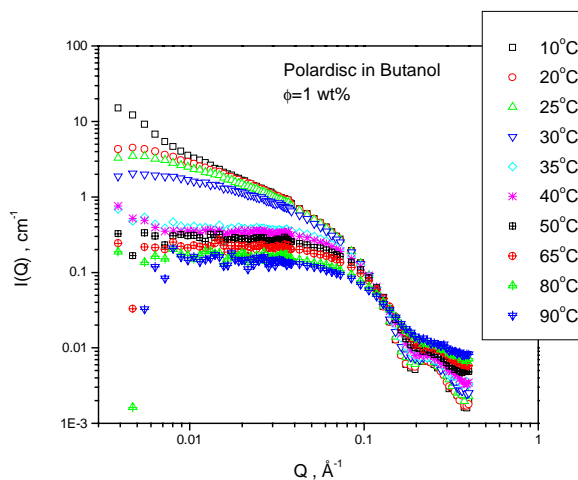
Fig. 2. Scattering intensity obtained at 1 wt% concentration in Butanol for different temperatures ranging from 10°C and 90°C.

[1] A. R. A. Palmans, J. A. J. M. Vekemans, R. A. Hikmet, H. Fischer and E. E. Meijer, Advanced Materials **10**, 873 (1998).

2.8.11. Structure and dynamics of asymmetric diblock copolymer systems in the orderestate[1, 2]

C. M. Papadakis, F. Rittig, G. Fleischer, *Faculty of Physics, University of Leipzig, Germany,* K. Almdal, K. Mortensen, *Danish Polymer Centre, Condensed Matter Physics and Chemistry Department, Risø National Laboratory,* P. Štepánek*, Institute of Macromolecular Chemistry, Academy of Sciences of the Czech Republic, Prague* and M. E. Vigild, *University of Minnesota, Minneapolis, USA*
e-mail: kell.mortensen@risoe.dk   http://www.risoe.dk/fys/Employee/kemo.htm

The dynamic processes in diblock copolymer melts are under intensive discussion. In compositionally symmetric diblock copolymers, the dynamic processes have been assigned as : 1) the cluster mode (diffusion of long-range heterogeneities), 2) the heterogeneity mode (single-chain diffusion), and modes corresponding to 3) undulations of the lamellar interfaces, 4) rotation of lamellas, and 4) segmental reorientational dynamics. In the present work, we have investigated the structure and dynamics of two asymmetric poly(ethylene propylene)-poly(dimethylsiloxane) (PEP-PDMS) diblock copolymers by means of small-angle neutron scattering, transmission of depolarized light, and dynamic light scattering (DLS).

The sample with volume fraction $f_{PEP} = 0.25$ forms at high temperature a disordered state and at low *T* a hexagonal structure. The DLS results are shown in Fig.1. In the disordered state the cluster (not shown) and the diffusive heterogeneity modes are observed. In the hexagonal phase, a broad mode is seen near T_{ODT} which at Lower *T* splits up into two component. The slower mode has an activation energy close to that of pure PEP, and is assigned to the diffusion of copolymers along the cylinder interfaces. The faster mode has an activation energy close to the one of pure PDMS and is attributed to the diffusion of "free" copolymer chains which are not bound to cylinders. The sample with $f_{PEP} = 0.22$ shows beyond the disordered state three ordered morphologies. At low temperatures and right below T_{ODT}, cubic structures are formed, whereas the intermediate phase is non-cubic[1]. This phase sequence is different from theoretical predictions and may reflect the vicinity to the hexagonal phase. In the disordered state, we find again cluster diffusion (not shown) and the heterogeneity mode (Fig. 2)[2]. In the cubic state right below T_{ODT}, we observe two diffusive processes. As the activation energy of the fast mode is close to that of PDMS and independent of *T* (i.e. of structure), we attribute this mode to the self-diffusion of free chains. The slow mode may be assigned to co-operative motions of entire micelles. In the intermediate, non-cubic state, an additional weak mode is observed, likely reflecting the non-cubic structure. In the low-temperature bcc phase, we only observe the self-diffusion of free chains through the PDMS matrix in our experimental time window. The results show that the molecular dynamics is closely related to the sample morphology.
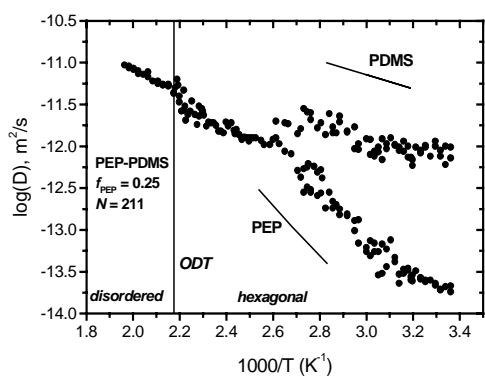
Fig. 1. Arrhenius diagram of the diffusion coefficients of the f_{PEP}=0.25. The single-chain diffusion of PEP and PDMS are also given.
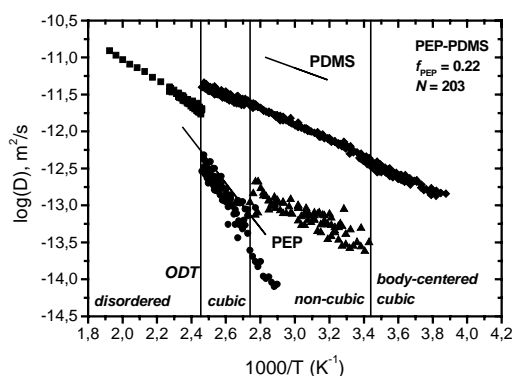
Fig. 2. Arrhenius diagram of the diffusion coefficients of the f_{PEP}=0.22. The single-chain diffusion of PEP and PDMS are also given.

[1] C. Papadakis, K. Almdal, K. Mortensen, M. Vigild and P. Stepanek. J. Chem. Phys **111**, 4319 (1999).

[2] C. Papadakis, K. Almdal, K. Mortensen, F. Rittig, G. Fleischer and P. Stepanek, Eur. Phys. J. Accepted for publication.

2.8.12. Structure of triblock copolymers subject to external deformation

I. W. Hamley , C. Daniel, *School of Chemistry, University of Leeds, UK* and K. Mortensen, *Danish Polymer Centre, Condensed Matter Physics and Chemistry Department, Risø National Laboratory, Denmark*

e-mail: kell.mortensen@risoe.dk   http://www.risoe.dk/fys/Employee/kemo.htm

Triblock copolymers with two polystyrene (PS) end blocks and a rubbery midblock are thermoplastic elastomers. The morphology of such block copolymers depends on the relative volume fractions of the two blocks. In the strong segregation limit, for small polystyrene contents a bcc phase of polystyrene spheres dispersed in a rubbery matrix is formed. Upon increasing the polystyrene content, a phase of hexagonal-packed PS cylinders can form and then for more nearly symmetric copolymers, a lamellar phase is stable.

We have examined the tensile mechanical response of polystyrene-poly(ethylene-co-butylene)-polystyrene triblock (PEBS) copolymers pre-oriented by planar extensional flow in a channel die.[1] Small angle neutron scattering (SANS) measurements revealed that a bcc-phase forming SEBS was oriented with the [111] direction along the flow axis. For the pre-oriented SEBS forming cylindrical microdomains, the cylinder axis were aligned along the extensional flow direction. The structural transformations during stretching were studied in different crystallographic orientations. Two-dimensional SANS patterns recorded at different strains at room temperature with processed G1657 are shown in Fig.1[1]. As the strain increases, the two equatorial (110) reflections move away from the beam center when the four other (110) reflections move closer to the beam center. This shows that interdomain distance along the drawing direction is elongated while the interdomain distance perpendicular to the drawing direction decreases. This deformation of the bcc lattice is affine with the macroscopic deformation of the sample. The deformation of the microstructure is reversible when deformation is suppressed. For the triblock copolymer with a cylindrical microdomain structure the deformation of the lattice was found to be non-affine.
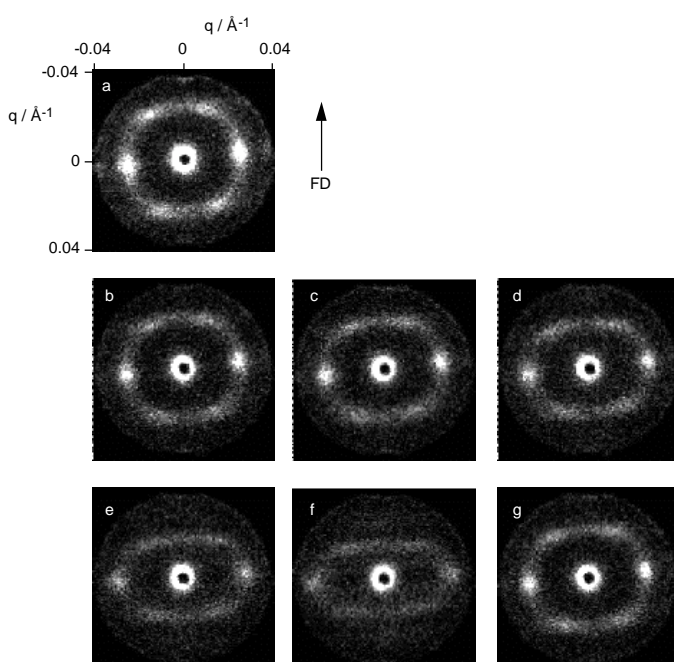
Fig. 1. SANS patterns for the sample G1657 obtained at the following extension rates:[1] (a) 0, (b) 5%, (c) 10%, (d) 20%, (e) 40%, (f) 63%, (g) 12%.

---

[1] I. W. Hamley, C. Daniel and K. Mortensen, Abstr. Pap. Am. Chem. Soc. **218** (1999).

2.8.13. Synthesis, characterization, and structural investigations of poly(ethyl acrylate)-*l*-polyisobutylene bicomponent conetwork[1]

K. Almdal, K. Mortensen, I. Johannsen, *Condensed Matter Physics and Chemistry Department, Risø National Laboratory, Denmark,* B. Iván, *Department of Polymer Chemistry and Material Science, Institute of Chemistry, Chemical Research Center, Hungarian Academy of Sciences, Hungary* and J. Kops, *Department of Chemical Engineering, Technical University of Denmark, Denmark*
e-mail: k.almdal@risoe.dk   http://www.risoe.dk/fys/Employee/kral.htm
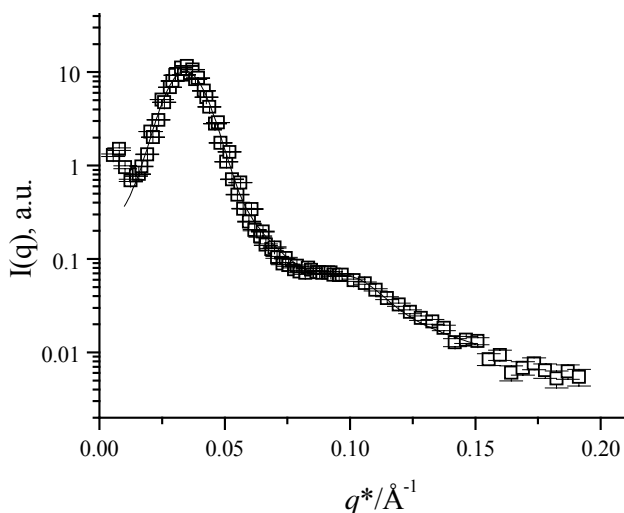
Fig. 1. Isotropic SANS. Azimuthally average data from 2 detector distances (3 m and 1.5 m) at 25°C. The line is a fit to two Lorenztians.

A new bicomponent conetwork, poly(ethyl acrylate)-*l*-polyisobutylene (PEtA-*l*-PIB) was synthesized by radical copolymerization of equal amounts of telechelic α,ω-dimethacrylic PIB (M_n = 11,200, M_w/M_n = 1.12 and MA/chain = 2.0) and ethyl acrylate in solution in a common solvent, tetrahydrofuran, followed by extraction and drying. Low amounts of extractable and nearly theoretical composition (51 % PEtA and 49 % PIB) of the resulting conetwork indicate efficient network formation. The structure of the conetwork was investigated by small angle neutron scattering (SANS) in the relaxed state and two correlation peaks were observed at $q^*/Å^{-1}$=0.035 and at $3q^*$ (see Figure 1). The macroscopically homogeneous conetwork is characterized by local layered like segregation with a correlation length of 445 Å and periodicity of 180 Å. Data collected at separately

at low *q* does not indicated any structure on longer length scales. The mechanical and structural properties on elongation were investigated. The resulting equilibrium stresses of the network are given in Figure 2. The sample is assumed to behave as a Hookean solid and the data is fit to the equation $\sigma_{eng}=(E/3)(\alpha-\alpha^{-2})$, where σ_{eng} is the engineering stress, α is the elongation ratio and *E* is Young's modulus. Young's moduli of 0.44 MPa at 25°C and 0.31 MPa at 60°C is obtained, respectively.

If one assumes perfect cross-linking and no influence of the microstructure on the modulus one can estimate Young's modulus from the theory of rubber elasticity. Each bifunctional PIB chain is connected to four elastic active chains of PEtA. However, each PEtA chain is also connected to another PIB-chain such that the number of elastic chains in the ideal case is three times the number of PIB chains. $E=3((f-2)/f)\nu RT$, where *f* is the functionality of the junction point (here 3) and ν is the number density of elastic chains. $\nu=3w\rho/M_{n,PIB}$, where *w* is the mass fraction of PIB in the network. With $M_{n,PIB}$/(kg/mol)=11.2, and the average density ρ/(g/cm^3)=1.01 *E*/MPa=0.32 which is surprisingly close to the measured modulus.
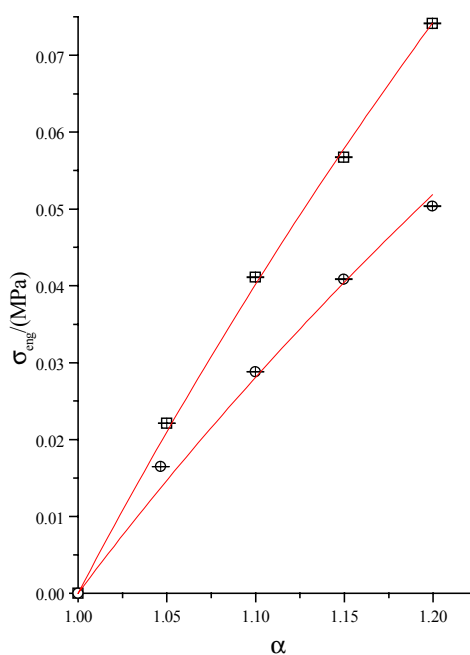
Fig. 2. The engineering stress of the PEtA-*l*-PIB network as a function of elongation ratio at 25°C (□) and 60°C (○). The lines are fits and represent a Hookean solid (see text).

---

[1] B. Iván, K. Almdal, K. Mortensen, I. Johannsen and J. Kops. Submitted to Macromolecules.

2.8.14. Crystallographic studies of triblock copolymer gels, applying neutron scattering and electron microscopy

K. Mortensen, K. Almdal, *Danish Polymer Centre, Condensed Matter Physics and Chemistry Department, Risø National Laboratory, Denmark*, R. Kleppinger, *FOM Institute Amsterdam, The Netherlands,* E. Theunissen, H. Reynaers, *Catholic University Leuven, Belgium* and R. Spontak, *North Carolina State University, USA*
e-mail: kell.mortensen@risoe.dk   http://www.risoe.dk/fys/Employee/kemo.htm

The ability of block copolymers to order into nanoscaled microstructures can be controllably modified through the addition of low-molar-mass solvents. We have studied the structure of triblock copolymers of the SEBS type: poly(styrene)-poly(ethylene bytylene)-poly(styrene) mixed with solvent selective for the PEB-midblock, such as tetradecane. The triblock copolymer system investigated within large regimes of the temperature/concentration phase diagram form spherical polystyrene micelles. At ambient temperatures these micelles are glassy resulting in a permanent network structure.
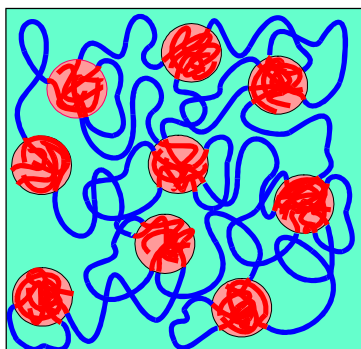
Fig. 1. Schematic illustration of the micellar network structure obtained from triblock copolymers in midblock selective solvents.

Upon annealing above the glass transition temperature, the micelles organize into a body centered cubic lattice. Upon exposure to oscillatory shear, the ordered domains align into basically defect free macroscopically ordered crystal, as verified by both neutron scattering and electron microscopy. The given orientation of the nanoscale ordered structure depends on both shear amplitude and frequency. For frequencies of the order of 1 sec^{-1} and shear amplitudes of the order of 50-100% the sample is single crystalline with shear gradient (∇) and vortex (**e**) direction parallel to respectively the [111] and [110] crystallographic axes. For shear amplitude of more than 100%, the sample form the bcc-twin structure with ∇ parallel to [110] axis and **e** parallel to the common [111] axis Fig.2 shows the SANS data of such shear aligned twin structure.
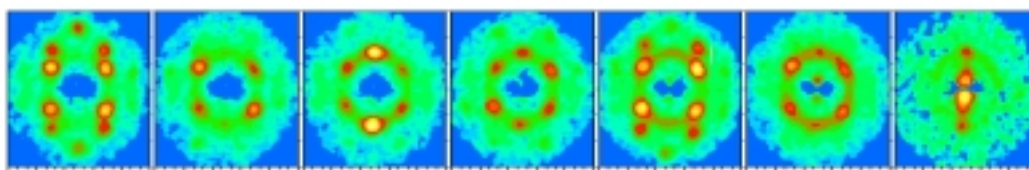
Fig. 2. SANS data of 30% SEBS-1650 in tetradecane, as obtained at *T*=65°C after large amplitude shear. The 9 pattern are obtained with the sample rotated in steps of 10 degree around the common [111]-axis of the two twin domains. The far-left figure corresponds to the (111,112) twin plane.

2.8.15. Characterisation of diblock copolymer blends

H. Frielinghaus, N. Hermsdorf, K. Almdal, K. Mortensen, *Condensed Matter Physics and Chemistry Department, Risø National Laboratory, Denmark*, N. Terrill, *CCLRC Daresbury Laboratory, Warrington, UK* and I. W. Hamley, *School of Chemistry, University of Leeds, UK*
e-mail: henrich.frielinghaus@risoe.dk   http://www.risoe.dk/fys/Employee/hefr.htm

The experimental determination of the phase diagram of diblock copolymer blends can be supported by SAXS, TEM and light microscopy. SAXS experiments were carried out at the SRS Daresbury, TEM measurements were performed at the University of Sheffield / MPI Berlin, and light microscopy at the Risø National Laboratory.

The SAXS data were collected at the station 8.2 at the SRS Daresbury. The samples were prepared into DSC-pans with MICA-windows, and heated by a Linkam-DSC-furnace. The sample spectra were corrected for detector sensitivity, background, sample transmission, and sample thickness. The scattering vector Q was calibrated by a rat-tail pattern of collagen.

A SAXS heating/cooling run is presented in Fig. 1 for a PS-PI/PI-PEO blend (M_W=20k/7k, Φ_{PI-PEO}=0.5). During heating the crystallised PEO-PI shows a broad intense peak in the SAXS pattern,

which vanishes at 50°C. Two sharp intense peaks show up with accompanying higher order peaks. All peaks can be indexed after a bcc sphere structure. At higher temperatures (160°C ≤ T ≤ 184°C) the broadening of the main peak indicates an order-disorder-transition, whereas the intense √2-peak remains sharp. The remaining higher order peaks can be indexed after a hexagonal cylinder phase. In a small temperature range (184°C ≤ T ≤ 193°C) two broad main peaks coexist before they merge into one. On the cooling cycle the reversed sequence is observed except for the crystallisation, which is regained at least after about one month's period. The state of this sample at temperatures in between 50°C and 160°C can hardly be judged, whether it is one commonly ordered phase or two separated, ordered phases. The Q-ratio of
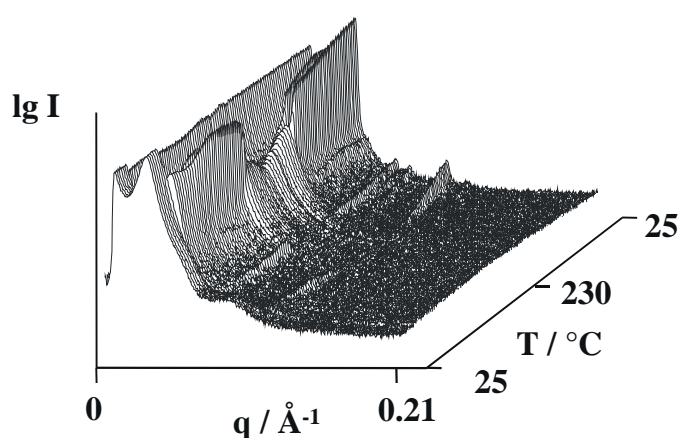
Fig. 1. SAXS data of a PS-PI/PI-PEO blend (f_{PI}=0.7/ Φ=0.5) on a heating/cooling run. During heating the PEO is crystalline at low temperatures. At intermediate temperatures two sharp main peaks indicate ordered phases. The higher order peaks help to resolve the ordered phase. The main peaks independently get broader, which means disorder. At high temperatures there is just one broad main peak, which indicates one homogeneous phase.

the intense peaks is about 6% larger than $\sqrt{2}$, which one expects for a commonly ordered bcc phase. This deviation is accurate within the peak width, but not within the statistical error (~0.3%).

The parallel measurements on the TEM show an ordered structure with circles and rectangles on the surface, which can result from spheres/cylinders and cylinders/lamellae, respectively. This observation supports the SAXS experiments that the sample is ordered at room temperature. The current TEM pictures cannot distinguish between a one-phase and two-phase sample. By polarisation light microscopy one finds a homogenous, non-turbid greyish sample for all temperatures (≤ 220°C), which might indicate the sample to be one phase.

The SAXS measurements and light microscopy cannot clearly distinguish between one- and two-phase, and therefore refined SAXS on shear aligned samples must help to clarify this point. Furthermore a larger amount of TEM pictures might help to identify the ordered phases.

2.8.16. Random phase approximation for diblock copolymer blends

H. Frielinghaus, N. Hermsdorf, K. Almdal, K. Mortensen, *Condensed Matter Physics and Chemistry Department, Risø National Laboratory, Denmark,* P. D. Olmsted and I. W. Hamley, *School of Chemistry, University of Leeds, UK*

e-mail: henrich.frielinghaus@risoe.dk   http://www.risoe.dk/fys/Employee/hefr.htm

The phase behaviour of diblock copolymers and of homopolymer blends has been of interest both experimentally and theoretically for some years. In this paper, we predict the phase behaviour of an A-b-B/B-b-C diblock copolymer blend from experimentally determined interaction parameters χ_{ij} between monomer species A, B and C.

The phase diagram depends besides χ_{ij} on the blend composition ϕ, and on architectural parameters of the diblock copolymers. The architecture of the single diblock copolymers is described by the degrees of polymerisation N and the chain length ratios f. The theory[1] was developed within the random phase approximation (RPA), and thus is a mean field theory. The two fluctuation amplitudes are associated with micro and macro phase separation, i.e. separation of A and C from B, and of A from C. Thus, there exist two spinodal lines, which are indicated by the criticality of the corresponding mode.

In the case of a 4k/17k PI-PEO/PI-PS blend [$f=f_1=f_2=\frac{1}{2}$] (Fig.1), a transition from the homogenous state at high temperatures to the macro phase separated state is predicted for intermediate compositions. That means the diblock copolymer blend is a two-phase system at low temperatures. Either of the two phases orders independently from the other. Against that, the almost pure diblock copolymers order first by cooling down from higher temperatures. The once ordered diblock copolymer blend tends to be a one-phase system even at lower temperatures. This behaviour is obtained by taking just the spinodal lines into account. The composition range of macro phase separation is extended by the refinement of the binodal line, which is calculated by the effective (macro phase separation)-interaction parameter $\chi_{macro}=\chi_{AC}(1-f_1)(1-f_2)+\chi_{AB}(1-f_1)(f_2-f_1)+\chi_{BC}(f_1-f_2)(1-f_2)$. This expression can be found as well for random copolymer theories, which do not take monomer sequences into account.

Fig. 1. RPA phase diagram predicted for a PI-PEO/ PI-PS blend, with molecular weight of 4k and 17k respectively. The spinodal of the macro phase separation (—) intersects the spinodal of the micro phase separation (▪▪▪▪▪). The binodal (·····) enlarges the composition range, where macro phase separation occurs.

The miscibility of the two diblock copolymers can be increased by a higher PI content. This feature is already obvious by discussing a system with the same chain length ratio $f=f_1=f_2$, because the effective (macro phase separation)-interaction parameter reads like $\chi_{macro} = \chi_{AC}(1-f)^2$ then. A chain length ratio of f=0.7 is sufficient for full miscibility, i.e. the spinodal of the microphase separation occurs at higher temperatures than the macrophase separation. This theory allows for the critical modes being mixed, i.e. the critical macrophase separation mode contains not only separation of PI from PS and PEO. Therefore, the microphase spinodal generally bends a bit down on the low PI-PEO-content side (Fig.1), and thus explains the quite high f-value of 0.7 for full miscibility.

To conclude, the miscibility of two diblock copolymers can be predicted by an effective (macro phase separation)-interaction parameter. The predicted microphase separation spinodal can deviate from a simple interpolation (≥ 50K). However, for chain length ratios f > 0.7 the considered diblock copolymers are predicted to microphase separate before they might macrophase separate.

---

[1] P. D. Olmsted and I. W. Hamley, Europhys. Lett. **45**, 83 (1999).

2.8.17. Phase behavior of ternary homopolymer/block copolymer blends near the mean-field Lifshitz point

K. Mortensen, K. Almdal, H. Frielinghaus, *Danish Polymer Centre, Condensed Matter Physics and Chemistry Department, Risø National Laboratory, Denmark*, F. S. Bates, W. W. Mauler, T. P. Lodge, *University of Minnesota, Minneapolis, USA* and D. Schwahn, *IFF, Forschungzentrum Jülich, Germany*
e-mail: kell.mortensen@risoe.dk   http://www.risoe.dk/fys/Employee/kemo.htm

A three component mixture of a critical binary homopolymer blend and the corresponding symmetrical diblock copolymer leads, for suitable choices of molar masses, to a diagram that beyond the homogeneous disordered phase include a single ordered phase, a two phase region and a microemulsion channel. Further, special critical features are observed near the mean-field predicted isotropic Lifshitz critical point. In the disordered high-*T* regime *blend-like* and *diblock-copolymer-like* properties are separated by the Lifshitz, i.e. for diblock content above the *LL* the maximum value $S(q^*)$ of the structure factor occurs at finite *q*-value, while below the *LL* $S(q^*)$ appear at $q^*=0$. Such unified type of phase diagram has been observed for three polymer systems, namely ternary systems of PE-PEP/PE/PEP, PE-PEO/PE/PEO and PEE-PDMS/PEE/PDMS[1]. Fig.1 shows the experimental phase diagram of the latter system.

According to mean field theory, there should be no microemulsion channel (*μE)*. The three phase lines should rather meet in a tri-critical Lifshitz point, *LP*. Even though fluctuations destroy this critical point, giving rise to the *μE,* there are clearly critical fluctuations emerging from the *LP*[2]. The measured susceptibilities has been analyzed by the scaling law according to $S^{-1}(0)=C_+^{-1} t^\gamma$ with the reduced temperature, $t=(T-T_{LP})/T$, and C_+ being the mean-field critical amplitude, giving the critical exponent γ and ν as shown in Fig.2. Relative far from the critical point (as obtained according to extrapolation) the critical exponent of the PEE-PDMS/PEE/PDMS system is $\gamma = 1.24$ in accordance with the Ising universality class. Near the *LP*, however, the exponent is significantly further enhanced, $\gamma = 2.44$, reflecting the major renormalization as a consequence of the large upper critical dimension of the Lifshitz universality class ($d_U=8$).
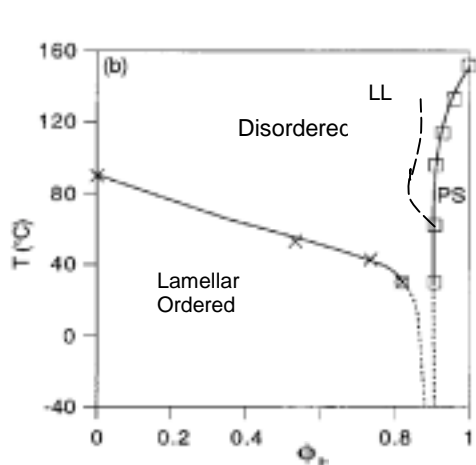
Fig. 1. Experimental phase diagram of ternary PEE-PDMS/PEE/PDMS polymer system.[1,2]
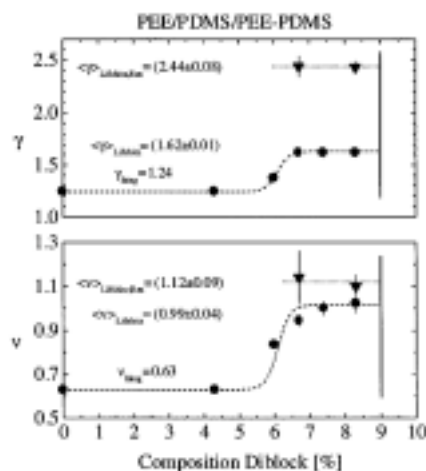
Fig. 2. Critical exponents, showing the significantly renormalized values near the mean-field expected Lifshitz point.[2]

[1] M. A. Hillmyer, W. W Maurer, T. P. Lodge and K. Almdal, J. Phys. Chem. **103**, 4814 (1999).
[2] D. Schwahn, K. Mortensen, H. Frielinghaus and K. Almdal, Phys. Rev. Lett. **82**, 5056 (1999).

2.8.18. SANS study of structure and inter-particle forces in composite materials

K. Jack, T. Cosgrove, *The School of Chemistry, The University of Bristol, UK* and J. S. Pedersen, *Condensed Matter Physics and Chemistry Department, Risø National Laboratory, Denmark*
e-mail: jan.skov.pedersen@risoe.dk   http://www.risoe.dk/fys/Employee/jask.htm

We have obtained SANS measurements for silica particles in polyethylene glycol (PEG) media as a function of particle concentration, at two different molecular weights of PEG, and for a range of PEG molecular weights at fixed particle loading. Furthermore, the structure of the particle matrix interface has been probed in a number of experiments in which an additional interfacial agent was added to the systems. The aim of these experiments is to investigate inter-particle forces in particle-polymer composites and the structures that these give rise to. Qualitative results from these experiments are discussed below, although, it should be noted that as these measurements were obtained very recently, quantitative analysis, by detailed simulation of these data, are still being carried out.

In Fig.1. we show the SANS scattering from a sample containing 20% silica in 600 molecular weight PEG upon addition of a third 'displacing' component, either dimethyl sulphoxide or poly (vinyl pyrollidone). It can be seen that the addition of both of these displacers leads to significant change in the scattering at low Q. It is believed that the increased scattering at low Q observed for the sample containing PVP (c.f. the sample containing no displacer) is due to an increased repulsive inter-particle interaction, e.g. due to steric repulsion of the PVP chains. Moreover, it is believed that the downturn in the scattering at low Q upon addition of the low molecular weight displacer (DMSO) may be a signature for depletion forces in this system.

The SANS measurements (not shown) of the silica in PEG show a complex trend as a function of particle loading and matrix molecular weight. We are currently fitting this data to a model in which the initial ordering of the silica particles become disrupted by adsorption and steric interactions of the polymer matrix material.
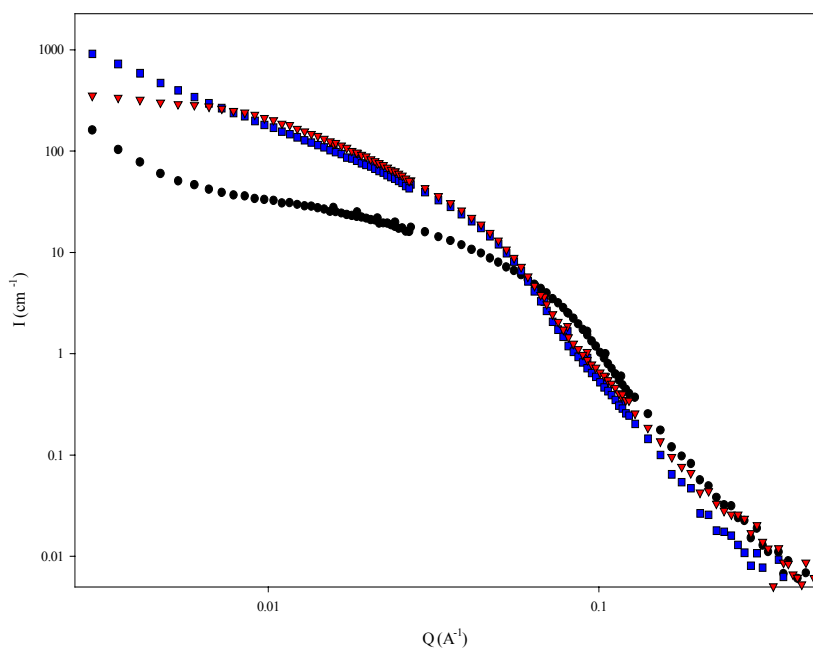
Fig. 1. SANS from a composite containing 20% silica in PEG 600 molecular weight. Pure composite (circles), with 100% coverage of PVP, as determined by NMR, (squares), with 1% DMSO (triangles).

2.8.19. A contrast variation SANS-study of the structure of polystyrene-polyisoprene block co-polymer micelles in decane

J. S. Pedersen, C. Svaneborg, K. Almdal, *Condensed Matter Physics and Chemistry Department, Risø National Laboratory, Denmark,* R. N. Young, *Department of Chemistry, University of Sheffield, UK* and I. W. Hamley, *School of Chemistry, University of Leeds, UK*
e-mail: jan.skov.pedersen@risoe.dk   http://www.risoe.dk/fys/Employee/jask.htm

The structure of micelles of three polystyrene-polyisoprene (PS-PI) diblock copolymers has been studied in n-decane, which is a selective solvent for PI. The polymers have relatively high molecular weights of the PI blocks and this result in strong excluded volume effects for the individual PI chain as well as en-forces relatively strong chain-chain interactions in the corona. Two of the polymers have a molecular weight of about 40k for the fully deuterated d-PS block and, respectively, about 40k and 80k for the PI block. The third polymer has molecular weight of about 12k and 48k of the d-PS and PI block, respectively. Samples with a polymer volume fraction of 2% were prepared in deuterated and protonated dec-ane. The samples were initially heated to 80°C, as suggested in the literature, to dissolve the polymer and to have equilibrium micelles forming. Small-angle x-ray scattering (SAXS) was performed in order to check the samples and it was found that the micelles of the polymers with PS of a molecular weight of 40k were different in protonated and deuterated decane. Only when the samples were heated above 100°C for more than 4 hours, were the micelles identical in the two solvents. SANS measurements were performed on these samples, and on samples prepared by mixing to give 33 and 67% deuterated decane (see Figure). Due to the strong intra- and inter-chain interactions in the corona, the data can not be fitted by the form factor for micelles with non-interacting chains[1]. The data was fitted simultaneously by a model developed from Monte Carlo simulation results. The micelle model has a compact core with a fraction of solvent included and a corona surrounding the core with a radial distribution described by (half of) a Gaussian function, which is centred at the core surface. The fluctuation scattering of the co-rona is described by a random phase type expression. Polydispersity of the micellar size is also included, and the particle interference effects are described by a hard-sphere model, which includes polydispersity of the interaction radius. The model fits the 0 and 100% data perfectly, however, it predicts a too low scattering intensity for the intermediate contrasts. These can also be fitted if part of the solvent in the core is assumed not to be exchanged in the mixtures, so that the micelles contains part of the original solvents from the 0 and 100% solutions. The reduced surface concentration of the PI chains relative to the overlap concentration can be calculated as $\sigma/\sigma^* = \pi R_g^2 / [4\pi(R + R_g)^2/N]$, where R_g is the radius of gyration, R is the core radius and N is the number of chains. The value is $\sigma/\sigma^* \approx 4$ suggesting a pro-nounced interaction between the chains as expected.
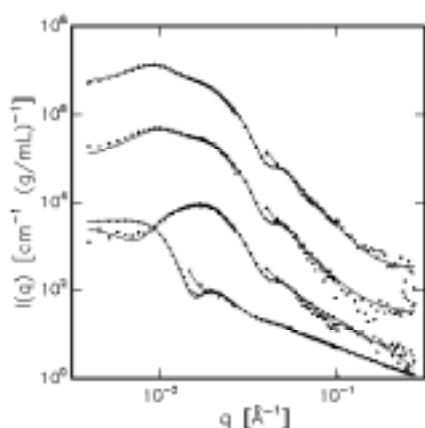
Fig. 1. Small-angle scattering contrast variation data for the polymer with molecular weight 40k and 40k for the PS and PI blocks. From bottom to top the data are the SANS results for 0, 33, 67 and 100% d-decane, respectively. For clarity the 0, 33 and 67% data have been multiplied by 1000, 100, and 10, respectively.

---

[1] J. S. Pedersen and M. C. Gerstenberg, Macromolecules **29**, 1363 (1996).

2.8.20. Form factors of block copolymer micelles with spherical, ellipsoidal and cylindrical cores

J. S. Pedersen, *Condensed Matter Physics and Chemistry Department, Risø National Laboratory, Denmark*

e-mail: jan.skov.pedersen@risoe.dk   http://www.risoe.dk/fys/Employee/jask.htm

When a block copolymer is dissolved in a solvent, which is a good solvent for one block and a poor solvent for the other block, micelles are formed. The insoluble blocks form a relatively compact core whereas the soluble blocks form a diffuse corona surrounding the core. The form factor of a micelle model with a spherical core and Gaussian polymer chains attached to the surface has previously been calculated analytically[1]. Non-penetration of the chains into the core region was mimicked in the analytical calculations by moving the center of mass of the chains R_g away from the surface of the core, where R_g is the radius of gyration of the chains. In the present work[2], the calculations have been extended to micelles with ellipsoidal and cylindrical cores. Non-penetration was also for these taken into account by moving the center of mass of the chains R_g away from the core surface. In addition results for worm-like micelles, disk-shape micelles and micelles with a vesicle shape are given. The figure shows the form factor of cylindrical micelles for homogeneous contrast, where core and chains have equal contrast, for core contrast, where only the core scatters and shell contrast, where only the chains are observed.
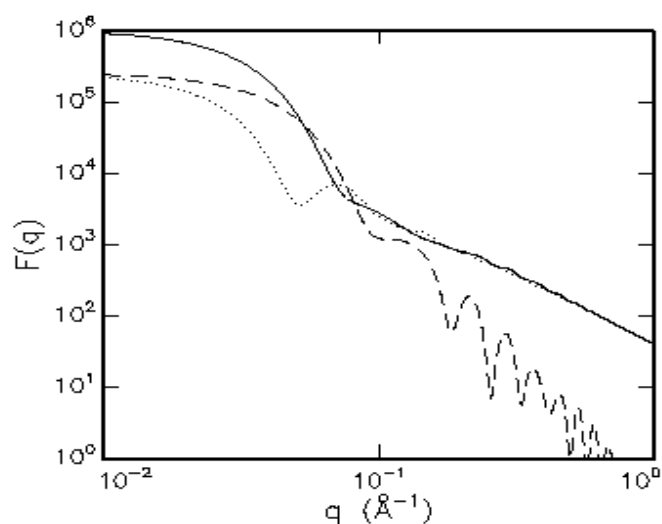
Fig. 1. Form factor of a micelle with a cylindrical core with radius $R = 40$ Å and length $L = 100$ Å. Full line: homogeneous contrast, broken line: core contrast, and dotted line: shell contrast.

---

[1] J. S. Pedersen and M. C. Gerstenberg, Macromolecules **29**, 1363 (1996).
[2] J. S. Pedersen, J. Applied Cryst. In the press.

2.8.21. Structure factors effects in small-angle scattering from block copolymer micelles and star polymers

J. S. Pedersen, *Condensed Matter Physics and Chemistry Department, Risø National Laboratory, Denmark*

e-mail: jan.skov.pedersen@risoe.dk   http://www.risoe.dk/fys/Employee/jask.htm

When a block copolymer is dissolved in a solvent, which is a good solvent for one block and a poor solvent for the other block, micelles are formed. The insoluble blocks form a relatively compact core whereas the soluble blocks form a diffuse corona surrounding the core. Results for the form factor of a block copolymers micelle model with a spherical core and Gaussian polymer chains attached to the surface has previously been calculated[1]. In the present work[2] the inclusion of particle interference effects in terms of a structure factor $S(q)$ is described, where q is the length of the scattering vector. The scattering intensity is described by the expression

$$I(q) = F_{mic}(q) + A^{av}{}_{mic}(q)^2 [S(q)-1],$$

where $F_{mic}(q)$ is the form factor of micelle and $A^{av}{}_{mic}(q)$ is the amplitude of the Fourier transform of the *centro-symmetrically averaged* (radial) scattering length density distribution. The expression is not a simple product of the form factor and the structure factor, which has the important consequence that the effective structure factor, defined as

$$S_{eff}(q)=I(q)/F_{mic}(q),$$

depends on the relative scattering contrast of the core and the corona of polymer chains. This is demonstrated in the Figure, where the effective structure factor is plotted for micelles interaction with a hard-sphere potential. The hard-sphere volume fraction is 0.3 and the interaction radius is equal to $R + 2 R_g$, where R is the core radius and R_g is the radius of gyration of the chains in the corona. The effective structure factors have large differences for $q > 0.04$ Å^{-1} where the effective structure factors of decay much faster to unity than the hard-sphere structure factor. Note that for shell contrast there is even a reduction of the first maximum in the structure factor relative to the pure hard-sphere structure factor. Similar effects as those described for the micelles are present for star polymers, as the form factor of star polymers is obtained from that of micelles by letting the radius approaching zero.
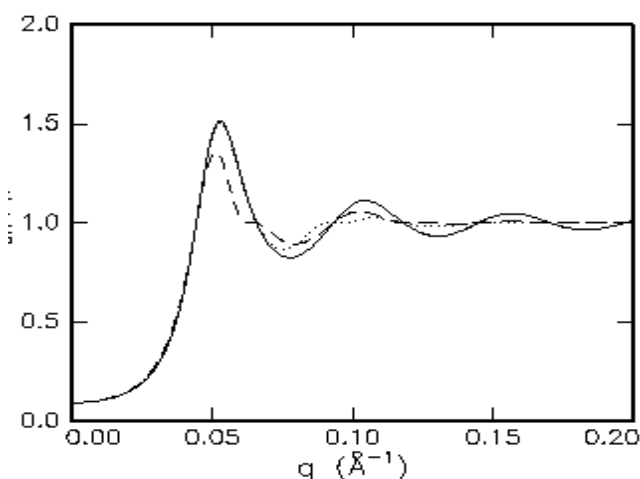
Fig. 1. The effective structure factor of a micelle with hard-sphere interactions and with equal scattering length of the core and the chains (broken curve) and of a micelle for which only the chains contribute to the scattering (dotted curve). The pure structure factor for a hard sphere is also shown (full curve).

---

[1] J. S. Pedersen and M. C. Gerstenberg, Macromolecules **29**, 1363 (1996).
[2] J. S. Pedersen. Submitted to J. Chem. Phys.

2.8.22. Analytical expression for the form factor of block copolymer micelles with chain-chain interactions

C. Svaneborg and J. S. Pedersen, *Condensed Matter Physics and Chemistry Department, Risø National Laboratory, Denmark*

e-mail: carsten.svaneborg@risoe.dk   http://www.risoe.dk/fys/Employee/casv.htm

A block copolymer micelle consists of a dense core of the insoluble blocks surrounded by a corona of solvated blocks. For micelles with a low surface coverage or in a theta solvent the corona scattering is very well described by the non-interacting model due to Pedersen and Gerstenberg[1]. However, chain-chain interaction becomes increasingly more significant at higher surface coverage fractions. To a first approximation the corona of interacting chains can be described by an radial density distribution of monomers (a core-shell model[2]), the radial density distribution can in turn be described empirically or be calculated from a self-consistent mean field theory. However, this level of approximation fails to account for effects associated with the polymer chain connectivity. Based on Monte Carlo simulations we have improved the core-shell model by using an Random Phase Approximation[3] expression to take account of the monomer density fluctuations introduced by the chain connectivity, and the effects on the single chain form factor by the interaction with other chains. We modify the model by including the RPA. chain form factor $P_{eff}(q) = P(q) / [1+\nu P(q)]$ in the core-shell expression for the corona scattering. Here ν is a concentration parameter, and $P(q)$ is the form factor of a non-interacting chain. In this approximation the corona is described as a semi-dilute polymer solution with a given radial density profile, which we model as a box profile with a Gaussian tail. The surface coverage fraction is defined as $\sigma/\sigma^* = N \pi R_g^2 / [4\pi(R_{co} + R_g)^2]$, where R_g is the chain radius of gyration, and R_{co} is the core radius. For the simulated polymer corona scattering shown in fig 1 (left) the surface coverage fraction is in the range from 0.02 to 5, and the model fits reproduce the MC simulation results within the statistical errors for $\sigma/\sigma^* < 1$, and they are in good agreement for $1 < \sigma/\sigma^* < 5$. Fig. 1 (right) shows that the concentration parameter derived from fits follow a power law as function of surface coverage fraction.
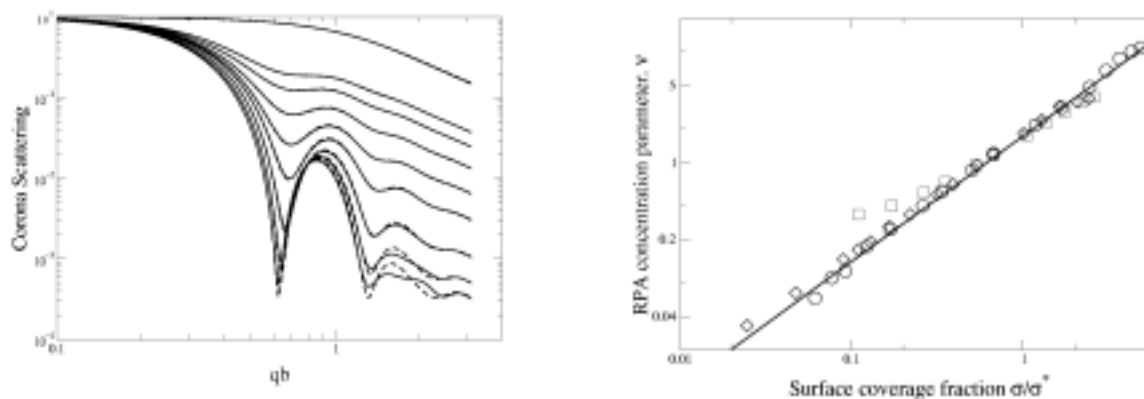
Fig. 1. (left) the model fitted to the simulated scattering from the micellar corona as a function of the number of chains, which is gradually increased from $N = 1$ to $N = 320$ (solid line simulation, dashed line fit). b is Kuhn length of the simulated chains. (right) The RPA concentration parameter ν against surface coverage fraction for a number of simulations varying number of chains (circles), chain length (boxes) and core radius (diamonds), the line is the power law $\nu = 1.76 \ (\sigma/\sigma^*)^{1.14}$.

1 J. S. Pedersen and M. C. Gerstenberg, Macromolecules **29**, 1363 (1996).

[2] S. Förster and C. Burger, Macromolecules **31**, 879 (1998).

[3] H. Beniot and M. Benmouna, Polymer **25**, 1059 (1984).

2.8.23. Monte Carlo simulation of block copolymer micelles with excluded volume interactions

C. Svaneborg and J. S. Pedersen, *Condensed Matter Physics and Chemistry Department, Risø National Laboratory, Denmark*

e-mail: carsten.svaneborg@risoe.dk   http://www.risoe.dk/fys/Employee/casv.htm

The effects of excluded volume interactions on the scattering from block copolymer micelles have been investigated by performing Monte Carlo simulations (MC). A micelle is represented as a number of semi-flexible chains tethered to a spherical core with radius R_{co}. Chains interact via hard-sphere interactions with the core and other chains. During an MC simulation the conformation averaged partial contributions to the micelle scattering are sampled, and they correspond to the scattering data available from a neutron contrast variation experiment. The averaged radius of gyration and average distance to the micelle core for each chain is also sampled. The scattering from the micelle depends on the scattering vector q and three dimensionless parameters: The surface coverage fraction defined as $\sigma/\sigma^* = N\pi R_g^2 / [4\pi(R_{co} + R_g)^2]$, where R_g is the radius of gyration, the surface curvature measured by R_g / R_{co}, and N the number of chains. Simulations have been performed varying the number of chains, the chain length (e.g. the chain radius of gyration), and the core radius. Similar simulations were carried out with chain-core interactions but without chain-chain interactions. The simulation data was analysed using a model, which describes micelles with non-interacting chains, but include effects due to chain connectivity and approximate the effects arising from core expulsion[1]. This model was chosen in order to understand to which extent it could provide accurate estimates for the structure of micelles with interactions, and to determine the effects due to excluded volume interactions on the micellar scattering. The model depends only on two parameters: the chain radius of gyration, and the chain average distance from the micelle core, both were sampled during the MC simulations. The conclusion is, that for $\sigma/\sigma^* \ll 1$ chains are only weakly perturbed by the other chains, and the model provide accurate estimates for the two parameters. For $\sigma/\sigma^* \sim 1$ excluded volume effects becomes significant, but the model still provides a reasonable estimate (radius of gyration with less than 10% deviation, and average chain distance within 20%). We modified the model slightly to approximate chain stretching close to the micelle surface, by describing the chains as consisting of two segments: a radially pointing rigid rod onto which a flexible chain is attached. This has improved the average chain distance to the micelle core estimate, but at the expense of a more inaccurate estimate of radius of gyration. It can also be considered as an improved representation of core expulsion effects for the chains, which are not mutually interacting.
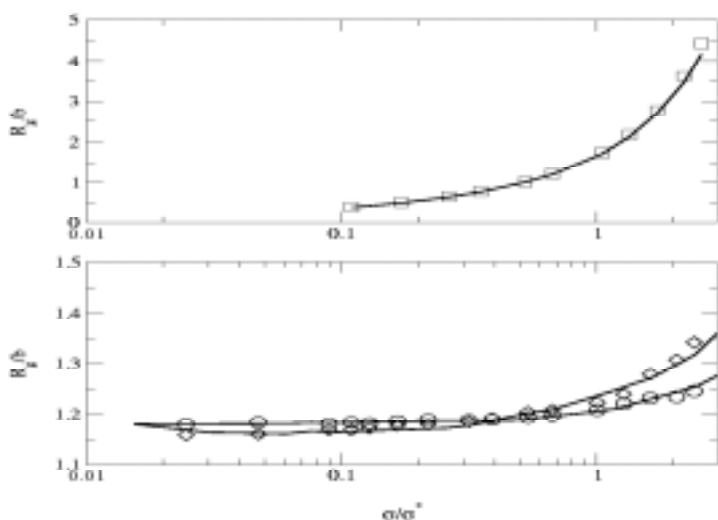
Fig. 1. Radius of gyration from simulations (lines) and estimates from model fits plotted against surface coverage. Symbols: Varying number of chains (diamond), varying core radius (circle), and varying chain length (boxes).

---

1 J. S. Pedersen and M. C. Gerstenberg, Macromolecules **29**, 1363 (1996).

2.8.24. Polymer tribology – water lubricated wear of carbon fibre reinforced PEEK (poly-ether-ether-ketone) sliding against stainless steel

T. Frello, S. Jensen, H. Jepsen, *Danfoss A/S, Nessie™ Water Hydraulics, Nordborg, Denmark*, K. Norrman, N. B. Larsen, K. Bechgaard and R. Feidenhans'l, *Condensed Matter Physics and Chemistry Department, Risø National Laboratory, Denmark*
e-mail: thomas.frello@risoe.dk   http://www.risoe.dk/fys/Employee/thfr.htm

In recent years an increasing number of hydraulic systems are using tap water both as pressure medium and as lubricant. Due to the intrinsic poor lubricant properties of water, the hydraulic components cannot be constructed from materials conventionally used in hydraulics. A tribologically well-suited combination displaying low friction and high wear resistance is carbon fibre reinforced PEEK sliding against stainless steel. The PEEK polymer has a unique combination of low water absorption, high chemical resistance and excellent mechanical and tribological properties. The microstructure of the carbon fibres is essentially graphitic with the graphite planes oriented along the length of the fibre. We have investigated the wear behaviour by Pin-on-Disc experiments, where a pin of PEEK slides against a rotating disc of stainless steel, while flushing with tap water. The velocity was 0.5 m/s and the pressure was 25 MPa. The worn PEEK surfaces have been investigated by AFM microscopy and TOF-SIMS. The TOF-SIMS analyses are used to monitor the chemical effects of various wear conditions in the Pin-on-Disc experiments. AFM images from two areas of the same pin are shown below.
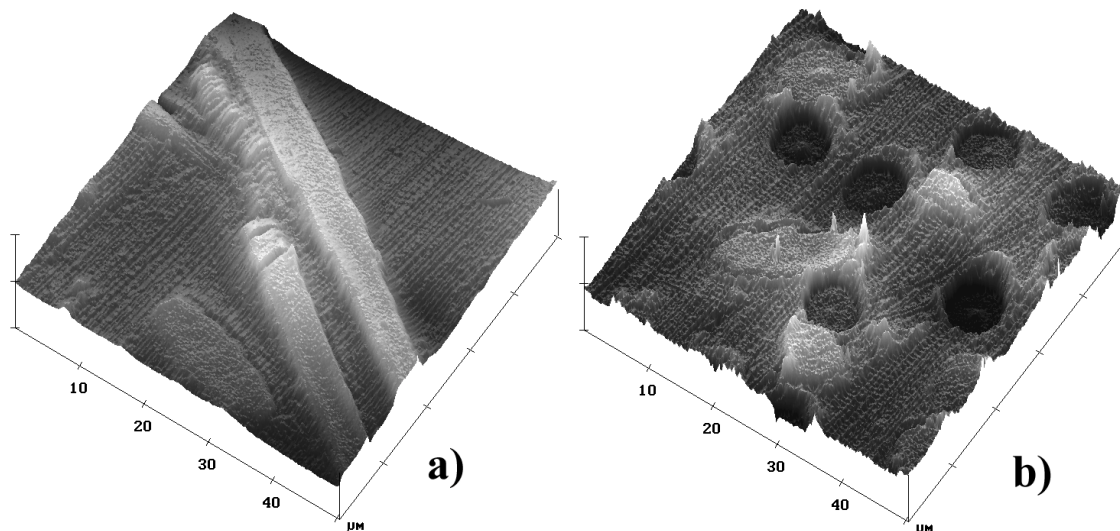
Fig. 1. AFM images of the worn surface of carbon fibre reinforced PEEK. The areas probed are 50×50 μm, the height difference (black to white) is 0-800 nm for a) and 0-250 nm for b). In a) the carbon fibres are oriented parallel to the surface, in b) most fibres are essentially perpendicular to the surface, appearing as circular pits, while fibres with less inclination to the surface appear elliptic

As seen from Fig. 1 there is a distinct angular dependence of the wear of the carbon fibres. Fibres oriented parallel to the surface in a) stand above the PEEK matrix level, while the fibres oriented normal to the surface in b) are below the matrix level. The pin area with dominantly normal fibre orientation display enhanced wear, and our conclusion is that a dominant wear mechanism is through chemical corrosion of the carbon fibres in water. This is consistent with the observed angular wear dependence: When the fibres are oriented normal to the surface the chemically active dangling bonds at the edges of the graphite planes are exposed, while this is not the case for the parallel orientation where the graphite planes are oriented essentially normal to the surface. Work is in progress to identify the reactions responsible for the carbon fibre corrosion.

2.9. Organic chemistry

2.9.1. Lithium-ion induced conformational change of 5,17-bis(9-fluorenyl)-25,26,27,28-tetrapropoxy calix[4]arene resulting in an egg shaped dimeric clathrate

A. Faldt, F. C. Krebs and M. Jørgensen, *Condensed Matter Physics and Chemistry Department, Risø National Laboratory, Denmark*
e-mail: frederik.krebs@risoe.dk   http://www.risoe.dk/fys/Employee/frkr.htm

The present study shows how a lithium ion can bind to the ether groups of a calix[4]arene to open up the structure. Two fluorenyl substituents placed opposite each other on the upper rim in the 5,17-positions are then allowed to make efficient π–π overlap with another calix[4]arene forming an egg-shaped cavity large enough to hold a solvent molecule of toluene. 5,17-Dibromo-calix[4]arene tetrapropoxyether was lithiated with Bu^{t}Li in THF in a halogen-to-metal exchange reaction and subsequently reacted with fluorenone to produce 5,17-bis(9-hydroxy-fluoren-9-yl)-calix[4]arene ether **1**. Reduction of **1** with HSiEt$_3$ proceeded smoothly to give the 5,17-Bis(9-fluorenyl)-calixarene **2**. It was expected that deprotonation at the 9-positions in both fluorene moieties followed by reaction with ZrCl$_4$ would result in the formation of a bis-fluorenyl zirconocene dichloride system placed upon the calix[4]arene platform. Crystals of the salt **3** were harvested from the solution and analyzed by X-ray crystallography which showed that the product was instead a lithium complex of the calixarene **2** with the protons in the 9-fluorenyl groups intact and zirconium pentachloride co-ordinated with THF present as counter ions.[1]
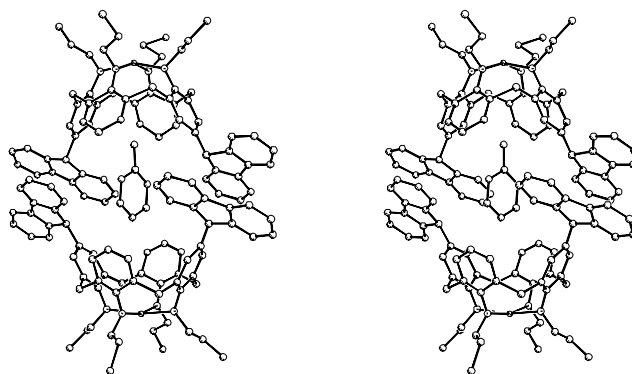
Fig. 1. A stereo view of the dimeric clathrate with bound lithium and included toluene
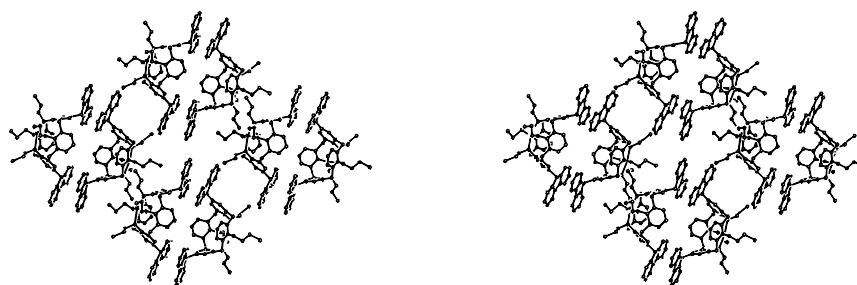
Fig. 2. A stereo view of the packing of the egg shaped dimers in the crystal.
.

---

[1] A. Faldt, F. C. Krebs and M. Jørgensen, Tetrahedron Letters. Accepted for publication.

2.10. Instrumentation

2.10.1. Developments on the neutron simulation package McStas

K. Nielsen, K. Lefmann and K. N. Clausen, *Condensed Matter Physics and Chemistry Department, Risø National Laboratory, Denmark*

e-mail: kristian.nielsen@risoe.dk   http://www.risoe.dk/fys/Employee/krni.htm

McStas is a software package for simulating neutron scattering instruments [1]. The program can calculate most aspects of the performance of an instrument. This way, is possible to optimise the design of a new instrument before starting expensive construction, to optimise the configuration of an instrument before starting experiments, and to calculate the effect of the instrument resolution on measured data after an experiment. Thanks to a unique design based on a neutron instrument meta-language and compiler technology, McStas makes it simple to set up simulations and is flexible enough to handle almost any aspects of the wide variety of neutron instrumentation being used.

McStas version 1.1 was released in March 1999, and is freely available on CD and on the Internet [2]. In 1999, the program has achieved widespread use at many neutron facilities throughout the world, including ILL in France, FRM-II in Germany, ISIS in Great Britain, Argonne in the USA, Tokyo Metropolitan University in Japan, China Institute of Atomic Energy, and others. Several users have contributed enhancements to the program in the form of simulations of specific instrument components; these are then made available to the entire McStas community. McStas has thus been very successful as a catalyst for co-operation among the different neutron facilities in the world. To accelerate the adoption of McStas, the program has been presented in seminars at the ILL in March and at Argonne National Laboratory in August, with a poster at the European Conference on Neutron Scattering in Budapest in September, and in an invited talk for the Neutron Optics workshop at the PSI in Switzerland. Philipp Bernhardt from FRM-II, Germany and Ross Piltz from Ansto, Australia visited Risø to learn about the program.

Several new developments on the program have been added in 1999. These will be included in a new release version 1.2 in January 2000. A graphical user interface McGui has been developed (see Fig. 1). This sits between the user and the command-line based part of McStas, converting menu and dialog actions into the appropriate command (the command line interface is of course still available for the users that prefer it). Several new components have also been developed. These include a crystal with Gaussian mosaic and $\Delta d/d$ that accepts an arbitrary list of reflections with structure factors. Another component is a neutron source that adapts its Monte Carlo sampling of initial neutron parameters to the behaviour of the simulation. This way, neutron parameters with a high chance of reaching the detector are sampled with a higher probability, improving the efficiency of the simulation. Many other enhancements and components developed at Risø and elsewhere will be available in the next version or from the Internet.

A large number of simulations has been performed using McStas at Risø and elsewhere. These include extensive simulations of the RITA instrument at Risø, simulations of the Risø neutron guides, guide designs for the new source FRM-II, simulations of instrument upgrades at the ILL, time focusing in time-of-flight instruments, and many more.
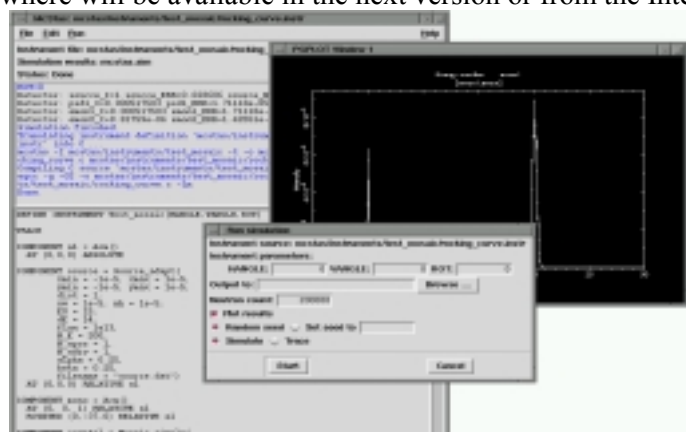
Fig. 1. McGui, showing message window, editor, simulation dialog, and result windows.

---

[1] K. Lefmann and K. Nielsen, Neutron News **10/3**, 20 (1999).

[2] From the McStas home page: http://neutron.risoe.dk/mcstas/.

2.10.2. Investigating the resolution function of RITA-1 by McStas simulations

K. Lefmann, K. Nielsen and K. N. Clausen, *Condensed Matter Physics and Chemistry Department, Risø National Laboratory, Denmark*

e-mail: kim.lefmann@risoe.dk   http://www.risoe.dk/fys/Employee/kile.htm

The new inelastic neutron spectrometer RITA-1 has a rather complex design with *e.g.* focusing neutron guides, a focusing monochromator, a 7-bladed analyser, and a position-sensitive detector[1]. This provides a large gain in flux and measurement efficiency at the cost of a much broader and more complex resolution function, which cannot be treated by standard analytical methods like Cooper-Nathans and Popovici. It is therefore important to find other means of calculating the resolution function in order to: a) Optimise the design and/or configuration of the spectrometer, b) Perform detailed experimental planning, and c) Analyse experimental data.

In order to calculate the RITA-1 resolution function we have modelled the spectrometer in McStas[2]. The computer model is quite accurate, with a few approximations: a) The source is equally bright everywhere, and its spectrum is flat. b) The mirrors in the guides are flat (no roughness), and they are perfectly aligned. c) The monochromator and analyser crystals have identical and perfect mosaic and are perfectly aligned, and d) no air scattering or gravity is included. The resolution function is obtained using a sample, which scatters uniformly in solid angle and energy and a detector, which records the energy and momentum transfer[3].

We have investigated the resolution function for RITA-1 in a mode where 5 of the analyser blades are used to perform monochromatic point-to-point focusing[1] at an incident energy of 5 meV and a nominal scattering vector of 1.87 Å^{-1}. The simulated (elastic part of the) resolution function in the scattering plane is shown in Fig. 1. The five spots with high intensity are the expected signals from the five blades in use, but the 2×5 weaker spots represent neutrons, which are reflected in the second focusing guide section after the monochromator. To investigate this further, we have simulated a rocking scan of a single crystal with a 30' mosaic with and without this guide section (see Fig. 2). It is clear that the second guide section is responsible the spurious side peaks without contributing to the main signal.

From this small investigation we conclude that the design of the focusing guides of RITA-1 could be improved, and that we have found the source of earlier observed spurious peaks. This example is a clear illustration of the usefulness of McStas in instrument design.
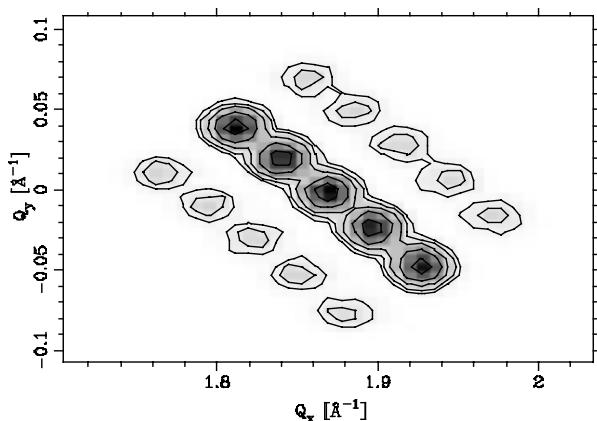
Fig. 1. Contour plot of the RITA-1 resolution function in the scattering plane (q_x, q_y) around zero energy transfer. The spectrometer is in the monochromatic point-to-point focusing mode.
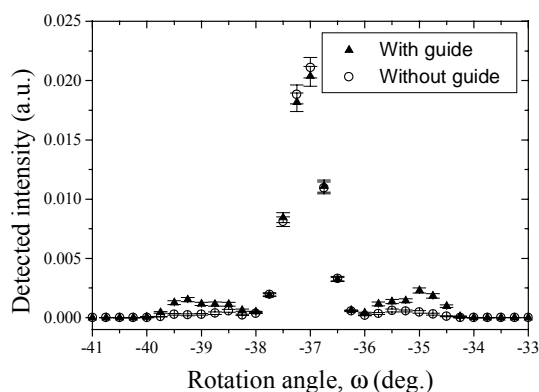
Fig. 2. Simulated rocking scans of a single crystal on RITA-1 with and without the second guide section (closed and open symbols, respectively).

---

[1] K. N. Clausen, D. F. McMorrow, K. Lefmann, G. Aeplli, T. E. Mason, A. Schröder, M. Issikii, M. Nohara and H. Takagi, Physica B **241-243**, 50 (1998); K. Lefmann, D. F. McMorrow, H. M. Rønnow, K. Nielsen, K. N. Clausen, B. Lake and G. Aeppli. To appear in Physica B.

[2] K. Lefmann and K. Nielsen, Neutron News **10 / 3**, 20 (1999); K. Nielsen and K. Lefmann,. To appear in Physica B.

[3] K. Lefmann, K. Nielsen, A. Tennant and B. Lake. To appear in Physica B.

2.10.3. Simulations of a beryllium filter

S. N. Klausen, K. Nielsen, H. M. Rønnow and D. F. McMorrow, *Condensed Matter Physics and Chemistry Department, Risø National Laboratory, Denmark*
e-mail: stine.nyborg.klausen@risoe.dk   http://www.risoe.dk/fys/Employee/stkl4768.htm

The neutron ray-tracing package *McStas*[1] makes it possible to optimise the efficiency of a filter by simulating different filter designs. This procedure has been used to determine the design of a Be filter for the new RITA-II spectrometer.

A Be filter removes neutrons with wavelengths below 4 Å from the beam, since these neutrons are Bragg-scattered away from the beam direction. However, neutrons may be scattered twice in the filter and hence they could reenter the beam. In order to minimise this effect the filter should be made of slices separated by a neutron absorbing material, *e.g.* B^{10} or Cd^{113}.

The ray-tracing in the Be filter is simulated in the following way: the penetration depth of the neutrons into the Be powder is determined by a exponentially decaying probability distribution given by the linear attenuation factor. The scattered neutrons are assumed to lie on the Debye-Scherrer cone for Bragg scattering in the Be powder. Only neutrons with a wave vector k, such that $\tau < 2k$, are scattered. Here τ is the minimal reciprocal lattice vector with a non-zero structure factor. Multiple scattering is included. Absorption is neglected since the absorption cross section of Be is small compared to the scattering cross section.

The simulations are made for a cubic Be filter with a side length of 10 cm. Fig. 1 and fig. 2 show results for simulations using only the first reflection, which cuts off at 4 Å (In future work all reflections will be considered). Typically, the neutrons will scatter five to ten times before they exit the filter. The filter slices are parallel to the neutron beam. They improve the efficiency of the filter considerably, as shown in fig. 2. When the number of intersections equals six only one fifth of the neutrons with wavelength below 4 Å are transmitted compared with the solid (non-sliced) filter.

The design with separated blocks yields in addition a collimating effect. The planned modes of operation of RITA-II include both linearly and radially collimated beams. Therefore each filter-slice is made of two trapezodially shaped blocks that can be combined to a rectangular or wedged slope. At the same time the number of absorbing plates can be chosen. This is a part of the general effort to make the components of RITA-II modular, leaving the user with flexibility to configure the spectrometer for the individual needs of each experiment.
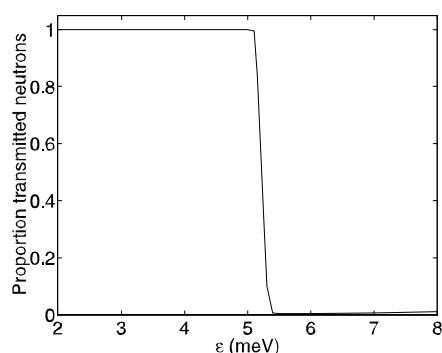
Fig. 1. Proportion transmitted neutrons in a Be filter as function of energy. If the energy spread is zero, the cut off is sharp. The shown result is for neutrons with an energy spread on 0.1 meV incident on a Be filter with a side length of 10 cm.
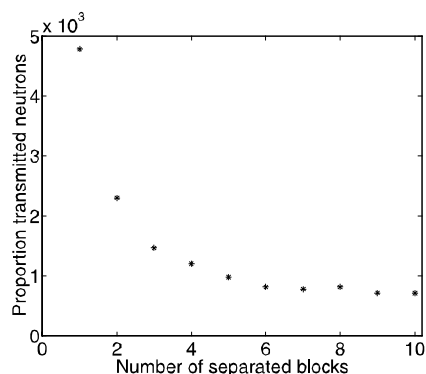
Fig. 2. Proportion transmitted neutrons in a Be filter as a function of number of slices separated by an absorbing material. The incoming neutrons have an energy of 6 ± 0.1 meV. The detector is placed 10 cm after the filter.

---

[1] K. Lefmann and K. Nielsen, Neutron News **10/3**, 20 (1999).

2.10.4. Magneto-optical measurement system

B. H. Larsen, S. Nielsen, T. Kjær, N. H. Andersen, T. Frello, P. Skaarup and M. R. Koblischka[1], *Condensed Matter Physics and Chemistry Department, Risø National Laboratory, Denmark*
e-mail: britt.h.larsen@risoe.dk   http://www.risoe.dk/fys/Employee/brla.htm

We have established a system for magneto-optic (MO) imaging. The technique enables spatially local and time resolved measurements of magnetic flux penetration and distribution in superconductors, which in turn may be converted into a critical current distribution. The system is suitable for studies of basic properties, e.g. kinetics of magnetic flux flow and penetration, as well as identification of weak current links in superconductor materials for technological applications, e.g. in BiSCCO tapes. This way significant information for optimising the fabrication processes and flux pinning properties of the tapes may be obtained.

The MO set-up is sketched in Fig. 1. It is based on an optical microscope and a flow cryostat mounted on an optical table. Monochromatic light from a Hg-lamp is polarised and shined onto an MO indicator film, which, due to the Faraday effect, rotates the polarisation of the light proportionally to the local magnetic field. A thin film mirror deposited on a substrate below the indicator film reflects the light, which is analysed by a polarisation filter, rotated 90 degrees compared to the polarising filter. This way the field distribution at the surface of a sample positioned below the indicator film can be monitored, see Fig. 2 where the Faraday effect is illustrated using a $YBa_2Cu_3O_7$ high-T_c superconducting thin film. The indicator films available at present are typically 2-10 μm thick and made of Bi-doped yttrium-iron-garnet (YIG) evaporated onto a YIG substrate covered with an Al-mirror. These films saturate at a magnetic field of 0.1 T, and the conversion factor from polarisation rotation angle to magnetic field is typically 5 mT/deg. A CCD video camera is used for data acquisition. The cryostat may be operated with a flow of liquid helium or nitrogen and temperatures between 4 and 300 K is stabilised with an electronic temperature controller. The magnetic field distribution may be determined with a spatial resolution of 2 μm and a time resolution of ~20 msec. The distance from the sample on the cold finger to the quartz window in the cryostat is 5 mm and the opening aperture has a diameter of 18 mm. A standard copper-wire solenoid is placed outside of the cryostat and supplies magnetic fields up to 125 mT. It is possible to bias the sample with a transport current during measurements.

An example of a MO study of a multifilamentary BiSCCO tape is presented in section 2.3.
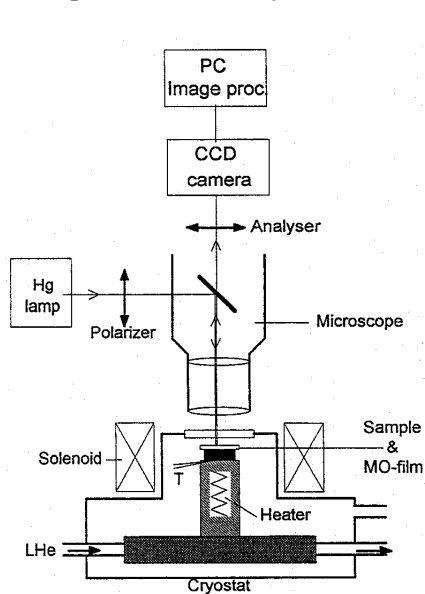
Fig.1. Schematical drawing of the set-up
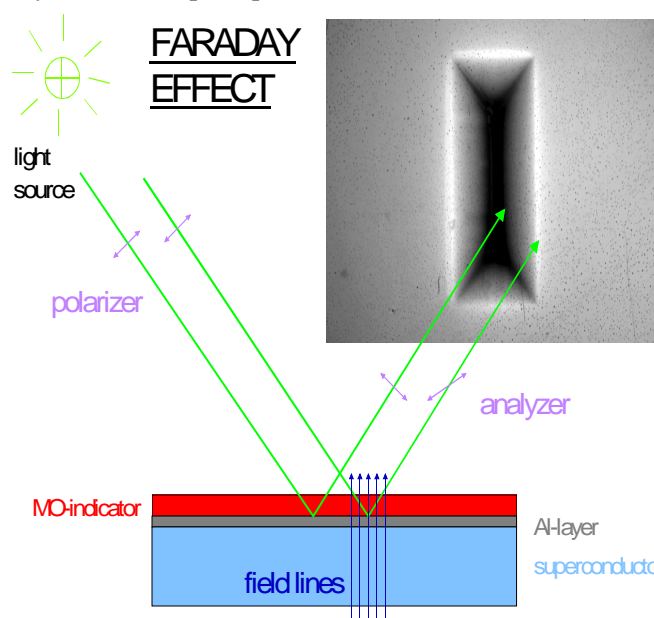
Fig. 2. Schematical drawing of the Faraday effect

[1] Also at Nordic Superconductor Technologies (NST) A/S, Brøndby, Denmark.

2.10.5. The facility for plastically deformed germanium single-crystal wafers

B. Lebech, K. Theodor and B. Breiting, *Condensed Matter Physics and Chemistry Department, Risø National Laboratory, Denmark*
e-mail: bente.lebech@risoe.dk   http://www.risoe.dk/fys/Employee/bele.htm

The Risø facility[1] for plastically deformed germanium single crystal wafers was inspired by Axe et al.[2] and motivated by the wish to optimise and improve the neutron flux at the thermal neutron beams at Risø as cost effectively as possible by producing better monochromators. The facility has been in routine operations since June 1996 and has been producing plastically deformed germanium wafers to be used in neutron monochromators for customers since early 1997.

The two first germanium composite monochromators (Fig. 1) have been installed at the TAS3/POW and PUS powder diffractometers at the DR3 and the JEEPII reactors at Risø National Laboratory, Denmark and Institute for Energy Technology, Norway by the end of January 1997. They have functioned satisfactorily since the commissioning. Figure 1 shows the two monochromators prior to installation, one of the seven cut composite wafer strips used in the monochromator (20 wafers slab, 4 strips per slab), a single bend wafer and a pencil for estimating size. Until now we have made monochromators with excellent performance for germanium wafers cut for reflection from the (511) and (311) planes. Test deformation of a few wafers cut for reflection from the (111) planes show very promising results in terms of reflectivity and mosaicity. Test deformation of wafers cut for reflection from the (711) planes is planned. During 1998 and 1999 the facility was used to deform germanium wafers for customers. They are now functioning as neutron monochromators at the powder diffractometers at the Hahn Meitner Institute in Germany and the Demokritos Research Centre in Greece. In addition, germanium wafers to be used for neutron monochromators at Oak Ridge National Laboratory and instruments at the FRMII in Munich, Germany are being processed as illustrated in Fig. 2.

Fig. 1. The composite germanium wafer monochromators used at Risø and Kjeller since early 1997. The seven 20-wafer composite strips are mounted in the Risø design focusing monochromator holder, which are commercially available. The monochromator holder may be mounted for horizontal focusing (as shown) or for vertical focusing (normal monochromator).
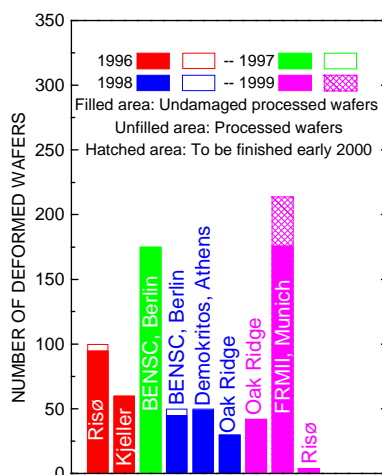
Fig. 2. Production of deformed germanium wafers for neutron monochromators at Risø National Laboratory**.**

.

[1] B. Lebech, K. Theodor, B. Breiting, P. G. Kealey, B. Hauback, J. Lebech, S. Aa. Sørensen and K. N. Clausen, Physica B **241-243**, 204 (1998), Risø-R-1014(EN). Editors: M. Nielsen, K. Bechgaard, K. N. Clausen, R. Feidenhans'l and I. Johansen, pp. 137 and 138 (1998). Risø-R-1099(EN). Editors: K. Bechgaard, K. N. Clausen, R. Feidenhans'l and I. Johansen, 137 (1999).
[2] J. D. Axe, S. Cheung, D. E. Cox, L. Passell, T. Vogt and S. Bar-Ziv, Neutron Research **2**, 85 (1994).

2.11. Training and Mobility of Researchers - Access to Large Installations

2.11.1. Training and Mobility of Researchers - Access to Large Installations

K. N. Clausen, *Condensed Matter Physics and Chemistry Department, Risø National Laboratory, Denmark*

e-mail: kurt.clausen@risoe.dk   http://www.risoe.dk/fys/Employee/kucl.htm

The CEC Large Installation Programme was initiated in order to make large national facilities available to users from the whole EU, to promote European collaboration and to make more facilities available to the less favoured regions in the EU. The cold neutron facilities at DR3 has been included in this programme since early 1992. The present TMR programme expires early 2000, but the user programme continues as an IHP programme under Framework 5 programme until mid 2003. The programme is in collaboration with the neutron scattering laboratory NFL at Studsvik in Sweden. News about the programme, information about the facilities and deadline for proposals can be found on the WWW pages: http://www.risoe.dk/fys/tmr.htm and http://www.studsvik.uu.se

Proposals for experiments are refereed by a group of six international experts, chaired by Prof. Jens Als-Nielsen from the University of Copenhagen. The TMR and IHP programmes covers marginal costs in connection with neutron scattering experiments at Risø. These costs are (1) Travel and subsistence for the users, (2) salaries to staff employed to run the user programme, (3) consumables and other running costs in connection with the experiments.

During 1999 a total of 49 beam weeks were allocated to 46 experiments. The experiments were performed by 37 user groups and involved 80 users from EU-countries or associated states (Norway, Iceland, Liechtenstein or Israel). In total the EC programme supported 798 visitor days at Risø, distributed over 95 visits.

The experiments carried out at Risø with support from the Commission of the European Communities during 1999 are listed below in chronological order. The column marked applicant is the name of the principal applicant.

Applicant	Title
Kleppinger	Small angle neutron scattering studies on dendrimers and open hyperbranched polymers
Kleppinger	Temperature-dependent morphologies in block copolymer solutions
Powell	Order-Disorder Transition in $NiCr_2S_4$
Coad	Quasi-elastic excitation in UGa_3
Cowley	Magnetic structures of rare earth alloys
Daymond	Effect of fatigue on load sharing in a particulate reinforced metal matrix composite
Almgren	Structure of micelles and micellar demixing in fluorocarbon/hydrocarbon surfactant mixtures
Dreismann	"Anomalous" reflectivity of the quartz/$(H_2O\text{-}D_2O)$ interface -- D content dependence
Hall	The accessibility of liquids into partially coked microporous HDS catalysts
Withers	Internal stress development during intern welding
Harrison	Spin-wave dispersion in a kagome antiferromagnet
Branger	"In situ" study of the cube texture formation and development in FeNi50% alloy
Harris	Diffuse magnetic scattering from geometrically-frustrated pyrochlores
Kamenev	Study of low-temperature magnetic ordering in a single crystal of layered $(La_{0.6}Nd_{0.4})_{1.2}$ $Sr_{1.8}Mn_2O_7$
Schwahn	Temperature- and pressure-dependent composition fluctuations in

Applicant	Title
	the 3 component polymer mixture of PB,PS and PB-PS
Williams	Crystal and magnetic structures of substituted iron oxides
Dann	Investigation of cancrinite scale formed in the Bayer process
Gradzielski	Gelation of ethylene glycol ester of silicic acid in the presence of surfactant mesophases and the interactions between them
Keimer	Low energy magnetic excitations in superconducting $YBa_2Cu_3O_{6+d}$
Schröder	Search for quantum critical fluctuations in $CeNi_2Ge_2$
Cowley	Magnetic structures of rare earth alloys
Schröder	Magnetic field tuning of the quantum critical fluctuations in $CeCu_{5.9}Au_{0.1}$
Mazza	Neutron powder diffraction B-11 enriched $La_5Si_2BO_{13}$
McLURE	Critical adsorption of near-critical d-C_4E_1+H2O liquid mixture at a chemically modified silicon-liquid interface
Mergia	Training in powder diffraction exemplified by studies of the magnetic structure of $mn_{1-x}fe_xsn_2$
Greaves	Nuclear and magnetic structures of chromium thiospinels
Visser	Acoustic phonon branches in hexagonal perovskite type ABX_3 halides around the zone-center
Bollinne	Assessment of density perturbations in thin polymer films near solid substrates
Cowley	Magnetic structures of rare earth alloys
Visser	Acoustic phonon branches in the hexagonal perovskites $CsFeBr_3$ and $RbNiCl_3$ around the Zone-Centre
Campbell	Magnetic order and magnetic excitations in 2D cmr manganites
Madgwick	Neutron driffraction strain measurements for direct testing of steady state creep calculations
Reynaers	Influence of the molecular topology change on the morphology of block copolymer physical gels
Hillman	Influence of pH on structure of oxidised poly (o-toluidine) films
Cowley	The magnetic phase transition of $CsNiCl_3$
Ceglie	Nematic ordering of giant wormlike micelles
Dreismann	"Anomalous" reflectivity of the Quartz/(H_2O-D_2O) interface -- D content dependance
Gomez-Sal	the magnetic ground state of the $CeNi_{0.4}Cu_{0.6}$ compound
Boothroyd	Magnetic excitations in $(Pr,Y)Ba_2Cu_3O_{6+x}$
Ramzi	Supramolecular assemblies of polystyrene-poly(propylene imine) dendrimer diblock copolymers
McEwen	Magnetic and quadrupolar phase transitions in $Ce_3Pd_{20}Ge_6$
Cosgrove	SANS study of structure and inter-particle forces in TiO_2 and Al_2O_3
Hillman	Electroactive poly(3-hexylthiophene) films with novel viscoelastic properties
Hall	Small angle neutron scattering to determine porosity development in biomss gasification
Korsunsky	A study of plastic deformation in polycrystalline metals and composites
Papadakis	Phase behavior of binary blends of compositionally symmetric polystyrene-polybutadiene and poly(d8-styrene)-poly(n-butyl methacrylate) didblock copolymers

3.   Publications, lectures, educational and organisational activities

3.1.   International publications

Aasmundtveit, K. E.; Samuelsen, E. J.; Pettersson, L. A. A.; Inganas, O.; Johansson, T.; Feidenhans'l, R., Structure of thin films of poly(3,4-ethylenedioxythiophene). Synth. Met. (1999) v. 101 p. 561-564..

Aeppli, G.; Bishop, D. J.; Broholm, C.; Bucher, E.; Cheong, S. W.; Dai, P.; Fisk, Z.; Hayden, S. M.; Kleiman, R.; Mason, T. E.; Mook, H. A.; Perring, T. G.; Schröder, A., Neutron scattering and the search for mechanisms of superconductivity. Physica C (1999) v. 317-318 p. 9-17.

Andersen, L. G.; Poulsen, H. F.; Frello, T.; Andersen, N. H.; Zimmermann, M. von, Cooling behavior of BSCCO/Ag tapes. IEEE Trans. Appl. Superconduct. (1999) v. 9 p. 2758-2761.

Andersen, N. H.; Zimmermann, M. von; Frello, T.; Kall, M.; Mønster, D.; Lindgård, P. -A.; Madsen, J.; Niemöller, T.; Poulsen, H. F.; Schmidt, O.; Schneider, J. R.; Wolf, T.; Dosanjh, P.; Liang, R.; Hardy, W. N., Superstructure formation and the structural phase diagram of $YBa_2Cu_3O_{6+x}$. Physica C (1999) v. 317-318 p. 259-269.

Andresen, T. L.; Krebs, F. C.; Larsen, M.; Thorup, N., Crystal structure of three compounds related to triphenylene and tetracyanoquinodimethane. Acta Chem. Scand. (1999) v. 53 p. 410-416.

Andruzzi, L.; Altomare, A.; Ciardelli, F.; Solaro, R.; Hvilsted, S.; Ramanujam, P. S., Holographic gratings in azobenzene side-chain polymethacrylates. Macromolecules (1999) v. 32 p. 448-454.

Baker, J.; Lindgård, P. -A., Heteroepitaxial strain in alkali halide thin films: KCl on NaCl. Phys. Rev. B (1999) v. 60 p. 16941-16949.

Balakrishnan, G.; Offersgaard, J. F.; Wilbrandt, R., Radical cation of 2,5-dimethyl-2,4-hexadiene: Resonance Raman spectrum and molecular orbital calculations. J. Phys. Chem. A (1999) v. 103 p. 10798-10804.

Basletic, M.; Hamzic, A.; Korin-Hamzic, B.; Bechgaard, K., Angular dependence of magnetoresistance in SDW state of (TMTSF)(2)PF6. Synth. Met. (1999) v. 103 p. 2044-2045.

Baunsgaard, D.; Balsami, M. El; Frederiksen, J.; Harrit, N.; Negri, F.; Orlandi, G.; Wilbrandt, R., The phosphorescence spectra of triphenylene and truxene: A combined experimental and theoretical investigation of the vibronic structure. Laser Chem. (1999) v. 19 p. 349-351.

Berfeld, M.; Kuzmenko, I.; Weissbuch, I.; Cohen, H.; Howes, P. B.; Kjær, K.; Als-Nielsen, J.; Leiserowitz, L.; Lahav, M., Use of diastereomeric interactions to probe the inplane attachment of water-soluble molecules to the polar head groups of Langmuir films of Cu-α-amino acid complexes. J. Phys. Chem. B (1999) v. 103 p. 6891-6899.

Bergmeier, M.; Gradzielski, M.; Hoffmann, H.; Mortensen, K., Behavior of ionically charged lamellar systems under the influence of a shear field. J. Phys. Chem. B (1999) v. 103 p. 1605-1617.

Bergström, M.; Pedersen, J. S., Formation of tablet-shaped and ribbonlike micelles in mixtures of an anionic and a cationic surfactant. Langmuir (1999) v. 15 p. 2250-2253.

Bergström, M.; Pedersen, J. S., Structure of pure SDS and DTAB micelles in brine determined by small-angle neutron scattering (SANS). Phys. Chem. Chem. Phys. (1999) v. 1 p. 4437-4446.

Bergström, M.; Pedersen, J. S., A small-angle neutron scattering (SANS) study of tablet-shaped and ribbonlike micelles formed from mixtures of an anionic and a cationic surfactant. J. Phys. Chem. B (1999) v. 103 p. 8502-8513.

Bergström, M.; Pedersen, J. S.; Schurtenberger, P.; Egelhaaf, S. U., Small-angle neutron scattering (SANS) study of versicles and lamellar sheets formed from mixtures of an anionic and a cationic surfactant. J. Phys. Chem. B (1999) v. 103 p. 9888-9897.

Biskup, N.; Vuletic, T.; Herman, D.; Tomic, S.; Nagasawa, M.; Bechgaard, K., Low frequency dielectric response in spin density wave phase of Bechgaard salts. Synth. Met. (1999) v. 103 p. 2052-2053.

Boothroyd, A. T.; Hill, J. P.; McMorrow, D. F.; Andersen, N. H.; Stunault, A.; Vettier, C.; Wolf, T., Incommensurate magnetism in non-superconducting $PrBa_2Cu_3O_{6.92}$. Physica C (1999) v. 317-318 p. 292-298.

Boothroyd, A. T.; Reynolds, J. M.; Andersen, N. H.; Brecht, E.; Wolf, T.; Chowdhury, A. J. S., Magnetic ordering of Nd^{3+} in single-crystal $NdBa_2Cu_3O_{6+x}$. Phys. Rev. B (1999) v. 60 p. 1400-140 8.

Brecht, E.; Schweiss, P.; Wolf, T.; Boothroyd, A. T.; Reynolds, J. M.; Andersen, N. H.; Lutgemeier, H.; Schmahl, W. W., Antiferromagnetic ordering states of oxygen-deficient $NdBa_2Cu_3O_{6+x}$ and $Nd_{1+y}Ba_{2-y}Cu_3O_{6+x}$ single crystals. Phys. R ev. B (1999) v. 59 p. 3870-3878.

Bronger, W.; Brassard, L. A.; Müller, P.; Lebech, B.; Schultz, T. M., K_2ReH_9, eine Neubestimmung der Struktur. Z. Anorg. Allg. Chem. (1999) v. 625 p. 1143-1146.

Bull, M. J.; McEwen, K. A.; Eccleston, R. S.; Clausen, K. N.; Kockelmann, W., Antiferromagnetism, crystal fields and hybridisation in $UxY_{1-x}Pd_3$ studied by neutron scattering. Physica B (1999) v. 261 p. 254-255.

Bunk, O.; Falkenberg, G.; Zeysing, J. H.; Lottermoser, L.; Johnson, R. L.; Nielsen, M.; Rasmussen, F. B.; Feidenhans'l, R., Structure determination of the indium-induced Ge(103)-(1x1) reconstruction by surface X-ray diffraction. Appl. Surf. Sci. (1999) v. 142 p. 88-93.

Bunk, O.; Falkenberg, G.; Zeysing, J. H.; Lottermoser, L.; Johnson, R. L.; Nielsen, M.; Rasmussen, F. B.; Baker, J.; Feidenhans'l, R., Structure determination of the indium-induced Si(111)-(4x1) reconstruction by surface X-ray diffraction. Phys. Rev. B (1999) v. 59 p. 12228-12231.

Bunk, O.; Falkenberg, G.; Zeysing, J. H.; Johnson, R. L.; Nielsen, M.; Feidenhans'l, R., Comment on "Structural model for the Si(001)4x3-In surface phase". Phys. Rev. B (1999) v. 60 p. 13905-13906.

Bunk, O.; Zeysing, J. H.; Falkenberg, G.; Johnson, R. L.; Nielsen, M.; Nielsen, M. M.; Feidenhans'l, R., Phase transitions in two dimensions: The case of Sn adsorbed on Ge (111) surfaces. Phys. Rev. Lett. (1999) v. 83 p. 2226-2229.

Carlsson, P.; Mattsson, B.; Swenson, J.; Torell, L. M.; Käll, M.; Börjesson, L.; McGreevy, R. L.; Mortensen, K.; Gabrys, B., Neutron-scattering studies of a polymer electrolyte, $PPO-LiClO_4$. Solid State Ionics (1998) v. 115 (no. Sp. issue) p. 139-147.

Cascales, C.; Puebla, E. G.; Klimin, S.; Lebech, B.; Monge, A.; Popova, M. N., Magnetic ordering in the rare earth iron germanates $HoFeGe_2O_7$ and $ErFeGe_2O_7$. Chem. Mater. (1999) v. 11 p. 2520-2526.

Castan, T.; Vives, E.; Lindgård, P. -A., Modeling premartensitic effects in Ni_2MnGa: A mean-field and Monte Carlo simulation study. Phys. Rev. B (1999) v. 60 p. 7071-7084.

Chen, X. Y.; Jankova, K.; Kops, J.; Batsberg Pedersen, W., Hydrolysis of 4-acetoxystyrene polymers prepared by atom transfer radical polymerization. J. Polym. Sci. A (1999) v. 37 p. 627-633.

Chretien, D.; Janosi, I.; Taveau, J. C.; Flyvbjerg, H., Microtubule's conformational cap. Cell Struct. Funct. (1999) v. 24 p. 299-303.

Christiansen, J. K. S.; Andersen, N. H.; Frello, T., Pinning of magnetic flux lines in Y-Ba-Cu-O superconductors by neutron irradiation and chemical route. IEEE Trans. Appl. Superconduct. (1999) v. 9 p. 2304-2307 Clarke, S. J.; Harrison, A.; Mason, T. E.; Visser, D., Characterisation of spin-waves in copper(II) deuteroformate tetradeuterate: A square $_{s=}1/2$ Heisenberg antiferromagnet. Solid State Commun. (1999) v. 112 p. 561-564.

Clausen, K. N., A focusing multi-element monochromator and analyser spectrometer. In: Steigenberger, U. (ed.), European Spallation Source. Contributions to the ESS Instrument Working Group on single crystal spectroscopy. ESS-98-74-T (1998) p. 57-60.

Derici, L.; Ledger, S.; Mai, S. M.; Booth, C.; Hamley, I. W.; Pedersen, J. S., Micelles and gels of oxyethylene-oxybutylene diblock copolymers in aqueous solution: The effect of oxyethylene-block length. Phys. Chem. Chem. Phys. (1999) v. 1 p. 2773-2785.

Eckstein, G. A.; Maupai, S.; Dakkouri, A. S.; Stratmann, M.; Nielsen, M.; Nielsen, M. M.; Feidenhans'l, R.; Zeysing, J. H.; Bunk, O.; Johnson, R. L., Surface structure of $AU_3Cu(001)$. Phys. Rev. B (1999) v. 60 p. 8321-8325.

Edgar, R.; Schultz, T. M.; Rasmussen, F. B.; Feidenhans'l, R.; Leiserowitz, L., Solvent binding to benzamide crystals: Morphology, induced twinning and direct observation by surface X-ray diffraction. J. Am. Chem. Soc. (1999) v. 121 p. 632-637.

Elllouze, C.; Selmane, T.; Kim, H. K.; Tuite, E.; Norden, B.; Mortensen, K.; Takahashi, M., Difference between active and inactive nucleotide cofactors in the effect of the DNA binding and the helical structure of RecA filament - Discussion of RecA-DNA complex by inactive nucleotides. Eur. J. Biochem. (1999) v. 262 p. 88-94.

Eskildsen, M. R.; Harada, K.; Gammel, P. L.; Andersen, N. H.; Ernst, G.; Ramirez, A. P.; Bishop, D. J.; Mortensen, K.; Canfield, P. C., Hysteresis in the field-induced magnetic structure in $TmNi_2B_2C$. Physica B (1999) v. 261 p. 582-583.

Fleischer, G.; Rittig, F.; Stepanek, P.; Almdal, K.; Papadakis, C. M., Self-diffusion of a symmetric PEP-PDMS diblock copolymer above and below the disorder-to-order transition. Macromolecules (1999) v. 32 p. 1956-1961.

Fleischer, G.; Rittig, F.; Karger, J.; Papadakis, C. M.; Mortensen, K.; Almdal, K.; Stepanek, P., Self-diffusion of an asymmetric diblock copolymer above and below the order-to-disorder transition temperature. J. Chem. Phys. (1999) v. 111 p. 2789-2796.

Fourmigué, M.; Mézière, C.; Canadell, E.; Zitoun, D.; Bechgaard, K.; Auban-Senzier, P., Covalent linking of β-slabs of EDT-TTF moieties: Bis (ethylenedithiotetrathiafulvalenyl)ethane and its 1:1 radical cation salt with $Au(CN)_2^-$. Adv. Mater. (1999) v. 11 p. 766-769.

Frello, T.; Baziljevich, M.; Johansen, T. H.; Andersen, N. H.; Wolf, T.; Koblischka, M. R., Flux turbulence in $NdBa_2Cu_3O_{6+x}$ and underdoped $YBa_2Cu_3O_{6+x}$ single crystals. Phys. Rev. B (1999) v. 59 p. R6639-R6642.

Frello, T.; Poulsen, H. F.; Andersen, L. G.; Andersen, N. H.; Bentzon, M. D.; Schmidberger, J., An in situ study of the annealing behaviour of BiSCCO Ag tapes. Supercond. Sci. Technol. (1999) v. 12 p. 293-300.

Fuente, C. de la; Cowley, R. A.; Goff, J. P.; Ward, R. C. C.; Wells, M. R.; McMorrow, D. F., The magnetic structures of holmium-yttrium superlattices in an applied magnetic field. J. Phys. Condens. Matter (1999) v. 11 p. 6529-6541.

Fyhn, M. F.; Chevallier, J.; Larsen, A. N.; Feidenhans'l, R.; Seibt, M., α-Sn and β-Sn precipitates in annealed epitaxial $Si_{0.95}Sn_{0.05}$. Phys. Rev. B (1999) v. 60 p. 5770-5777.

Gadegaard, N.; Almdal, K.; Larsen, N. B.; Mortensen, K., The lamellar period in symmetric diblock copolymer thin films studied by neutron reflectivity and AFM. Appl. Surf. Sci. (1999) v. 142 p. 608-613.

Gammel, P. L.; Barber, B. P.; Ramirez, A. P.; Varma, C. M.; Bishop, D. J.; Canfield, P. C.; Kogan, V. G.; Eskildsen, M. R.; Andersen, N. H.; Mortensen, K.; Harada, K., Effects of magnetic order on the superconducting length scales and critical fields in single crystal $ErNi_2B_2C$. Phys. Rev. Lett. (1999) v. 82 p. 1756-1759.

Gammel, P. L.; Bishop, D. J.; Eskildsen, M. R.; Mortensen, K.; Andersen, N. H.; Fisher, I. R.; Cheon, K. O.; Canfield, P. C.; Kogan, V. G., Systematic studies of the square-hexagonal flux line lattice transition in $Lu(Ni_{1-x}Co_x)2B_2C$: The role of nonlocality. Phys. Rev. Lett. (1999) v. 82 p. 4082-4085.

Goff, J. P.; Sarthour, R. S.; McMorrow, D. F.; Yakhou, F.; Stunault, A.; Vigliante, A.; Ward, R. C. C.; Wells, M. R., X-ray resonant scattering study of spin-density waves in a superlattice. J. Phys. Condens. Matter (1999) v. 11 p. L139-L146.

Greve, D. R.; Reitzel, N.; Hassenkam, T.; Bøgelund, J.; Kjær, K.; Howes, P. B.; Larsen, N. B.; Jayaraman, M.; McCullough, R. D.; Bjørnholm, T., Directed self-assembly of amphiphilic regioregular polythiophenes on the nanometer scale. Synth. Met. (1999) v. 102 p. 1502-1505.

Hansen, T.; Itoua, S.; Kamounah, F. S.; Christensen, J. B.; Bjørnholm, T.; Schaumburg, K.; Bechgaard, K.; Wilkes, S. B., STM investigations of physisorbed monolayers of dialkoxy-substituted aromatics. J. Mater. Chem. (1999) v. 9 p. 1107-1113.

Hasegawa, H.; Sakamoto, N.; Takeno, H.; Jinnai, H.; Hashimoto, T.; Schwahn, D.; Frielinghaus, H.; Janssen, S.; Imai, M.; Mortensen, K., Small-angle neutron scattering studies on phase behavior of block copolymers. J. Phys. Chem. Solids (1999) v. 60 p. 1307-1312.

Helbig, M.; Ruseckas, A.; Grage, M. M. -L.; Birckner, E.; Rentsch, S.; Sundstrøm, V., Resolving the radical cation formation from the lowest-excited singlet (S-1) state of terthiophene in a TiO_2-SiO_2 hybrid polymer matrix. Chem. Phys. Lett. (1999) v. 302 p. 587-594.

Hillmyer, M. A.; Maurer, W. W.; Lodge, T. P.; Bates, F. S.; Almdal, K., Model bicontinuous microemulsions in ternary homopolymer/block copolymer blends. J. Phys. Chem. B (1999) v. 103 p. 4814-4824.

Holme, N. C. R.; Nikolova, L.; Hvilsted, S.; Rasmussen, P. H.; Berg, R. H.; Ramanujam, P. S., Optically induced surface relief phenomena in azobenzene polymers. Appl. Phys. Lett. (1999) v. 74 p. 519-521.

Holme, N. C. R.; Nikolova, L.; Norris, T. B.; Hvilsted, S.; Pedersen, M.; Berg, R. H.; Rasmussen, P. H.; Ramanujam, P. S., Physical processes in azobenzene polymers on irradiation with polarized light. Macromol. Symp. (1999) v. 137 p. 83-103.

Hooker, J. C.; Burghardt, W. R.; Torkelson, J. M., Birefringence and second-order nonlinear optics as probes of polymer cooperative segmental mobility: Demonstration of Debye-type relaxation. J. Chem. Phys. (1999) v. 111 p. 2779-2788.

Ishibashi, S.; Manuel, A. A.; Vasumathi, D.; Shukla, A.; Suortti, P.; Kohyama, M.; Bechgaard, K., Electron momentum density of TTF-TCNQ (tetrathiafulvalene-tetracyanoquinodimethane) studied by Compton scattering. J. Phys. Condens. Matter (1999) v. 11 p. 9025-9032.

Jankova, K.; Kops, J.; Chen, X. Y.; Batsberg Pedersen, W., Synthesis by ATRP of poly(ethylene-co-butylene)-block-polystyrene, poly(ethylene-co-butylene)-block-poly(4-acetoxystyrene) and its hydrolysis product poly(ethylene-co-butylene)-block-poly(hydroxystyrene). Macromol. Rapid Commun. (1999) v. 20 p. 219-223.

Jankova, K.; Truelsen, J. H.; Chen, X.; Kops, J.; Batsberg Pedersen, W., Controlled-"living" atom transfer radical polymerization of styrene in the synthesis of amphiphilic diblock copolymers from a poly(ethyleneglycol) macroinitiator. Polym. Bull. (1999) v. 42 p. 153-158.

Jensen, T. R.; Hazell, R. G., A novel layered templated lithium zinc phosphate prepared by an unusual solution mediated technique. Chem. Commun. (1999) v. 4 p. 371-372.

Jäger, E. W. H.; Smela, E.; Inganas, O., On-chip microelectrodes for electrochemistry with moveable PPy bilayer actuators as working electrodes. Sens. Actuators B (1999) v. 56 p. 73-78.

Jäger, E. W. H.; Smela, E.; Inganas, O.; Lundström, I., Polypyrrole microactuators. Synth. Met. (1999) v. 102 p. 1309-1310.

Kaganer, V. M.; Brezesinski, G.; Möhwald, H.; Howes, P. B.; Kjær, K., Positional order in Langmuir monolayers: An X-ray diffraction study. Phys. Rev. E (1999) v. 59 p. 2141-2152.

Keszthelyi, T.; Grage, M. M. L.; Wilbrandt, R.; Svendsen, C.; Mortensen, O. S., The radical cation of bithiophene; An experimental and theoretical study. Laser Chem. (1999) v. 19 p. 393-396.

Koblischka, M. R.; Murakami, M.; Johansen, T. H.; Baziljevich, M.; Frello, T.; Wolf, T., Instability of the critical state in $NdBa_2Cu_3O_{7-\delta}$ single crystals. Phys. Stat. Sol. B (1999) v. 215 p. R11-R12.

Koblischka, M. R.; Murakami, M.; Koishikawa, S.; Johansen, T. H.; Baziljevich, M.; Frello, T.; Wolf, T., Instability of the critical state in $NdBa_2Cu_3O_7-^d$elta single crystals. J. Low Temp. Phys. (1999) v. 117 p. 1483-1487.

Korin-Hamzic, B.; Basletic, M.; Hamzic, A.; Bechgaard, K., Change of the activation energy in SDW state of (TMTSF)(2)PF6. Synth. Met. (1999) v. 103 p. 2125-2126.

Krebs, F. C.; Faldt, A.; Thorup, N.; Bechgaard, K., Arrested handedness and disordered stacking in crystals of the pre-helical molecule 7,8-dioxa[6]helicene. CrystEngComm (1999) (no. 6) p. 1-3.

Krebs, F. C.; Jørgensen, M.; Larsen, M., On the saddle-shaped nature of 14,15-dimethylbenzo[s]picene. J. Org. Chem. (1999) v. 64 p. 8758-8760.

Krebs, F. C.; Larsen, M.; Jørgensen, M.; Jensen, P. R.; Bielecki, M.; Schaumburg, K., Synthesis and structural properties of 5,17-bis (N-methyl-N-arylaminocarbonyl)calix[4]arenes. Directing the substituents toward the cavity by use of the cis-generating property of the N-methylaminocarbonyl linker. J. Org. Chem. (1998) v. 63 p. 9872-9879.

Krebs, F. C.; Laursen, B. W.; Johannsen, I.; Faldt, A.; Bechgaard, K.; Jacobsen, C. S.; Thorup, N.; Bou-bekeur, K., The geometry and structural properties of the 4,8,12-trioxa-4,8,12c-tetrahydrodibenzo[*cd,-mn*]pyrene system in the cationic state. Structures of a planar organic cation with various monovalent and divalent anions. Acta Cryst. B (1999) v. 55 p. 410-423.

Kuhl, T. L.; Majewski, J.; Howes, P. B.; Kjær, K.; Nahmen, A. von; Lee, K. Y. C.; Ocko, B.; Israelachvili, J. N.; Smith, G. S., Packing stress relaxation in polymer-lipid monolayers at the air-water interface: An X-ray grazing-incidence diffraction and reflectivity study. J. Am. Chem. Soc. (1999) v. 121 p. 7682-7688.

Kuzmenko, I.; Kjær, K.; Als-Nielsen, J.; Lahav, M.; Leiserowitz, L., Detection of chiral disorder in langmuir monolayers undergoing spontaneous chiral segregation. J. Am. Chem. Soc. (1999) v. 121 p. 2657-2661.

Lake, B.; Aeppli, G.; Mason, T. E.; Schröder, A.; Mcmorrow, D. F.; Lefmann, K.; Ishiki, M.; Nohara, M.; Takagi, H.; Hayden, S. M., Spin gap and magnetic coherence in a clean high-temperature superconductor. Nature (1999) v. 400 p. 43-46.

Langridge, S.; Paixao, J. A.; Bernhoeft, N.; Vettier, C.; Lander, G. H.; Gibbs, D.; Sørensen, S. Å.; Stunault, A.; Wermeille, D.; Talik, E., Changes in 5d band polarization in rare-earth compounds. Phys. Rev. Lett. (1999) v. 82 p. 2187-2190.

Larsen, F. H.; Rasmussen, T.; Batsberg Pedersen, W.; Nielsen, N. C.; Jakobsen, H. J., Observation of immobile regions in natural rubber at ambient temperature by solid-state C-13 CP/MAS NMR spectroscopy. Polymer (1999) v. 40 p. 7013-7017.

Larsen, M.; Krebs, F. C.; Harrit, N.; Jørgensen, M., Synthesis and conformational studies of a series of 5,17-bis-aryl-25,26,27,28-tetrapropoxycalix[4]arenes: The influence of pi-pi interactions on the molecular structure. J. Chem. Soc. Perkin Trans. 2 (1999) (no. 8) p. 1749-1757.

Lee, K. Y. C.; Majewski, J.; Kjær, K.; Howes, P. B.; Lipp, M. M.; Waring, A. J.; Zasadzinski, J. A., Incorporation of lung surfactant specific protein SP-B into lipid monolayers at the air-fluid interface: A synchrotron X-ray study. Biophys. J. (1999) v. 76 p. A216.

Lefmann, K.; Bødker, F.; Hansen, M. F.; Vazquez, H.; Christensen, N. B.; Lindgård, P. -A.; Clausen, K. N.; Mørup, S., Magnetic dynamics of small α-Fe_2O_3 particles studied by neutron scattering. Eur. Phys. J. D (1999) v. 9 p. 491-494.

Lefmann, K.; Nielsen, K., McStas, a general software package for neutron ray-tracing simulations. Neutron News (1999) v. 10 (no. 3) p. 20-23.

Lindgård, P. -A., Reply to "Equivalence of the *p*-degenerate and ordinary Blume-Emery-Griffiths models". Phys. Rev. B (1999) v. 60 p. 12504.

Lister, S. J. S.; Boothroyd, A. T.; Andersen, N. H.; Zhokhov, A. A.; Christensen, A. N.; Wolf, T., Magnetic excitations and pressure studies on single-crystals of $PrBa_2Cu_3O_{6+x}$. Physica C (1999) v. 317-318 p. 572-574.

Lorenzo, J. E.; Regnault, L. P.; Langridge, S.; Vettier, C.; Sutter, C.; Grübel, G.; Souletie, J.; Lussier, J. G.; Schoeffel, J. P.; Pouget, J. P.; Stunault, A.; Wermeille, D.; Dhalenne, G.; Revcolevschi, A., Observation of a Kosterlitz-Thouless state at the spin-Peierls phase transition in $CuGeO_3$. Europhys. Lett. (1999) v. 45 p. 45-51.

McLaughlin, W. L.; Silverman, J.; Al-Sheikhly, M.; Chappas, W. J.; Liu, Z. J.; Miller, A.; Batsberg Pedersen, W., High-density polyethylene dosimetry by transvinylene FTIR analysis. Radiat. Phys. Chem. (1999) v. 56 p. 503-508.

McMorrow, D. F.; Gibbs, D.; Bohr, J., X-ray scattering studies of lanthanide magnetism. In: Handbook on the physics and chemistry of rare earths, vol. 26. Gschneidner, K. A.; Eyring, L. (eds.), (Elsevier, Amsterdam, 1999) p. 1-85.

Meunier, I.; Gay, J. M.; Lapena, L.; Aufray, B.; Oughaddou, H.; Landemark, E.; Falkenberg, G.; Lotter-moser, L.; Johnson, R. L., Atomic structure of the SbCu surface alloy: A surface X-ray diffraction study. Surf. Sci. (1999) v. 422 p. 42-49.

Morkved, T. L.; Chapman, B. R.; Bates, F. S.; Lodge, T. P.; Stepanek, P.; Almdal, K., Dynamics of ternary polymer blends: Disordered, ordered and bicontinuous microemulsion phases. Faraday Discuss. (1999) v. 112 p. 335-350.

Mortensen, K., Block copolymer micelles, micellar networks and mesophases (Invited review). Fibre Diffr. Rev. (1999) (no. 7) p. 25-31.

Müller-Gerking, J.; Pfurtscheller, G.; Flyvbjerg, H., Designing optimal spatial filters for single-trial EEG classification in a movement task. Clin. Neurophysiol. (1999) v. 110 p. 787-798.

Møller, P. J.; Feidenhans'l, R.; Adams, D. L. (eds.), ICSFS-9. Proceedings. 9. International conference on solid films and surfaces, Copenhagen (DK), 6-10 Jul 1998. (Elsevier, Amsterdam, 1999) (Applied Surface Science, v. 142, no. 1-4) 677 p.

Mønster, D.; Lindgård, P. -A.; Andersen, N. H., Simple solution to problems concerning oxygen ordering in $YBa_2Cu_3O_{6+x}$. Phys. Rev. B (1999) v. 60 p. 110-113.

Naydenova, I.; Nikolova, L.; Ramanujam, P. S.; Hvilsted, S., Light-induced circular birefringence in cyanoazobenzene side-chain liquid-crystalline polyester films. J. Opt. A (1999) v. 1 p. 438-441.

Ndoni, S.; Jannasch, P.; Larsen, N. B.; Almdal, K., Lubricating effect of thin films of styrene-dimethylsiloxane block copolymers. Langmuir (1999) v. 15 p. 3859-3865.

Nielsen, M.; Feidenhans'l, R.; Howes, P. B.; Vedde, J.; Rasmussen, K.; Benamara, M.; Grey, F., The interface structure in directly bonded silicon crystals studied by synchrotron x-ray diffraction. Surf. Sci. (1999) v. 442 p. L989-L994.

Niemøller, T.; Hunnefeld, H.; Frello, T.; Andersen, N. H.; Ichikawa, N.; Uchida, S.; Schneider, J. R., Detailed study of charged stripes in $La_{1.6-x}Nd_{0.4}Sr_xCuO_4$. J. Low Temp. Phys. (1999) v. 117 p. 455-459.

Niemöller, T.; Ichikawa, N.; Frello, T.; Hünnefeld, H.; Andersen, N. H.; Uchida, S.; Schneider, J. R.; Tranquada, J. M., Charge stripes seen with X-rays in $La_{1.45}Nd_{0.4}Sr_{0.15}CuO_4$. Eur. Phys. J. B (19 99) v. 12 p. 509-513.

Niemöller, T.; Zimmermann, M. von; Uhlenbruck, S.; Friedt, O.; Buchner, B.; Frello, T.; Andersen, N. H.; Berthet, P.; Pinsard, L.; Leon-Guevara, A. M. De; Revcolevschi, A.; Schneider, J. R., The charge ordered phase in $La_{1-x}Sr_xMnO_3$ studied by means of high energy x-ray diffraction. Eur. Phys. J. B (1999) v. 8 p. 5-8.

Niemöller, T.; Zimmermann, M. von; Schneider, J. R.; Frello, T.; Andersen, N. H.; Uhlenbruck, S.; Friedt, O.; Buchner, B.; Berthet, P.; Pinsard, L.; Revcolevschi, A., Hard x-ray diffraction studies of $La_{1-x}Sr_xMnO_3$. J. Superconduct. (1999) v. 12 p. 317-318.

Ohnuma, M.; Hono, K.; Onodera, H.; Pedersen, J. S.; Linderoth, S., Cu clustering stage before the crystallization in Fe-Si-B-Nb-Cu amorphous alloys. Nanostruct. Mater. (1999) v. 12 p. 693-696.

Ohnuma, M.; Hono, K.; Onodera, H.; Pedersen, J. S.; Mitani, S.; Fujimori, H., Distribution of Co particles in Co-Al-O granular thin films. Adv. Nanocryst. (1999) v. 307 p. 171-176.

Ohnuma, M.; Pryds, N. H.; Linderoth, S.; Eldrup, M.; Schrøder Pedersen, A.; Pedersen, J. S., Bulk amorphous $(Mg_{0.98}Al_{0.02})_{60}Cu_{30}Y_{10}$ alloy. Scr. Mater. (1999) v. 41 p. 889-893.

Papadakis, C. M.; Almdal, K.; Mortensen, K.; Vigild, M. E.; Stepanek, P., Unexpected phase behavior of an asymmetric diblock copolymer. J. Chem. Phys. (1999) v. 111 p. 4319-4326.

Pavese, A.; Prencipe, M.; Tribaudino, M.; Aagaard Sørensen, S., X-ray and neutron single-crystal study of P4/n vesuvianite. Can. Mineralogist (1998) v. 36 p. 1029-1037.

Pedersen, J. S., Analysis of small-angle scattering data from micelles and microemulsions: Free-form approaches and model fitting. Curr. Opin. Colloid Interface Sci. (1999) v. 4 p. 190-196.

Pedersen, J. S.; Schurtenberger, P., Static properties of polystyrene in semidilute solutions: A comparison of Monte Carlo simulation and small-angle neutron scattering results. Europhys. Lett. (1999) v. 45 p. 666-672.

Pedersen, M.; Hvilsted, S.; Holme, N. C. R.; Ramanujam, P. S., Influence of the substituent on azobenzene side-chain polyester optical storage materials. Macromol. Symp. (1999) v. 137 p. 115-127.

Poulsen, H. F.; Andersen, L. G.; Frello, T.; Prantontep, S.; Andersen, N. H.; Garbe, S.; Madsen, J.; Abrahamsen, A. B.; Bentzon, M. D.; Zimmermann, M. von, In situ study of equilibrium phenomena and kinetics in a BiSCCO Ag tape. Physica C (1999) v. 315 p. 254-262.

Ramanujam, P. S.; Hvilsted, S., Instant holography. Holography Newslett. (1999) v. 10 (no. 2) p. 1,5.

Ramanujam, P. S.; Pedersen, M.; Hvilsted, S., Instant holography. Appl. Phys. Lett. (1999) v. 74 p. 3227-3229.

Rapaport, H.; Kim, H. S.; Kjær, K.; Howes, P. B.; Cohen, S.; Als-Nielsen, J.; Ghadiri, M. R.; Leiserowitz, L.; Lahav, M., Crystalline cyclic peptide nanotubes at interfaces. J. Am. Chem. Soc. (1999) v. 121 p. 1186-1191.

Rasmussen, P. H.; Ramanujam, P. S.; Hvilsted, S.; Berg, R. H., A remarkably efficient azobenzene peptide for holographic information storage. J. Am. Chem. Soc. (1999) v. 121 p. 4738-4743.

Rasmussen, P. H.; Ramanujam, P. S.; Hvilsted, S.; Berg, R. H., Accelerated optical holographic recording using bis-DNO. Tetrahedron Lett. (1999) v. 40 p. 5953-5956.

Rittig, F.; Fleischer, G.; Karger, J.; Papadakis, C. M.; Almdal, K.; Stepanek, P., Anisotropic self-diffusion in a hexagonally ordered asymmetric PEP-PDMS diblock copolymer studied by pulsed field gradient NMR. Macromolecules (1999) v. 32 p. 5872-5877.

Rittig, F.; Karger, J.; Papadakis, C. M.; Fleischer, G.; Stepanek, P.; Almdal, K., Self-diffusion investigations on a series of PEP-PDMS diblock copolymers with different morphologies by pulsed field gradient NMR. Phys. Chem. Chem. Phys. (1999) v. 1 p. 3923-3931.

Rønne, C.; Åstrand, P. -O.; Keiding, S. R., THz spectroscopy of liquid H_2O and D_2O. Phys. Rev. Lett. (1999) v. 82 p. 2888-2891.

Rønnow, H. M.; McMorrow, D. F.; Harrison, A., High-temperature magnetic correlations in the 2D S=1/2 antiferromagnet copper formate tetradeuterate. Phys. Rev. Lett. (1999) v. 82 p. 3152-3155.

Sarthour, R. S.; Goff, J. P.; McMorrow, D. F.; Yakhou, F.; Stunault, A.; Lidstrom, E.; Vigliante, A.; Ward, R. C. C.; Wells, M. R., Induced magnetic order in Nd/Pr superlattices. J. Magn. Magn. Mater. (1999) v. 198/199 p. 288-290.

Schwahn, D.; Mortensen, K.; Frielinghaus, H.; Almdal, K., Crossover from 3D ising to isotropic Lifshitz critical behavior in a mixture of a homopolymer blend and diblock copolymer. Phys. Rev. Lett. (1999) v. 82 p. 5056-5059.

Singh-Zocchi, M.; Andreasen, A.; Zocchi, G., Osmotic pressure contribution of albumin to colloidal interactions. Proc. Nat. Acad. Sci. USA (1999) v. 96 p. 6711-6715.

Sirringhaus, H.; Brown, P. J.; Friend, R. H.; Nielsen, M. M.; Bechgaard, K.; Langeveld-Voss, B. M. W.; Spiering, A. J. H.; Janssen, R. A. J.; Meijer, E. W.; Herweg, P.; Leeuw, D. M. de, Two-dimensional charge transport in self-organized, high-mobility conjugated polymers. Nature (1999) v. 401 p. 685-688.

Smela, E., Microfabrication of PPy microactuators and other conjugated polymer devices. J. Micromech. Microeng. (1999) v. 9 p. 1-18.

Smela, E., A microfabricated movable electrochromic "pixel" based on polypyrrole. Adv. Mater. (1999) v. 11 p. 1343-1345.

Smela, E.; Gadegaard, N., Surprising volume change in PPy(DBS): An atomic force microscopy study. Adv. Mater. (1999) v. 11 p. 953-957.

Smela, E.; Kallenbach, M.; Holdenried, J., Electrochemically driven polypyrrole bilayers for moving and positioning bulk micromachined silicon plates. J. Microelectromech. Syst. (1999) v. 8 p. 373-383.

Svensson, B.; Olsson, U.; Alexandridis, P.; Mortensen, K., A SANS investigation of reverse (water-in-oil) micelles of amphiphilic block copolymers. Macromolecules (1999) v. 32 p. 6725-6733.

Sylvester-Hvid, K. O.; Åstrand, P. -O.; Ratner, M. A.; Mikkelsen, K. V., Frequency-dependent molecular polarizability and refractive index: Are substituent contributions additive?. J. Phys. Chem. A (1999) v. 103 p. 1818-1821.

Thestrup, B.; Schou, J.; Nordskov, A.; Larsen, N. B., Electrical and optical properties of thin indium tin oxide films produced by pulsed laser ablation in oxygen or rare gas atmospheres. Appl. Surf. Sci. (1999) v. 142 p. 248-252.

Vaqueiro, P.; Hull, S.; Lebech, B.; Powell, A. V., High temperature neutron diffraction studies of phase transformations in $NiCr_2S_4$. J. Mater. Chem. (1999) v. 9 p. 2859-2863.

Verclas, S. A. W.; Howes, P. B.; Kjær, K.; Wurlitzer, A.; Weygand, M.; Büldt, G.; Dencher, N. A.; Lösche, M., X-ray diffraction from a single layer of purple membrane at the air/water interface. J. Mol. Biol. (1999) v. 287 p. 837-843.

Verheul, M.; Pedersen, J. S.; Roefs, S. P. F. M.; Kruif, K. G. de, Association behavior of native beta-lactoglobulin. Biopolymers (1999) v. 49 p. 11-20.

Vries, S. A. de; Goedtkindt, P.; Huisman, W. J.; Zwanenburg, M. J.; Feidenhans'l, R.; Bennett, S. L.; Smilgies, D. M.; Stierle, A.; Yoreo, J. J. De; Enckevort, W. J. P. van; Bennema, P.; Vlieg, E., X-ray diffraction studies of potassium dihydrogen phosphate (KDP) crystal surfaces. J. Cryst. Growth (1999) v. 205 p. 202-214.

Weygand, M.; Wetzer, B.; Pum, D.; Sleytr, U. B.; Cuvillier, N.; Kjær, K.; Howes, P. B.; Lösche, M., Bacterial S-layer protein coupling to lipids: X-ray reflectivity and grazing incidence diffraction studies. Biophys. J. (1999) v. 76 p. 458-468.

Wilkins, C. J. T.; Rainford, B. D.; Goff, J. P.; Ward, R. C. C.; Wells, M. R.; McMorrow, D. F.; McIntyre, G. J., Magnetic characterisation of Tm/Y and Tm/Lu superlattices. J. Magn. Magn. Mater. (1999) v. 198/199 p. 509-512.

Åstrand, P. -O.; Ruud, K.; Mikkelsen, K. V.; Helgaker, T., Rovibrationally averaged magnetizability, rotational g factor, and indirect spin-spin coupling of the hydrogen fluoride molecule. J. Chem. Phys. (1999) v. 110 p. 9463-9468.

3.2.   Publications for a broader readership, theses and reports

Aagaard Sørensen, S., Neutron scattering studies of modulated magnetic structures. Risø-R-1125(EN) (1999) 83 p.

Bechgaard, K.; Clausen, K. N.; Feidenhans'l, R.; Johannsen, I. (eds.), Annual progress report of the Condensed Matter Physics and Chemistry Department 1 January - 31 December 1998. Risø-R-1099(EN) (1999) 186 p.

Berg Madsen, N., Modification and characterization of the interface in polymer/inorganic composites. Risø-R-1113(EN) (1999) 149 p. (ph. d. thesis).

Eskildsen, M. R., Eksotiske hvirvler. Fluxliniegitteret i magnetiske superledere. In: Samfinansiering 1. Seks unge danske samfinansierede forskerstuderende fortæller om deres igangværende forskning - og deres syn på det at være samfinansieringsstipendiat. (Forskerakademiet, Århus, 1999) p. 27-29.

Feidenhans'l, R.; Gerward, L.; Staun Olsen, J., Fri-elektron laseren - Næste generation af brillante synkrotronstrålingskilder. Kvant (1999) v. 10 (no. 2) p. 16-24.

Flyvbjerg, H., The Danish Research Academy's Graduate School of Biophysics: 1998 activity report. (Niels Bohr Institute, Copenhagen, 1999) 54 p.

Frello, T., Structural and superconducting properties of high-T_c superconductors. Risø-R-1086(EN) (1999) vp. (ph. d. thesis).

Krebs, F. C., Initium sapientiæ timor domini. Risø-R-1144(EN) (2000) 480 p. (ph. d. thesis).

Lindgård, P. -A., Det Europæiske Fysiske Selskab. Kvant (1999) v. 10 (no. 2) p. 27-28.

Mortensen, K., Polymerer til ingelligente materialer. Risønyt (1999) (no. 2) p. 20-24.

Nielsen, K.; Lefmann, K., User and programmers guide to the neutron ray-tracing package McStas, version 1. 1. (Risø National Laboratory, Roskilde, 1999) 122 p.

Nielsen, M. M., De nye chips er af plast. Risønyt (1999) (no. 2) p. 13-16.

Nørgaard, K., Neutron scattering studies of the magnetic structures in the borocarbide superconductor $TmNi_2B_2C$. (Risø National Laboratory, Roskilde, 1999) 75 p.

Pedersen, J. S., Structural studies by small-angle scattering and specular reflectivity. Risø-R-1166(EN) (1999) 104 p.

Rasmussen, P. H., Pseudopeptide structures for reversible holographic storage and combinatorial applications. Risø-R-1124(EN) (1999) vp. (ph. d. thesis).

Sommer-Larsen, P., Polymeraktuatorer som kunstige muskler. Risønyt (1999) (no. 2) p. 17-19.

3.3. Conference lectures, published and lectures, incl. published abstracts

3.3.1. Conference lectures, published

Bak, P.; Flyvbjerg, H., Punctuated equilibria vs Darwin?. In: Nonlinear cooperative phenomena in biological systems. Adriatico research conference, Trieste (IT), 19-22 Aug 1997. Matsson, L. (ed.), (World Scientific, Singapore, 1998) p. 68-85.

Berg, R. H.; Rasmussen, P. H.; Hvilsted, S.; Ramanujam, P. S., Optical holographic data storage using peptides. In: Peptides. Frontiers of peptide science. Proceedings. 15. American peptide symposium, Nashville, TN (US), 14-19 Jun 1997. Tam, J. P.; Kaumaya, P. T. P. (eds.), (Kluwer Academic Publishers, Dordrecht, 1999) p. 88-90.

Flyvbjerg, H., Error estimates on averages of correlated data. In: Advances in computer simulation. International summer school and workshop on advances in computer simulations. Bolyai College. Eötvös University, Budapest (HU), 16-20 Jul 1996. Kertész, J.; Kondor, I. (eds.), (Springer-Verlag, Berlin, 1998) (Lecture notes in physics, 501) p. 88-103.

Hvilsted, S.; Ramanujam, P. S., Azobenzene side-chain liquid crystalline polyesters - A prodigious potential for optical information storage. In: Abstract book and general information. 6. International Bayreuth polymer and materials research symposium (BPS'99), Bayreuth (DE), 11-13 Apr 1999. (Universität Bayreuth, Bayreuth, 1999) 3 p. (L20).

Jobs, E.; Wolf, D. E.; Flyvbjerg, H., Modeling microtubule oscillations. In: Biological physics. 3. International symposium on biological physics, Santa Fe, NM (US), 20-24 Sep 1998. Frauenfelder, H.; Hummer, G.; Garcia, R. (eds.), (American Institute of Physics, Melville, NY, 1999) (AIP conference proceedings, 487) p. 279-287.

Jobs, E.; Wolf, D. E.; Flyvbjerg, H., Modeling microtubule oscillations. In: Statistical mechanics of biocomplexity. 15. Sitges conference, Barcelona (ES), 8-12 Jun 1998. Reguera, D.; Vilar, J. M. G.; Rubi, J. M. (eds.), (Springer-Verlag, Berlin, 1999) (Lecture notes in physics, 527) p. 46-55.

Lebech, B., Magnetic structures studied by neutron scattering (invited paper). In: Proceedings. Conference: Physics and its applications, Krakow (PL), 24-25 Jun 1999. Wierzbanowski, K. (ed.), (University of Mining and Metallurgy, Faculty of Physics and Nuclear Techniques, Krakow, 1999) p. 39-44.

McMorrow, D. F., From thin films to superlattices studied with X-ray and neutron scattering. In: Complementarity between neutron and synchrotron X-ray scattering. 6. Summer school of neutron scattering, Zuoz (CH), 8-14 Aug 1998. Furrer, A. (ed.), (World Scientific, Singapore, 1998) p. 199-217.

Mønster, D.; Lindgård, P. -A.; Andersen, N. H., Monte Carlo study of oxygen ordering in $Yba_2Cu_3O_{6+x}$. In: Proceedings. 11. Annual workshop on computer simulation studies in condensed- matter physics, Athens, GA (US), 22-27 Feb 1998. Landau, D. P.; Schüttler, H. -B. (eds.), (Springer-Verlag, Berlin, 1999) (Springer proceedings in physics, 84) p. 150-154.

Ramanujam, P. S.; Holme, N. C. R.; Berg, R. H.; Hvilsted, S., Holographic memory. In: Selected papers from Photonics India '98. International conference on fiber optics and photonics, New Delhi (IN), 14-18

Dec 1998. Sharma, A.; Gupta, B. D.; Ghatak, A. K.; (eds.), (International Society for Optical Engineering, Bellingham, WA, 1999) (Proceedings of SPIE, v. 3666) p. 611-617.

Rasmussen, P. H.; Ramanujam, P. S.; Hvilsted, S.; Berg, R. H., Improved peptides for holographic data storage. In: Peptides. Frontiers of peptide science. Proceedings. 15. American peptide symposium, Nashville, TN (US), 14-19 Jun 1997. Tam, J. P.; Kaumaya, P. T. P. (eds.), (Kluwer Academic Publishers, Dordrecht, 1999) p. 168-169.

Sahlén, F.; Geisler, T.; Hvilsted, S.; Holme, N. C. R.; Ramanujam, P. S.; Petersen, J. C., Combined main- and side-chain azobenzene polyesters: A potential for photoinduced nonlinear waveguides. In: Proceedings. Symposium on organic nonlinear optical materials and devices, San Francisco, CA (US), 6-9 Apr 1999. Kippelen, B.; Lackritz, H. S.; Claus, R. O. (eds.), (MRS, Warrendale, PA, 1999) (Materials Research Society symposium proceedings, 561) p. 57-62.

Thomsen, A. B.; Schmidt, A. S.; Toftegaard, H.; Batsberg Pedersen, W.; Woidemann, A.; Lilholt, H., Natural plant fibre composites based on wet-oxidised wheat straw and polypropylene. In: Proceedings. 6. Symposium on renewable resources for the chemical industry; 4. European symposium on industrial crops and products, Bonn (DE), 23-25 Mar 1999. (Landwirtschaftsverlag GmbH, Münster, 1999) (Schriftenreihe "Nachwachsende Rohstoffe", 14) p. 762-771.

3.3.2. Lectures, incl. published abstracts

Abrahamsen, A. B.; Eskildsen, M. R.; Andersen, N. H.; Gammel, P. L.; Bishop, D. J.; Canfield, P. C., Flux line lattice reorientation in TmNi$_2$B$_2$C studied by Bitter decoration. APS Centennial meeting. Session UC27 - Vortices in superconputers 8: Imaging and structure, Atlanta, GA (US), 21-26 Mar 1999. Unpublished. Abstract available.

Alexandridis, P.; Olsson, U.; Lindman, B.; Linse, P.; Khan, A.; Mortensen, K.; Svensson, B.; Svensson, M.; Tsianou, M.; Holmqvist, P., Morphological versatility of solvated block copolymers. In: Nordic polymer days 1999. Nordic polymer days, Danish Society for Polymer Technology, Copenhagen (DK), 31 May - 2 Jun 1999. (Ingeniørforeningen i Danmark, Copenhagen, 1999) 5. 1.

Almdal, K., Dynamic mechanical spectroscopy. 1. Polymer conference, Oleinitec, Bornholm (DK), 15-16 Apr 1999. Unpublished.

Almdal, K., Orientation of microstructured polymers melts in oscillatory shear flow. 1. Polymer conference, Oleinitec, Bornholm (DK), 15-16 Apr 1999. Unpublished.

Almdal, K., Dynamical mechanical spectroscopy and viscosity measurements. Introduction and practical examples. Short course on interpretation of rheological measurements at the Nordic rheology conference, Lyngby (DK), 9 Jun 1999. Unpublished.

Almdal, K., Thermodynamics of and non-equilibrium phenomena in polydimethylsiloxane (PDMS) containing diblock copolymers. Meeting at the Max Planck Institute of Colloids and Interfaces, Teltow (DE), 27 Jan 1999. Unpublished.

Almdal, K.; Vigild, M. E.; Mortensen, K., Fluctuations effects in ordered diblock copolymers. In: Nordic polymer days 1999. Nordic polymer days, Danish Society for Polymer Technology, Copenhagen (DK), 31 May - 2 Jun 1999. (Ingeniørforeningen i Danmark, Copenhagen, 1999) 5. 3.

Almdal, K.; Vigild, M. E.; Mortensen, K., On the coupling of composition fluctuations to shear fields in ordered diblock copolymers. ESF workshop on field - responsive polymers, composite organic materials and gels with controlled supramolecular structure, Heraklion (GR), 23-24 Apr 1999. Unpublished.

Andersen, N. H., Superconductors for power transmission and magnetic applications. Møde i Dansk Magnetisk Forening, Odense (DK), 2 Mar 1999. Unpublished.

Andersen, N. H., Keramiske superledere: Grundlæggende egenskaber og anvendelsesmuligheder. Dansk Keramisk Selskabs forårsmøde og MUP-2 seminar om superledere, Risø (DK), 5 May 1999. Unpublished. Abstract available.

Andersen, N. H., Keramiske højtemperatur superledere: Grundlæggende egenskaber og anvendelsesmuligheder. DAKS forårsmøde '99, Risø (DK), 5 May 1999. Tidsskr. Dansk Keramisk Selskab (1999) v. 2 (no. 2) p. 28.

Andersen, T. H.; Tougaard, S.; Hubert, L.; Johannsen, I., Surface morphology of diblock copolymers during annealing. In: Programme. Abstracts. List of participants. Annual meeting of the Danish Physical Society, Nyborg (DK), 3-4 Jun 1999. (HCØ Tryk, København, 1999) p. FF41P.

Arleth, L.; Pedersen, J. S., Scattering vector dependence of the small-angle scattering from mixture of hydrogenated and deuterated organic solvents. SAS'99. 11. International conference on small-angle scattering, New York, NY (US), 17-20 May 1999. Unpublished.

Avdeev, M. V.; Pedersen, J. S.; Almasy, L.; Wiedenmann, A.; Serdyuk, I. N., Use of apoferritin to study resolution effects for SANS instruments. SAS'99. 11. International conference on small-angle scattering, New York, NY (US), 17-20 May 1999. Unpublished.

Bailey, L.; Henderson, M. J.; Hillman, A. R.; Gadegaard, N., In Situ neutron reflectivity study of poly-o-toluidine films. In: Conference programme and abstracts. 2. European conference on neutron scattering (ECNS '99). Session C, Budapest (HU), 1-4 Sep 1999. Cser, L.; Grósz, T.; Rosta, L. (eds.), (Technical University of Budapest, Budapest, 1999) p. 109.

Batsberg Pedersen, W., Size exclusion chromatographic and MALDI-TOF analysis of polymers - a comparison. Danish Society for Polymer Technology (PTS) thematic meeting, Risø (DK), 5 Oct 1999. Unpublished. Abstract available.

Bergström, M.; Pedersen, J. S., The growth from small disk-shaped to larger tablet-shaped or ribbon-like surfactant micelles investigated by small-angle neutron scattering. SAS'99. 11. International conference on small-angle scattering, New York, NY (US), 17-20 May 1999. Unpublished.

Borbély, S.; Pedersen, J. S., Temperature induced aggregation in aqueous solutions of pluronic F68 triblock copolymer containing small amount of o-xylene. In: Conference programme and abstracts. 2. European conference on neutron scattering (ECNS '99). Session C, Budapest (HU), 1-4 Sep 1999. Cser, L.; Grósz, T.; Rosta, L. (eds.), (Technical University of Budapest, Budapest, 1999) p. 105.

Borg, J.; Tiana, G.; Lindgård, P. -A., Models of protein folding and protein interactions. In: Book of abstracts. Topical meeting on biophysics-biological physics, Copenhagen (DK), 21 Apr 1999. (Niels Bohr Institute, Copenhagen, 1999) 1 p.

Busson, P.; Hult, A.; Hvilsted, S.; Ramanujam, P. S., Synthesis and characterization of azobenzene functionalized dendritic macromolecules for holographic storage applications. In: Nordic polymer days 1999. Nordic polymer days, Danish Society for Polymer Technology, Copenhagen (DK), 31 May - 2 Jun 1999. (Ingeniørforeningen i Danmark, Copenhagen, 1999) 1. 4.

Calderon, H. A.; Cruz, J.; Pedersen, J. S., Evolution and coherent γ pricipitates in a Ni-12 at. % Al alloy with a bimodal particle size distribution. In: Collected abstracts. 18. IUCr congress and general assembly, Glasgow (GB), 4-13 Aug 1999. (International Union of Crystallography, Glasgow, 1999) p. 223.

Canfield, P. C.; Fisher, I. R.; Cheon, K. O.; Eskildsen, M. R.; Gammel, P. L., Effect of rare-earth, Ni and B site substitutions on T_c, the electrical resistivity and the flux line lattice in the borocarbide superconductors $LuNi_2B_2C$ and YNi_2B_2C. APS Centennial meeting. Session VC26 - Organics and borocarbides, Atlanta, GA (US), 21-26 Mar 1999. Unpublished. Abstract available.

Christensen, N. B.; Lefmann, K.; Johannsen, I.; Jørgensen, O., Magnetic Bloch oscillations in the near-Ising 1D ferromagnet $CoCl_2\bullet2D_2O$. In: Conference programme and abstracts. 2. European conference on neutron scattering (ECNS '99). Session G, Budapest (HU), 1-4 Sep 1999. Cser, L.; Grósz, T.; Rosta, L. (eds.), (Technical University of Budapest, Budapest, 1999) p. 241.

Clausen, K. N., Eksempler på brug af neutroner i materialeforskning. Møde om neuytronspektroskopi i materialforskning, Kjeller (NO), 15-19 Mar 1999. Unpublished.

Clausen, K. N., Nye neutronkilder. Møde om neuytronspektroskopi i materialforskning, Kjeller (NO), 15-19 Mar 1999. Unpublished.

Clausen, K. N., Neutron scattering studies of nano-particles. Meeting on Physics and chemistry of nanostructures, Danish Technical University, Lyngby (DK), 16 Sep 1999. Unpublished.

Clausen, K. N., McStas a package for Monte Carlo simulation of neutron scattering instruments. 6. ESS general meeting, Portonovo/Ancona (IT), 20-23 Sep 1999. Unpublished.

Clausen, K. N., Neutron instrumentation and the neutron round-table. Conference on neutron optics for the next millennium, NOP99, Villigen (CH), 25-27 Nov 1999. Unpublished.

Clausen, K. N.; Bødker, F.; Kuhn, L. T.; Hansen, M. F.; Lefmann, K.; Lindgård, P. -A.; Mørup, S., Dynamics of magnetic nanoparticles (invited lecture). In: Conference programme and abstracts. 2. European conference on neutron scattering (ECNS '99). Session I, Budapest (HU), 1-4 Sep 1999. Cser, L.; Grósz, T.; Rosta, L. (eds.), (Technical University of Budapest, Budapest, 1999) p. 263.

Clegg, P. S.; Cowley, R. A.; Goff, J. P.; McMorrow, D. F.; Ward, R. C. C.; Wells, M. R., Anomalous magnetic ordering in Dy_xPr_{1-x} alloys. In: Conference programme and abstracts. 2. European conference on neutron scattering (ECNS '99). Session F, Budapest (HU), 1-4 Sep 1999. Cser, L.; Grósz, T.; Rosta, L. (eds.), (Technical University of Budapest, Budapest, 1999) p. 211.

Enderle, M.; Kiefer, K.; McIntyre, G.; Lefmann, K.; Kamp, R. van de, Quantum features in the spin dynamics of S=1/2 and S=1 Heisenberg antiferromagnets in spite of long-range ordered phases. In: Conference programme and abstracts. 2. European conference on neutron scattering (ECNS '99). Session G, Budapest (HU), 1-4 Sep 1999. Cser, L.; Grósz, T.; Rosta, L. (eds.), (Technical University of Budapest, Budapest, 1999) p. 240.

Enderle, M.; Regnault, L. -P.; Broholm, C.; Reich, D.; Zaliznyak, I.; Rønnow, H. M.; McMorrow, D., High-field spin dynamics of antiferromagnetic quantum spin chains. In: Conference programme and abstracts. 2. European conference on neutron scattering (ECNS '99). Session F, Budapest (HU), 1-4 Sep 1999. Cser, L.; Grósz, T.; Rosta, L. (eds.), (Technical University of Budapest, Budapest, 1999) p. 179.

Eskildsen, M. R.; Abrahamsen, A. B.; Andersen, N. H.; Mortensen, K.; Gammel, P. L.; Bishop, D. J.; Canfield, P. C., Temperature dependence of the flux line lattice square to hexagonal symmetry transition in LuNi2B2C: A crossover from London to Ginzburg-Landau behaviour. In: Programme. Abstracts. List of participants. Annual meeting of the Danish Physical Society, Nyborg (DK), 3-4 Jun 1999. (HCØ Tryk, København, 1999) p. FF07.

Eskildsen, M. R.; Abrahamsen, A. B.; Andersen, N. H.; Mortensen, K.; Gammel, P. L.; Bishop, D. J.; Fisher, I. R.; Cheon, K. O.; Kogan, V. G.; Canfield, P. C., Flux line lattice symmetries in the borocarbide superconductors. 1. Euroconference on vortex matter in superconductors, Crete (GR), 18-24 Sep 1999. Unpublished.

Eskildsen, M. R.; Gammel, P. L.; Bishop, D. J.; Andersen, N. H.; Mortensen, K.; Fisher, I. R.; Canfield, P. C., Flux line lattice symmetries in the borocarbide superconductors. 1. Regional conference on magnetic and supercomputing materials, Tehran (IR), 27-30 Sep 1999. Unpublished.

Eskildsen, M. R.; Gammel, P. L.; Bishop, D. J.; Abrahamsen, A. B.; Andersen, N. H.; Mortensen, K.; Canfield, P. C., Temperature dependence of the flux line lattice hexagonal to square symmetry transition in $LuNi_2B_2C$: A crossover from London to Ginzburg-Landay behaviour. 1. Regional conference on magnetic and supercomputing materials, Tehran (IR), 27-30 Sep 1999. Unpublished.

Feidenhans'l, R., Interfacial structures of bonded Si wafers. 6. International conference on surface X-ray and neutron scattering (6SXNS), Noordwijkerhout (NL), 13-17 Sep 1999. Unpublished.

Feidenhans'l, R., Structures of metals on semiconductor surfaces. Users EC round table, Paris (FR), 31 May 1999. Unpublished.

Feidenhans'l, R., Metal-induced restructuring of semiconductor surfaces. Meeting at University of Erlangen-Nürnberg, Nürnberg (DE), 6 May 1999. Unpublished.

Feidenhans'l, R., X-ray scattering from semiconductor surfaces and interfaces. Meeting at ETH Zürich, Zürich (CH), 16 Nov 1999. Unpublished.

Feidenhans'l, R.; Nielsen, M.; Howes, P. B.; Weichert, S.; Grey, F.; Vedde, J., Interfacial structures of bonded Si wafers. In: Collected abstracts. 18. IUCr congress and general assembly, Glasgow (GB), 4-13 Aug 1999. (International Union of Crystallography, Glasgow, 1999) p. 51.

Flyvbjerg, H., Supramolecular structures (invited talk). Nordita workshop on biophysics, Copenhagen (DK), 1-2 Feb 1999. Unpublished.

Flyvbjerg, H., Kinetics of self-assembling microtubules: An 'inverse problem' in biochemistry (invited talk). Seminar at Physics Department, Trondheim University, Trondheim (NO), 8 Apr 1999. Unpublished.

Flyvbjerg, H., Modeling microtubule dunamics (invited talk). Colloquium at Physics Department, Trondheim University, Trondheim (NO), 8 Apr 1999. Unpublished.

Flyvbjerg, H., Hvordan man laver en forskerskole under Forskerakademiet: Forskerskolen i Biofysik som eksempel. Seminar om forskerskoler, Copenhagen (DK), 23 Aug 1999. Unpublished.

Flyvbjerg, H., Micro- and macro-canonical ensembles and the Boltzmann distribution (guest lecture). Course on Thermodynamics and statistical mechanics, University of Copenhagen, Copenhagen (DK), 28 Sep 1999. Unpublished.

Flyvbjerg, H., Modeling microtubule dynamics: Doing molecular biology with the tools of theoretical physics (invited talk). Seminar at AMOLF (FOM Institute for Atomic and Molecular Physics), Amsterdam (NL), 3 Nov 1999. Unpublished.

Flyvbjerg, H., Modeling microtubule dynamics: Doing molecular biology with the tools of theoretical physics (invited talk). Seminar at Institute for Theoretical Physics, Utrecht (NL), 4 Nov 1999. Unpublished.

Flyvbjerg, H., The microtubule cap: Myths, models, and meagre facts (invited talk). Seminar at AMOLF (FOM Institute for Atomic and Molecular Physics), Amsterdam (NL), 5 Nov 1999. Unpublished.

Flyvbjerg, H., Nucleation-polymerization models for actin and tubulin. Forelæsning. M. Sc. course on physics of proteins, Copenhagen (DK), 17 Nov 1999. Unpublished.

Flyvbjerg, H., The ising model (guest lecture). Course on Thermodynamics and statistical mechanics, University of Copenhagen, Copenhagen (DK), 14 Dec 1999. Unpublished.

Flyvbjerg, H., Microtubule's conformational cap. In: Book of abstracts. Topical meeting on biophysics-biological physics, Copenhagen (DK), 21 Apr 1999. (Niels Bohr Institute, Copenhagen, 1999) 1 p.

Frello, T., Magneto-optical investigations of high-temperature superconductors. Dansk Keramisk Selskabs forårsmøde og MUP-2 seminar om superledere, Risø (DK), 5 May 1999. Unpublished. Abstract available.

Frello, T., Magneto-optical investigations of high-temperature superconductors. DAKS forårsmøde '99, Risø (DK), 5 May 1999. Tidsskr. Dansk Keramisk Selskab (1999) v. 2 (no. 2) p. 28.

Frielinghaus, H., Polymer blends and corresponding diblock copolymers in comparison. In: Nordic polymer days 1999. Nordic polymer days, Danish Society for Polymer Technology, Copenhagen (DK), 31 May - 2 Jun 1999. (Ingeniørforeningen i Danmark, Copenhagen, 1999) 1 p.

Frielinghaus, H.; Mortensen, K.; Almdal, K., Corresponding polymer blends and diblock copolymers in comparison. In: Conference programme and abstracts. 2. European conference on neutron scattering (ECNS '99). Session C, Budapest (HU), 1-4 Sep 1999. Cser, L.; Grósz, T.; Rosta, L. (eds.), (Technical University of Budapest, Budapest, 1999) p. 109.

Frielinghaus, H.; Mortensen, K.; Almdal, K., Comparison of a polyethyleneoxide/polystyrene polymer blend and corresponding diblock copolymer. In: Conference programme and abstracts. 6. European symposium on polymer blends. Session B, Mainz (DE), 16-19 May 1999. (Max Planck Institute, Mainz, 1999) 1 p.

Gadegaard, N., The effect of surface topography and chemistry on microorganism viability. In: Book of abstracts. Topical meeting on biophysics-biological physics, Copenhagen (DK), 21 Apr 1999. (Niels Bohr Institute, Copenhagen, 1999) 1 p.

Gammel, P. L.; Bishop, D. J.; Eskildsen, M. R.; Mortensen, K.; Andersen, N. H.; Fisher, I. R.; Cheon, K. O.; Canfield, P. C.; Kogan, V. G., SANS studies of the role of non-locality on the flux line lattice square-hexagonal symmetry transition. APS Centennial meeting. Session UC27 - Vortices in superconputers 8: Imaging and structure, Atlanta, GA (US), 21-26 Mar 1999. Unpublished. Abstract available.

Gammel, P. L.; Eskildsen, M. R.; Isaacs, E. D.; Detlefs, C.; Mortensen, K.; Bishop, D. J., Compound refractive optics for focusing and imaging with low-energy neutrons. SAS'99. 11. International conference on small-angle scattering, New York, NY (US), 17-20 May 1999. Unpublished. Abstract available.

Gerstenberg, M. C.; Pedersen, J. S.; Smith, G. S., Surface induced ordering of micelles at the solid-liquid interface. SAS'99. 11. International conference on small-angle scattering, New York, NY (US), 17-20 May 1999. Unpublished.

Glidle, A.; Cooper, J. M.; Gadegaard, N., Determination of the solvation and reactivity profile within activated electropolymerised films and their subsequent metal ion chelating properties using neutron reflectivity. In: Conference programme and abstracts. 2. European conference on neutron scattering (ECNS '99). Session C, Budapest (HU), 1-4 Sep 1999. Cser, L.; Grósz, T.; Rosta, L. (eds.), (Technical University of Budapest, Budapest, 1999) p. 104.

Goff, J. P.; Sarthour, R. S.; McMorrow, D. F.; Yakhou, F.; Vigliante, A.; Gibbs, D.; Ward, R. C. C.; Wells, M. R., Diffuse magnetic scattering from dhcp Ho-Ce alloys. In: Conference programme and abstracts. 2. European conference on neutron scattering (ECNS '99). Session F, Budapest (HU), 1-4 Sep 1999. Cser, L.; Grósz, T.; Rosta, L. (eds.), (Technical University of Budapest, Budapest, 1999) p. 211.

Grivel, J. -C.; Liu, Y. L.; Poulsen, H. P.; Andersen, L. G.; Frello, T.; Andersen, N. H.; Wang, W. G., Bi,Pb(2212) grain growth and relationship between the initial and final texture in Ag-sheathed Bi,Pb(2223) tapes. In: Programme. Technical sessions. Exhibition. Abstracts. 4. European conference on applied superconductivity, Sitges (ES), 14-17 Sep 1999. (Organisation Committee of EUCAS '99, Sitges, 1999) p. 114.

Hamley, I. W.; Daniel, C.; Mortensen, K., Structure and mechanical properties of triblock copolymers subject to extensional deformation. 218. ACS national meeting, New Orleans, LA (US), 22-26 Aug 1999. Abstr. Pap. Am. Chem. Soc. (1999) v. 218 p. 639-POLY.

Hansen, M. F.; Bødker, F.; Mørup, S.; Lefmann, K.; Clausen, K. N.; Lindgård, P. -A., Magnetic dynamics of fine particles studied by inelastic neutron scattering. 3. Euroconference on magnetic properties of fine particles and their relevance to materials science, Barcelona (ES), 19-22 Oct 1999. Unpublished. Abstract available.

Hooker, J. C., Polymer gels: Materials for actuation devices. MODECS Spring meeting 1999: Gels - Science and technology, Værløse (DK), 27 May 1999. Unpublished.

Hooker, J. C., Complementary probe tack techniques for measuring adhesion of a model PSA. Meeting at Coloplast, Humlebæk (DK), 24 Nov 1999. Unpublished.

Hooker, J. C.; Creton, C.; Tordjeman, P.; Shull, K. R., Surface effects on the microscopic adhesion mechanisms of styrene-isoprene-styrene + resin PSA's. 22. Annual meeting of the Adhesion Society, Panama City, FL (US), 21-24 Feb 1999. Unpublished.

Hooker, J. C.; Kofod, G.; Smela, E.; Gadegaard, N.; Sommer-Larsen, P.; West, K.; Skaarup, S.; Benslimane, M.; Gravesen, P., Polymer actuators. In: Nordic polymer days 1999. Nordic polymer days, Danish Society for Polymer Technology, Copenhagen (DK), 31 May - 2 Jun 1999. (Ingeniørforeningen i Danmark, Copenhagen, 1999) P13.

Hooker, J. C.; Sommer-Larsen, P.; Johannsen, I.; Eskildsen, J.; Smela, E., Monitoring volume expansion of PPy(DBS) with AFM and Dektak profilometry: Effects of DBS isomers. 4. Workshop on multifunctional and smart polymer systems, Malahide (IE), 20-23 Sep 1999. Unpublished.

Howes, P.; Nielsen, M.; Feidenhans'l, R.; Grey, F., Probing the structure of wafer bonded interfaces: A comparison of X-ray diffraction data with keating energy calculations. 1999 Joint international meeting: 196. Meeting of the Electrochemical Society; 1999 Fall meeting of the Electrochemical Society of Japan, Honolulu, HI (US), 17-22 Oct 1999. Unpublished.

Hvilsted, S., Prodigious optical information storage polyesters. The matrix-integrated azobenzene puzzle. Lecture at Departamento Fisica de la Materia Condensada Facultad de Ciencias, Universidad de Zaragoza, Zaragoza (ES), 30 Mar 1999. Unpublished.

Hvilsted, S., Design of azobenzene side-chain liquid crystalline polyesters - A prodigious potential for optical information storage. Lecture at Departamento de Quimica Orgánica, Facultad de Ciencias, Universidad Autónoma de Madrid, Madrid (ES), 9 Apr 1999. Unpublished.

Hvilsted, S., Photoadressable LC polyesters: Synthesis and applications for optical information storage. Lecture at Fachbereich 8 Chemie, Universität und Gesamthochschule Essen, Essen (DE), 14 Apr 1999. Unpublished.

Hvilsted, S., Azobenzene side-chain materials - A prodigious potential for optical information storage. LC Photonet meeting, Southampton (GB), 11-13 Feb 1999. Unpublished. Abstract available.

Hvilsted, S., Prodigious optical storage polyester materials - The matrix-integrated azobenzene puzzle. Meeting at Laboratory of Polymer Chemistry, Chemistry Department, University of Helsinki, Helsinki (FI), 22 Oct 1999. Unpublished.

Hvilsted, S., Prodigious optical storage materials - The matrix-integrated azobenzene puzzle. Meeting at Department of Chemistry, University of Aarhus, Aarhus (DK), 9 Nov 1999. Unpublished.

Hvilsted, S., The ordered azobenzene in a polymer matrix puzzle - how polarization FTIR can help. Møde om polymer-spektroskopi. Dansk Forening for Molekylspektroskopi, København (DK), 25 Nov 1999. Unpublished.

Hvilsted, S., Small LC domains in an amorphous phase through tailoring of block copolymers - A potential optical information storage material?. In: Experimental and theoretical investigation of complex polymer structures (SUPERNET). Kick off workshop, Strasbourg (FR), 19-21 Nov 1999. Sundholm. F. (ed.), (European Science Foundation, Strasbourg, 1999) 1 p.

Hvilsted, S.; Ramanujam, P. S., Light induced surface relief in azobenzene materials. In: 2. Symposium on phthalocyanines and related compounds. Abstracts. COST action 518. Molecular materials and functional polymers for advanced devices. First Working Group 2 meeting, Madrid (ES), 28-29 May 1999. (Cost Action 518, Madrid, 1999) 1 p.

Hvilsted, S.; Ramanujam, P. S., Azobenzene side-chain LC polyesters for optical information storage. SICL '99 workshop: Applications of liquid crystals, Portonovo di Ancona (IT), 23-26 Jun 1999. Unpublished. Abstract available.

Ishøy, T., Scattering studies of protein/peptide self-assembly and interactions with lipid layers. In: Book of abstracts. Topical meeting on biophysics-biological physics, Copenhagen (DK), 21 Apr 1999. (Niels Bohr Institute, Copenhagen, 1999) 1 p.

Ishøy, T.; Larsen, S., How crystallisation of turkey lysozyme is affected by contamination with hen lysozyme. Workshop: Pathways in protein folding and protein aggregation, University of Copenhagen, Copenhagen (DK), 6-9 Oct 1999. Unpublished.

Ishøy, T.; Larsen, S., How crystallisation of turkey lysozyme is affected by contamination with hen lysozyme. Summer school: Protein, lipid and membrane traffic: Pathways and targeting, Cargèse (FR), 7-9 Jun 1999. Unpublished.

Jensen, T. R., Model systems for biological membranes investigated by X-ray reflectivity and grazing incidence diffraction. In: Book of abstracts. Topical meeting on biophysics-biological physics, Copenhagen (DK), 21 Apr 1999. (Niels Bohr Institute, Copenhagen, 1999) 2 p.

Jensen, T. R., Structural investigation of novel zinc orthophosphates. In: Program and collected abstracts. 30. Danske krystallografmøde, Risø (DK), 20-21 May 1999. (Forskningscenter Risø, Roskilde, 1999) 1 p.

Jensen, T. R.; Kjær, K.; Howes, P. B.; Balashev, K.; Reitzel, N.; Bjørnholm, T., Model systems for biological membranes; Lipid-lipase interaction investigated by X-ray reflectivity and grazing incidence diffraction. In: Program and collected abstracts. 30. Danske krystallografmøde, Risø (DK), 20-21 May 1999. (Forskningscenter Risø, Roskilde, 1999) 1 p.

Johannsen, I., Overfladeanalyse - en introduktion. Temadag om industriel anvendelse af avanceret overfladeanalyse arrangeret af Risø og Teknologisk Institut, Risø (DK), 18 May 1999. Unpublished.

Kawano, S.; Lebech, B.; Shigeoka, T.; Iwata, N., Neutron diffraction studies of the magnetic structures of TbRu$_2$Si$_2$. In: Conference programme and abstracts. 2. European conference on neutron scattering (ECNS '99). Session F, Budapest (HU), 1-4 Sep 1999. Cser, L.; Grósz, T.; Rosta, L. (eds.), (Technical University of Budapest, Budapest, 1999) p. 185.

Kjær, K., Monolayer films at the air-liquid interface. EU workshop: Research with synchrotron radiation, HASYLAB at DESY, Hamburg (DE), 28 Jan 1999. Unpublished.

Kjær, K., X-ray diffraction from protein monolayers at the air/water interface. In: Book of abstracts. Topical meeting on biophysics-biological physics, Copenhagen (DK), 21 Apr 1999. (Niels Bohr Institute, Copenhagen, 1999) 2 p.

Kjær, K., Lipid-lipase interactions investigated by synchrotron X-ray reflectivity and grazing-incidence diffraction. International conference: Lipases and lipids. Structure, function and biotechnological applications, Santorini (GR), 6-8 May 1999. Unpublished.

Kjær, K., Progress report on X-ray studies of lipid-lipase interaction in Langmuir films. 4. Meeting of the EU funded lipid lipase project BIO4 CT97 2365, Santorini (GR), 10-11 May 1999. Unpublished.

Kleppinger, R.; Mortensen, K.; Almdal, K., An in-situ study on structural and viscoelastic consequences of physical network formation in triblock copolymer solutions. SAS'99. 11. International conference on small-angle scattering, New York, NY (US), 17-20 May 1999. Unpublished.

Kofod, G.; Faldt, A.; Sommer-Larsen, P., Dielectric spectroscopy and rheology of graphite filled elastomer. In: Nordic polymer days 1999. Nordic polymer days, Danish Society for Polymer Technology, Copenhagen (DK), 31 May - 2 Jun 1999. (Ingeniørforeningen i Danmark, Copenhagen, 1999) P4.

Kops, J.; Chen, X.; Jankova, K.; Truelsen, J. H.; Batsberg Pedersen, W., Atom-transfer radical polymerization of p-acetoxystyrene for the synthesis of amphiphilic block copolymers. 218. ACS national meeting, New Orleans, LA (US), 22-26 Aug 1999. Abstr. Pap. Am. Chem. Soc. (1999) v. 218 p. 357-POLY.

Krebs, F. C.; Jørgensen, M., Conformational analysis of 5,17-disubstituted and 5,11,17,23-tetrasubstituted calix[4]arenes using NMR and X-ray diffraction. In: Program and collected abstracts. 30. Danske krystallografmøde, Risø (DK), 20-21 May 1999. (Forskningscenter Risø, Roskilde, 1999) 1 p.

Kuhn, L. T.; Lefmann, K.; Clausen, K. N.; Pedersen, J. S., Small angle neutron scattering from a magnetic vortex structure in a cubic nanoparticle. In: Programme. Abstracts. List of participants. Annual meeting of the Danish Physical Society, Nyborg (DK), 3-4 Jun 1999. (HCØ Tryk, København, 1999) p. FF40P.

Lake, B.; Aeppli, G.; Mason, T. E.; Schröder, A.; McMorrow, D. F.; Lefmann, K.; Ishiki, M.; Nohara, M.; Takagi, H.; Hayden, S. M., Inelastic neutron scattering studies of the spin excitations in La$_{2-\chi}$Sr$_\chi$CuO$_4$. In: Abstracts. 22. International conference on low temperature physics (LT 22), Espoo and Helsinki (FI), 4-11 Aug 1999. (Helsinki University of Technology, Espoo, 1999) p. 623.

Lake, B.; Mason, T. E.; Lefmann, K.; McMorrow, D. F.; Aeppli, G.; Hedegård, P.; Schröder, A.; Hayden, S.; Ishiki, M.; Nohara, M.; Takagi, H., Neutron scattering studies of magnetic excitations in the high-$_{Tc}$ superconductor La$_{2-x}$Sr$_x$CuO$_4$. In: Programme. Abstracts. Lis t of participants. Annual meeting of the Danish Physical Society, Nyborg (DK), 3-4 Jun 1999. (HCØ Tryk, København, 1999) p. FF09.

Larsen, N. B., Undersøgelse af polymeroverflader med AFM. Temadag om industriel anvendelse af avanceret overfladeanalyse arrangeret af Risø og Teknologisk Institut, Risø (DK), 18 May 1999. Unpublished.

Larsen, N. B., Chemical and topographical surface analysis of polymers. Danish Society for Polymer Technology (PTS) thematic meeting, Risø (DK), 5 Oct 1999. Unpublished. Abstract available.

Le, T. D.; Olsson, U.; Wennerström, H.; Mortensen, K., Lamellar-liposome transformation in binary nonionic systems. In: Conference programme and abstracts. 2. European conference on neutron scattering (ECNS '99). Session C, Budapest (HU), 1-4 Sep 1999. Cser, L.; Grósz, T.; Rosta, L. (eds.), (Technical University of Budapest, Budapest, 1999) p. 110.

Lebech, B., Magnetic structures with long periods studied by small angle neutron scattering of single crystals (invited paper). 6. Workshop on magnetism and intermetallics, Porto (PT), 11-12 Nov 1999. Unpublished. Abstract available.

Lebech, B.; Menshikov, A.; Vokhmyanin, A., Magnetic structure determinations and phase transitions in $(Mn_{1-x}Fe_x)Sn_2$. In: Collected abstracts. 18. IUCr congress and general assembly, Glasgow (GB), 4-13 Aug 1999. (International Union of Crystallography, Glasgow, 1999) p. 517-518.

Lebech, B.; Theodor, K.; Breiting, B.; Clausen, K. N., The Risø facility for plastic deformation of germanium single crystals wafers. In: Program and collected abstracts. 30. Danske krystallografmøde, Risø (DK), 20-21 May 1999. (Forskningscenter Risø, Roskilde, 1999) 1 p.

Lefmann, K.; Ipsen, J.; Rasmussen, F. B.; Rischel, C., Thermodynamics of Rh nuclear spins calculated by exact diagonalization. In: Abstracts. 22. International conference on low temperature physics (LT 22), Espoo and Helsinki (FI), 4-11 Aug 1999. (Helsinki University of Technology, Espoo, 1999) p. 109.

Lefmann, K.; McMorrow, D. F.; Rønnov, H. M.; Nielsen, K.; Clausen, K. N.; Aeppli, G., Added flexibility in triple axis spectrometers: The two RITAs at Risø. Conference on neutron optics for the next millennium, NOP99, Villigen (CH), 25-27 Nov 1999. Unpublished. Abstract available.

Lefmann, K.; Nielsen, K., McStas 1. 1: A freeware package for neutron Monte Carlo ray-tracing simulations. In: Conference programme and abstracts. 2. European conference on neutron scattering (ECNS '99). Session A, Budapest (HU), 1-4 Sep 1999. Cser, L.; Grósz, T.; Rosta, L. (eds.), (Technical University of Budapest, Budapest, 1999) p. 37.

Lister, S. J. S.; Boothroyd, A. T.; Andersen, N. H.; Zhokhov, A. A.; Christensen, A. N.; Wolf, T., Magnetic excitations in $PrBa_2Cu_3O_{6.2}$. In: Conference programme and abstracts. 2. European conference on neutron scattering (ECNS '99). Session G, Budapest (HU), 1-4 Sep 1999. Cser, L.; Grósz, T.; Rosta, L. (eds.), (Technical University of Budapest, Budapest, 1999) p. 245.

Madsen, G. K. H.; Krebs, F. C.; Larsen, F. K.; Lebech, B., The charge density and the dipole moment of phosphangulene, a molecular pyroelectric material. In: Program and collected abstracts. 30. Danske krystallografmøde, Risø (DK), 20-21 May 1999. (Forskningscenter Risø, Roskilde, 1999) 1 p.

Makovicky, E.; Wenzel Andreasen, J.; Lebech, B., Determination of structural role of iron in tetrahedrite $Cu_{12-x}Fe_xSb_4S_{13}$ by means o f neutron diffraction. In: Program and collected abstracts. 30. Danske krystallografmøde, Risø (DK), 20-21 May 1999. (Forskningscenter Risø, Roskilde, 1999) 1 p.

McMorrow, D. F., Resonant scattering studies of magnetic and orbital order. Meeting at ESRF, Grenoble (FR), Jul 1999. Unpublished.

McMorrow, D. F., Spectrometers for the 21st century: RITA and other developments at Risø. Meeting at Institute Laue Langevin, Grenoble (FR), Jun 1998. Unpublished.

McMorrow, D. F.; Rønnow, H. M.; Harrison, A., Cross over from renormalised classical to quantum criticality in the 2D S=1/2 HAF?. Aspen Winter conference on quantum criticality, Aspen, CO (US), 3-9 Jan 1999. Unpublished.

Mortensen, K.; Almdal, K.; Kleppinger, R.; Reynaers, H.; Theunissen, L., Block copolymer micellar networks. Response to stretching, shear and temperature changes. In: Nordic polymer days 1999. Nordic polymer days, Danish Society for Polymer Technology, Copenhagen (DK), 31 May - 2 Jun 1999. (Ingeniørforeningen i Danmark, Copenhagen, 1999) 5. 4.

Mortensen, K.; Almdal, K.; Reynaers, H.; Theunissen, L.; Mischenko, N.; Kleppinger, R., Structural response to the structure of micellar mesophases and networks when exposed to oscillatory and steady shear (Invited paper). COST Action P1 workshop. Time resolved measurements of structure evolution in soft condensed matter under flow, Leuven (BE), 22-23 Jan 1999. Unpublished.

Mortensen, K.; Almdal, K.; Reynaers, H.; Kleppinger, R.; Mischenko, N.; Theunissen, L., Shear and temperature dependence of the cubic structure of a SEBS micellar network. APS Centennial meeting. Session XC11 - Solutions and chain confirmation, Atlanta, GA (US), 21-26 Mar 1999. Unpublished. Abstract available.

Mortensen, K.; Almdal, K.; Reynaers, H.; Theunissen, L.; Kleppinger, R., Response to the structure of micellar mesophases and networks when exposed to shear and stretching. SAS'99. 11. International conference on small-angle scattering, New York, NY (US), 17-20 May 1999. Unpublished.

Mortensen, K.; Almdal, K.; Kleppinger, R.; Reynaers, H.; Theunissen, L., Block copolymer micellar networks exposed to stretch, shear and temperature. In: Conference programme and abstracts. 2. European conference on neutron scattering (ECNS '99). Session A, Budapest (HU), 1-4 Sep 1999. Cser, L.; Grósz, T.; Rosta, L. (eds.), (Technical University of Budapest, Budapest, 1999) p. 39.

Mortensen, K.; Frielinghaus, H.; Schwahn, D., Pressure dependence of the phase behaviour of polymer blends and diblock copolymers (Invited paper). In: Collected abstracts. 18. IUCr congress and general assembly, Glasgow (GB), 4-13 Aug 1999. (International Union of Crystallography, Glasgow, 1999) p. 137.

Mortensen, K.; Schwahn, D.; Frielinghaus, H.; Almdal, K., Crossover from 3D-ising to isotropic Lifshitz critical behavior in a mixture of a homopolymer blend and diblock copolymer. SAS'99. 11. International conference on small-angle scattering, New York, NY (US), 17-20 May 1999. Unpublished.

Nielsen, K., McStas, a new neutron ray-tracing package. Meeting at Institute Laue Langevin, Grenoble (FR), 2-3 Mar 1999. Unpublished.

Nielsen, K., McStas, the neutron ray-tracing package. Meeting at Argonne National Laboratory, Chicago, IL (US), 12 Mar 1999. Unpublished.

Nielsen, K.; Lefmann, K., Monte Carlo simulations of neutron scattering instruments using McStas. Conference on neutron optics for the next millennium, NOP99, Villigen (CH), 25-27 Nov 1999. Unpublished. Abstract available.

Nielsen, M.; Feidenhans'l, R.; Howes, P. B.; Grey, F.; Weichel, S.; Vedde, J., The interface structure of directly bonded Si(001) wafers, studied by X-ray diffraction. In: Programme and abstracts. Condensed matter and materials physics conference (CMMP '99), Leicester (GB), 19-22 Dec 1999. (Institute of Physics, London, 1999) p. 3.

Nielsen, M.; Feidenhans'l, R.; Howes, P. B.; Grey, F.; Weichel, S.; Vedde, J.; Rasmussen, K., The interface structure of directly bonded Si crystals studied by synchrotron X-ray diffraction. 1999 Joint international meeting: 196. Meeting of the Electrochemical Society; 1999 Fall meeting of the Electrochemical Society of Japan, Honolulu, HI (US), 17-22 Oct 1999. Unpublished.

Nørgaard, K.; Eskildsen, M. R.; Andersen, N. H.; Canfield, P. C., Magnetic structure of TmNi2B2C in applied magnetic fields. In: Programme. Abstracts. List of participants. Annual meeting of the Danish Physical Society, Nyborg (DK), 3-4 Jun 1999. (HCØ Tryk, København, 1999) p. FF08.

Pedersen, J. S., Modelling and goodness of fit for small-angle scattering data reduction. CANSAS (Collective Aid for Normadic Small-Angle Scatterers), Brookhaven National Laboratory, New York, NY (US), 17-20 May 1999. Unpublished.

Pedersen, J. S., Analytical calculations of the form factors of block copolymer micelles with spherical, ellipsoidal and cylindrical cores. SAS'99. 11. International conference on small-angle scattering, New York, NY (US), 17-20 May 1999. Unpublished.

Pedersen, J. S., Small-angle neutron and X-ray scattering studies of block polymer micelles: Isotope effects. In: Collected abstracts. 18. IUCr congress and general assembly, Glasgow (GB), 4-13 Aug 1999. (International Union of Crystallography, Glasgow, 1999) p. 48.

Pedersen, J. S., Small-angle neutron scattering. 3. Neutron scattering course of the Spanish Neutron Scattering Society, Oviedo (ES), 2-5 Jun 1999. Unpublished.

Pedersen, J. S., Structure of aggregates in mixed surfactant systems determined by small-angle neutron scattering. Physikalisch-chemisches Kolloquium, University of Graz, Graz (AT), 30 Apr 1999. Unpublished.

Pedersen, J. S.; Schurtenberger, P., Monte Carlo simulations applied in the analysis of SANS data from micellar and polymer systems. In: Conference programme and abstracts. 2. European conference on neutron scattering (ECNS '99). Session C, Budapest (HU), 1-4 Sep 1999. Cser, L.; Grósz, T.; Rosta, L. (eds.), (Technical University of Budapest, Budapest, 1999) p. 101.

Pedersen, J. S.; Schurtenberger, P., Monte Carlo simulations applied in the analysis of small-angle scattering data from micellar and polymer systems. SAS'99. 11. International conference on small-angle scattering, New York, NY (US), 17-20 May 1999. Unpublished. Abstract available.

Pedersen, J. S.; Schurtenberger, P., The use of Monte Carlo simulations in the analysis of small-angle scattering data from worm-like micelles and polymers. Erich Schmid colloquium, University of Leoben, Leoben (AT), 29 Apr 1999. Unpublished.

Poulsen, L., Confocal Raman microscopy on polymer materials. Danish Society for Polymer Technology (PTS) thematic meeting, Risø (DK), 5 Oct 1999. Unpublished. Abstract available.

Ramanujam, P. S.; Hvilsted, S., Optical storage in azobenzene polymers. In: Nordic polymer days 1999. Nordic polymer days, Danish Society for Polymer Technology, Copenhagen (DK), 31 May - 2 Jun 1999. (Ingeniørforeningen i Danmark, Copenhagen, 1999) 2. 2.

Rasmussen, F. B., Small angle X-ray scattering used in catalysis research. In: Programme. Abstracts. List of participants. Annual meeting of the Danish Physical Society, Nyborg (DK), 3-4 Jun 1999. (HCØ Tryk, København, 1999) p. FF04.

Rasmussen, F. B.; Knuuttila, T.; Tuoriniemi, J. T.; Lefmann, K., Two-spin NMR mode in Rhodium at high polarization. In: Programme. Abstracts. List of participants. Annual meeting of the Danish Physical Society, Nyborg (DK), 3-4 Jun 1999. (HCØ Tryk, København, 1999) p. FF59P.

Rasmussen, P. H.; Ramanujam, P. S.; Hvilsted, S.; Berg, R. H., Remarkably efficient proline-based azobenzene peptides for optical information storage. In: Program and abstracts. 16. American peptide symposium: Peptides for the new millennium, Minneapolis, MN (US), 26 Jun - 1 Jul 1999. (American Peptide Society, Minneapolis, 1999) p. 275 (P438).

Rønnow, H. M.; Enderle, M.; Hoser, A.; Regnault, L. -P.; McMorrow, D. F.; Dhalenne, G.; Revcholev-schi, A., On the nature of the field-induced incommensurate phase in $CuGeO_3$. In: Conference programme and abstracts. 2. European conference on neutron scattering (ECNS '99). Session F, Budapest (HU), 1-4 Sep 1999. Cser, L.; Grósz, T.; Rosta, L. (eds.), (Technical University of Budapest, Budapest, 1999) p. 207.

Rønnow, H. M.; McMorrow, D. F., Correlations and fluctuations in the 2D $_{S=}$1/2 Heisenberg antiferro-magnet. In: Programme. Abstracts. List of participants. Annual meeting of the Danish Physical Society, Nyborg (DK), 3-4 Jun 1999. (HCØ Tryk, København, 1999) p. FF10.

Rønnow, H. M.; Wildes, A. R., Magnetic correlations in the 2D $_{S=}$5/2 honeycomb antiferromagnet $MnPS_3$. In: Conference programme and abstracts. 2. European conference on neutron scattering (ECNS '99). Session F, Budapest (HU), 1-4 Sep 1999. Cser, L.; Grósz, T.; Rosta, L. (eds.), (Technical University of Budapest, Budapest, 1999) p. 207.

Schmidt, A. S.; Lawther, J. M.; Hvilsted, S.; Thomsen, A. B., Properties of wheat straw and beechwood fibre fraction prepared by wet oxidation and enzyme treatment. Natural fibres performance forum conference: Plant fibre products - essential for the future, Copenhagen (DK), 27-28 May 1999. Unpublished.

Schrenk, R.; Rasmussen, F. B.; Lefmann, K.; Tuoriniemi, J. T.; Vuorinen, R. T.; Siemensmeyer, K.; Steiner, M., On the transition to nuclear order in Ag. In: Programme and abstracts. International symposium on ultralow temperature physics, St. Petersburg (RU), 12-15 Aug 1999. (Ioffe Physico-Technical Institute, St. Petersburg, 1999) p. 69.

Schwahn, D.; Mortensen, K.; Frielinghaus, H.; Almdal, K., Crossover from 3d-ising to isotropic Lifshitz critical behavior in a mixture of a homopolymer blend and diblock copolymer. APS Centennial meeting. Session YC11 - Block copolymers, Atlanta, GA (US), 21-26 Mar 1999. Unpublished. Abstract available.

Schwahn, D.; Mortensen, K.; Frielinghaus, H.; Almdal, K., 3d-ising and Lifshitz critical behavior in a mixture of a polymer blend and a diblock copolymer. In: Conference programme and abstracts. 2. European conference on neutron scattering (ECNS '99). Session C, Budapest (HU), 1-4 Sep 1999. Cser, L.; Grósz, T.; Rosta, L. (eds.), (Technical University of Budapest, Budapest, 1999) p. 103.

Sommer, C.; Cannavacciuolo, L.; Egelhaaf, S. U.; Pedersen, J. S.; Schurtenberger, P., Flexibility and interaction effects in equilibrium polyelectrolytes. In: Conference programme and abstracts. 2. European conference on neutron scattering (ECNS '99). Session C, Budapest (HU), 1-4 Sep 1999. Cser, L.; Grósz, T.; Rosta, L. (eds.), (Technical University of Budapest, Budapest, 1999) p. 102.

Sommer-Larsen, P., Dielectrical spectroscopy of polymers. Danish Society for Polymer Technology (PTS) thematic meeting, Risø (DK), 5 Oct 1999. Unpublished. Abstract available.

Swann, M. J.; Glidle, A.; Cooper, J. M.; Gadegaard, N., Odour permeation profiles within 'electronic nose' polymer membranes determined by neutron reflectivity. In: Conference programme and abstracts. 2. European conference on neutron scattering (ECNS '99). Session C, Budapest (HU), 1-4 Sep 1999. Cser, L.; Grósz, T.; Rosta, L. (eds.), (Technical University of Budapest, Budapest, 1999) p. 103.

Thestrup, B.; Schou, J.; Larsen, N. B., Pulsed laser deposition of transparent, conducting AZO and ITO films. In: Programme. Abstracts. List of participants. Annual meeting of the Danish Physical Society, Nyborg (DK), 3-4 Jun 1999. (HCØ Tryk, København, 1999) p. KF09P.

Thestrup, B.; Schou, J.; Larsen, N. B., Transparent, conducting AZO and ITO films produced by pulsed laser ablation at 355 nm. COLA 99, 5. International conference on laser ablation, Göttingen (DE), 19-23 Jul 1999. Unpublished. Abstract available.

Thom, V.; Altankov, G.; Groth, T.; Jankova, K.; Jonsson, G.; Ulbricht, M., Control of cell - surface interactions by photo-grafting of poly(ethylene glycol)(PEG). 15. European conference on biomaterials (ESB), Bordeaux/Arcachon (FR), 8-12 Sep 1999. Unpublished.

Thom, V.; Ulbricht, M.; Jankova, K.; Altankov, G.; Groth, T.; Jonsson, G.; Johannsen, I., Control of protein/cell interactions with polymer surfaces via photo-grafting of poly(ethylene glycol) (PEG). Nordic polymer days, Danish Society for Polymer Technology, Copenhagen (DK), 31 May - 2 Jun 1999. Unpublished. Abstract available.

Thom, V.; Ulbricht, M.; Jankova, K.; Altankov, G.; Groth, T.; Jonsson, G., Control of protein and cell interactions with polymeric films and membranes by photo-grafting of poly(ethylene glycol) (PEG). EUROMEMBRANE '99, Leuven (BE), 19-22 Sep 1999. Unpublished.

Thomsen, A. B.; Schmidt, A. S.; Toftegaard, H.; Batsberg Pedersen, W.; Woidemann, A.; Lilholt, H., Wet-oxidised wheat straw used as reinforcement for polypropylene composites. Natural fibres performance forum conference: Plant fibre products - essential for the future, Copenhagen (DK), 27-28 May 1999. Unpublished.

Travas-Sejdic, J.; Easteal, R.; Knott, R.; Pedersen, J. S., Small-angle neutron scattering from poly(NIPA-co-AMPS) gels. SAS'99. 11. International conference on small-angle scattering, New York, NY (US), 17-20 May 1999. Unpublished.

Truelsen, J. H.; Kops, J.; Batsberg Pedersen, W., Synthesis by ATRP of triblock copolymers with densely grafted styrenic end blocks from a polyisobutylene macroinitiator. In: Nordic polymer days 1999. Nordic polymer days, Danish Society for Polymer Technology, Copenhagen (DK), 31 May - 2 Jun 1999. (Ingeniørforeningen i Danmark, Copenhagen, 1999) P2.

Vaqueriro, P.; Powell, A. V.; Lebech, B., Order-disorder transitions in $NiCr_2S_4$. In: Conference programme and abstracts. 2. European conference on neutron scattering (ECNS '99). Session B, Budapest (HU), 1-4 Sep 1999. Cser, L.; Grósz, T.; Rosta, L. (eds.), (Technical University of Budapest, Budapest, 1999) p. 64.

Vigild, M. E.; Almdal, K.; Mortensen, K., Mesomorphic crystallography of the gyroid structure in a diblock copolymer. APS Centennial meeting. Session YC11 - Block copolymers, Atlanta, GA (US), 21-26 Mar 1999. Unpublished. Abstract available.

Wolny, J.; Lebech, B.; Wnek, A., Modulated magnetic structures of light rare earth metals and their compounds. Sudeten workshop, Duszniki (PL), 1-3 Jul 1999. Unpublished.

Wurlitzer, A.; Politsch, E.; Gutberlet, T.; Weygand, M.; Hübner, S.; Howes, P.; Kjær, K.; Cevc, G.; Lösche, M., Neutron and x-ray reflection measurements from surface monolayers of a new lipopolymer. In: Conference programme and abstracts. 2. European conference on neutron scattering (ECNS '99). Session C, Budapest (HU), 1-4 Sep 1999. Cser, L.; Grósz, T.; Rosta, L. (eds.), (Technical University of Budapest, Budapest, 1999) p. 99.

Åstrand, P. -O., Intermolecular interactions. Ph. D. course on computational methods in chemistry, University of Copenhagen, Department of Chemistry, Copenhagen (DK), 19 Jan 1999. Unpublished.

Åstrand, P. -O., Simulations of liquids. Ph. D. course on computational methods in chemistry, University of Copenhagen, Department of Chemistry, Copenhagen (DK), 18 Jan 1999. Unpublished.

3.4. Patent applications

Batsberg Pedersen, W.; Berg, R. H.; Almdal, K.; Winther, L., Tværbundet polyolefin substrat. EP patentansøgning 94918770. 0; US application 08/569. 255.

Feidenhans'l, R.; Howes, P. B.; Nielsen, M.; Vedde, J.; Grey, F., Nanometer-scale modulation. DK patentansøgning PA 1999 00918.

Hvilsted, S.; Berg, R. H.; Ramanujam, P. S., Peptidbaseret hologram. EP patentansøgning 96916021. 7; US Application 08/973,179.

Lauritsen, J. B.; Bechgaard, K., A prostetic device. DK patentansøgning PA 1999 01811.

Smela, E.; Sommer-Larsen, P.; Johannsen, I., Conjugated polymer actuator. EP patentansøgning 99200250. 1

3.5. Meeting and Courses

3.5.1. Ph.D. Course on "Statistical Physics and Soft Matter "

From February to May 1999.

"Graduate School of Biophysics" and "Graduate School in Non-Linear Science" supported by The Danish Research Academy

Organisers:
Risø National Laboratory, Denmark: *P.-A. Lindgård*
The Technical University of Denmark: *O. G. Mouritsen* and *L. Miao*

The lectures were given by:
P.-A. Lindgård, Risø National Laboratory, Denmark
O. G. Mouritsen, The Technical University of Denmark
H. C. Fogedby, University of Århus, Denmark
G. Besold, The Technical University of Denmark
L. Miao, The Technical University of Denmark
J. H. Ipsen, The Technical University of Denmark
S. Toxværd, University of Copenhagen, Denmark
G. Peters, The Technical University of Denmark
J. Dyre, Roskilde University Centre, Denmark
E. Præstgård, Roskilde University Centre, Denmark
I. Vattualinen, The Technical University of Denmark
T. Bohr, The Technical University of Denmark

3.5.2. XENNI meeting

May 5 to 6, Risø National Laboratory and Copenhagen Star Hotel

Organisers:
M. Johnson, ISIS Facility, UK*, K. Lefmann, K. N. Clausen and A. Liljenström,* Risø National Laboratory, Denmark:

The meeting was the half-annual meeting of the European network XENNI on neutron instrumentation: Detectors, neutron optics, polarised neutrons, and data visualisation. This meeting further contained preparation of three FP-5 networks, which are to replace the XENNI network.

The contributors to the programme were:

Wednesday May 5	*C. Van Eijk, C. Wilkinson/D. Myles, D. Sivia, P. Böni, C. Fermon, J. Dreyer, L.-P. Regnault and K. Habicht*
Thursday May 6	*A. Rupp, T. Roberts, G. Evrard, R. McGreevy, M. Johnson and W. Svendsen*

Participants:

M. Johnson, G. Evrard, E. Schooneveld and D. Sivia, ISIS Facility, UK
Louis-Pierre Regnault and Jochen Dreyer, CEA, Grenoble, France
D. Myles, C. Wilkinson, F. Tasset, T. Roberts, Institute Laue Langevin, Grenoble, France
C. Fermon, CEA, Saclay, France
C. van Eijk, Delft University of Technology, The Netherlands
B. Alefeld, Kernforschungscenter Jülich, Germany
A. Rupp and K. Habicht, Hahn Meitner Institute, Berlin, Germany

R. McGreevy, The Studsvik Neutron Research Laboratory, Sweden
P. Böni, Paul Sherrer Institute, Switzerland
W. Svendsen, Niels Bohr Institute, University of Copenhagen, Denmark
K. Nielsen, K. N. Clausen and K. Lefmann, Risø National Laboratory, Denmark

3.5.3. Thematic day on Surface Analysis.

Thursday May 18, Risø National Laboratories.

Organisers: *A. Liljenström, N. B. Larsen, R. Feidenhans'l, Risø National Laboratory, Denmark and L. H. Christensen, Danish Technological Institute, Denmark.*

In collaboration with the Danish Technological Institute (TI) we organised a thematic day on surface analysis, where Risø and TI presented their equipment and possibilities with surface characterisation for Danish Industry. There were 30 participants from private companies Danish Companies and about 15 from TI and Risø

The program contained:

Surface characterisation –an introduction, *I. Johannsen,* Risø National Laboratory, Denmark
Industrial use of TOF-SIMS, *R. Kersting,* TASCON, Germany
Investigation of polymer surfaces by AFM, *N. B. Larsen*, Risø National Laboratory, Denmark
SEM at the Danish Technological Institute, *L. H. Christensen,* Danish Technological Institute, Denmark
SEM, ESEM and LV-SEM illustrated by practical examples, *J. Bilde-Sørensen*, Risø National Laboratory, Denmark
3D topographical characterisation of surfaces, *L. H. Christensen,* Danish Technological Institute, Denmark
The new Camera TOF-SIMS facility, *N. B. Larsen,* Risø National Laboratory, Denmark

3.5.4. 30th Meeting of the Danish Crystallographers

May 20-21, Risø National Laboratory

Organisers: *A. Liljenström, B. Lebech and R. Feidenhans'l, Risø National Laboratory, Denmark*

The 30th Meeting of the Danish Crystallographers was held at Risø May 20-21. There were 51 participants, out of which about 20 were Ph.D. or Master students.

The Meeting started with a session on Protein Crystallography, where Prof. Sine Larsen, KU, gave an excellent overview with the title 'Macromolecular Crystallography – Results and Projects'. A poster session with 21 contributions followed and the scientific part of the day ended by a talk by Prof. E. Mokovicky, University of Copenhagen, about asymmetries in art and science. The dinner was enjoyed in the scenic Borrevejle Idrætscenter, where the beach and the nice weather tricked many informal discussions on Crystallography and Danish science funding policy.

On the following day, Karsten Joenson form Osmic Inc. gave a vivid overview on the new possibilities using multilayers and Bo Brummerstedt from University of Copenhagen told how accurate crystallographic information can be used to improved the properties of materials, in his case clathratets as new thermoelectric materials.

'Kemisk Forening' and Acta Chemica Scandinavica supported the meeting.

3.5.5. Nordic Polymer Days 1999

May 31 - June 2, 1999, IDA House, Kalvebod Brygge 31-33, Copenhagen, Denmark

An international symposium organized by Danish Society for Polymer Technology in co-operation with Technical University of Denmark, Risø National Laboratory, and Aalborg University. The symposium covered all aspects of polymer chemistry and physics, rheology and processing of polymers, polymer composites and blends, and recycling of polymer materials. In addition to the below listed five plenary lectures, 66 short oral presentations were given, and 19 posters were presented. An exhibition featuring 8 companies presenting mostly analytical equipment was offered. A total of 177 scientists, industrialists and students participated.

Organisation:

J. Lyngaae-Jørgensen, Technical University of Denmark, Denmark
S. Hvilsted, Risø National Laboratory, Denmark
J. de Caville Christiansen, Aalborg University, Denmrk
C. Hansen, FORCE Institute, Denmark
L. D. Clausen¸ Radiometer Medical A/S, Denmark
U. Nøsted, Novo Nordisk A/S, Denmark
J. D. Larsen, Coloplast A/S, Denmark
A. Sørensen, Novo Nordisk A/S, Denmark
B. K. Storm, Aalborg University, Esbjerg, Denmark

Plenary lectures:

New structures and properties through metallocene catalyzed polymerizations, *J. Seppälä,* Helsinki University of Technology, Finland
Developments in controlled radical polymerizations, J. *Kops,* Technical University of Denmark, Denmark
Diffusion of small-molecule penetrants in polymers, *U. W. Gedde,* Royal Institute of Technology, Sweden
Structure - function relationships in chitosans, *O. Smidsrød,* Norwegian University of Science and Technology, Norway
Raman Microspectroscopy, Scanning Probe Microscopy and *R. Pyrz,* Aalborg University, Denmark

3.5.6. Microsymposia organised at the XVIII IUCR Congress and General Assembly

August 4 to 13, Glasgow, Scotland

Organisers from Risø staff: *R. Feidenhans'l, B. Lebech and J. Skov Pedersen*

R. Feidenhans'l was a member of the programme committee of the XVIII IUCR Congress and General Assembly and held the overall responsibility for the following Microsymposia:
- **Advances in Liquid Structure Determination**, August 6, 10:00 to 12:30
- **Interfaces, Thin Films and Multilayers**, August 6, 10:00 to 12:30, 14:15 to 17:15
- **Amorphous Materials: Small Angle Scattering**, August 7, 10:00 to 12:30
- **Opto-Electronic Materials**, August 9, 14:15 to 17:15

Two of Microsymposia at the XVIII IUCR Congress and General Assembly were planned and organised by Risø staff members. They are:

- **X-ray and Neutron Complementarity**
  Organised by B. *Lebech and J. W. White*, August 6, 14:45 to 17:15

  ○ C. Vettier, *European Synchrotron Radiation Facility, Grenoble, France*. Overview of complementarity between neutrons and x-rays with typical examples.
  ○ J. P. Hill[1], A. T. Boothroyd[2], D. F. McMorrow[3], N. H. Andersen[3], A. Stunault, C. Vettier[4], Th. Wolf[5], *[1]Department of Physics, Brookhaven National Laboratory, Upton NY, USA, [2]Clarendon Laboratory, Oxford University, Oxford, UK, [3]Condensed Matter Physics and Chemistry Department, Risø National Laboratory, Roskilde, Denmark, [4]European Synchrotron Radiation Facility, Grenoble, France, [5]Forschungszentrum Karlsruhe, Karlsruhem,German.*, $PrBa_2CU_3O_{6+x}$, a case study in the complementarity of x-ray and neutronmagnetic scattering.
  ○ E. Lelièvre-Berna and F. Tasset, *Institut Laue Langevin, Avenue des Martyrs, Grenoble, France*. Spherical neutron polarimetry and complementarity with x-rays.
  ○ N. Niimura, *Advanced Science Research Center, Japan Atomic Energy Research Institute, Tokaimura, Japan*. Neutron protein crystallog-raphy by the use of a neutron imaging plate.
  ○ J. Skov Pedersen, *Condensed Matter Physics and Chemistry Department, Risø National Laboratory, Roskilde, Denmark*. Small-angle neutron and x-ray scattering studies of block copolymer micelles: isotope effect.

- **Amorphous materials: Small angle scattering**
  Organised by *G. Kostorz and J. S. Pedersen*, August 7, 10:00 to 12:30

  ○ P. Lamparter, S. Schempp, J. Bill and F. Aldinger, *Max-Planck-Institut für Metallforschung, Stuttgart, Germany*. X-ray and neutron small angle scattering with amorphous Si-C-N ceramics.
  ○ F. Craievich, *Instituto de Física, São Paulo, SP, Brasil*. Structural transformations in nanostructured materials.
  ○ J. F. Löffler[1], H. B. Braun[2], W. Wagner[2], A. Wiedenmann[3] and G. Kostorz[4], *[1]California Institute of Technology, W. M. Keck Laboratory, Pasadena, USA, [2]Paul Scherrer Institut, PSI Villigen, Switzerland, [3]Hahn-Meitner-Institut, Berlin, Germany, [4]ETH, Institut für Angewandte Physik, Zürich, Switzerland*. Magnetic microstructure of nanostructured metals studied by small-angle neutron scattering.
  ○ H. Seto[1], D. Okuhara[1], Y. Kawabata[1], and T. Takeda[1] and M. Nagao[2], *[1]Faculty of Integrated Arts and Sciences, Hiroshima University, Japan, [2]Neutron Scattering Laboratory, Institute for Solid State Physics, The University of Tokyo, Tokai, Japan*. Small angle scattering studies on a pressure induced phase transition in a ternary microemulsion.
  ○ E. P. Gilbert, P. A. Reynolds and J. W. White, *Research School of Chemistry, Australian National University, Canberra, Australia*. Induced structural changes at paraffin-graphite interfaces.

3.5.7. Advanced Analytical Methods for Polymeric Materials

October 5, 1999, Risø National Laboratory

A symposium organized by Søren Hvilsted, Risø National Laboratory, jointly under the auspices of Danish Society for Polymer Technology and Danish Polymer Centre. 85 scientists and industrialists attended the symposium. After the lecture program tours to the analytical chemistry and laser laboratories at Risø National Laboratory were conducted.

The following lecture programme was presented by staff nembers at Risø National Laboratory:

S. Hvilsted,	Welcome and Introduction.
N. B. Larsen	Chemical and Topographical Surface Analysis of Polymers.
P. S. Ramanujam	Optical Techniques for Analysis of Polymers.
L. Poulsen	Confocal Raman Microscopy on Polymer Materials.
P. Sommer-Larsen	Dielectric Spectroscopy of Polymers.
H. Egsgaard	Investigation of Low Molar Mass Polymers by Use of Electrospray Ionization and Mass Spectrometry.
W. B. Pedersen	Size Exclusion Chromatography and MALDI-TOF Analysis of Polymers - A Comparison.

3.6.   Memberships of committees and boards

N. H. Andersen
Member of Consultant for the Swedish Superconductivity Consortium
Expert evaluator for INTAS, the International Association for the promotion of Co-operation with scientists from the new independent states of the former Soviet Union
Member of Fagligt forum

K. Bechgaard
Member of Advisory Board of Journal of Materials Chemistry
Member of Assessment Committee for an associate professorship in experimental biological physics at the Niels Bohr Institute and Risø National Laboratory
Member of ATV, Akademiet for de Tekniske Videnskaber
Board member of Dansk Polymercenter
Member of EEC COST D-4 Committee
Member of Nationalkomiteen for Kemi

R. H. Berg
Councillor of the European Peptide Society
Member of Editorial Board of Journal of Peptide Science

K. N. Clausen
Board member of the Danish Research Academy's Graduate School of Biophysics
Member of Editorial Board of Journal of Neutron Research
Member of The ENSA (European Neutron Scattering Association) Committee
Member of International Union of Pure and Applied Physics, Magnetism Section
Chairman of Round Table of Neutron Sources
Member of SNS Instrument Oversight Committee

R. Feidenhans'l
Board member for Center for Metrologi og Funktionalitet
Member of Council of the European Synchrotron Radiation Society
Chairman of Den Danske Nationalkomité for Krystallografi
Member of Forschungsberat Synchrotronstrahlung HASYLAB, DESY. Hamburg
Member of IUCr Commission on Synchrotron Radiation
Member of MAXLAB, Program Advisory Committee
Member of Nordsync, Danish representative
Chairman of Center for Udnyttelse af Synkrotronstråling

H. Flyvbjerg
Member of Advisory Committee on Biophysics, reporting to the Physics Study Committee of the Faculty of Science at the University of Copenhagen

Chairman of Assessment Committee for an associate professorship in experimental biological physics at the Niels Bohr Institute and Risø National Laboratory
Chairman of Board of the Danish Research Academy's Graduate School of Biophysics
Board member of the Solid State Section of the Danish Physical Society
Member of Organizing Committee of the International Summer school "Physics of Bio-Molecules and Cells", Les Houches (FR), 2001

S. Hvilsted
Chairman of Management Committee for COST Action 518: Molecular Materials and Functional Polymers for Advanced Devices. Project 5: Polymers for Holography
Board member Dansk Polymercenter
Board member Polymerteknisk Selskab
Member of International Advisory Boardon International Conference on New Trends in Functional Polymer, Huangshan (CN), 8-13 May 2000
Member of International Union of Pure and Applied Chemistry, Macromolecular Division
Member of Kontaktudvalg for Dansk Selskab for Termoanalyse
Member of Organizing committee of the 12. International conference on thermal analysis and calorimetry. Copenhagen, Denmark 12-16 Aug 2000
Member of Steering Committee for Experimental and Theoretical Investigation of Complex Polymer Structures (SUPERNET) from 1999 to 2003

I. Johannsen
Member of Biological Materials and Products Research Board
Chairman of MODECS Research Forum
Chairman of Programkommiteen for "Kostbart Udstyr"
Member of Statens Teknisk-Videnskabelige Forskningsråd

K. Kjær
Member of European Synchrotron Radiation Facility (ESRF) Review Committee on Soft Condensed Matter

B. Lebech
Member of Den Danske Nationalkomité for Krystallografi
Member of The ENSA (European Neutron Scattering Association) Committee
Chairman of Dansk Neutronspredningsselskab
Expert evaluator for INTAS, the International Association for the promotion of Co-operation with scientists from the new independent states of the former Soviet Union

K. Lefmann
Board member of Dansk Neutronspredningsselskab

P.-A. Lindgaard
Chairman of EPS-Communications and Interdivisional Relation Group
Member of EU TMR Evaluation Panel
Member of Executive Committee of the European Physical Society. Including Financial Subcommittee and Editorial Subcommittee for Europhysics News
Member of Programme Committee of the European conference: Physics of Magnetism 99, Poznan (PL), 21-25 Jun 1999

D.F. McMorrow
Member of Editorial board of Journal of Physics: Condensed Matter
Member of European Synchrotron Radiation Facility (ESRF) Review Committees
Member of ISIS Scheduling Panel, RAL (GB)

K. Mortensen
Member of Advisory Committee for 8. European Macromolecular Club meeting: Physical aspects of macromolecules: Polymers and polyelectrolytes
Board member of the Danish Research Academy's Graduate School of Biophysics
Board member of Dansk Neutronspredningsselskab
Member of Editorial Board of Journal of Macromolecular Science

J. S. Pedersen
Member of Co-editor of Journal of Applied Crystallography
Member of IUCr Commission on Neutron Scattering
Member of IUCr Commission on Small-Angle Scattering

## 4.	Staff, guests, students, degrees and awards
http://www.risoe.dk/fys/Employee/

Scientific staff and consultants

Aeppli, Gabriel (Consultant)
Almdal, Kristoffer
Als-Nielsen, Jens (Consultant)
Andersen, Niels Hessel
Bechgaard, Klaus (Head of the Department)
Berg, Rolf H.
Clausen, Kurt N. (Head of Research Programme)
Feidenhans'l, Robert (Head of Research Programme)
Flyvbjerg, Henrik
Hvilsted, Søren
Jensen, Jens (Consultant)
Johannsen, Ib (Head of Research Programme)
Jørgensen, Mikkel
Kjær, Kristian
Larsen, Niels B.
Lebech, Bente
Lebech, Jens
Lefmann, Kim
Lindgård, Per-Anker
McMorrow, Des
Mortensen, Kell (Research Professor)
Nielsen, Kristian
Nielsen, Mourits
Pedersen, Jan Skov
Pedersen, Walther Batsberg
Skaarup, Per
Smela, Elisabeth (Until February 28)
Sommer-Larsen, Peter
Wilbrandt, Robert (On leave from August 1)

Post-docs

Bergström, Magnus (Until March 31)
Eskildsen, Morten Ring (Stationed in Geneva from July 1)
Frello, Thomas
Frielinghaus, Henrich
Hermsdorf, Nadja (From May 1)
Hooker, Jacob
Jensen, Torben René
Koblischka, Michael (From September 1)
Kumpf, Christian (From February 1)
Larsen, Britt Hvolbæk
Nielsen, Martin Meedom
Norrman, Kion (From March 1)
Papra, Alexander (From May 1)
Rasmussen, Frank Berg
Thom, Volkmar
Åstrand, Per-Olof

Temporary scientific staff

Eskildsen, Jørgen (Until June 30)
Klausen, Stine Nyborg (From October 13)
Kuhn, Louise (From January 1 until March 31)
Poulsen, Lars (From August 9 to November 8)
Wang, Christian (From February 1)
Zuccarello, Guido (Until February 15)

Ph.D. students and other students

Abrahamsen, Asger
Arleth, Lise
Borg, Jesper
Bøgelund, Jesper Poder (Until April 1)
Christensen, Niels Bech
Faldt, André
Gadegaard, Nikolaj
Grage, Mette
Ishøy, Torben
Jacobsen, Birgitte Abery (From August 11)
Jensen, Lasse
Kofod, Guggi
Krebs, Frederik
Lausen, Bo Wegge
Mentzel, Søren
Nørgaard, Katrine
Petterson, Robert (From November 1)
Poulsen, Mette (From September 23)
Rasmussen, Palle H.
Reynisson, Jóhannes
Rønnow, Henrik M.
Somolinos, Carlos Sánchez (From October 1 until October 30)
Steenstrup, Frederik
Svaneborg, Carsten
Tiana, Guido
Thomsen, Kristina

Technical staff

Alstrup, Jan (From September 20)
Bang, Steen
Berntsen, Allan Nørtoft
Breiting, Bjarne
Hansen , Thomas Agertoft
Heinvig, Tania (Trainee until April 30)
Hubert, Lene
Jensen, Birgit
Jørgensen, Ole
Kjær, Kristine (Until May 31)
Kjær, Torben
Larsen, Bent Lykke
Mazur, Tanja (From October 1)

Nielsen, Anne Bønke (Until September 30)
Nielsen, Lotte
Nielsen, Steen
Nielsen, Thomas (Trainee from September 1)
Rasmussen, Helle D.
Rasmussen, Ove
Saxild, Finn
Stahl, Kim
Sørensen, Carsten Gynther
Theodor, Keld

Secretaries

Frederiksen, Lajla
Liljenström, Anette
Schlichting, Bente O.
Studinski, Ca
Thomsen, Alice

Guest scientists and long time visitors

Chuai, C. Z.
Balakrishnan, Gurusamy
Bøgelund, Jesper Poder (From August 1)
Goff, Jon
Mosler, Stephan

Short time visitors under the EC-TMR programme

Abbas, Basil	Forschungszentrum Jülich GmbH , Institut für Festkörperforschung (DE)
Abdul-Redah, Tyno	Technical University of Berlin, I.N. Stranski Institute, Berlin (DE)
Almgren, Mats	University of Uppsala, Department of Physical Chemistry (SE)
Armstrong, Jennifer A.	Loughborough University, Department of Chemistry (UK)
Ayub, Ibrar	Open University, South West Regional Centre (UK)
Bailey, Lee	University of Leicester, Department of Chemistry (UK)
Bancroft, Nicky	University of Warwick, Department of Physics (UK)
Berry, Frank	Open University, South West Regional Centre (UK)
Boerakker, Mark	Eindhoven Univ of Technology, Eindhoven Polymer Laboratories (NL)
Bollinne, Cecile	Université catholique de Louvain, Laboratoire de Physique et de Chimie des Hauts Polymeres (BE)
Bramwell, Steve	LLB (CEA) Saclay, (FR)
Branger, Vincent	LLB (CEA) Saclay, (FR)
Brown, Steve	University of Strathclyde, Department of Pure and Applied Chemistry (UK)
Brunsveld, Luc	Eindhoven Univ of Technology, Eindhoven Polymer Laboratories (NL)
Castro, Miguel	University of Strathclyde, Department of Pure and Applied Chemistry (UK)
Cegli, Andrea	University of Molise, DISTAAM (IT)
Clegg, Paul S.	University of Oxford, Department of Physics (UK)
Coad, Suzanna	ILL, (FR)
Cosgrove, Terence	Bristol University, School of Chemistry (UK)

Cossardo, Maria Teresa	Politecnico di Torino, Dipartimento di Scienza dei Materiali e Ing. Chimica (IT)
Cowley, Roger	University of Oxford, Department of Physics (UK)
Dann, Sandra	Loughborough University, Department of Chemistry (UK)
Daub, Carsten	Technical University of Berlin, I.N.Stranski-Institute (DE)
Daymond, Mark	ISIS, Rutherford Appleton Laboratory (DE)
Escalanta, Jose	University of Bayreuth, Department of Physical Chemistry I (DE)
Espeso, José	University of Cantabria, CITIMAC (ES)
Fernandez, John	University of Strathclyde, Department of Pure and Applied Chemistry (UK)
Fernandez, Luis	University of Cantabria, CITIMAC (ES)
Fitzparick, Mike	Open University, Materials Discipline, Fac. of Technology (UK)
Glidle, Adrew	University of Glasgow, Department of Electronics & Electrical Engineering (UK)
Goff, Jon	University of Oxford, Department of Physics (UK)
Greaves, Colin	University of Birmingham, School of Chemistry (UK)
Grier, Elisabeth	University of Oxford , Department of Physics (UK)
Hall, Peter J.	University of Strathclyde, Department of Pure and Applied Chemistry (UK)
Harris, Mark	ISIS Facility, Rutherford Appleton Laboratory (UK)
Harrison, Andrew	University of Edinburgh, Department of Chemistry (UK)
Hemon, Stephanie	University of Oxford, Department of Physics (UK)
Henderson, Mark	University of Leicester, Department of Chemistry (UK)
Hiess, Arno	ILL, Grenoble (FR)
Howse, Jon	University of Shieffield, (UK)
Jackson, Angela	University of Leicester, Chemistry Department (UK)
James, Karen	University of Newcastle, Department of Mechanical and Manufacturing Engineering (UK)
Kamenev, Konstantin	University of Warwick, Department of Physics (UK)
Keimer, Bernhard	Max-Planck-Institute of Solid State Research, Stuttgart (DE)
Kleppinger, Ralf	FOM Institute for Atomic & Molecular Physics, Amsterdam (NL)
Kunze, Matthias	University of Marburg, Institute for Physical Chemistry (DE)
Lister, Stephen	University of Oxford, Department of Physics (UK)
Madgwick, Alexander	University of Cambridge, Department of Materials (UK)
Mathon, Marie-Helene	LLB (CEA) Saclay, (F)
Mazza, Daniele	Politecnico di Torino, Dipartimento di Scienza dei Materiali e Ing. Chimica (IT)
McEwen, Keith A	University College London, Department of Physics and Astronomy ()
McLure, Ian A.	University of Shieffield, Department of Chemistry (UK)
Monteith, Andrew	Royal Institution of Great Britain, London (UK)
Oakley, Gareth	University of Edinburgh, Department of Chemistry (UK)
Olsson, Ulf	University of Lund, Physical Chemistry I (SE)
Palmer, Helen	University of Birmingham, School of Chemistry (UK)
Papadakis, Christine	Universität Leipzig, Fakultät für Physik und Geowissenschaffen (DE)
Powell, Antony V.	Heriot-Watt University, Department of Chemistry (UK)
Rauchs, Gaston	University of Manchester, Manchester Materials Science Center (UK)
Roberts, Claire	Bristol University, School of Chemistry (UK)
Schmoelzer, Stefan	Universität Bayreuth, Lehrstuhl für Physikalische Chemie I (DE)
Schröder, Almut	Universität Karlsruhe, Physikalisches Institut (DE)
Schwan, Dietmar	Forschungszentrum Jülich GmbH , Institut für Festkörperforschung (DE)
Sperling, Jan	Technical University of Berlin, I.N. Stranski-Institute, (DE)
Theunissen, Liesbeth	K.U. Leuven, Department of Chemistry (BE)
Tuck, Jonathan	University of Newcastle upon Tyne, Department of Mechanical and Manufacturing Engineering (UK)
Ulbrich, Werner	Universität Bayreuth, Lehrstuhl für Physikalische Chemie I (DE)

Vaqueiro, Paz	Heriot-Watt University, Department of Chemistry (UK)
Visser, Dirk	University of Warwick, Physics Department (UK)
Wang, Ke	University of Uppsala, Department of Physics and Chemistry (SE)
Weller, Mark	University of Southampton, Department of Chemistry (UK)
Williams, Ruth	Open University, South West Regional Centre (UK)

Short time visitors

Andersen, Trine	Odense Universitet (DK)
Angelico, Ruggero	Dept of Food Technology, University of Molise (IT)
Antoun, Sayed	Labo MSC, Katholieke Universiteit Leuven (BE)
Apperloo, Joke	Dept of Polymers & Organic Chemistry, Eindhoven University of Technology (NL)
Barker, Anna	Department of Chemistry, University of Warwick (UK)
Bernhardt, Philipp	Lehrstuhl für Kristallographie und Strukturphysik, Universität Erlangen/Nürnberg (DE)
Bergström, Magnus	Department of Physical Chemistry, Royal Institute of Technology (SE)
Bishop, David	Bell Laboratories, Innovations for Lucent Technologies (US)
Brezesinski, Gerald	Berlin, Max-Planck-Institut of Colloids and Interfaces (DE)
Busson, Philippe	Stockholm, Kungliga Tekniska Högskolan (SE)
Buyers, William	Chalk River Laboratories, National Research Council Canada (CA)
Cannavacciuolo, Luigi	ETHZ (CH)
Caruana, Daren	Department of Chemistry, University College London (UK)
Chung, Emma	Department of Physics, University of Warwick (UK)
Christensen, Axel Nørlund	Department of Inorganic Chemistry, University of Aarhus (DK)
Coldea, Radu	Rutherford Appleton Laboratory, ISIS Facility (UK)
Dönni, Andreas	Department of Physics, Niigata University (JP)
Egelhaaf, Stefan	Department of Physics, University of Edingburgh (UK)
Gammel, Peter	Bell Laboratories, Innovations for Lucent Technologies (US)
Goderis, Bart	Structure & Morphology of Materials Section PAC-MC, DSM Research (NL)
Haramus, Vasyl	Geesthacht, GKSS Research Center (DE)
Hayden, Stephen	H.H. Wills Physics Laboratory, University of Bristol (UK)
Herrmannsdoerfer, Thilo	Laboratory for Neutron Scattering, ETHZ & PSI (CH)
Horsch, Sebastian	University of Aarhus (DK)
Kenzelmann, Michael	Department of Physics, University of Oxford (UK)
Kersting, Reinhard	Münster, TASCON GmbH (DE)
Khakhar, Jan	Physical Chemistry 1, University of Lund (SE)
Korsunsky, Alexander	Department of Engineering Science, University of Oxford (UK)
Kuhn, Luise Theil	Laboratory for Solid State Physics and Magnetism, Katholieke Universiteit Leuven (BE)
Ivan, Bela	Dept of Polymer Chemistry & Material Science, Hungarian Academy of Sciences (HU)
Jack, Kevin	School of Chemistry, Bristol University (UK)
Janssen, Renee	Dept of Polymers & Organic Chemistry, Eindhoven University of Technology (NL)
Juntunen, Kirsi	Low Temperature Laboratory, Helsinki University of Technology (FI)
Lake, Bella	Oak Ridge National Laboratory, Solid State Division (US)
Lopez, Omar Daniel	Bell Laboratories, Innovations for Lucent Technologies (US)
Madsen, Georg	Department of Chemistry, University of Aarhus (DK)
Mayer, Hans-Michael	BENSC, Hahn-Meitner-Institute Berlin GmbH (DE)
Mori, Tsuutomu	Department of Materials, University of Cambridge (UK)
Nagler, Stephen E.	Oak Ridge National Laboratory, Solid State Division (CA)
Nedelmann, Lorentz	Dept of Materials & Interfaces, Weizman Institute of Science (Israel)

Niemöller, Thomas	HASYLAB, DESY (DE)
Nohara, Minorou	Dept of Advanced Material Science, University of Tokyo (JP)
Nylander, Tommy	Physical Chemistry 1, University of Lund (SE)
Parthasarathy, Raghuver	James Franck Institute, University of Chicago (US)
Palazzo, Gerardo	Department of Chemistry, University of Bari (IT)
Pettersson, Robert	Stockholm, Kungliga Tekniska Högskolan (SE)
Pontak, Richard	North Carolina State Univ (US)
Posselt, Dorthe	IMFUFA - Department of Mathematics and Physics, University of Roskilde (DK)
Rading, Derk	TASCON (DE)
Ramzi, Aissa	Eindhoven Polymer Laboratories, Eindhoven University of Technology (NL)
Rittig, Frank	Leipzig, Leipzig Universitet (DE)
Rudershausen, Sandra	Rostock-Warnemünde, Partikeltechnologie GmbH (DE)
Samseth, Jon	Trondheim, SINTEF Energiforskning (NO)
Sanchez, Carlos	Universidad de Zaragoza (ES)
Scherrenberg, Rolf	Structure & Morphology of Materials Section PAC-MC, DSM Research (NL)
Sørensen, Lasse Holst	Roskilde, CAT (DK)
Sørensen, Thore	Dept of Chemical Engineering, Norwegian University of Science and Technology (NO)
Taashi, Karen Inge	Department of Inorganic Chemistry, University of Aarhus (DK)
Tallon, Jeff	New Zealand Institute for Industrial Research (NZ)
Vass, Szabolcs	Laboratory of Physical Chemistry, Institute of Atomic Energy Research (HU)
Vickers, Phil	Mechanical Material Engineering, University of Surrey (UK)
Wildes, Andrew	Grenoble, Institut Laue-Langevin (FR)

Degrees and awards

Frello, Thomas, Ph.D. degree
Rasmussen, Palle H., Ph.D. degree
Thom, Volkmar, Ph.D. degree
Åstrand, Per-Olof, *Docent* in theoretical chemistry, University of Lund (SE)

Direct phone numbers, fax numbers and e-mail:-mail addresses of the scientific staff of the Condensed Matter Physics and Chemistry Department

Name	Direct phone	Fax no.	e-mail
Abrahamsen, Asger	+45 4677 4741	+45 4677 4790	asger.abrahamsen@risoe.dk
Almdal, Kristoffer	+45 4677 4785	+45 4677 4791	k.almdal@risoe.dk
Als-Nielsen, Jens	+45 4677 4528	+45 4677 4790	als@xray.fys.dk
Andersen, Niels Hessel	+45 4677 4711	+45 4677 4790	niels.hessel@risoe.dk
Arleth, Lise	+45 4677 4726	+45 4677 4790	lise.arleth@risoe.dk
Bechgaard, Klaus	+45 4677 4701	+45 4677 4790	klaus.bechgaard@risoe.dk
Berg, Rolf H.	+45 4677 4782	+45 4677 4791	rolf.berg@risoe.dk
Chuai, Chengzhi	+45 4677 4796	+45 4677 4791	chengzhi.chuai@risoe.dk
Clausen, Kurt N.	+45 4677 4704	+45 4677 4790	kurt.clausen@risoe.dk
Eskildsen, Morten Ring	+45 4677 4713	+45 4677 4790	morten.eskildsen@risoe.dk
Faldt, André	+45 4677 4261	+45 4677 4791	andre.faldt@risoe.dk
Feidenhans'l, Robert	+45 4677 4708	+45 4677 4790	robert.feidenhansl@risoe.dk
Flyvbjerg, Henrik	+45 4677 4528	+45 4677 4790	henrik.flyvbjerg@risoe.dk
Frello, Thomas	+45 4677 4719	+45 4677 4790	thomas.frello@risoe.dk
Frielinghaus, Henrich	+45 4677 4779	+45 4677 4791	henrik.frielinghaus@risoe.dk
Gadegaard, Nikolaj	+45 4677 4746	+45 4677 4790	nikolaj.gadegaard@risoe.dk
Gerstenberg, Michael C.	+45 4677 4713	+45 4677 4790	michael.gerstenberg@.risoe.dk
Hermsdorf, Nadja	+45 4677 4753	+45 4677 4791	nadja.hermsdorf@risoe.dk
Hooker, Jacob	+45 4677 4748	+45 4677 4791	jacob.hooker@risoe.dk
Hvilsted, Søren	+45 4677 4784	+45 4677 4791	s.hvilsted@risoe.dk
Ishøy, Torben	+45 4677 4720	+45 4677 4790	torben.ishoy@risoe.dk
Jensen, Torben René	+45 4677 4745	+45 4677 4790	torben.rene.jensen@risoe.dj
Johannsen, Ib	+45 4677 4747	+45 4677 4791	ib.johannsen@risoe.dk
Jørgensen, Mikkel	+45 4677 4717	+45 4677 4791	mikkel.joergensen@risoe.dk
Kjær, Kristian	+45 4677 4709	+45 4677 4790	kristian.kjaer@risoe.dk
Klausen, Stine Nyborg	+45 4677 4730	+45 4677 4791	stine.nyborg.klausen@risoe.dk
Koblischka, Michael	+45 4677 4720	+45 4677 4790	michael.koblischka@risoe.dk
Kofod, Guggi	+45 4677 4748	+45 4677 4791	guggi.kofod@risoe.dk
Krebs, Frederik	+45 4677 4261	+45 4677 4791	frederik.krebs@risoe.dk
Kumpf, Christian	+45 4677 4745	+45 4677 4790	christian.kumpf@risoe.dk
Larsen, Britt Hvolbæk	+45 4677 4712	+45 4677 4790	britt.h.larsen@risoe.dk
Larsen, Niels B.	+45 4677 4721	+45 4677 4790	niels.b.larsen@risoe.dk
Laursen, Bo Wegge	+45 4677 4261	+45 4677 4791	bo.laursen@risoe.dk
Lebech, Bente	+45 4677 4705	+45 4677 4790	bente.lebech@risoe.dk
Lebech, Jens	+45 4677 4761	+45 4677 4792	jens.lebech@risoe.dk
Lefmann, Kim	+45 4677 4726	+45 4677 4790	kim.lefmann@risoe.dk
Lindgård, Per-Anker	+45 4677 4706	+45 4677 4790	p.a.lindgard@risoe.dk
Madsen, Nils Berg	+45 4677 4743	+45 4677 4791	mak-nibm@risoe.dk
McMorrow, Des	+45 4677 4723	+45 4677 4790	des.mcmorrow@risoe.dk
Mortensen, Kell	+45 4677 4710	+45 4677 4790	kell.mortensen@risoe.dk
Nielsen, Kristian	+45 4677 5515	+45 4677 4790	kristian.nielsen@risoe.dk
Nielsen, Martin Meedom	+45 4677 4741	+45 4677 4790	martin.m.nielsen@risoe.dk
Nielsen, Mourits	+45 4677 4703	+45 4677 4790	mourits.nielsen@risoe.dk
Norrman, Kion	+45 4677 4793	+45 4677 4790	kion.norrman@risoe.dk
Nørgaard, Katrine	+45 4677 4719	+45 4677 4790	katrine.noergaard@risoe.dk

Name	Direct phone	Fax no.	e-mail
Papra, Alexander	+45 4677 4795	+45 4677 4790	alexander.papra@risoe.dk
Pedersen, Jan Skov	+45 4677 4718	+45 4677 4790	jan.skov.pedersen@risoe.dk
Pedersen, Walther Batsberg	+45 4677 4783	+45 4677 4791	walther.batsberg@risoe.dk
Rasmussen, Frank Berg	+45 4677 4722	+45 4677 4790	frank.berg.rasmussen@risoe.dk
Rønnow, Henrik M.	+45 4677 4715	+45 4677 4790	henrik.roennow@risoe.dk
Skaarup, Per	+45 4677 5512	+45 4677 4790	per.skaarup@risoe.dk
Sommer-Larsen, Peter	+45 4677 4744	+45 4677 4791	peter.sommer.larsen@risoe.dk
Steenstrup, Frederik	+45 4677 4754	+45 4677 4791	frederik.steenstrup@risoe.dk
Svaneborg, Carsten	+45 4677 4722	+45 4677 4790	carsten.svaneborg@risoe.dk
Thom, Volkmar	+45 4677 4746	+45 4677 4790	volkmar.thom@risoe.dk
Wang, Christian	+45 4677 4753	+45 4677 4791	christian.wang@risoe.dk
West, Keld	+45 4677 4787	+45 4677 4791	keld.west@risoe.dk
Åstrand, Per-Olof	+45 4677 4712	+45 4677 4790	per-olof.aastrand@risoe.dk

Bibliographic Data Sheet   **Risø-R-1156(EN)**

Abstract (max. 2000 characters)

The Condensed Matter Physics and Chemistry Department is concerned with both fundamental and applied research into the physical and chemical properties of materials. The principal activities in the year 1999 are presented in this progress report.

The research in physics is concentrated on neutron and x-ray scattering measurements and the problems studied include two- and three-dimensional structures, magnetic ordering and spin dynamics, superconductivity, phase transitions and nano-scale structures. The research in chemistry includes chemical synthesis and physico-chemical investigation of small molecules and polymers, with emphasis on polymers with new optical properties, block copolymers, surface-modified polymers, and supramolecular structures. Theoretical work related to these problems is undertaken, including Monte Carlo simulations, computer simulation of molecules and polymers and methods of data analysis.